STAINLESS STEEL REINFORCEMENT AS A REPLACEMENT FOR EPOXY-COATED STEEL IN BRIDGE DECKS

By

James Lafikes

Scott Storm

David Darwin

JoAnn Browning

Matthew O'Reilly

A Report on Research Sponsored by

OKLAHOMA DEPARTMENT OF TRANSPORTATION
ODOT SPR ITEM NUMBER 2231

KU TRANSPORTATION RESEARCH INSTITUTE

Structural Engineering and Engineering Materials
SL Report 11-4

THE UNIVERSITY OF KANSAS CENTER FOR RESEARCH, INC.
LAWRENCE, KANSAS
November 2011

ABSTRACT

The performance of different types of reinforcement in concrete bridge decks is evaluated in this study. Application of deicing salts has directly led to deterioration of roadway bridge decks due the corrosion of reinforcing steel. Epoxy-coated reinforcement (ECR) is currently the most commonly used alternative in this application; however, it does not guarantee a long lifespan. In some cases, poorly adhering epoxy coatings have resulted in increased corrosion rates, which is a concern for all epoxy coatings. As a comparison, two types of stainless reinforcing steel are evaluated; a 2304 duplex stainless steel and NX-SCR^{TM} stainless steel clad bars, alongside conventional reinforcement and ECR. Upon the completion of testing, the projected cost of each system will be calculated to determine if the increased initial costs can be justified over a design life. Two tests are performed on specimens – a 15 week rapid macrocell test and a series of 96 week bench-scale tests. Completed test results for the rapid macorcell tests are presented, while bench-scale tests are partially completed with specimens aged 26-31 weeks. Results have shown that ECR and stainless steel reinforcement perform better in test media than conventional reinforcement. Pickling 2304 duplex stainless steel bars has a considerable effect on the performance of test specimens, with as-received bars failing ASTM A955 limits on corrosion rates in rapid macrocell and cracked beam tests. Repickling a series of specimens for rapid macrocell testing resulted in a passing of these test limits. Bending stainless steel clad reinforcement did not cause the specimens to exceed the maximum corrosion rate threshold to be surpassed in rapid macrocell testing, while corrosion initiation has not yet occurred in Southern Exposure specimens. Upon initiation, chloride contents at the level of reinforcement are lowest for conventional steel and highest for damaged stainless steel clad specimens.

Keywords: chlorides, concrete, corrosion, disbondment, duplex stainless steel reinforcement epoxy-coated reinforcement, stainless steel clad reinforcement

ACKNOWLEDGEMENTS

This report is based on a project submitted by James Lafikes and Scott Storm in partial fulfillment of the requirements of the M.S. degree. Major funding was provided by the Oklahoma Department of Transportation under SPR Item Number 2231 and the KU Transportation Research Institute. Material support was also provided by the Epoxy Interest Group of the Concrete Reinforcing Steel Institute (CRSI), Talley Metals, and NX Infrastructure.

TABLE OF CONTENTS

ABSTRACT iii
ACKNOWLEDGEMENTS iv
TABLE OF CONTENTS v
LIST OF TABLES vi
LIST OF FIGURES vii
1. INTRODUCTION 1
2. EXPERIMENTAL WORK 1
2.1 Materials 1
2.2 Rapid macrocell test 4
2.2.1 Experimental Procedure 4
2.2.2 Test Procedure 6
2.3 Bench-scale tests 8
2.3.1 General 8
2.3.2 Concrete mix design and aggregate properties 9
2.4 Southern Exposure (SE) and cracked beam (CB) tests 10
2.4.1 Description 10
2.4.2 Fabrication 11
2.4.3 Test Procedure 13
2.4.4 Corrosion Measurements 14
2.4.5 Chloride Sampling for SE Specimens 15
2.4.6 Chloride Sampling Procedure 15
2.4.7 Chloride Analysis 16
2.5 Test Equipment 17
3. TEST PROGRAM 20
4. RESULTS 24
4.1 Rapid Macrocell Tests 24
4.1.1 Control Specimens 30
4.1.2 2304 Stainless steel 31
4.1.3 NX-SCRTM stainless steel clad reinforcement 37
4.1.4 Autopsy 47
4.2 Bench-Scale Tests 57
4.2.1 Corrosion losses 57
4.2.2 Mat-to-mat resistance 64
4.2.3 Corrosion potential 66
4.2.4 Corrosion rates 72
4.2.5 Critical chloride threshold for Southern Exposure specimens 75
5. SUMMARY AND CONCLUSIONS 78
6. REFERENCES 81

APPENDIX A 82
APPENDIX B 108
APPENDIX C 110

LIST OF TABLES

Table 1: Chemical compositions of steels (provided by manufacturer) 2

Table 2: Mixture proportions for lab and field specimens based on SSD aggregate 9

Table 3: Test Program – number of test specimens 22

Table 4: Casting schedule 23

Table 5: Concrete properties per batch 23

Table 6: Corrosion losses at 15 weeks based on total area for macrocell specimens 25

Table 7: Disbonded area (in2) for damaged ECR specimens 1-6 48

Table 8: Corrosion losses based on total area for Southern Exposure specimens 57

Table 9: Corrosion losses based on total area for cracked beam specimens 59

Table 10a: Chloride contents for specimens with conventional reinforcement 75

Table 10b: Chloride contents for specimens with conventional (top) and 2304 (bottom) reinforcement 76

Table 10c: Chloride contents for specimens with conventional (top) and stainless steel clad (bottom) reinforcement 76

Table 10d: Chloride contents for specimens with epoxy-coated reinforcement 77

Table 10e: Chloride contents for specimens with damaged stainless steel clad reinforcement 77

Table B1: Total losses of rapid macrocell test specimens 109

LIST OF FIGURES

Figure 1: 2304 duplex stainless steel bars in the as-received (left) and re-pickled (right) conditions 2

Figure 2: Rapid macrocell specimens, ECR and NX-SCRTM stainless steel clad damaged bars (0.83% damaged area) 4

Figure 3: Rapid macrocell test 5

Figure 4: Macrocell test of a bent bar 6

Figure 5: Southern Exposure (SE) specimen 10

Figure 6: Cracked Beam (CB) specimen 11

Figure 7: Southern Exposure chloride sampling 16

Figure 8: Heat tent dimensions 19

Figure 9: Average corrosion losses based on total area for conventional, ECR, and undamaged ECR rapid macrocell specimens 26

Figure 10: Average corrosion losses based on total area for conventional, ECR, and undamaged ECR rapid macrocell specimens (Different Scale) 26

Figure 11: Average corrosion losses based on total area for conventional, 2304, 2304-p, mixed 2304/conventional, and mixed conventional/2304 rapid macrocell Specimens 27

Figure 12: Average corrosion losses based on total area for conventional, 2304, 2304-p, mixed 2304/conventional and mixed conventional/2304 rapid macrocell specimens (Different Scale) 28

Figure 13: Average corrosion losses based on total area for conventional, stainless steel clad, damaged stainless steel clad, uncapped stainless steel clad, bent stainless steel clad, mixed stainless steel clad/conventional, and mixed conventional/stainless steel clad rapid macrocell specimens 29

Figure 14: Average corrosion losses based on total area for conventional, stainless steel clad, damaged stainless steel clad, uncapped stainless steel clad, bent stainless steel clad, mixed stainless steel clad/conventional, and mixed conventional/stainless steel clad rapid macrocell specimens (Different Scale) 29

Figure 15: Average corrosion rates of conventional, ECR, and undamaged ECR Specimens 31

Figure 16: Average corrosion rates of ECR and undamaged ECR specimens 31

Figure 17: Macrocell average corrosion rates of conventional, ECR, ECR-ND, 2304, 2304-p, mixed 2304/conventional, and mixed conventional/2304 rapid macrocell specimens, specimens 1-6 32

Figure 18: Macrocell average corrosion rates of, ECR, ECR-ND, 2304, 2304-p, and mixed 2304/conventional rapid macrocell specimens, specimens 1-6 (Different Scale) 33

Figure 19: Macrocell individual corrosion rates of 2304 stainless steel, specimens 1-6 34

Figure 20: Macrocell individual corrosion rates of re-pickled 2304 stainless steel, specimens 1-6 35

Figure 21: Macrocell individual corrosion rates of mixed 2304 stainless steel (anode/cathode), specimens 1-6 36

Figure 22: Macrocell individual corrosion rates of mixed 2304 stainless steel (anode/cathode), specimens 1-6 (Different Scale) 37

Figure 23: Staining of anode of 2304 stainless steel, mixed 2304/conventional steel macrocell specimen 37

Figure 24: Average corrosion rate of conventional, stainless steel clad, damaged v stainless steel clad, uncapped stainless steel clad, bent stainless steel clad, mixed stainless steel clad/conventional, and mixed conventional/stainless steel clad rapid macrocell specimens 39

Figure 25: Average corrosion rate of stainless steel clad, damaged stainless steel clad, uncapped stainless steel clad, bent stainless steel clad, and mixed stainless steel clad/conventional steel clad rapid macrocell specimens (Different Scale) 39

Figure 26: Macrocell individual corrosion rates of undamaged NX-SCRTM stainless steel clad bars, specimens 1-6. Figure 27: Bar end with protective cap removed at end of rapid macrocell test, NX-SCRTM stainless steel clad (cathodes) 40

Figure 27: Bar end with protective cap removed at end of rapid macrocell test, NX-SCRTM stainless steel clad (cathodes). 41

Figure 28: Photograph of Specimen 6 upon completion of the rapid evaluation test, NX-SCRTM stainless steel clad (anode on top, cathode on bottom). 41

Figure 29: Photograph of Specimen 6 upon completion of the rapid evaluation test, NX-SCRTM stainless steel clad (close-up of cathode) 42

Figure 30: Macrocell individual corrosion rates of uncapped NX-SCRTM stainless steel clad bars, specimens 1-6. 43

Figure 31: Uncapped bar end upon autopsy, NX-SCRTM stainless steel clad. 43

Figure 32: Macrocell individual corrosion rates of bent NX-SCRTM stainless steel clad bars, specimens 1-6 44

Figure 33: Corrosion staining on bent section upon autopsy, bent NX-SCRTM stainless steel clad bar (close-up)..... 44

Figure 34: Macrocell individual corrosion rates of 0.83% damaged area NX-SCR™ stainless steel clad bars, specimens 1-6. 45

Figure 35: Macrocell individual corrosion rates of mixed NX-SCRTM stainless steel clad bars (anode/cathode), specimens 1-6 46

Figure 36: Macrocell individual corrosion rate of mixed NX-SCRTM stainless steel clad bars (anode/cathode), specimens 1-6 (Different Scale) 46

Figure 37: Corrosion under protective cap at end of evaluation, NX-SCRTM stainless steel clad bar, Specimen 2 (close-up). 47

Figure 38: Rapid macrocell specimen upon completion of test, conventional steel (anode on top, cathode on bottom) 49

Figure 39: Rapid macrocell specimen upon completion of test, undamaged ECR (anode on top, cathode on bottom) 50

Figure 40: Rapid macrocell specimen upon completion of test, ECR (close-up of damage site after disbondment test)..... 50

Figure 41: Rapid macrocell specimen upon completion of test, 2304 stainless steel (anode on top, cathode on bottom) 51

Figure 42: Rapid macrocell specimen upon completion of test, re-pickled 2304 stainless steel (anode on top, cathode on bottom)..... 51

Figure 43: Rapid macrocell specimen upon completion of test, mixed 2304/conventional steel (anode on top, cathode on bottom) 52

Figure 44: Rapid macrocell specimen upon completion of test, mixed conventional/2304 stainless steel (anode on top, cathode on bottom)..... 52

Figure 45: Rapid macrocell specimen upon completion of test, undamaged stainless steel clad reinforcement (anode on top, cathode on bottom) 53

Figure 46: Rapid macrocell specimen upon completion of test, undamaged stainless steel clad reinforcement (close-up of bar end after cap has been removed) 53

Figure 47: Rapid macrocell specimen upon completion of test, damaged stainless steel clad reinforcement (anode on top, cathode on bottom) 54

Figure 48: Rapid macrocell specimen upon completion of test, uncapped stainless visteel clad reinforcement (anode on top, cathode on bottom) 54

Figure 49: Rapid macrocell specimen upon completion of test, uncapped stainless steel clad reinforcement (close-up of bar end) 55

Figure 50: Rapid macrocell specimen upon completion of test, bent stainless steel clad reinforcement (anode) 55

Figure 51: Rapid macrocell specimen upon completion of test, mixed conventional/stainless steel clad reinforcement (anode on top, cathode on bottom 56

Figure 52: Rapid macrocell specimen upon completion of test, mixed stainless steel clad/conventional steel (anode on top, cathode on bottom) 56

Figure 53a: Average corrosion losses (μm) based on total area for Southern Exposure specimens with conventional and epoxy-coated reinforcement 60

Figure 53b: Average corrosion losses based on total area for Southern Exposure specimens with conventional and 2304 stainless steel reinforcement (Different Scale) 61

Figure 54c: Average corrosion losses based on total area for Southern Exposure specimens with conventional and stainless steel clad reinforcement (Different Scale) 61

Figure 55a: Average corrosion losses based on total area for cracked beam specimens 62

Figure 55b: Average corrosion losses based on total area for cracked beam specimens (Different Scale) 63

Figure 56a: Average mat-to-mat resistances based on total area for Southern Exposure specimens with conventional and epoxy-coated reinforcement 64

Figure 56b: Average mat-to-mat resistances based on total area for Southern Exposure specimens with conventional and 2304 stainless steel reinforcement (Different Scale)..... 65

Figure 56c: Average mat-to-mat resistances based on total area for Southern Exposure specimens with conventional and stainless steel clad reinforcement (Different Scale)..... 65

Figure 57: Average mat-to-mat resistances based on total area for cracked beam Specimens 66

Figure 58a: Average top-mat potentials with respect to CSE for Southern Exposure specimens with conventional and epoxy-coated reinforcement 67

Figure 58b: Average top-mat potentials with respect to CSE for Southern Exposure specimens with conventional and 2304 stainless steel reinforcement. 68

Figure 58c: Average top-mat potentials with respect to CSE for Southern Exposure specimens with conventional and stainless steel clad reinforcement. 68

Figure 59: Average top-mat potentials with respect to CSE for cracked beam specimens..... 69

Figure 60a: Average bottom-mat potentials with respect to CSE Southern Exposure specimens with conventional and epoxy-coated reinforcement 70

Figure 60b: Average bottom-mat potentials with respect to CSE Southern Exposure specimens with conventional and 2304 stainless steel reinforcement..... 71

Figure 60c: Average bottom-mat potentials with respect to CSE Southern Exposure specimens with conventional and stainless steel clad reinforcement. 71

Figure 61: Average bottom-mat potentials with respect to CSE for cracked beam Specimens 72

Figure 62a: Individual corrosion rates (μm/yr) based on total area for cracked beam specimens with 2304 reinforcement. 74

Figure 62b: Individual corrosion rates (μm/yr) based on total area for cracked beam specimens with stainless steel clad reinforcement..... 74

Figure A.1: Macrocell individual corrosion rate of conventional steel, specimens 1-6..... 82

Figure A.2: Macrocell individual corrosion potentials with respect to SCE. Conventional steel bars in pore solution with salt (anode), specimens 1-6..... 82

Figure A.3: Macrocell individual corrosion potentials with respect to SCE. Conventional steel bars in pore solution (cathode), specimens 1-6 83

Figure A.4: Average corrosion potentials with respect to SCE. Conventional steel bars, specimens 1-6 83

Figure A.5: Macrocell individual corrosion loss of conventional steel, specimens 1-6 84

Figure A.6: Macrocell individual corrosion rates of 0.83% damaged area ECR, specimens 1-6 84

Figure A.7: Macrocell individual corrosion potentials with respect to SCE. 0.83% damaged area ECR in pore solution with salt (anode), specimens 1-6 85

Figure A.8: Macrocell individual corrosion potentials with respect to SCE. 0.83% damaged area ECR in pore solution (cathode), specimens 1-6 85

Figure A.9: Average corrosion potentials with respect to SCE. 0.83% damaged area ECR, specimens 1-6 86

Figure A.10: Macrocell individual corrosion loss of 0.83% damaged area ECR, specimens 1-6 86

Figure A.11: Macrocell individual corrosion rates of undamaged ECR, specimens 1-6 87

Figure A.12: Macrocell individual corrosion potentials with respect to SCE. Undamaged ECR in pore solution with salt (anode), specimens 1-6 87

Figure A.13: Macrocell individual corrosion potentials with respect to SCE. Undamaged ECR in pore solution (cathode), specimens 1-6 88

Figure A.14: Average corrosion potentials with respect to SCE. Undamaged ECR, specimens 1-6 88

Figure A.15: Macrocell individual corrosion loss of undamaged ECR, specimens 1-3 89

Figure A.16: Macrocell individual corrosion potentials with respect to SCE. 2304 stainless steel bars in pore solution with salt (anode), specimens 1-6 89

Figure A.17: Macrocell individual corrosion potentials with respect to SCE. 2304 stainless steel bars in pore solution (cathode), specimens 1-6 90

Figure A.18: Average corrosion potentials with respect to SCE. 2304 stainless steel bars, specimens 1-6 90

Figure A.19: Macrocell individual corrosion loss of 2304 stainless steel, specimens 1-6..... 91

Figure A.20: Macrocell individual corrosion potentials with respect to SCE. Re-pickled 2304 stainless steel bars in pore solution with salt (anode), specimens 1-6 91

Figure A.21: Macrocell individual corrosion potentials with respect to SCE. Re-pickled 2304 stainless steel bars in pore solution with salt (cathode), specimens 1-6..... 92

Figure A.22: Average corrosion potentials with respect to SCE. Re-pickled 2304 stainless steel bars, specimens 1-6 92

Figure A.23: Macrocell individual corrosion loss of 2304 re-pickled stainless steel, specimens 1-6..... 93

Figure A.24: Macrocell individual corrosion potentials with respect to SCE. Mixed 2304 stainless steel (anode/cathode) in pore solution with salt (anode), specimens 1-6..... 93

Figure A.25: Macrocell individual corrosion potentials with respect to SCE. Mixed 2304 stainless steel (anode/cathode) in pore solution (cathode), specimens 1-6..... 94

Figure A.26: Average anode corrosion potentials with respect to SCE. Mixed 2304 stainless steel (anode/cathode), specimens 1-6 94

Figure A.27: Average cathode corrosion potentials with respect to SCE. Mixed 2304 stainless steel (anode/cathode), specimens 1-6 95

Figure A.28: Macrocell individual corrosion loss of mixed 2304 stainless steel, specimens 1-6..... 95

Figure A.29: Macrocell individual corrosion loss of mixed 2304 stainless steel, specimens 1-6 (different scale 96

Figure A.30: Macrocell individual corrosion potentials with respect to SCE. Undamaged NX-SCR™ stainless steel clad bars in pore solution with salt (anode), specimens 1-6..... 96

Figure A.31: Macrocell individual corrosion potentials with respect to SCE. Undamaged NX-SCR™ stainless steel clad bars in pore solution (cathode), specimens 1-6..... 97

Figure A.32: Average corrosion potentials with respect to SCE. Undamaged NX-SCR™ stainless steel clad bars, specimens 1-6 97

Figure A.33: Macrocell individual corrosion loss of undamaged NX-SCR™ stainless steel clad bars, specimens 1-6 98

Figure A.34: Macrocell individual corrosion potentials with respect to SCE. Uncapped NX-SCR™ stainless steel clad bars in pore solution with salt (anode), specimens 1-6..... 98

Figure A.35: Macrocell individual corrosion potentials with respect to SCE. Uncapped NX-SCR™ stainless steel clad bars in pore solution (cathode), specimens 1-6..... 99

Figure A.36: Average corrosion potentials with respect to SCE. Uncapped NX-SCR™ stainless steel clad bars, specimens 1-6 99

Figure A.37: Macrocell individual corrosion loss of uncapped NX-SCR™ stainless steel clad bars, specimens 1-6 100

Figure A.38: Macrocell individual corrosion potentials with respect to SCE. Bent NX-SCR™ stainless steel clad bars in pore solution with salt (anode), specimens 1-6..... 100

Figure A.39: Macrocell individual corrosion potentials with respect to SCE. Bent NX-SCR™ stainless steel clad bars in pore solution (cathode), specimens 1-6 101

Figure A.40: Average corrosion potentials with respect to SCE. Bent NX-SCR™ stainless steel clad bars, specimens 1-6 101

Figure A.41: Macrocell individual corrosion loss of bent NX-SCR™ stainless steel clad bars, specimens 1-6 102

Figure A.42: Macrocell individual corrosion potentials with respect to SCE. 0.83% damaged area NX-SCR™ stainless steel clad bars in pore solution with salt (anode), specimens 1-6..... 102

Figure A.43: Macrocell individual corrosion potentials with respect to SCE. 0.83% damaged area NX-SCR™ stainless steel clad bars in pore solution (cathode), specimens 1-6 103

Figure A.44: Average corrosion potentials with respect to SCE. 0.83% damaged area NX-SCR™ stainless steel clad bars, specimens 1-6..... 103

Figure A.45: Macrocell individual corrosion loss of 0.83% damaged area NX-SCR™ stainless steel clad bars, specimens 1-6 104

Figure A.46: Macrocell individual corrosion potentials with respect to SCE. Mixed NX-SCR™ stainless steel clad bars (anode/cathode) in pore solution with salt (anode), specimens 1-6 104

Figure A.47: Macrocell individual corrosion potentials with respect to SCE. Mixed NX-SCR™ stainless steel clad bars (anode/cathode) in pore solution (cathode), specimens 1-6 105

Figure A.48: Average anode corrosion potentials with respect to SCE. Mixed NX-SCR™ stainless steel clad bars (anode/cathode), specimens 1-6 105

Figure A.49: Average cathode corrosion potentials with respect to SCE. Mixed NX-SCR™ stainless steel clad bars (anode/cathode), specimens 1-6 106

Figure A.50: Macrocell individual corrosion loss of mixed NX-SCR™ stainless steel clad bars, specimens 1-6 106

Figure A.51: Macrocell individual corrosion loss of mixed NX-SCR™ stainless steel clad bars, specimens 1-6 (different scale) 107

Figure C.1: Southern Exposure corrosion rates – conventional steel, w/c = 0.45 110

Figure C.2: Southern Exposure corrosion losses – conventional steel, w/c = 0.45 110

Figure C.3: Southern Exposure mat-to-mat resistances – conventional steel, w/c = 0.45 .. 111

Figure C4: Southern Exposure corrosion potentials with respect to CSE – conventional steel, top mat, w/c = 0.45 111

Figure C5: Southern Exposure corrosion potentials with respect to CSE – conventional steel, bottom mat, w/c = 0.45 112

Figure C.6: Cracked beam corrosion rates – conventional steel, w/c = 0.45 112

Figure C.7: Cracked beam corrosion losses – conventional steel, w/c = 0.45 113

Figure C.8: Cracked beam mat-to-mat resistances – conventional steel, w/c = 0.45 113

Figure C.9: Cracked beam corrosion potentials with respect to CSE – conventional steel, top mat, w/c = 0.45 114

Figure C.10: Cracked beam corrosion potentials with respect to CSE – conventional steel, bottom mat, w/c = 0.45 114

Figure C.11: Southern Exposure corrosion rates (based on total area) – epoxy coated steel, w/c = 0.45 115

Figure C.12: Southern Exposure corrosion rates (based on exposed area) – epoxy coated steel, w/c = 0.45 115

Figure C.13: Southern Exposure corrosion losses (based on total area) – epoxy coated steel, w/c = 0.45 116

Figure C.14: Southern Exposure corrosion losses (based on exposed area) – epoxy coated steel 116

Figure C.15: Southern Exposure mat-to-mat resistances – epoxy coated steel, w/c = 0.45 117

Figure C.16: Southern Exposure corrosion potentials with respect to CSE – epoxy coated steel, top mat, w/c = 0.45 117

Figure C.17: Southern Exposure corrosion potentials with respect to CSE – epoxy coated steel, bottom mat, w/c = 0.45 118

Figure C.18: Cracked beam corrosion rates (based on total area) – epoxy coated steel, w/c = 0.45 118

Figure C.19: Cracked beam corrosion rates (based on exposed area) – epoxy coated steel, w/c = 0.45 119

Figure C.20: Cracked beam corrosion losses (based on total area) – epoxy coated steel, w/c = 0.45 119

Figure C.21: Cracked beam corrosion losses (based on exposed area) – epoxy coated steel, w/c = 0.45 120

Figure C.22: Cracked beam mat-to-mat resistances – epoxy coated steel, w/c = 0.45 120

Figure C.23: Cracked beam corrosion potentials with respect to CSE – epoxy coated steel, top mat, w/c = 0.45 121

Figure C.24: Cracked beam corrosion potentials with respect to CSE – epoxy coated steel, bottom mat, w/c = 0.45 121

Figure C.25: Southern Exposure corrosion rates– epoxy coated (no damage) steel, w/c = 0.45 122

Figure C.26: Southern Exposure corrosion losses – epoxy coated (no damage) steel, w/c = 0.45 122

Figure C.27: Southern Exposure mat-to-mat resistances – epoxy coated (no damage) steel, w/c = 0.45 123

Figure C.28: Southern Exposure corrosion potentials with respect to CSE – epoxy coated (no damage) steel, top mat, w/c = 0.45 123

Figure C.29: Southern Exposure corrosion potentials with respect to CSE – epoxy coated (no damage) steel, bottom mat, w/c = 0.45 124

Figure C.30: Cracked beam corrosion rates – epoxy coated steel, w/c = 0.45 124

Figure C.31: Cracked beam corrosion losses – epoxy coated steel, w/c = 0.45 125

Figure C.32: Cracked beam mat-to-mat resistances – epoxy coated steel, w/c = 0.45 125

Figure C.33: Cracked beam corrosion potentials with respect to CSE – epoxy coated steel, top mat, w/c = 0.45 126

Figure C.34: Cracked beam corrosion potentials with respect to CSE – epoxy coated steel, bottom mat, w/c = 0.45 126

Figure C.35: Southern Exposure corrosion rates – 2304 steel, w/c = 0.45 127

Figure C.36: Southern Exposure corrosion losses – 2304 steel, w/c = 0.45 127

Figure C.37: Southern Exposure mat-to-mat resistances – 2304 steel, w/c = 0.45 128

Figure C.38: Southern Exposure corrosion potentials with respect to CSE – 2304, top mat, w/c = 0.45 128

Figure C.39: Southern Exposure corrosion potentials with respect to CSE –2304, bottom mat, w/c = 0.45 129

Figure C.40: Cracked beam corrosion rates – 2304 steel, w/c = 0.45 129

Figure C.41: Cracked beam corrosion losses – 2304 steel, w/c = 0.45 130

Figure C.42: Cracked beam mat-to-mat resistances – 2304 steel, w/c = 0.45 130

Figure C.43: Cracked beam corrosion potentials with respect to CSE – 2304, top mat, w/c = 0.45 131

Figure C.44: Cracked beam corrosion potentials with respect to CSE – 2304, bottom mat, w/c = 0.45 131

Figure C.45: Southern Exposure corrosion rates – 2304 (top mat) / conventional steel (bottom mat), w/c = 0.45 132

Figure C.46: Southern Exposure corrosion losses – 2304 (top mat) / conventional steel (bottom mat), w/c = 0.45 132

Figure C.47: Southern Exposure mat-to-mat resistances – 2304 (top mat) / conventional steel (bottom mat), w/c = 0.45 133

Figure C.48: Southern Exposure corrosion potentials with respect to CSE – specimens with 2304 (top mat) / conventional steel (bottom mat), top mat potentials, w/c = 0.45 133

Figure C.49: Southern Exposure corrosion potentials with respect to CSE – specimens with 2304 (top mat) / conventional steel (bottom mat), bottom mat potentials, w/c = 0.45 134

Figure C.50: Southern Exposure corrosion rates – conventional steel (top mat) / 2304 (bottom mat), w/c = 0.45 134

Figure C.51: Southern Exposure corrosion losses – conventional steel (top mat) / 2304 (bottom mat), w/c = 0.45 135

Figure C.52: Southern Exposure mat-to-mat resistances – conventional steel (top mat) / 2304 (bottom mat), w/c = 0.45 135

Figure C.53: Southern Exposure corrosion potentials with respect to CSE – specimens with conventional steel (top mat) / 2304 (bottom mat), top mat potentials, w/c = 0.45 136

Figure C.54: Southern Exposure corrosion potentials with respect to CSE – specimens with conventional steel (top mat) / 2304 (bottom mat), bottom mat potentials, w/c = 0.45 136

Figure C.55: Southern Exposure corrosion rates (based on total area) – stainless steel clad (damaged), w/c = 0.45 137

Figure C.56: Southern Exposure corrosion rates (based on exposed area) – stainless steel clad (damaged), w/c = 0.45 137

Figure C.57: Southern Exposure corrosion losses (based on total area) – stainless steel clad (damaged), w/c = 0.45 138

Figure C.58: Southern Exposure corrosion losses (based on exposed area) – stainless steel clad (damaged), w/c = 0.45 138

Figure C.59: Southern Exposure mat-to-mat resistances – stainless steel clad (damaged), w/c = 0.45 139

Figure C.60: Southern Exposure corrosion potentials with respect to CSE – stainless steel clad (damaged), top mat, w/c = 0.45 139

Figure C.61: Southern Exposure corrosion potentials with respect to CSE – stainless steel clad (damaged), bottom mat, w/c = 0.45 140

Figure C.62: Southern Exposure corrosion rates – stainless steel clad, w/c = 0.45 140

Figure C.63: Southern Exposure corrosion losses – stainless steel clad, w/c = 0.45 141

Figure C.64: Southern Exposure mat-to-mat resistances – stainless steel clad, w/c = 0.45 141

Figure C.65: Southern Exposure corrosion potentials with respect to CSE – stainless steel clad, top mat, w/c = 0.45 142

Figure C.66: Southern Exposure corrosion potentials with respect to CSE – stainless steel clad, bottom mat, w/c = 0.45 142

Figure C.67: Cracked beam corrosion rates – stainless steel clad, w/c = 0.45 143

Figure C.68: Cracked beam corrosion losses – stainless steel clad, w/c = 0.45 143

Figure C.69: Cracked beam mat-to-mat resistances – stainless steel clad, w/c = 0.45 144

Figure C.70: Cracked beam corrosion potentials with respect to CSE – stainless steel clad, top mat, w/c = 0.45 144

Figure C.71: Cracked beam corrosion potentials with respect to CSE – stainless steel clad, bottom mat, w/c = 0.45 145

Figure C.72: Southern Exposure corrosion rates – stainless steel clad (180° bend), w/c = 0.45 145

Figure C.73: Southern Exposure corrosion losses – stainless steel clad (180° bend), w/c = 0.45 146

Figure C.74: Southern Exposure mat-to-mat resistances – stainless steel clad (180° bend), w/c = 0.45 146

Figure C.75: Southern Exposure corrosion potentials with respect to CSE – stainless steel clad (180° bend), top mat, w/c = 0.45 147

Figure C.76: Southern Exposure corrosion potentials with respect to CSE – stainless steel clad (180° bend), bottom mat, w/c = 0.45 147

Figure C.77: Southern Exposure corrosion rates – stainless steel clad (top mat) / conventional steel (bottom mat), w/c = 0.45 148

Figure C.78: Southern Exposure corrosion losses – stainless steel clad (top mat) / conventional steel (bottom mat), w/c = 0.45 148

Figure C.79: Southern Exposure mat-to-mat resistances – stainless steel clad (top mat) / conventional steel (bottom mat), w/c = 0.45 149

Figure C.80: Southern Exposure corrosion potentials with respect to CSE – stainless steel clad (top mat) / conventional steel (bottom mat), top mat, w/c = 0.45 149

Figure C.81: Southern Exposure corrosion potentials with respect to CSE – stainless steel clad (top mat) / conventional steel (bottom mat), bottom mat, w/c = 0.45 150

Figure C.82: Southern Exposure corrosion rates – conventional steel (top mat) / stainless steel clad (bottom mat), w/c = 0.45 150

Figure C.83: Southern Exposure corrosion losses – conventional steel (top mat) / stainless steel clad (bottom mat), w/c = 0.45 151

Figure C.84: Southern Exposure mat-to-mat resistances – conventional steel (top mat) / stainless steel clad (bottom mat), w/c = 0.45 151

Figure C.85: Southern Exposure corrosion potentials with respect to CSE – conventional steel (top mat) / stainless steel clad (bottom mat), top mat, w/c = 0.45 152

Figure C.86: Southern Exposure corrosion potentials with respect to CSE – conventional steel (top mat) / stainless steel clad (bottom mat), bottom mat, w/c = 0.45 152

1. INTRODUCTION

This report describes corrosion performance testing of 2304 duplex stainless steel and NX-SCR™ stainless steel clad reinforcement during the first year of the study. Performance tests include rapid macrocell tests, which are performed in accordance with ASTM A955, and bench-scale tests. The 2304 duplex stainless steel is evaluated in the as-received condition and after re-pickling. The NX-SCR™ stainless steel clad reinforcement is evaluated in the damaged, undamaged, and uncapped conditions. Performance is compared with that of epoxy-coated reinforcement in the damaged and undamaged conditions and conventional reinforcing steel. The results of the rapid macrocell tests and the first 31 weeks of bench-scale tests are described.

2. EXPERIMENTAL WORK

2.1 Materials

Tests were performed on 2304 duplex stainless steel bars in the as-received and re-pickled conditions and on NX-SCR™ stainless steel clad bars in the damaged, undamaged, and uncapped conditions, as well as on conventional steel reinforcement and on epoxy-coated reinforcement (ECR) in the damaged and undamaged conditions. The stainless steel cladding is Type 316L austenitic stainless steel with an average thickness of 19.1 mils (484 μm). The ECR coating is DuPont™ Nap-Gard® 7-2719 Epoxy Powder with an average thickness of 11.2 mils (284 μm). The thickness of the stainless steel cladding and epoxy coating were measured with a pull-off gage, per ASTM A775. The conventional steel and ECR bars are from the same heat of steel. The chemical compositions of the bars used for the study are listed in Table 1.

Table 1: Chemical compositions of steels (provided by manufacturer)

Material	C	Mn	P	S	Si	Cu	Cr	Ni	Mo	V	Co	Sn	Al	N	B
ECR and Conventional	0.39	1.18	0.01	0.037	0.23	0.31	0.16	0.15	0.045	0.002	0.001	0.012	0.002	-	-
2304	0.02	1.72	0.02	0.001	0.41	0.3	22.71	3.58	0.25	-	-	-	-	0.18	0.002
NX-SCR™ - cladding	0.018	1.37	0.034	0.003	0.37	-	16.87	10	2	-	-	-	-	0.058	-
NX-SCR™ core	0.34	1.04	0.014	0.026	0.25	-	-	-	-	-	-	-	-	-	-

All tests were performed on No. 5 (No. 16) bars, with the exception of the NX-SCR™ stainless steel clad bars, which, based on weight per unit length, had an average diameter of 0.673 in. (17.1 mm).

The stainless steel clad bars, conventional reinforcement, and ECR were inspected upon arrival and found to be in good condition. The 2304 bars arrived with a dark and mottled appearance, possibly due to incomplete pickling (Figure 1). As a result, macrocell tests were performed on the 2304 stainless steel bars in both the as-received condition and after re-pickling.

Figure 1: 2304 duplex stainless steel bars in the as-received (left) and re-pickled (right) conditions

Re-pickling was performed at the University of Kansas. The procedure consisted of submerging the bars in a solution of 25% nitric acid and 5% hydrofluoric acid for thirty minutes at room temperature (72° F, 22° C). The bars were then removed from the solution and rinsed thoroughly with distilled water, producing a bright, shiny surface on the metal.

To protect the exposed steel at the submerged ends of both the ECR and stainless steel clad specimens in the rapid macrocell tests, one end of each bar was covered with a protective cap. To apply the cap, 3M Scotchkote Liquid Epoxy Coating Patch Compound 323R was applied to the exposed ends and left to dry overnight. A second coat of the epoxy patch compound was then applied to the ends, and a 0.5-in. (12.5-mm) deep vinyl cap, half-filled with the epoxy, was placed on the end of the bar. One set of stainless steel clad specimens was tested without the use of the protective cap.

The coating on most ECR bars and the cladding on some of the NX-SCR^{TM} bars were penetrated using a 1/8-in. (3.2-mm) diameter four-flute drill bit to simulate damage that may occur in the field. The number and spacing of the drilled holes varied between the rapid macrocell specimens and bench-scale specimens.

For the rapid macrocell specimens, two holes were placed on each side of a bar, for a total of four holes, exposing 0.83% of the bar area. The holes were located approximately 1 in. (25.4 mm) from the bottom end of the bar with the second spaced 1 in. (25.4 mm) from the first hole. For the bench-scale specimens, damage varied based on steel type. Selected ECR specimens were damaged with 10 evenly spaced holes, exposing 0.5% of the bar area. Selected stainless steel clad specimens were damaged with 4 evenly spaced holes, exposing 0.2% of the bar area. Holes were drilled to a depth so as to expose the underlying conventional steel and, for the rapid macrocell specimens, located approximately 1.5 in. (38.1 mm) and 2.5 in. (63.5 mm) from the bottom end of the bar. The exact spacing of the holes varied slightly to avoid drilling at deformations, as shown in Figure 2.

Figure 2: Rapid macrocell specimens, ECR and NX-SCR^{TM} stainless steel clad damaged bars (0.83% damaged area)

2.2 RAPID MACROCELL TEST

2.2.1 Experimental Procedure

Six specimens for each of the series of specimens were tested in accordance with the rapid macrocell test outlined in Annexes A1 and A2 of ASTM 955/A955M-10 and illustrated in Figure 3, with the exception of undamaged ECR, mixed NX-SCR^{TM} stainless steel/conventional and mixed 2304 duplex stainless steel/conventional specimens for which three specimens were tested.

The bars used in rapid macrocell test are cut to a length of 5 in. (127 mm) and drilled and tapped at one end to accept a 0.5-in. (12.7-mm), 10-24 stainless steel machine screw. To remove any oil and surface contaminants introduced when machining the bars, conventional, stainless steel clad, and 2304 specimens are cleaned with acetone prior to testing. ECR bars are cleaned with soap and water. A length of 16-gauge insulated copper wire is attached to each bar with a machine screw. To prevent corrosion from occurring at the electrical connection, 3M Scotchkote Liquid Epoxy Coating Patch Compound 323R is used to thoroughly coat the tops of the bars. After the first coat of epoxy has dried overnight, a second coat is applied to ensure complete coverage.

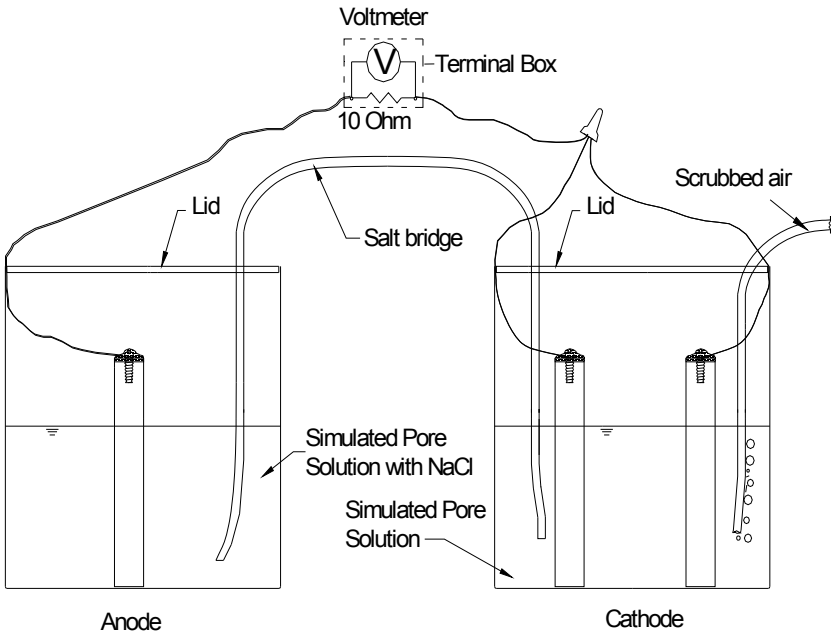

Figure 3: Rapid macrocell test

Extra precautions are taken when preparing the ECR specimens. To avoid coating damage where the bar is clamped in the lathe for drilling and tapping, the bars are cut to a length in excess of 5 in. (127 mm). The area that is damaged by the clamp is then removed, providing the 5-in. (127-mm) specimen with, at most, minimal damage to the epoxy coating. When selecting anode and cathode bars, the bars with minimal damage to the epoxy coating are used as cathode bars, while the bars with no damage are used as anode bars. Prior to testing, the ECR bars are inspected to ensure that no perforations in the coating, other than drilled holes, are present.

To prepare the bent stainless steel clad bars, the specimens are initially cut to a length of 18 in. (457 mm). The specimens are then bent to form a 180° bend around a 3.25-in. (82.6-mm) diameter pin. The excess length of bar is then removed with a band saw, providing a specimen that fits in the testing container. One end of the bent bar is drilled and tapped, thus allowing it to accept a machine screw for the electrical connection. The end that is to be electrically connected receives multiple coats of the epoxy patch compound, as described earlier. The other end of the

bar is fit with the protective capping system. The cap is then clipped with an alligator clamp and attached to a wire, which is used to stabilize the specimen in the container by securing the wire to the lid. A rapid macrocell test on a bent bar is shown in Figure 4.

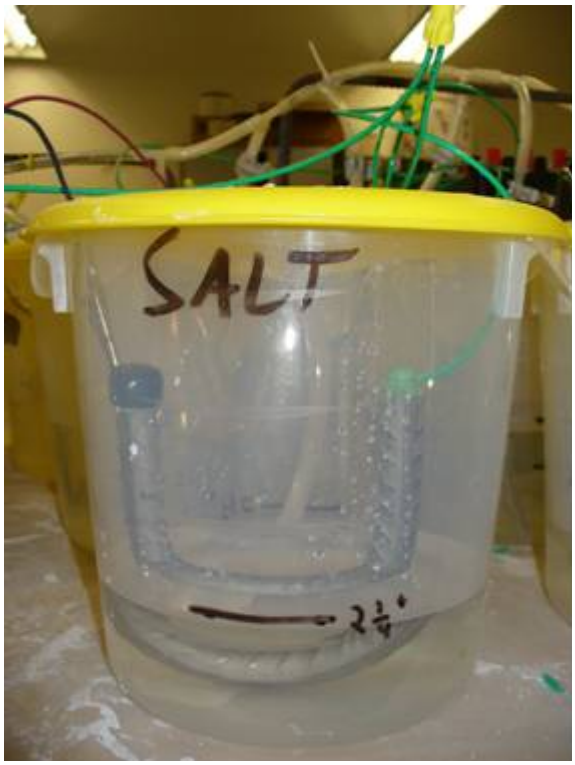

Figure 4: Macrocell test of a bent bar

2.2.2 Test Procedure

A single rapid macrocell test consists of an anode and a cathode, as shown in Figure 3. The cathode consists of two bars placed in a plastic container, which are submerged in simulated concrete pore solution. One liter of pore solution consists of 974.8 g of distilled water, 18.81 g of potassium hydroxide, and 17.87 g of sodium hydroxide. The solution has a pH of 13.9. Air, which is scrubbed to remove carbon dioxide, is bubbled into the cathode solution. The anode consists of a single bar submerged in the simulated concrete pore solution with 15 percent sodium chloride solution. The "salt" solution is prepared by adding 172.1 g of NaCl to one liter of pore solution. To limit the effects of carbonation, the solutions are changed every five weeks.

The anode and cathode are electrically connected across a 10-ohm resistor. An ionic connection is provided between the anode and cathode using a potassium chloride salt bridge (Figure 3).

In accordance with Annex A2 of ASTM 955, bars are submerged in the solution to a depth of 3 in. (76 mm), which exposes 6.20 in.^{2} (4000 mm^2) to the solution. In the case of the ECR and stainless steel clad bars that receive a protective cap, the solution depth is 3.5 in. (89 mm), which provides a nearly equal amount of exposed area as obtained for bars without a vinyl cap. The capped specimens submerged to a depth of 3.5 in. (89 mm) have roughly 4% less exposed area than the typical specimens submerged to a depth of 3 in. (76 mm). This small difference in exposed area is included in the expressions when calculating corrosion rates. The slightly larger diameter of the NX-SCR^{TM} stainless steel have an exposed area of 6.34 in.^{2} (4090 mm^2) when submerged with an exposed length of 3 in. (76 mm), as well. The bent stainless steel clad bars are placed in a solution to a depth of 2.25 in. (57 mm), which provides an exposed area of 12.7 in.^{2} (8194 mm^2). The exposed areas are used to calculate the corrosion rate, which is calculated based on the voltage drop measured across the 10-ohm resistor using Faraday's equation.

$$\text{Rate} = K \frac{V \cdot m}{n \cdot F \cdot D \cdot R \cdot A} \qquad (1)$$

where the Rate is given in μm/yr, and

K = conversion factor = $31.5 \cdot 10^4$ amp·μm ·sec/μA·cm·yr

V = measured voltage drop across resistor, millivolts

m = atomic weight of the metal (for iron, m = 55.8 g/g-atom)

n = number of ion equivalents exchanged (for iron, n = 2 equivalents)

F = Faraday's constant = 96485 coulombs/equivalent

D = density of the metal, g/cm^3 (for iron, D = 7.87 g/cm^3)

R = resistance of resistor, ohms = 10 ohms for the test

A = surface area of anode exposed to solution

In addition to determining the corrosion rate by taking voltage readings across the 10-ohm resistor, the corrosion potential is measured at both the anode and cathode using a saturated calomel electrode (SCE). Voltage drop and potential readings are taken daily for the first week and then weekly thereafter for a total of 15 weeks. Linear polarization resistance (LPR) tests are performed every 3 weeks, and data from LPR can be found in Appendix B.

For stainless steels to qualify in accordance with the rapid macrocell test guidelines listed in ASTM A955, the corrosion rate of the individual specimens may not exceed 0.50 μm/yr, and the average corrosion rate for all specimens in a series may not exceed 0.25 μm/yr. In some cases, the corrosion current may appear to be negative. This, however, does not indicate negative corrosion; rather it is caused by minor differences in the oxidation rate between the single anode bar and the two cathode bars.

2.3 BENCH-SCALE TESTS

2.3.1 General

The bench-scale tests in this study include Southern Exposure (SE) and cracked beam (CB) tests. These tests take approximately two years to complete. During this time, the specimens are exposed to alternate ponding and drying cycles with a 15 percent sodium chloride solution. The data collected allows for the monitoring of the corrosion rate via the voltage drop between top and bottom bars in the specimen. Mat-to-mat resistances and corrosion potentials are also recorded. In addition to these readings, the Southern Exposure specimens are sampled for chlorides at corrosion initiation.

2.3.2 Concrete Mix Design and Aggregate Properties

The concrete used in the study matches that used in bridge-decks. The materials used in the concrete mixtures were:

Water – Municipal tap water from the City of Lawrence.

Cement – Type I/II portland cement.

Coarse Aggregate – Crushed limestone from Fogle quarry. Nominal maximum size = 0.75 in. (19 mm), bulk specific gravity (SSD) = 2.58, absorption = 2.3%, unit weight = 95.9 lb/ft^3 (1536 kg/m^3).

Fine Aggregate – Kansas River sand. Bulk specific gravity (SSD) = 2.62, absorption = 0.8%, fineness modulus = 2.51.

Air-Entraining Agent – Daravair 1400, a saponified rosin-based air-entraining agent manufactured by W. R. Grace.

The concrete mixture proportions are detailed in Table 2. The mixture proportions for all test specimens have a 0.45 water-cement ratio, a target slump of 3 ± 0.5 in. (75 ± 13 mm), a target air content of 6 ± 1%, and a target 28-day compressive strength of 4000 psi.

Table 2: Mixture proportions for lab and field specimens based on SSD aggregate

Mix	**Water lb/yd^3 (kg/m^3)**	**Cement lb/yd^3 (kg/m^3)**	**Coarse Aggregate lb/yd^3 (kg/m^3)**	**Fine Aggregate lb/yd^3 (kg/m^3)**	**Air-entraining Agent oz/yd^3 (mL/m^3)**
Batch 1-7	269 (160)	598 (355)	1484 (880)	1435 (851)	2.33 (90)

2.4 SOUTHERN EXPOSURE (SE) AND CRACKED BEAM (CB) TESTS

2.4.1 Description

The Southern Exposure (SE) and cracked beam (CB) tests expose the test specimen to cyclic ponding and drying with a 15% sodium chloride (NaCl) solution. Southern Exposure specimens (Figure 5) are prisms measuring 12 × 12 × 7 in. (305 × 305 × 178 mm). No. 5 (No. 16) reinforcing bars are cast in the specimen in two mats and measure 12-in. (305-mm) in length. The top and bottom mats consist of two and four bars, respectively, each with 1-in. (25.4-mm) clear cover. The bars in each mat are centered horizontally within the prism and are spaced 2.5 in. (64 mm) from each other. The bars in the top and bottom mats are electrically connected though a terminal box across a 10-ohm resistor to allow for macrocell corrosion rate measurements. A 0.75-in. (19-mm) deep concrete dam is integrally cast with the specimen to contain the ponded salt solution. Southern Exposure tests represent conditions in uncracked reinforced concrete.

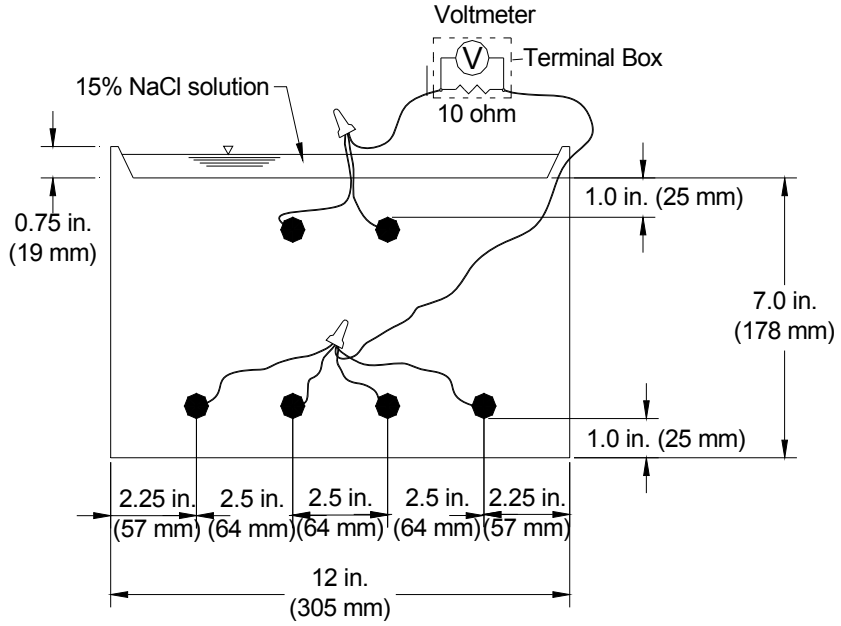

Figure 5: Southern Exposure (SE) specimen

Cracked beam specimens (Figure 6) are half the width of the Southern Exposure specimens, measuring 12 × 6 × 7 in. (305 × 152 × 178 mm). These specimens contain two mats of steel. The top mat consists of a single No. 5 (No. 16) bar; the bottom mat consists of two No. 5 (No. 16) bars. This test simulates exposure conditions in cracked concrete. Prior to casting, a 12-mil (0.3-mm) thick × 6-in. (152-mm) long stainless steel shim is affixed in the mold in direct contact with the top reinforcing bar. This results in direct infiltration of chlorides at the beginning of the test. The shim is removed about 12 hours after casting.

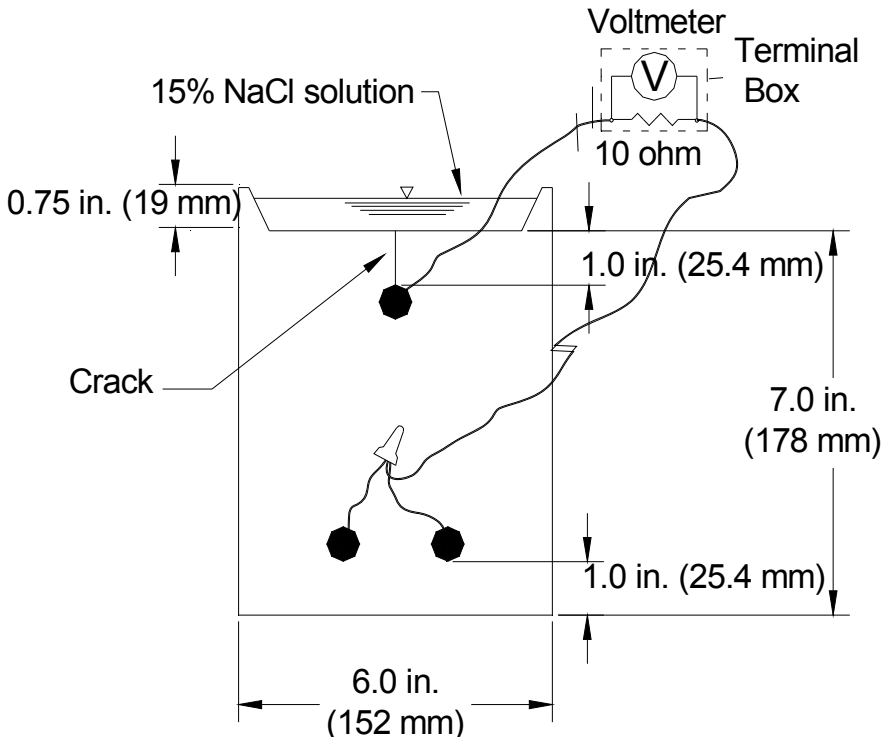

Figure 6: Cracked Beam (CB) specimen

2.4.2 Fabrication

Specimen fabrication for Southern Exposure and cracked beam specimens proceeds as follows:

1. Reinforcing bars are cut to 12 in. (305 mm) with a band saw.
2. Both ends of each bar are drilled and tapped to a 0.75-in. (19-mm) depth with 10-24 threading.
3. When appropriate, epoxy-coated and stainless steel clad bars are intentionally damaged, as previously described.
4. Epoxy-coated bars are cleaned with warm soapy water, rinsed, and allowed to dry. Conventional, stainless steel, and stainless steel clad bars are soaked in acetone for a minimum of two hours and scrubbed to remove any oil.
5. The forms are assembled, and the reinforcement is attached. Reinforcing bars with penetrations in the coating or cladding are aligned so that the holes face the top and bottom of the specimen. Forms and reinforcement are held in place using 1.25-in. (32-mm) long 10-24 threaded stainless steel machine screws.
6. Specimens are cast using concrete with the mixture proportions shown in Table 2. Specimens are filled in two layers, with each layer consolidated using a 0.75-in. (19-mm) diameter vibrator. The free surface of the concrete (the bottom of the specimen) is finished with a trowel.
7. Specimens are cured for 24 hours at room temperature. A plastic cover is used to minimize evaporation. Stainless steel shims are removed from CB specimens after 12 hours, when the concrete has set.
8. Formwork is removed after 24 hours.
9. Specimens are cured for an additional two days in a plastic bag containing deionized water, then air-cured for 25 days.

10. Prior to test initiation, wire leads are connected to the test bars using 10-24 × 0.5 in. (13 mm) stainless steel screws and a No. 10 stainless steel washer. Sewer Guard HBS 100 Epoxy is applied to the vertical sides of the specimens, while the top and bottom of the specimens are left uncoated.
11. The two mats of steel are connected to the terminal box. Specimens are left connected across the 10-ohm resistor, except when readings are taken (see the section on Corrosion Measurements). Specimens are placed on 2 × 2 studs to allow air flow under the specimens. Tests begin 28 days after casting.

2.4.3 Test Procedure

Southern Exposure and cracked beam test procedures involve alternate cycles of ponding and drying. The test begins with 12 weeks of ponding and drying, followed by 12 weeks of ponding, for a total of 24 weeks. This exposure regime is then repeated for the duration of testing. The tests conclude after 96 weeks. The procedures are described below.

Ponding and Drying Cycles:

A 15% NaCl solution is ponded on the surface of the specimens. SE specimens receive 600 mL of solution; CB specimens receive 300 mL of solution. The specimens are covered with plastic sheeting during ponding to minimize evaporation. Readings are taken on day 4. After all readings are completed, the specimens are vacuumed to remove the salt solution, and the heat tents are placed over the specimens. The heat tent keeps the specimens at 100 ± 3° F (38 ± 2° C) for three days. The tent is then removed, and the specimens are again ponded with the NaCl solution to start the second week of testing. Ponding and drying cycles continue for 12 weeks.

Ponding Cycle:

After 12 weeks of the ponding and drying, specimens are ponded for 12 weeks with the 15% NaCl solution and covered with plastic sheeting. The NaCl solution remains on the specimens throughout the 12 weeks at room temperature. Readings are continue to be taken on a weekly basis. Deionized water is added to maintain the desired solution depth on the specimens during this time. After 12 weeks, the specimens are again subjected to the weekly ponding and drying cycles. The two testing regimes are repeated for a total of 96 weeks.

2.4.4 Corrosion Measurements

The measurements taken weekly on the Southern Exposure and cracked beam specimens include macrocell voltage drop, mat-to-mat resistance, corrosion potential, and linear polarization resistance. The macrocell corrosion rate is determined from the voltage drop, based on Faraday's Law.

Following the measurement of the voltage drop, the electrical connection is interrupted to measure mat-to-mat resistance. This is completed using the ohmmeter. The specimens then remain disconnected for a minimum of two hours before measuring corrosion potentials, mat-to-mat resistance and performing linear polarization resistance (LPR) readings. Potentials and LPR are measured with respect to a saturated calomel electrode. After these readings are taken, the mats are then reconnected using the switch on the terminal box.

The corrosion rate is calculated based on the voltage drop across the 10-ohm resistor using Faraday's equation [Eq. (1)].

2.4.5 Chloride Sampling for SE Specimens

Upon the initiation of corrosion, Southern Exposure specimens are sampled for chlorides at the level of the top mat of steel. Cracked beam specimens are not sampled for chlorides, because the simulated crack shim allows for direct infiltration of the salt solution. Corrosion initiation is marked by voltage drops that signify macrocell corrosion rates above 0.3 μm/yr and top-mat corrosion potentials more negative than –0.275 V with respect to a saturated calomel electrode, as per ASTM C876.

2.4.6 Chloride Sampling Procedure

Chloride sampling is performed after all corrosion measurements are taken for a SE specimen. Prior to sampling, the specimen is rinsed on all four sides with tap water and again rinsed with deionized water. After drying, the specimens are marked for drilling in line with the top of the top mat of steel (Figure 7). Samples are obtained from the sides of the specimen, perpendicular to the mat of steel, with a 0.25-in. (6.4-mm) masonry drill bit. Three or five samples are taken from each side of the specimen for a total of six or ten samples. Sample sites are randomly chosen along the side of the specimen, with the exception that no samples are taken within 1.5 in. (38 mm) of the edge of the specimen.

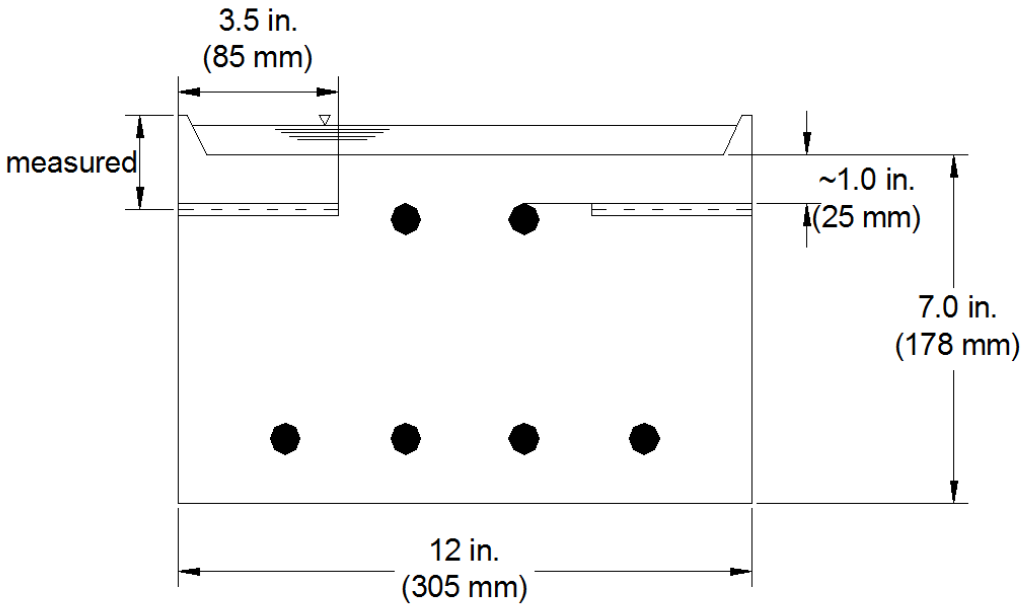

Figure 7: Southern Exposure chloride sampling.

For each sample site, a 0.5-in. (12.7-mm) deep hole is initially drilled. The resulting powder is then removed and discarded. The drill bit is then rinsed, reinserted, and used to penetrate to a depth of 3.5 in. (89 mm). This sample is collected in a plastic bag and labeled for analysis. Each sample provides approximately four grams of material. The drill bit is rinsed with reverse osmosis filtered water between specimens. The holes left from drilling are filled with clay, and the specimen is reconnected for continued testing.

2.4.7 Chloride Analysis

Concrete samples are analyzed for water-soluble chloride content using Procedure A of AASHTO T 260-94, "Standard Method of Test for Sampling and Testing for Chloride Ion in Concrete and Concrete Raw Materials." Each chloride sample is boiled in reverse osmosis water to free any water-soluble chlorides. Solutions rest for 24 to 28 hours after boiling and are then

filtered. The solution is acidified with nitric acid and then titrated with silver nitrate ($AgNO_3$). The potential with respect to a chloride sensitive electrode is measured throughout titration. For an incremental addition of silver nitrate, the change in potential with respect to each endpoint is indicated by the inflection point of the potential-volume curve. This point is indicated by the greatest change in potential for a given incremental addition of silver nitrate. This procedure gives the chloride concentration in terms of percent chloride by mass of sample. In this study, values are presented in lb/yd^3 (kg/m^3) by multiplying by the unit weight of concrete, taken as 3786 lb/yd^3 (2246 kg/m^3).

2.5 TEST EQUIPMENT

The following materials and equipment are used for the rapid macrocell and bench-scale tests.

Wire – The anode and cathode in rapid macrocell test and top and bottom mats of steel in the bench-scale tests are connected to a terminal box using 16-gauge multi-strand copper wire.

Terminal Box – To provide an electrical connection between the bars, each specimen is connected to an individual station in the terminal box. The terminal box allows the bars to be connected across a 10-ohm resistor. Internal box connections are made using solid 22-gauge copper wire. All connections are housed within the terminal box to protect the connections from unintentional salt exposure. This arrangement allows the voltage drop across the 10-ohm resistor to be measured. A switch is provided to interrupt the connection between the two bars to obtain corrosion potential, linear polarization

resistance measurements, and in the case of bench-scale specimens, mat-to-mat resistance.

Voltmeter – An Agilent model 34401A nanovoltmeter is used to measure voltage drop and corrosion potential.

Ohmmeter – An Agilent 4338B milliohmmeter is used to measure mat-to-mat resistance of SE and CB specimens.

Reference Electrode – A saturated calomel electrode (SCE) is used for corrosion potential measurements.

Epoxy – Sewer Guard HBS 100 Epoxy, manufactured by BASF, is used on the sides of the specimen to confine the chlorides within the specimen and to prevent corrosion of electrical connections.

Epoxy Patch – Scotchkote Liquid Epoxy Coating Patch Compound 323R, manufactured by 3M, is used to prevent corrosion of the specimen electrical connections and also to apply the protective cap to the bottom of the rapid macrocell specimens.

Stainless Steel Screws/Washers – Used to hold reinforcement in place in the formwork and to connect wires to specimens during testing. Described further in the section on Fabrication.

Wet/Dry Vacuum – A wet/dry vacuum is used to remove the salt solution from the bench-scale specimens, as described in the section on Test Procedure.

Potentiostat and Measuring System– A PC4/750 Potentiostat is used in obtaining Linear Polarization Resistance readings. The potentiostat forces the specimen away from equilibrium potential and a DC105 computer-controlled corrosion measurement system measures the resulting change in current.

Heating Tent – Heating tents are used to expose bench-scale specimens to a temperature of 100 ± 3° F (38 ± 2° C) during drying. A schematic is shown in Figure 8. The tents are 8 ft (2.44 m) long by 4 ft (1.22 m) wide by 3.5 ft (1.07 m) high. The faces and roofs of the tents are fabricated using 0.75-in. (19-mm) plywood with six 2 x 4 studs bracing the tent. Two sheets of plastic sheeting cover the space between the studs. Three 250-watt heat lamps are spaced along the inside roof of the tent to provide heat. The lamps are 1.5 ft (0.45 m) above the surface of the bench-scale specimens. Temperature is controlled with a thermostat.

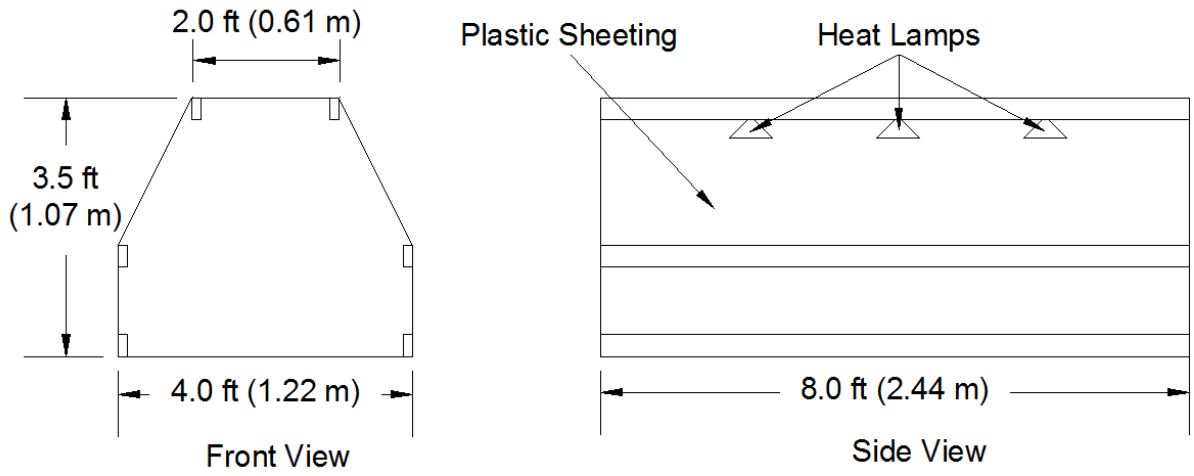

Figure 8: Heat tent dimensions.

Formwork – The formwork for the bench-scale specimens is constructed using 0.75-in. (19-mm) plywood, sealed with polyurethane. The forms consist of four face pieces and a base. The specimens are cast upside-down. The formwork has tapered inserts centered and affixed to the base to create the concrete dam used to pond the solution on the specimen. SE formwork inserts measure 10.5 × 10.5 × 0.75 in. (267 × 267 × 19 mm), and CB formwork inserts measure 4.5 ×

10.5 × 0.75 in. (114 × 267 × 19 mm) at their widest dimensions. CB forms also contain a slot centered and cut in the tapered insert to accommodate the 12-mil (0.3-mm) shim. Holes are drilled on two opposing faces to allow for the reinforcement to be held in place during casting. The faces and base are held together using 10-24 stainless steel machine screws that connect to threaded inserts in the sides of the forms. Prior to placement of the reinforcement and casting of the concrete, the interior surfaces of the forms are coated with mineral oil and the metal shim is affixed for the CB specimens.

3. TEST PROGRAM

Rapid macrocell tests were performed on six specimens of each type, with the exception of the undamaged ECR, mixed NX-SCR™ stainless steel clad/conventional and mixed 2304 duplex stainless steel/conventional specimens, for which tests were run on three specimens, as shown in Table 3, which includes the specimen designations used for the study (Conv., ECR, ECR-ND, 2304, 2304-p, SSClad, SSClad-NC, SSClad-4h, 2304/Conv., Conv./2304, SSClad/Conv., and Conv./SSClad). An additional mixed stainless steel clad/conventional specimen was tested, as one specimen demonstrated possibly errant results.

Bench-scale tests (also shown in Table 3) were performed on six specimens of each type for both Southern Exposure and cracked beam tests, with the exception of undamaged ECR, mixed NX-SCR™ stainless steel/conventional and mixed 2304 duplex stainless steel/conventional specimens, for which tests were run on three specimens. This distribution of specimens among separate batches was designed to minimize the effect of differences in concrete properties for the different types of steel.

The casting schedule for the bench-scale specimens, summarized in Table 4, was established to reduce possible effects of variations in concrete properties from batch to batch. One specimen of each type, therefore, was cast in each batch with the exception of the ECR-ND specimens, which were cast in the first three batches, and the mixed specimens, Conv./2304, 2304/Conv., Conv./SSClad, and SSClad/Conv., which were to be cast in every other batch. The mixed specimens were not included in some batches, however, requiring additional specimens to be cast in Batch 7.

The concrete mixture, as mentioned earlier, had a 0.45 water-cement ratio, a target slump of 3 ± 0.5 in. (76 ± 13 mm), a target air content of 6 ± 1%, and a target 28-day compressive strength of 4000 psi (27.6 MPa). The measured slump ranged between 1.75 in. (44.45 mm) and 6.5 in. (165 mm), with an average slump of 3.9 in. (99 mm). The measured air content ranged from 5.4% to 6.1%, with an average air content of 5.8%. At 28 days, the compressive strengths ranged from 3900 to 5160 psi (26.9 to 35.6 MPa), with an average 28-day compressive strength of 4650 psi (32.0 MPa). Table 5 summarizes the resulting concrete properties.

Table 3: Test Program – number of test specimens

Test	Macrocell		Southern Exposure[a]		Cracked Beam[a]
System	Straight Bar	Bent Bar	Straight Bar	Bent Bar	Straight Bar
Conventional reinforcement (Conv.)	6	--	6	--	6
ECR (ECR and ECR-ND) [b]	9	--	9	--	9
2304 stainless steel (2304)	6	--	6	--	6
Repickled 2304 stainless steel (2304-p) [c]	6	--	--	--	--
2304 stainless steel/conventional steel (2304/Conv.) [d]	3	--	3	--	--
Conv./2304 stainless steel (Conv./2304) [d]	3	--	3	--	--
NX-SCR™ stainless steel clad (SSClad)	6	6	6	6	6
Damaged NX-SCR™ stainless steel clad (SSClad-4h) [e]	6	--	6	--	--
NX-SCR™ without a cap at the end of the bar (SSClad-NC)	6	--	--	--	--
NX-SCR™/conventional steel (SSClad/Conv.) [d]	4	--	5	--	--
Conventional/NX-SCR™ (Conv./SSClad) [d]	3	--	3	--	--

[a] Water cement ratio = 0.45. Epoxy-coated bars have ten 1/8-in. (3-mm) diameter holes in coating.

[b] For ECR bars, three specimens with undamaged coating (ECR-ND), six specimens with four (macrocell) or ten (Southern Exposure) 1/8-in. (3-mm) diameter holes in coating (ECR).

[c] 2304-p stainless steel designates 2304 steel that was pickled a second time at the University of Kansas

[d] Mixed steel specimen titles are written with the first steel as the anode and section steel as the cathode, i.e. anode/cathode

[e] stainless steel clad reinforcement with four 1/8-in. (3-mm) diameter holes through the cladding

Table 4: Casting schedule

Steel Type[a]	Batch 1	Batch 2	Batch 3	Batch 4	Batch 5	Batch 6	Batch 7
Conv.	1	1	1	1[b]	1	1	1
ECR-10d	1	1	1	1	1	1	-
ECR-ND	1	1	1	-	-	-	-
2304	1	1	1	1	1	1	-
SSClad-4h	1	1	1	1	1	1	1[c]
SSClad-ND	1	1	1	1	1	1	-
SSClad-b	1	1	1	1	1	1	-
Conv./2304	-	1	1	1[b]	1[b]	1[b]	1
2304/Conv.	1	-	-	-	-	-	2
Conv./SSClad	1	-	-	-	-	-	2
SSClad/Conv.	-	1	1	1	1[c]	1[c]	-

[a] Conv. = conventional reinforcement, ECR = epoxy-coated reinforcement with ten 1/8-in. diameter holes through the epoxy, ECR-ND = undamaged ECR, 2304 = 2304 stainless steel, SSClad-4h = NX-SCR™ stainless steel clad reinforcement with four 0.125-in. diameter holes through the cladding, SSClad = undamaged NX-SCR™ stainless steel clad reinforcement, SSClad-b = bent NX-SCR™ stainless steel clad reinforcement. For mixed specimens, the reinforcement in the top mat is listed first.
[b] Corrosion observe at electrical connection – specimen taken out of testing
[c] Extra specimens
"-" = No specimen cast in this batch.

Table 5: Concrete properties per batch

	Batch 1	Batch 2	Batch 3	Batch 4	Batch 5	Batch 6	Batch 7
Casting Date:	12/3/2010	12/10/2010	12/17/2010	12/24/2010	1/4/2011	1/10/2011	4/18/2011
Slump (in.)	2.75	3	2	1.75	5.25	6.5	6
Temp. (^{o}F)	53	63	60	64	55	45	65
Air content (%)	5.4	5.5	6.0	5.8	6.0	5.9	6.1
Unit weight (lb/ft^3)	143.9	144.4	142.2	142.7	143.9	142.6	143.3
Strength (psi)							
7 day	3880	3560	3780	3680	3400	3290	3340
28 day	4990 4770 4950	4370 4580 5080	4850 4850 4830	4910 4950 5160	4290 4470 4810	4200 4460 4440	4400 4340 3900
Avg. 28 day	4900	4680	4840	5010	4520	4370	4210

Note: 1 in. = 25.4 mm, Temp. in ^{o}C = 5/9 (Temp. in ^{o}F – 32), 1 lb/ft^3 = 16.02 kg/m^3

4. RESULTS

4.1 Rapid Macrocell Tests

The rapid macrocell tests are complete, and the specimens have been autopsied. Individual corrosion losses for macrocell specimens are listed in Table 6. Plots showing individual corrosion rate are presented in Appendix A. Some specimens listed in the table show negative losses. The negative values can result from corrosion occurring at the location of the electrical connection or can be caused by minor differences in the oxidation rates of the single anode bar and two cathode bars. Upon completion of the test, all specimens were autopsied and no corrosion at the electrical connection was found. The negative readings, therefore, are likely caused by current drift due to differences in oxidation rates between the single anode bar and the two cathode bars and do not actually indicate "negative" corrosion.

Conventional steel displays the greatest corrosion loss, with values ranging between 6.21 and 12.4 μm and an average corrosion loss of 10.9 μm (Table 6). Corrosion losses for damaged ECR based on total area of the bar range from 0.037 μm to 0.244 μm, with an average of 0.107 μm. Corrosion losses for NX-SCR^{TM} stainless steel clad reinforcement with four 1/8-in. (3.2-mm) holes through the cladding range from –0.005 to 0.803 μm, with an average of 0.195 μm. Conventional steel with 2304 stainless steel as the cathode (Conv./2304) demonstrates corrosion losses very similar to conventional steel alone, with a mean corrosion loss of 10.4 μm. Also, conventional specimens with stainless steel clad bars as the cathode shows relatively high corrosion losses, with an average of 4.63 μm. Both of the "mixed" specimen sets with conventional steel at the cathode (2304/Conv. and SSClad/Conv.) show corrosion losses significantly below those for the mixed specimen sets with conventional steel as the anode but higher than the values recorded for specimens with 2304 stainless steel clad bars at both the

anode and the cathode suggested the possibility of a galvanic effect due to the combination of the stainless steels with conventional steel. To date, no galvanic effects have been apparent in the bench-scale tests, as will be described below. The rest of the specimens demonstrate minimal corrosion losses.

Table 6: Corrosion losses at 15 weeks based on total area for macrocell specimens

System[a]	Specimen							
	1	2	3	4	5	6	Mean	Standard deviation
	Corrosion Loss (µm)							
Conv.	9.09	12.4	10.9	15.5	6.21	11.1	10.9	3.12
ECR	0.072	0.058	0.104	0.037	0.127	0.244	0.107	0.0744
ECR-ND	0	0	-0.010	-	-	-	-0.0033	0.00577
2304	0.099	-0.101	0.008	-0.092	-0.018	-0.200	-0.0507	0.103
2304-p	-0.012	-0.025	-0.035	-0.030	-0.031	-0.007	-0.0233	0.0113
2304/Conv.	0.058	-0.066	0.490	-	-	-	0.161	0.292
Conv./2304	10.9	9.61	10.8	-	-	-	10.4	0.697
SSClad-4h	0.163	0.055	0.803	0.105	0.050	-0.005	0.195	0.303
SSClad	-0.028	-0.029	-0.076	-0.052	-0.004	0.063*	-0.021	0.0478
SSClad-b	-0.013	-0.096	-0.067	-0.066	-0.038	-0.044	-0.054	0.0289
SSClad/Conv.	0.172	1.11	0.011	0.445	-	-	0.435	0.487
Conv./SSClad	4.88	4.69	4.35	-	-	-	4.63	0.268

[a] Conv. = conventional reinforcement, ECR = epoxy-coated reinforcement with four 1/8-in. (3.2-mm) diameter holes through the epoxy, ECR-ND= undamaged ECR, 2304 = 2304 stainless steel, 2304-p = re-pickled 2304 stainless steel, SSClad-4h = stainless steel clad reinforcement with four 1/8-in. (3.2-mm) diameter holes through the cladding, SSClad = undamaged stainless steel clad reinforcement, SSClad-b = bent stainless steel clad reinforcement.
For mixed specimens, the reinforcement on the top mat is listed first.
"-" = No specimen tested in this set.
*Specimen exhibited corrosion at electrical connection.

`

Figures 9 and 10 show the average corrosion loss based on total area for the control specimens, conventional, ECR, and undamaged ECR rapid macrocell specimens, Conventional steel exhibits a corrosion loss of 10.9 µm. The ECR specimens exhibit average corrosion losses of 0.107 µm, while undamaged ECR exhibits no significant losses. Individual corrosion rate data

supports these findings, with conventional steel exhibiting very high corrosion rates and ECR and undamaged ECR exhibiting much lower corrosion rates (Appendix A).

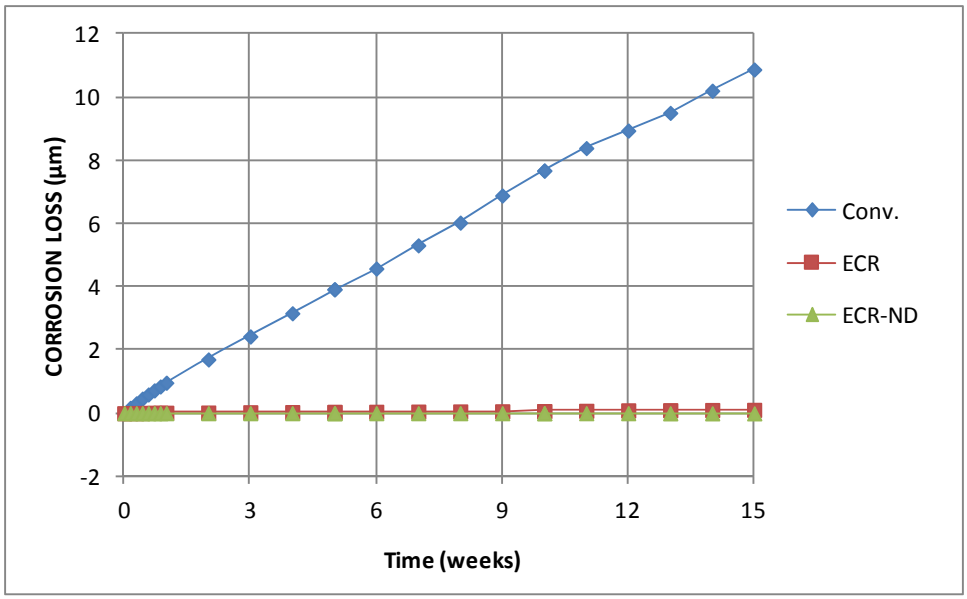

Figure 9: Average corrosion losses based on total area for conventional, ECR, and undamaged ECR rapid macrocell specimens

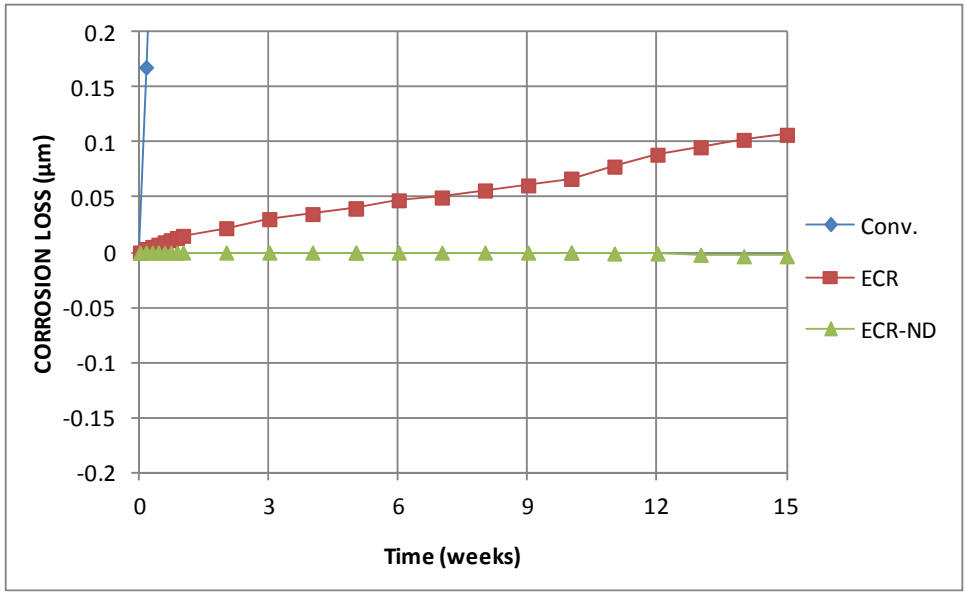

+

Figure 10: Average corrosion losses based on total area for conventional, ECR, and undamaged ECR rapid macrocell specimens (different scale)

Figures 11 and 12 show the corrosion losses based on total area for conventional, 2304 stainless steel, re-pickled 2304 stainless steel, and mixed 2304/Conv. and Conv./2304 stainless

steel rapid macrocell specimens. The Conv. and Conv./2304 stainless steel specimens exhibit relatively high corrosion losses of about 11 and 10 µm, respectively (Figure 11). As shown in Figure 12, the 2304 and 2304-p rapid macrocell specimens exhibit slightly negative losses, which is most likely due to the different oxidation rates of the anode and cathode bars, as discussed earlier. The mixed 2304/Conv. specimens exhibit minimal losses until week 12 with an average loss of about 0.15 µm at week 15. This increase in average corrosion loss is due to one specimen, which exhibited significant increases in corrosion rate at week 12 due to corrosion staining, as will be demonstrated later in this section.

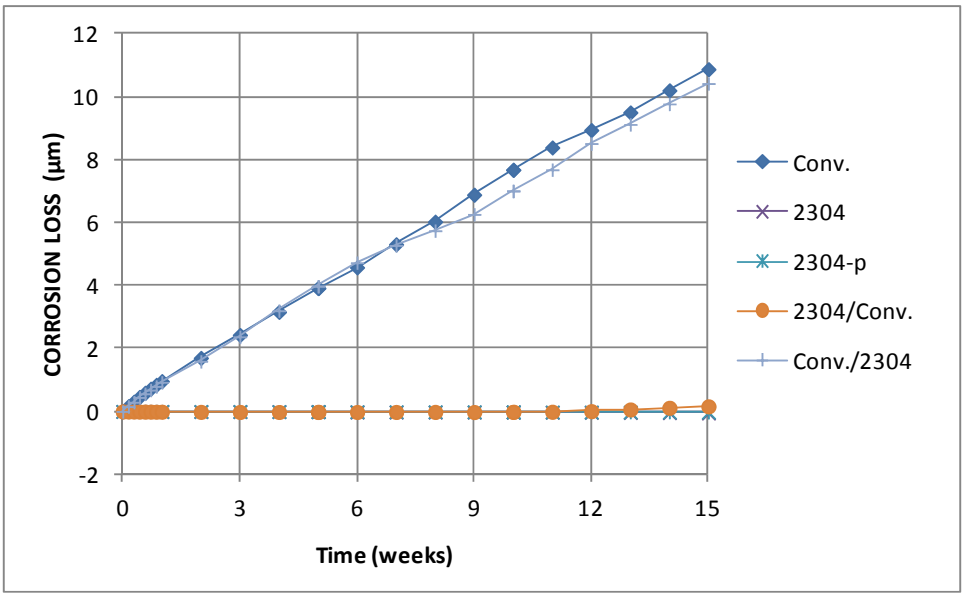

Figure 11: Average corrosion losses based on total area for conventional, 2304, 2304-p, mixed 2304/conventional, and mixed conventional/2304 rapid macrocell specimens

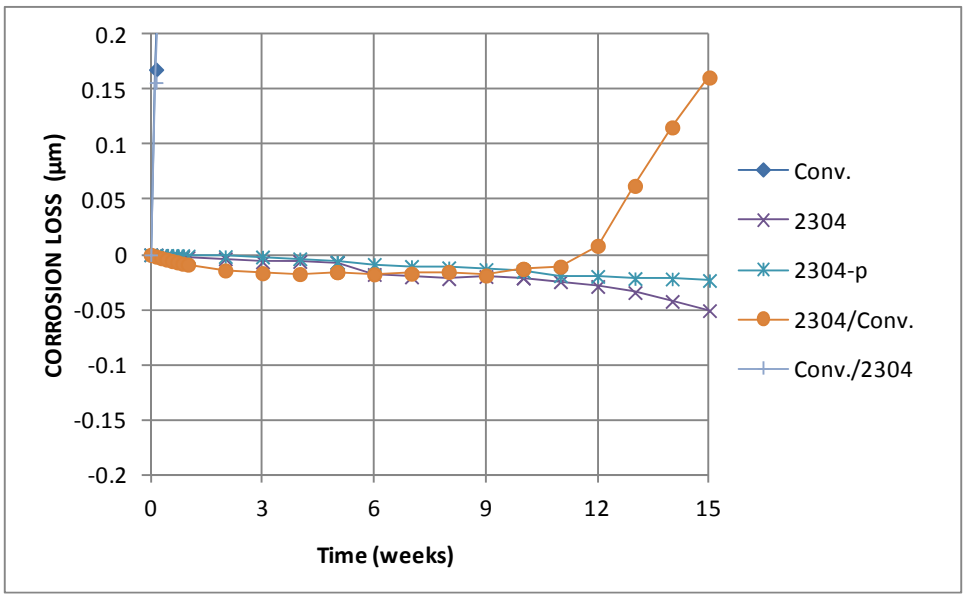

Figure 12: Average corrosion losses based on total area for conventional, 2304, 2304-p, mixed 2304/conventional and mixed conventional/2304 rapid macrocell specimens (different scale)

Figures 13 and 14 show the corrosion losses based on total area for conventional, undamaged stainless steel clad, damaged stainless steel clad, uncapped stainless steel clad, bent stainless steel clad, and mixed stainless steel clad/conventional specimens. The mixed Conv./SSClad specimens exhibit roughly half of the corrosion losses of conventional steel (Conv.), or 4.6 µm, over the course of the 15 week test (Figure 13). The uncapped stainless steel clad (SSClad-NC) specimens exhibit the highest losses of the specimens with stainless steel clad bars at the anode, with an average corrosion loss of 1.0 µm. The other specimens, which include SSClad, SSclad-4h, SSClad-b, and mixed SSClad/Conv., exhibit average corrosion losses under 0.5 µm (Figure 14). The undamaged stainless steel clad and bent stainless steel clad reinforcement specimens exhibit slightly negative corrosion losses. Damaged stainless steel clad reinforcement exhibits average corrosion losses of 0.20 µm, which is roughly half of the 0.42 µm loss recorded for the mixed SSClad/Conv. specimens.

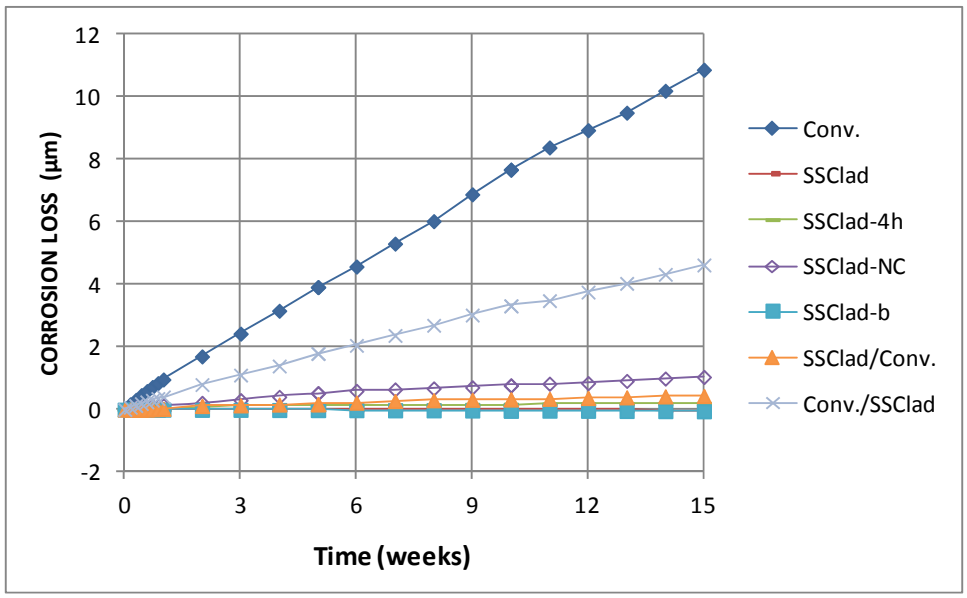

Figure 13: Average corrosion losses based on total area for conventional, stainless steel clad, damaged stainless steel clad, uncapped stainless steel clad, bent stainless steel clad, mixed stainless steel clad/conventional, and mixed conventional/stainless steel clad rapid macrocell specimens

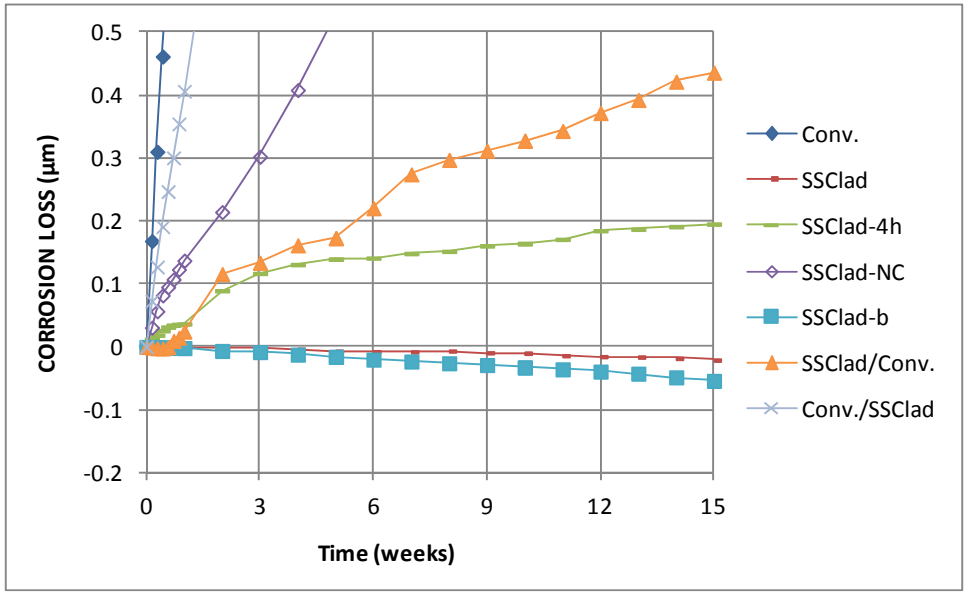

Figure 14: Average corrosion losses based on total area for conventional, stainless steel clad, damaged stainless steel clad, uncapped stainless steel clad, bent stainless steel clad, mixed stainless steel clad/conventional, and mixed conventional/stainless steel clad rapid macrocell specimens (different scale)

4.1.1 Control Specimens

The control specimens include conventional steel (Conv.), epoxy-coated reinforcement with 1/8-in. (3.2 mm) diameter holes through the epoxy (ECR), and undamaged epoxy-coated reinforcement (ECR-ND). As stated earlier, all specimens tested in the control group are from the same heat of steel. Figures 15 and 16 show the average corrosion rates of the control group. As shown in Figure 15, the conventional steel specimens exhibit an average corrosion rate of about 60 μm/yr at the beginning of the test, which drops, with some variations, to about 40 μm/yr for the duration of the test. The ECR specimens exhibit an average corrosion rate of about 1.2 μm/yr at the beginning of the test, dropping to about 0.3 μm/yr for the duration of the test (Figure 16). ECR-ND demonstrates an average corrosion rate of basically zero for the entire test, with a slight negative average corrosion rate from week 10 until the end of the test (Figure 16). For all control specimens, individual corrosion rates, individual/average corrosion potentials, and individual corrosion losses are found in Appendix A. The ECR-ND bars were autopsied at the end of the test. No signs of corrosion were observed on any ECR-ND specimen. The slight negative corrosion readings may be due to a small amount of current drift between the anodes and the cathodes.

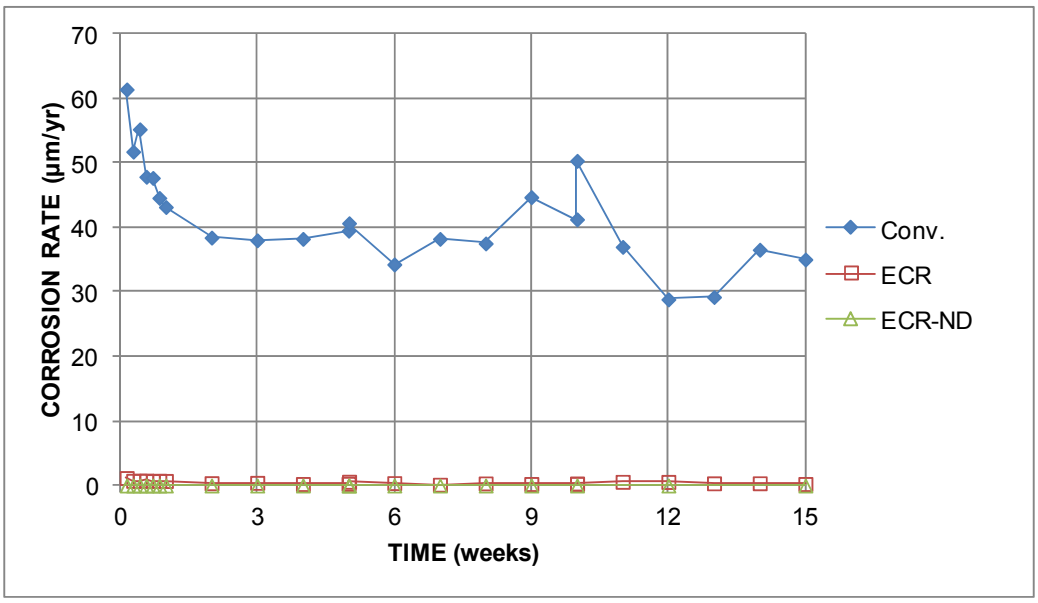

Figure 15: Average corrosion rates of conventional, ECR, and undamaged ECR specimens.

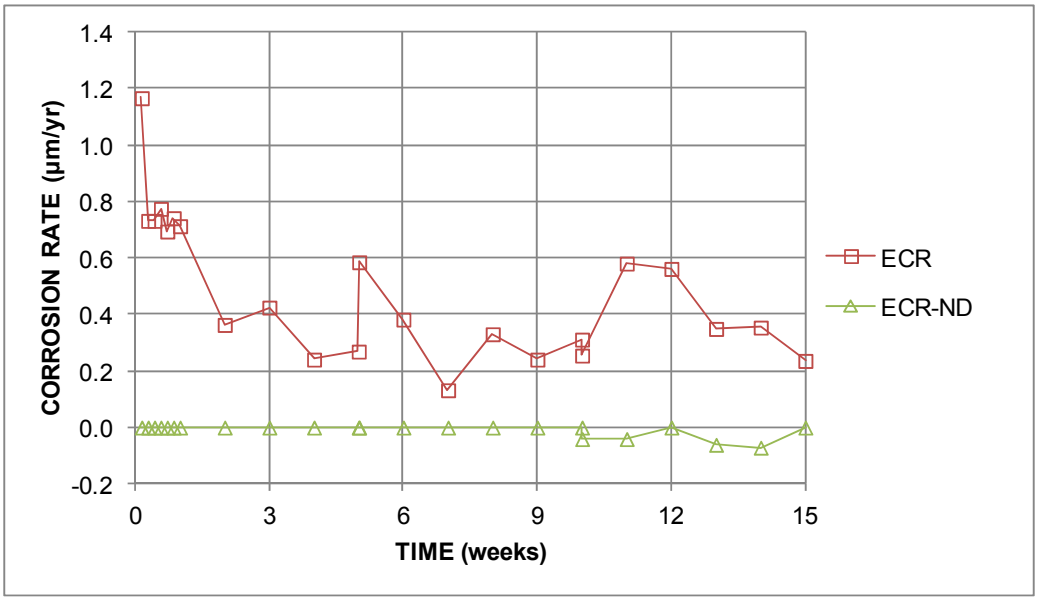

Figure 16: Average corrosion rates of ECR and undamaged ECR specimens.

4.1.2 2304 Stainless Steel

The average corrosion rates for the specimens containing 2304 stainless steel are shown in Figures 17 and 18. The rates for the conventional, ECR, and ECR-ND specimens are also plotted for comparison. The average corrosion rate of all stainless steel specimen sets must be below +0.25 µm/yr for the steel to qualify under the provisions of ASTM A955. For all 2304

specimens, individual/average corrosion potentials, and individual corrosion losses are found in Appendix A.

The behavior of the mixed Conv./2304 specimens is similar to that of the Conv. specimens and demonstrate average corrosion rates between 25 and 60 µm/yr throughout the test. The mixed 2304/Conv. specimens exhibit an average corrosion rate between –0.6 and 3.0 µm/yr. The 2304/Conv. specimens exhibit average corrosion rates that are in excess of the +0.25 µm/yr threshold specified in ASTM A955, although mixed-steel tests are not required by ASTM A955. As shown in Figure 18, the average corrosion rates of the 2304 and 2304-p specimens are nearly equal to that of the ECR-ND specimens. The 2304 and 2304-p specimens exhibit average corrosion rates of less than +0.25 µm/yr throughout the 15-week test, satisfying the requirement in ASTM A955.

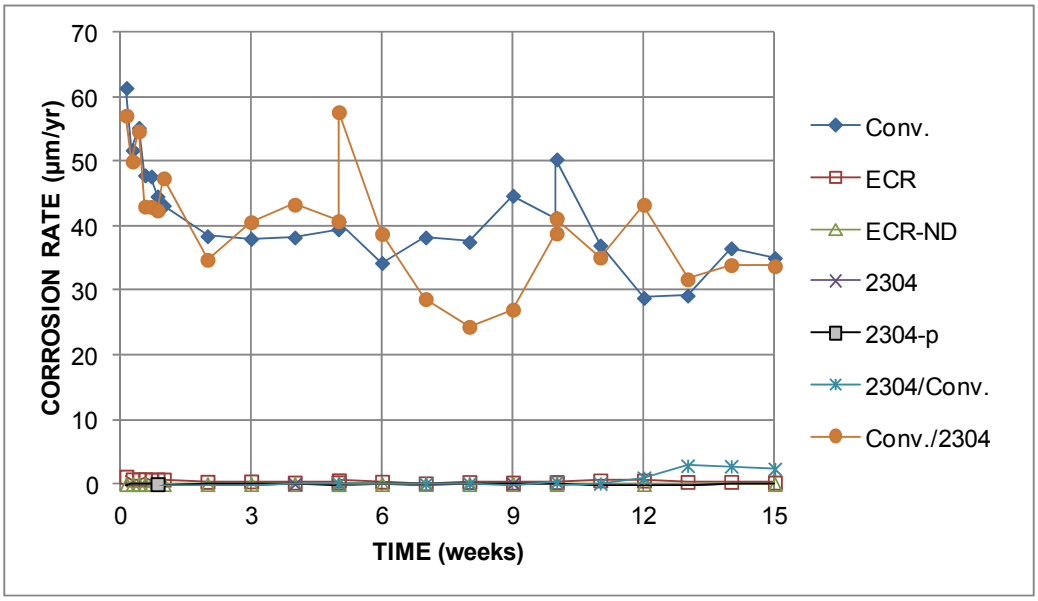

Figure 17: Macrocell average corrosion rates of conventional, ECR, ECR-ND, 2304, 2304-p, mixed 2304/conventional, and mixed conventional/2304 rapid macrocell specimens, specimens 1-6.

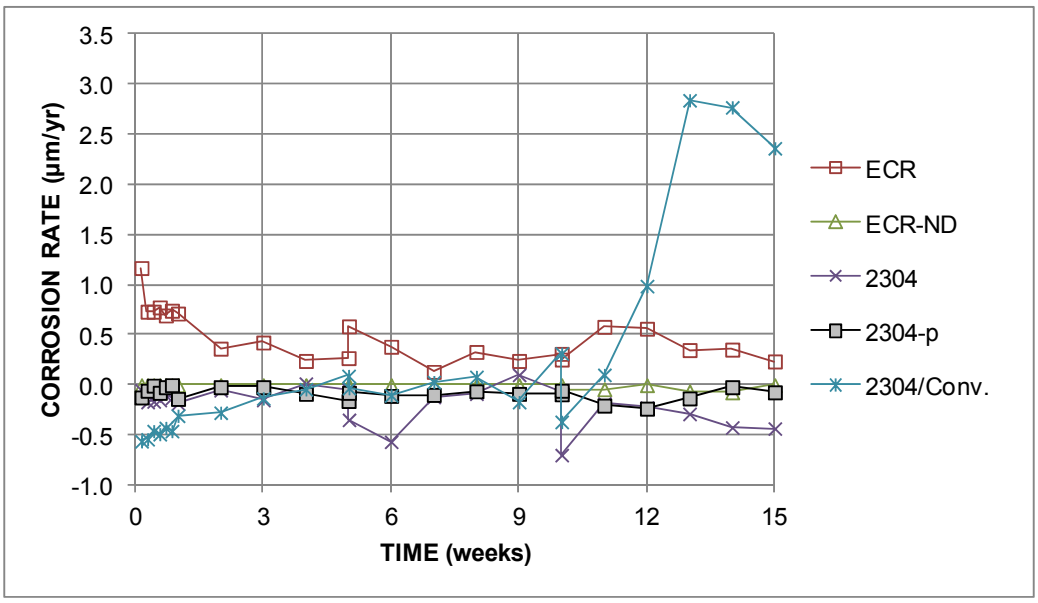

Figure 18: Macrocell average corrosion rates of, ECR, ECR-ND, 2304, 2304-p, and mixed 2304/conventional rapid macrocell specimens, specimens 1-6 (different scale).

The individual corrosion rates for the 2304 stainless steel specimens in the as-received condition are shown in Figure 19. As discussed earlier, most values are "negative," which is caused by minor differences in the oxidation rates of the single anode bar and the two cathode bars. The rates exhibit significant scatter, with values ranging between 1.10 µm/yr and –2.60 µm/yr. Individual corrosion potentials are also demonstrate significant scatter (Appendix A). While these data points may appear to be outliers, several specimens consistently exhibited corrosion rates in excess of +0.50 µm/yr maximum permitted by ASTM A955. Specimens 1, 2, and 3 exceeded +0.50 µm/yr one or more times during the test, although no corrosion products were observed on the bars.

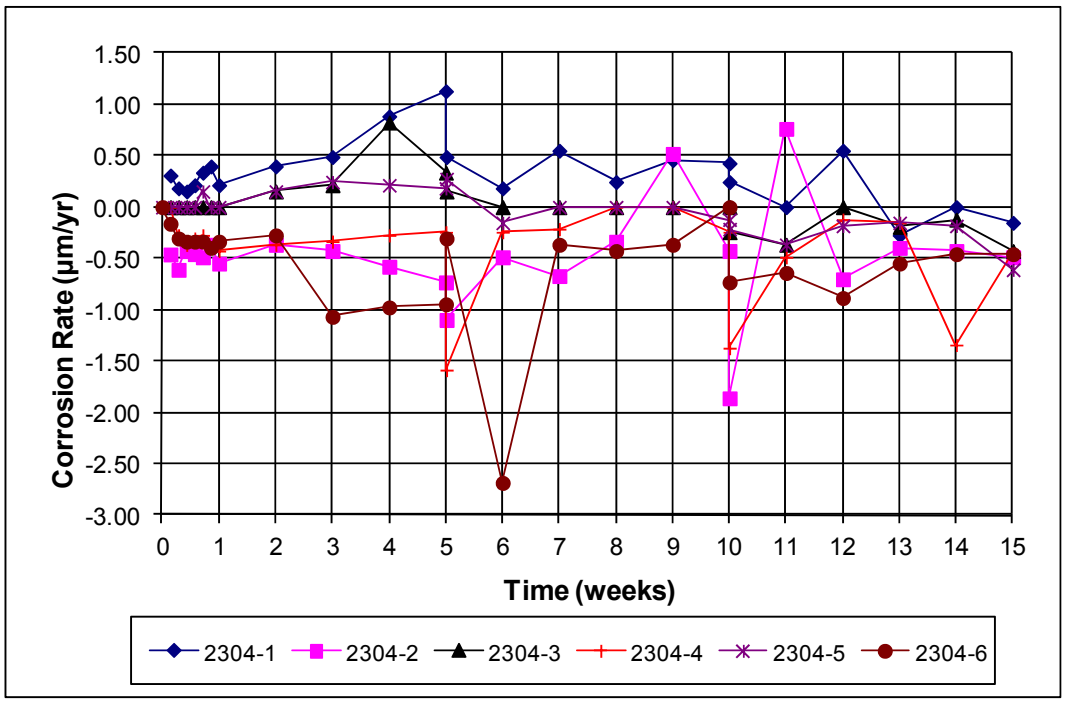

Figure 19: Macrocell individual corrosion rates of 2304 stainless steel, specimens 1-6.

As described earlier, the 2304 stainless steel in the as-received condition had a dull, mottled finish. As a result, a set of specimens was re-pickled to a bright, uniformly light surface. The individual corrosion rates for the re-pickled 2304 stainless steel bars are shown in Figure 20. The individual corrosion rates for the 2304-p specimens range between +0.15 and –0.50 µm/yr, with the largest scatter in the corrosion rates occurring in the first week of the test. Thereafter, individual corrosion rates of the re-pickled 2304 stainless steel were very tightly grouped, with values ranging for the most part between 0 and –0.30 µm/yr. Also, individual corrosion potentials for the 2304-p specimens demonstrate little scatter (Appendix A). The criteria for qualifying stainless steel per ASTM 955 were met, with no individual reading exceeding +0.50 µm/yr (Figure 20) and the average not exceeding +0.25 µm/yr during the test (Figure 18).

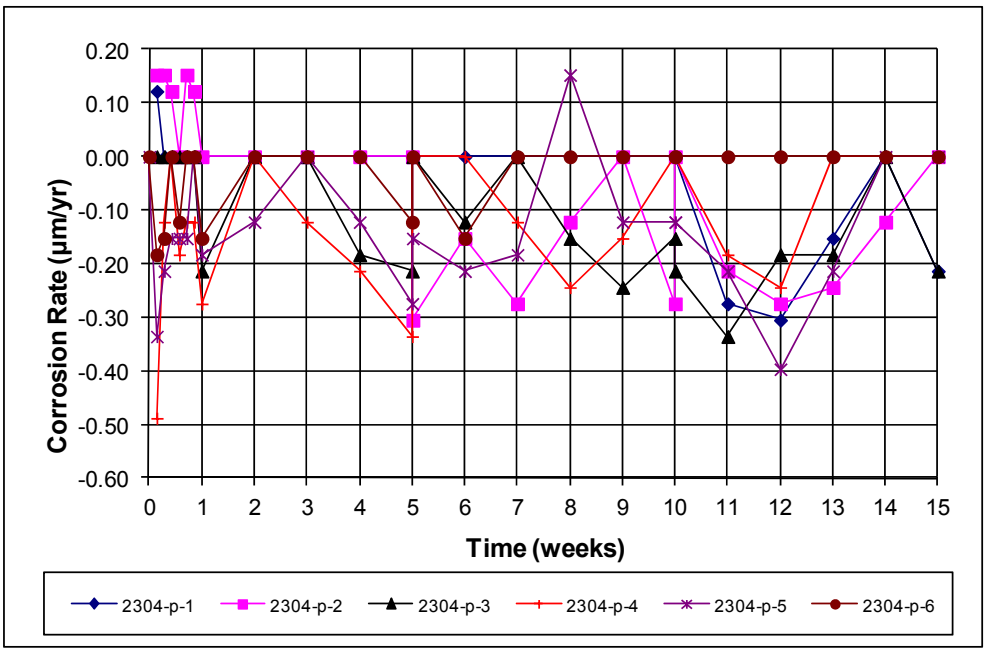

Figure 20: Macrocell individual corrosion rates of re-pickled 2304 stainless steel, specimens 1-6.

To assess the potential for galvanic effects, mixed-steel specimens were tested that included both conventional and 2304 stainless steel reinforcement. The 2304 stainless steel used in the mixed tests was tested in the as-received condition. Three specimens were tested with 2304 stainless steel as the anode and conventional reinforcement as the cathode, and three sets of specimens were tested with conventional reinforcement as the anode and 2304 stainless steel as the cathode.

The individual corrosion rates for the six mixed specimens are shown in Figures 21 and 22. In Figure 21, the corrosion rates of the Conv./2304 specimens are similar to that of conventional reinforcement. As shown in Figure 22, three of the 2304/Conv. specimens have corrosion rates that are similar to those of the 2304 stainless steel specimens in the as-received condition. As shown in Figure 22, the three mixed 2304/Conv. specimens exhibit individual corrosion rates in excess of +0.50 µm/yr at least once during the 15-week test. After week 12, specimen 2304/Conv.-3 corrodes at rates exceeding 1.5 µm/yr with a spike at week 12, reaching

a maximum of 10 µm/yr in week 14. Staining of the anode was observed, as shown in Figure 23. Individual corrosion potential data supports this, as a drop in the anode corrosion potential is seen in week 12 (Appendix A). As a result, the average corrosion rate of all the 2304/Conv. specimens is in excess of +0.25 µm/yr (Figure 18).

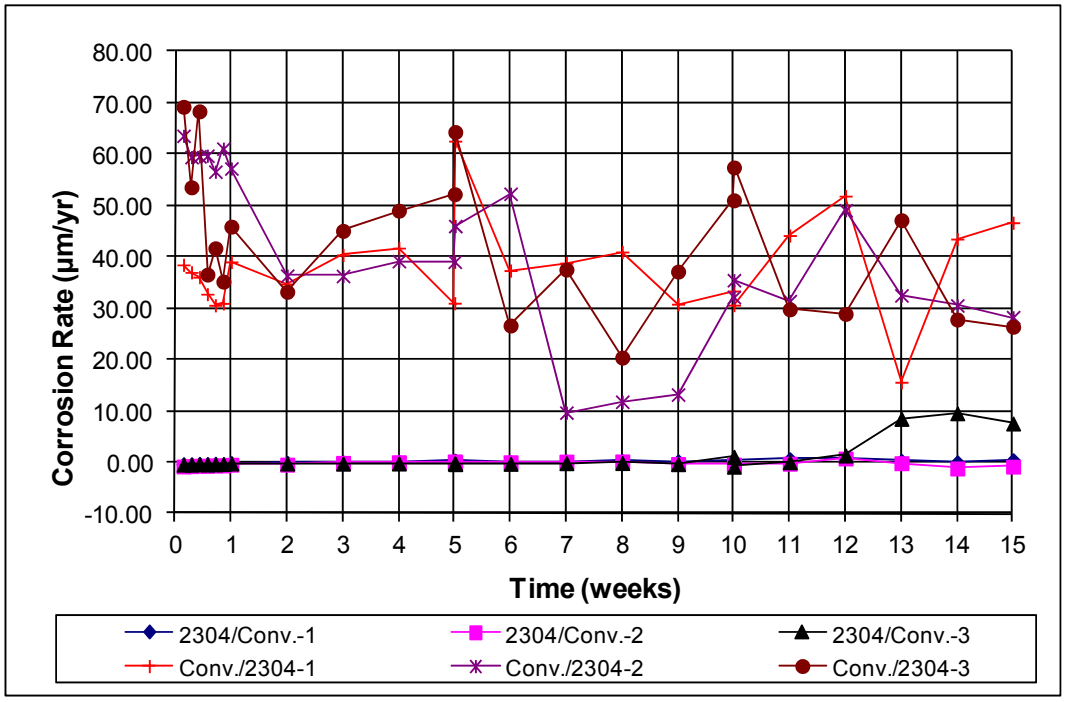

Figure 21: Macrocell individual corrosion rates of mixed 2304 stainless steel (anode/cathode), specimens 1-6.

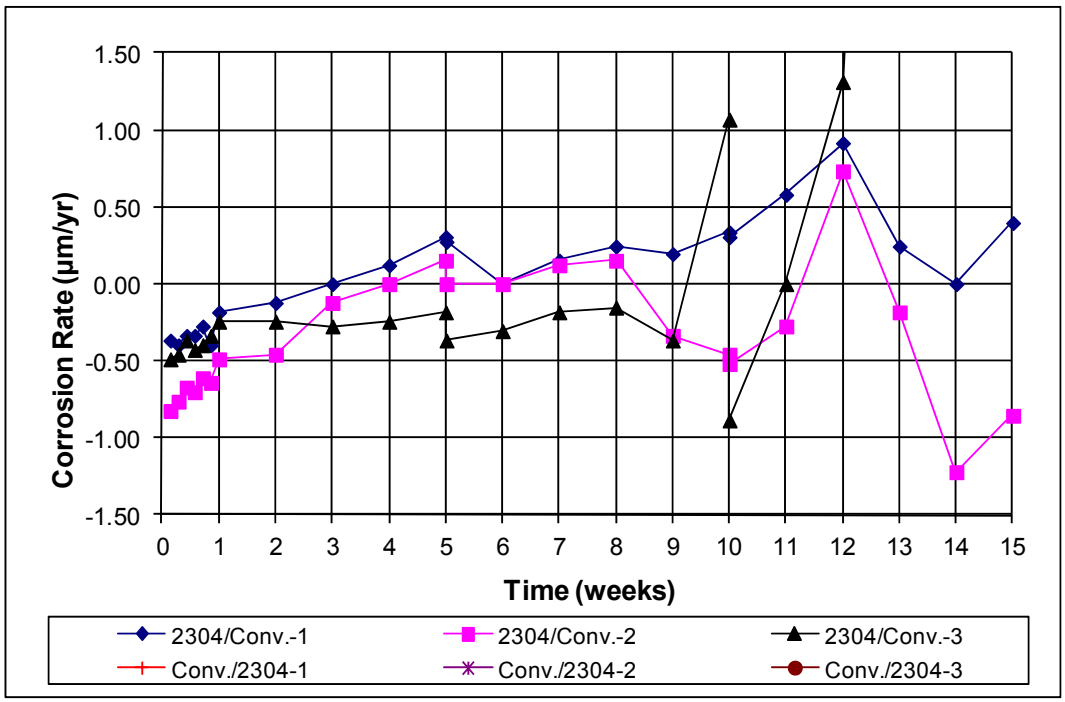

Figure 22: Macrocell individual corrosion rates of mixed 2304 stainless steel (anode/cathode), specimens 1-6 (different scale).

Figure 23: Staining of anode of 2304 stainless steel, mixed 2304/conventional steel macrocell specimen.

4.1.3 NX-SCR™ Stainless Steel Clad Reinforcement

The average corrosion rates for the specimens containing NX-SCR™ stainless steel clad reinforcement (SSClad) are shown in Figures 24 and 25. The results of the control specimens, conventional, ECR, and ECR-ND, are also plotted for comparison. For all SSClad specimens,

individual/average corrosion potentials, and individual corrosion losses are found in Appendix A.

The mixed Conv./SSClad specimens exhibited the highest average corrosion rate among rapid macrocell specimens containing stainless steel clad reinforcement. The average corrosion rate, which was between 9 and 26 μm/yr, was roughly half of the average corrosion rate of conventional steel.

The SSClad-NC and SSClad-4h bars had conventional steel exposed at the uncapped ends of the bars or at the holes drilled through the cladding. The SSClad-NC specimens exhibited average corrosion rates between 1 and 12 μm/yr, and the SSClad-4h specimens exhibited average corrosion rates between 0.2 and 5 μm/yr.

The average corrosion rates of the undamaged and bent stainless steel clad specimens never exceeded zero for the duration of the test. This seemingly "negative" corrosion has been discussed previously. Moreover, the average corrosion rate of both the undamaged and bent stainless steel clad reinforcement remained below +0.25 μm/yr throughout the duration of the test, satisfying this requirement of ASTM A955.

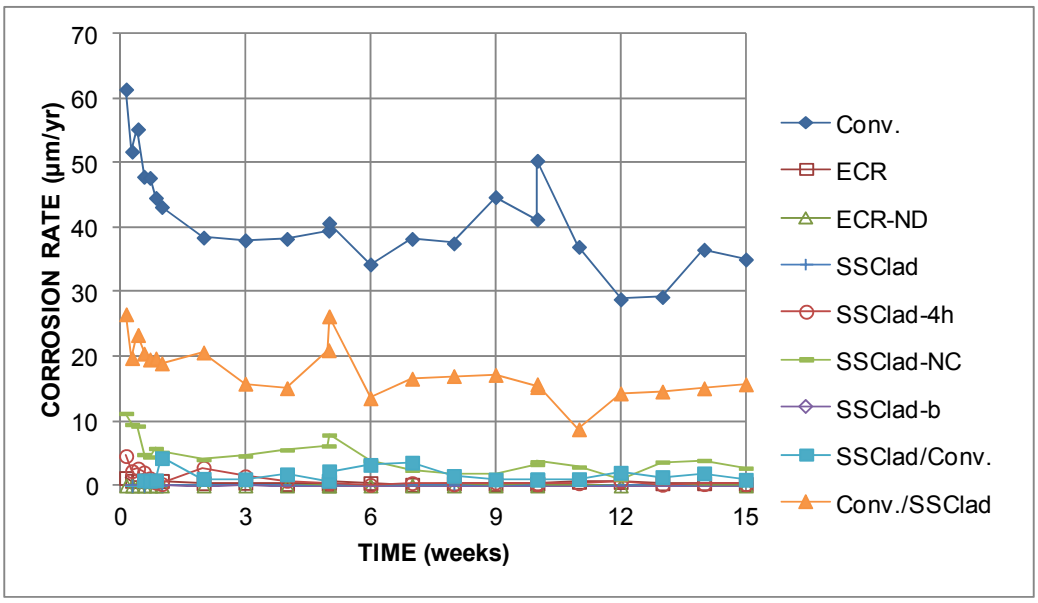

Figure 24: Average corrosion rate of conventional, stainless steel clad, damaged stainless steel clad, uncapped stainless steel clad, bent stainless steel clad, mixed stainless steel clad/conventional, and mixed conventional/stainless steel clad rapid macrocell specimens.

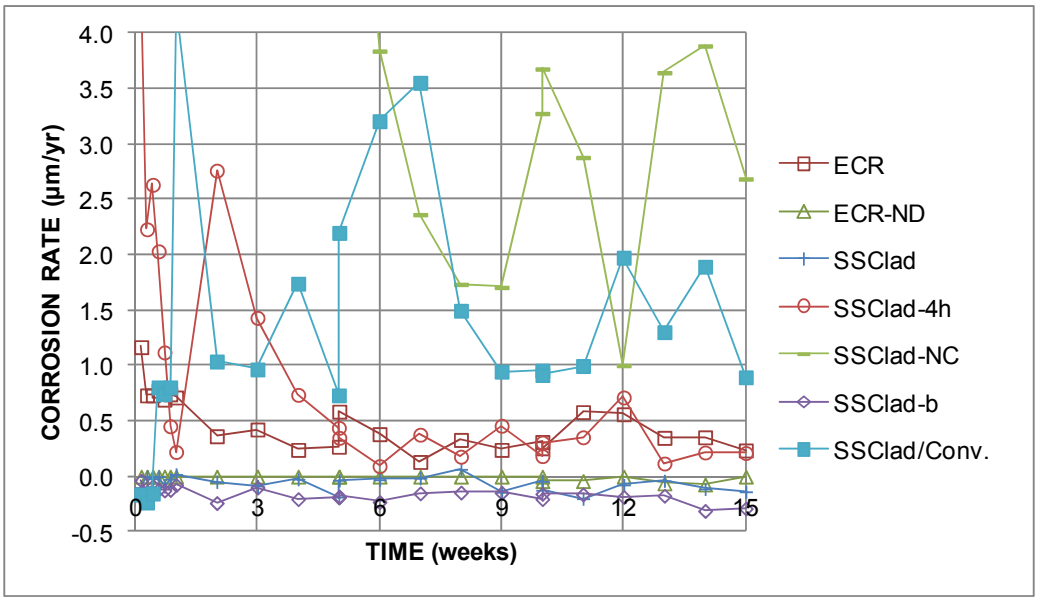

Figure 25: Average corrosion rate of stainless steel clad, damaged stainless steel clad, uncapped stainless steel clad, bent stainless steel clad, and mixed stainless steel clad/conventional steel clad rapid macrocell specimens (different scale).

The corrosion rates for the individual SSClad specimens are shown in Figure 26. Individual corrosion rates range from –0.60 to +0.90 µm/yr, although all but one specimen exhibited corrosion rates below 0.42 µm/yr. Upon completion of the evaluation, the specimens

were autopsied and the protective caps on both the anode bar and two cathode bars were removed to inspect the bar ends for signs of corrosion. Figure 27 shows the condition of a typical bar end. All specimens, with the exception of Specimen 6, performed satisfactorily, in that the individual corrosion rate did not exceed +0.50 µm/yr. Specimen 6, which exhibited very minor corrosion staining at the electrical connection of the anode and significant staining along the side of a cathode bar, is shown in Figures 28 and 29. Individual corrosion potential data supports this, as a large drop in anode potential is seen in Specimen 6. The failure of this specimen to meet the 0.50 µm/yr is not considered as representing a failure of the SSClad bars.

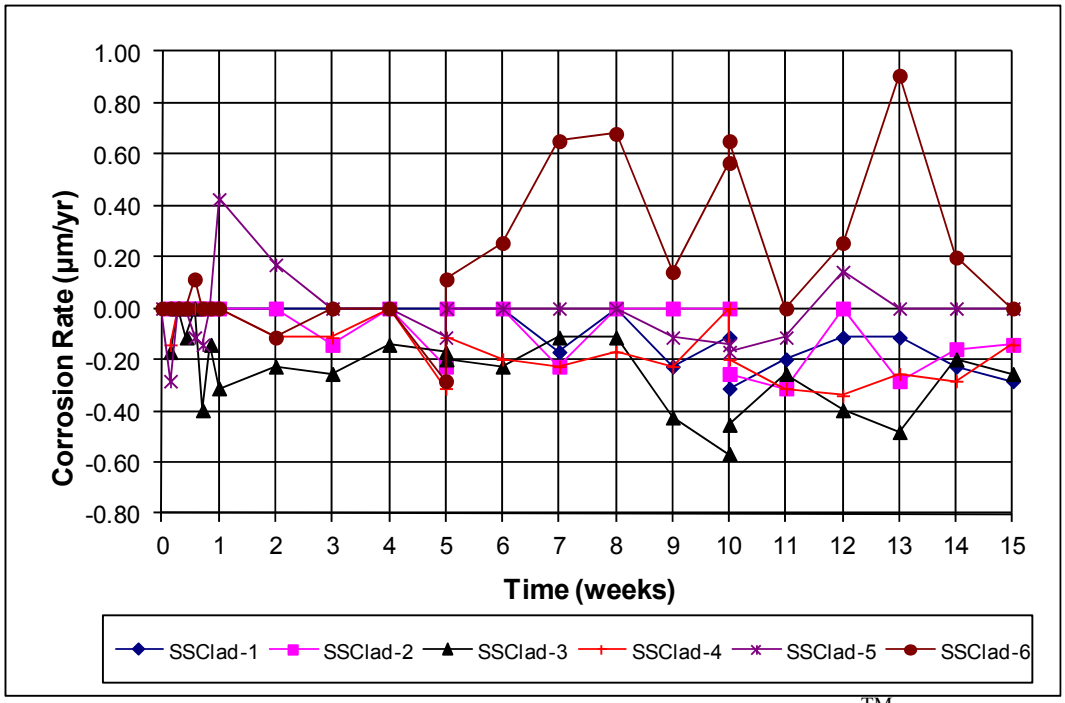

Figure 26: Macrocell individual corrosion rates of undamaged NX-SCR™ stainless steel clad bars, specimens 1-6.

Figure 27: Bar end with protective cap removed at end of rapid macrocell test, NX-SCR™ stainless steel clad (cathodes)

Figure 28: Photograph of Specimen 6 upon completion of the rapid evaluation test, NX-SCR™ stainless steel clad (anode on top, cathode on bottom)

Figure 29: Photograph of Specimen 6 upon completion of the rapid evaluation test, NX-SCR^{TM} stainless steel clad (close-up of cathode)

Individual corrosion rates are shown for uncapped stainless steel clad bars in Figure 30. Corrosion rates were highest in week 1, reaching values in excess of 25 μm/yr. Although the individual corrosion rates of the specimens was rather high due to the exposed conventional steel core of the NX-SCR^{TM} stainless steel clad bars, individual corrosion rates were much lower than the conventional reinforcement. Upon autopsy of the bars, it was discovered that a significant amount of corrosion was present at the location of the uncapped bar ends, as shown in Figure 31.

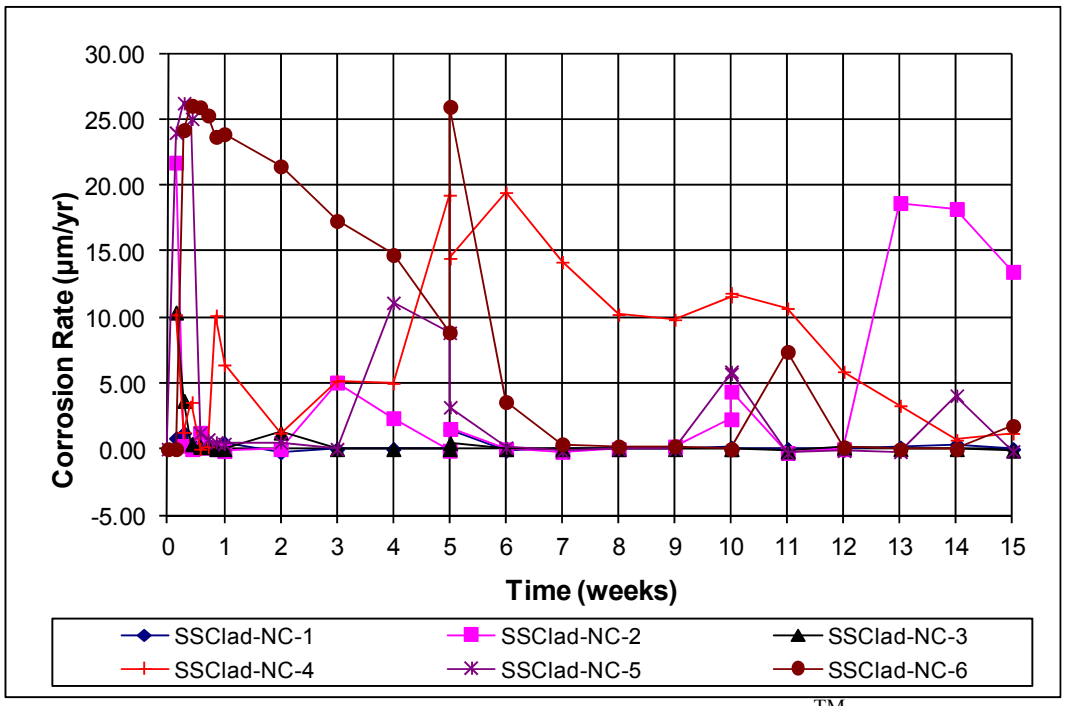

Figure 30: Macrocell individual corrosion rates of uncapped NX-SCR™ stainless steel clad bars, specimens 1-6.

Figure 31: Uncapped bar end upon autopsy, NX-SCR™ stainless steel clad.

The corrosion rates for the individual bent NX-SCR™ stainless steel clad (SSClad) bars are shown in Figure 32. The individual corrosion rates ranged from +0.4 to –0.4 µm/yr, satisfying the maximum value of +0.50 µm/yr in accordance with ASTM A955. Minimal

corrosion staining was observed on the bent stainless steel clad bars. A typical specimen is shown in Figure 33.

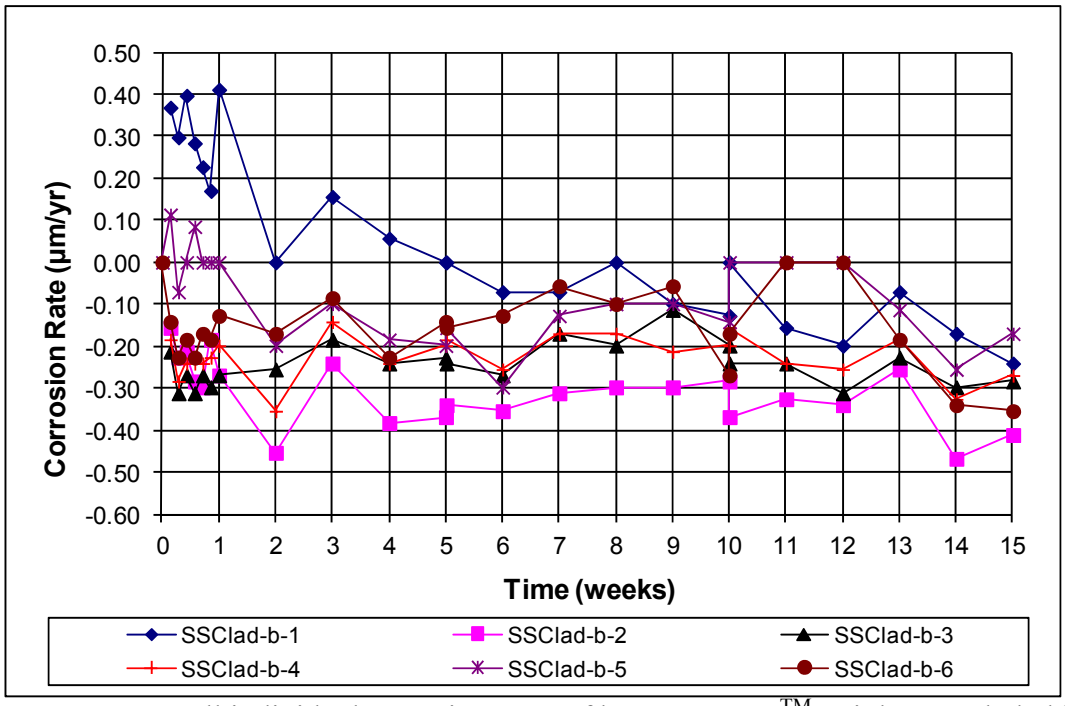

Figure 32: Macrocell individual corrosion rates of bent NX-SCR™ stainless steel clad bars, specimens 1-6.

Figure 33: Corrosion staining on bent section upon autopsy, bent NX-SCR™ stainless steel clad bar (close-up)

The corrosion rates for the individual damaged NX-SCR™ stainless steel clad specimens (SSClad-4h) are shown in Figure 34. Some individual corrosion rates, which range from just

below 0 to over 15 µm/yr, are rather high due to the exposed conventional steel core. Despite these corrosion rates, no visible signs of corrosion were present when the specimens were autopsied at completion of the test. As was the case for the undamaged, capped stainless steel clad (SSClad) bars, the bar caps were removed during the autopsy to determine if corrosion had occurred beneath the protective cap. No corrosion was discovered under the cap or at the holes through the cladding.

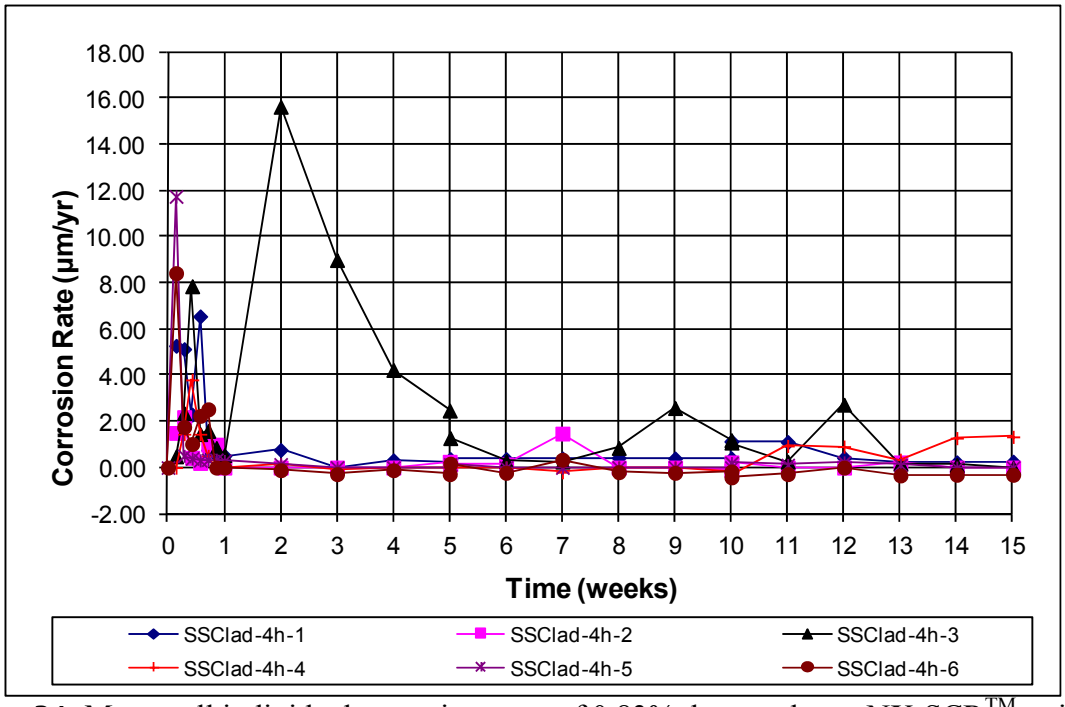

Figure 34: Macrocell individual corrosion rates of 0.83% damaged area NX-SCR™ stainless steel clad bars, specimens 1-6.

The corrosion rates for the individual SSClad/Conv. and Conv./SSClad specimens are shown in Figures 35 and 36. As shown in Figure 35, the specimens with a conventional bar as the anode performed much like the Conv. specimens, with corrosion rates around 35 µm/yr at the onset of the test, settling to about 15 µm/yr after about 6 weeks.

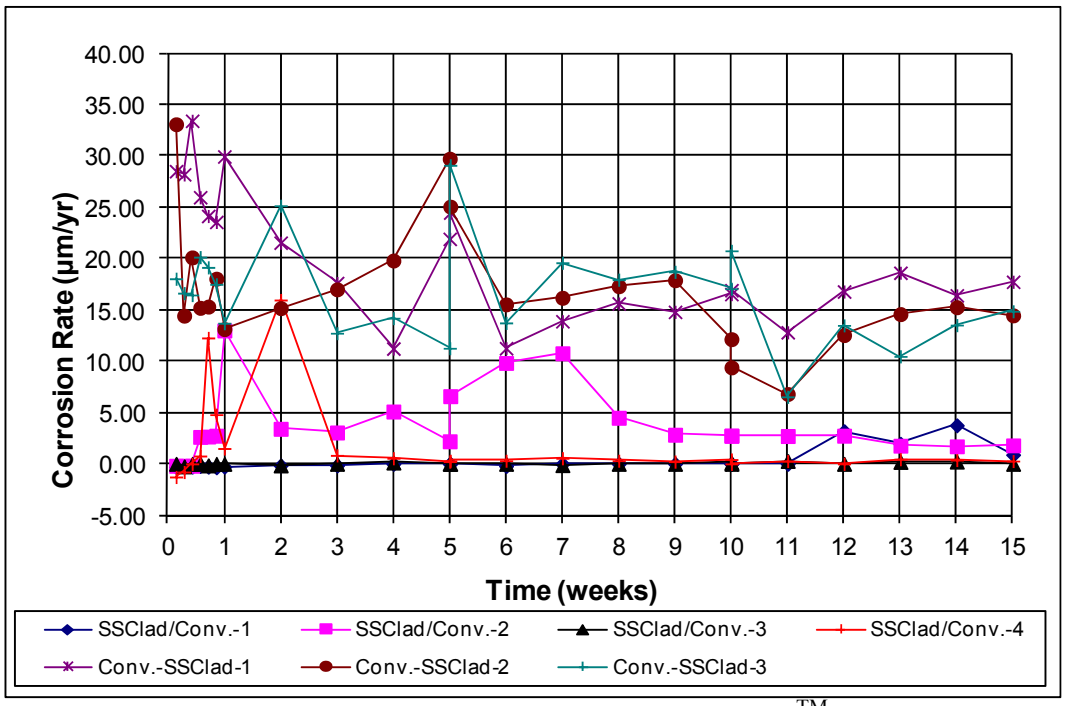

Figure 35: Macrocell individual corrosion rates of mixed NX-SCR™ stainless steel clad bars (anode/cathode), specimens 1-6.

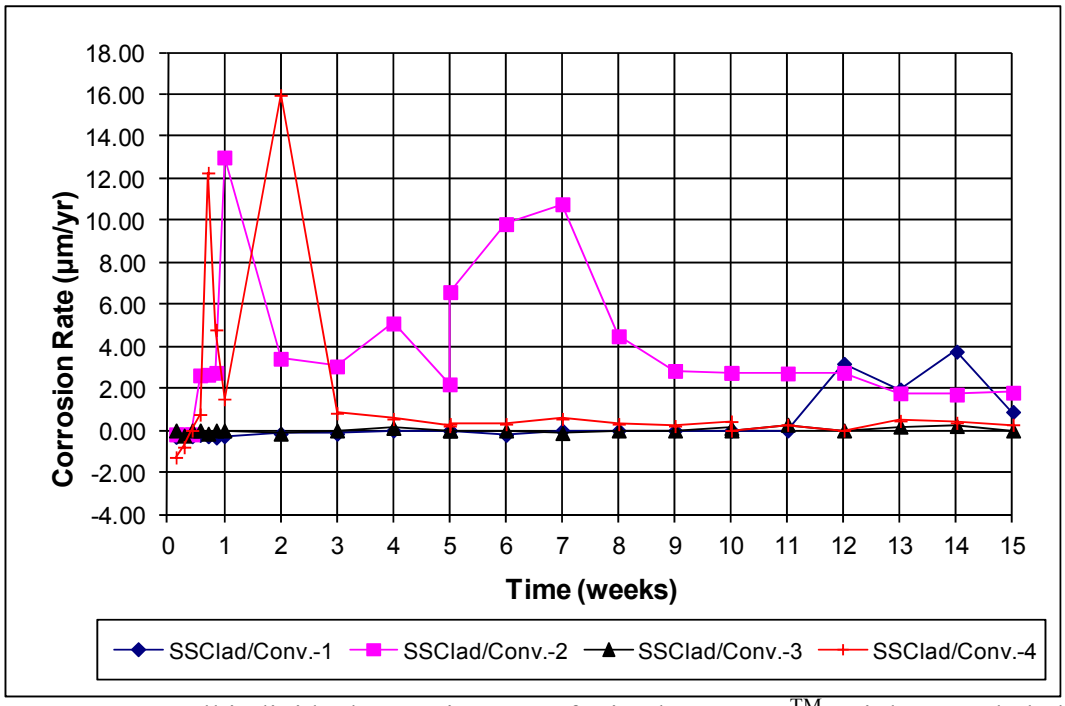

Figure 36: Macrocell individual corrosion rate of mixed NX-SCR™ stainless steel clad bars (anode/cathode), specimens 1-6 (different scale).

The mixed specimens with a stainless steel clad bar as the anode (SSClad/Conv.) performed much better, with the exception of specimen SSClad/Conv.-2, which had a corrosion rate of approximately 3 μm/yr during most of the test, with a spike in corrosion rate at week 7 to approximately 10 μm/yr. Because this specimen experienced such a high corrosion rate, it was thought that the protective cap on the end of this stainless steel clad bar may have been ineffective. As a result, an additional mixed SSClad/Conv. reinforcement specimen was tested, but it also exhibited a high corrosion rate. Upon the autopsy of specimen SSClad/Conv.-2, a significant amount of corrosion was discovered underneath the protective cap (Figure 37) indicating that the cap rather than the bar failed. Specimen SSClad/Conv.-4 exhibited a small amount of corrosion under the cap, suggesting that the high corrosion observed for that specimen was also caused by a failure of the cap.

Figure 37: Corrosion under protective cap at end of evaluation, NX-SCR™ stainless steel clad bar, Specimen 2 (close-up).

4.1.4 Autopsy

Upon completion of the 15-week rapid macrocell evaluation, all test specimens were autopsied, using the following procedure:

1. Specimens are removed from the solution and lightly patted dry with paper towels.
2. The electrical connection of each specimen is closely examined for signs of corrosion.

3. Photographs are taken of each specimen on two sides.
4. In the case of capped specimens, the protective caps on the ends are removed with a pen knife and inspected for signs of corrosion.
5. If applicable, photographs are taken of each specimen that has noteworthy corrosion staining.
6. In the case of ECR and ECR-ND specimens, disbondment tests are performed upon each anode bar.

The disbondment test is performed at the four locations of intentional damage on ECR bars and at the same locations on the undamaged ECR-ND bars. At each test site, a sharp utility knife is used to make two cuts through the epoxy at 45° from the axis of the bar, forming an "X" centered on the damage site. An attempt is made to peel back the epoxy coating with the knife around the "X" until either (1) the coating will no longer peel back or (2) a longitudinal rib is reached in the circumferential direction or the second deformation on either side of the damage site is reached along the specimen. In the case of the ECR-ND specimens, the coating was scraped with a pen knife in order to attempt to detect any softening of the coating that may be present. The disbonded area is measured with 0.01-in. (0.254-mm) grid paper. The originally damaged 1/8-in. (3.2-mm) diameter area is not included in the disbonded area. The values of the disbonded area for each of the originally damaged ECR specimens are shown in Table 7. The originally undamaged bars exhibited no disbondment.

Table 7: Disbonded area ($in.^2$)* for damaged ECR specimens 1-6

Specimen	1	2	3	4	5	6
Site 1	0.18	0.16	0.11	0.19	0.06	0.33
Site 2	0.14	0.19	0.21	0.08	0.32	0.20
Site 3	0.13	0.17	0.10	0.15	0.09	0.52
Site 4	0.13	0.22	0.26	0.08	0.09	0.09

Note: 1.0 $in.^2$ = 645 mm^2 *Values do not include area of original hole.

As mentioned earlier, each specimen is photographed on two sides upon completion of the rapid macrocell test. Anomalies observed during the autopsy were discussed earlier in this chapter. The photographs in Figures 38 through 58 are representative of typical specimens. Where corrosion products and staining are shown, it can be inferred that these effects were observed for all specimens in a set.

Figure 38: Rapid macrocell specimen upon completion of test, conventional steel (anode on top, cathode on bottom)

Figure 39: Rapid macrocell specimen upon completion of test, undamaged ECR (anode on top, cathode on bottom)

Figure 40: Rapid macrocell specimen upon completion of test, ECR (close-up of damage site after disbondment test)

Figure 41: Rapid macrocell specimen upon completion of test, 2304 stainless steel (anode on top, cathode on bottom)

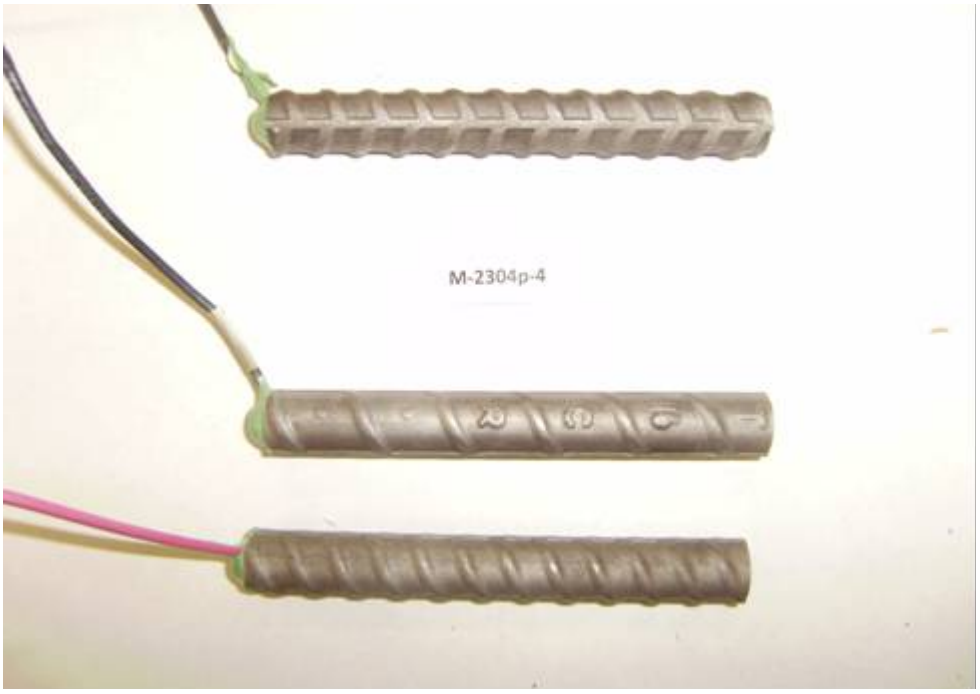

Figure 42: Rapid macrocell specimen upon completion of test, re-pickled 2304 stainless steel (anode on top, cathode on bottom)

Figure 43: Rapid macrocell specimen upon completion of test, mixed 2304/conventional steel (anode on top, cathode on bottom)

Figure 44: Rapid macrocell specimen upon completion of test, mixed conventional/2304 stainless steel (anode on top, cathode on bottom)

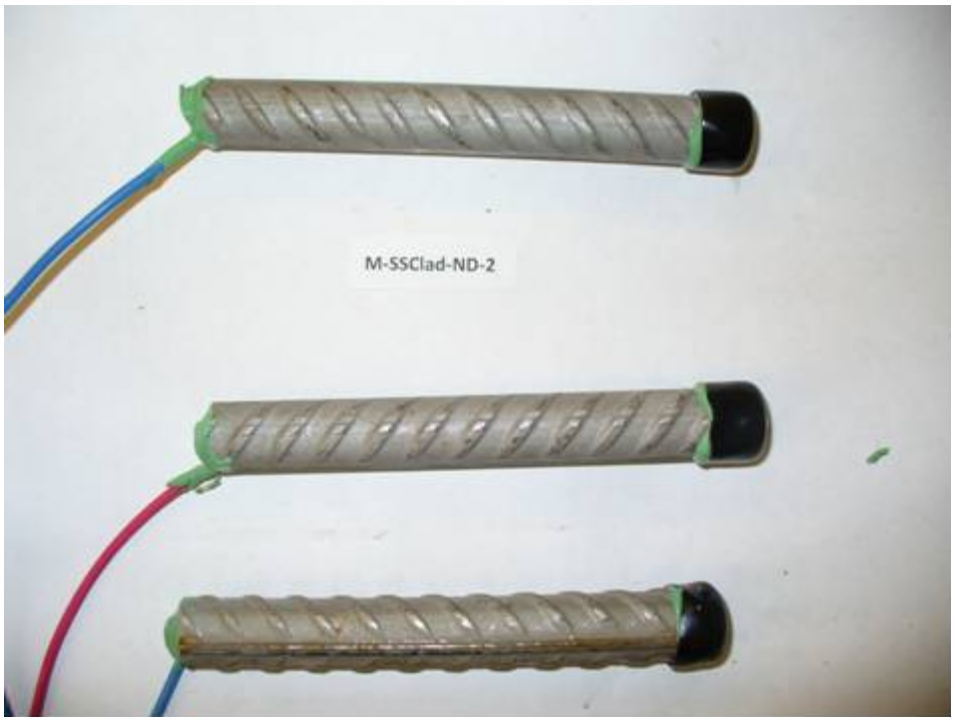

Figure 45: Rapid macrocell specimen upon completion of test, undamaged stainless steel clad reinforcement (anode on top, cathode on bottom)

Figure 46: Rapid macrocell specimen upon completion of test, undamaged stainless steel clad reinforcement (close-up of bar end after cap has been removed)

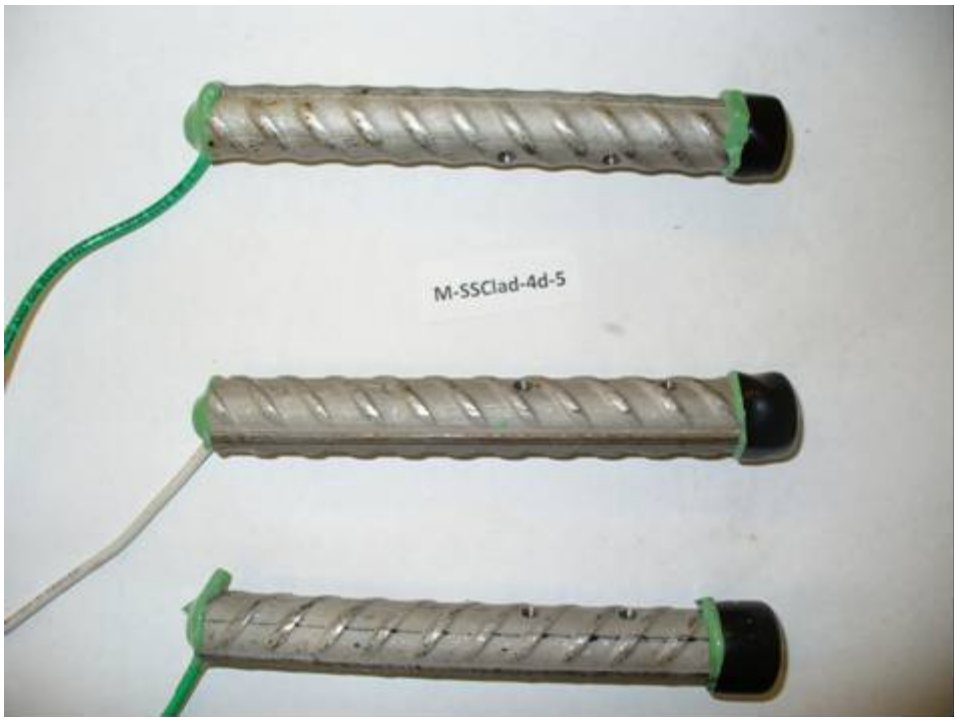

Figure 47: Rapid macrocell specimen upon completion of test, damaged stainless steel clad reinforcement (anode on top, cathode on bottom)

Figure 48: Rapid macrocell specimen upon completion of test, uncapped stainless steel clad reinforcement (anode on top, cathode on bottom)

Figure 49: Rapid macrocell specimen upon completion of test, uncapped stainless steel clad reinforcement (close-up of bar end)

Figure 50: Rapid macrocell specimen upon completion of test, bent stainless steel clad reinforcement (anode)

Figure 51: Rapid macrocell specimen upon completion of test, mixed conventional/stainless steel clad reinforcement (anode on top, cathode on bottom)

Figure 52: Rapid macrocell specimen upon completion of test, mixed stainless steel clad/conventional steel (anode on top, cathode on bottom)

4.2 Bench-Scale Tests

4.2.1 Corrosion losses

The bench-scale tests have been underway for between 31 and 36 weeks. Corrosion losses for the individual Southern Exposure and cracked beam specimens are listed in Tables 8 and 9, respectively. Some specimens in these tables exhibit negative loss values. Negative readings can result from corrosion at the external wiring. They can also result from corrosion of the bottom mat of steel. To date, however, inspections of these specimens have indicated no signs of corrosion at these locations. Similar to the macrocell results, these readings are likely due to current drift because of the greater number of bars in the bottom mat of steel and do not actually indicate "negative corrosion."

Table 8: Corrosion losses based on total area for Southern Exposure specimens

System[a]	Specimen					
	1	2	3	4	5	6
	Week					
	36	35	34	33	32	31
	Corrosion Loss (μm)					
Conv.	3.63	4.27	8.86	0.90[b]	2.42	2.51
ECR	0.03	0.13	0.06	0.05	0.06	0.13
ECR-ND	-0.01	0.00	0.00	-	-	-
2304	0.01	0.00	0.00	0.00	0.00	0.00
2304/Conv.	0.01	0.00[b]	0.00[b]	-	-	-
Conv./2304	-	5.27	6.11	2.85[b]	-	-
SSClad-4h	0.03	0.02	0.30	0.04	0.05	0.07
SSClad	-0.01	0.00	-0.01	-0.02	0.00	0.01
SSClad-b	0.03	0.01	-0.02	-0.01	-0.02	-0.02
SSClad/Conv.	-	-0.01	0.01	-0.04	-0.01	-0.02
Conv./SSClad	5.83	0.85[b]	0.37[b]	-	-	-

[a] Conv. = conventional reinforcement, ECR = epoxy-coated reinforcement with ten 1/8-in. (3.2-mm) diameter holes through the epoxy, ECR-ND= undamaged ECR, 2304 = 2304 stainless steel, SSClad-4h = stainless steel clad reinforcement with four 0.125-in. diameter holes through the cladding, SSClad = undamaged stainless steel clad reinforcement, SSClad-b = bent stainless steel clad reinforcement.
For mixed specimens, the reinforcement in the top mat is listed first.
- = No specimen cast in this batch.
[b] Specimen age = 17 weeks

Table 8 shows the corrosion losses for the individual Southern Exposure specimens. The values are obtained by integration of the corrosion rates that are measured on a weekly basis. Corrosion has initiated on all Conv., ECR, Conv./2304, Conv./SSClad specimens, along with four of the specimens with stainless steel clad bar with holes through the cladding, SSClad-4h-3, SSClad-4h-4, SSClad-4h-5, and SSClad-4h-6. Losses for two Conv./2304 specimens exceed the average losses exhibited by the Conv. alone. The other Conv./2304 specimen has not been under testing as long and is currently at 17 weeks. The loss for Conv./SSClad-1 also exceeds the average loss exhibited by Conv. specimens. The other two Conv./SSClad specimens are currently at 17 weeks of testing. Losses for all other Southern Exposure specimens are less than 1 μm.

Corrosion losses for the individual cracked beam specimens are presented in Table 9. The greatest corrosion loss is exhibited by specimen Conv.-1 (13.34 μm) at 36 weeks. Specimens containing ECR with 10 1/8-in. (3.2-mm) diameter holes through the epoxy (ECR) exhibit losses between 0.129 and 0.295 μm based on the total area of the bar. The undamaged ECR (ECR-ND) specimens are exhibiting no significant corrosion losses to date. Specimens containing 2304 stainless steel exhibit losses similar or somewhat less than those of damaged ECR. The 2304 corrosion loss values range between –0.05 and 0.18 μm. Specimens containing undamaged stainless steel clad reinforcement (SSClad) exhibit losses between 0.01 and 0.11 μm.

Table 9: Corrosion losses based on total area for cracked beam specimens

System[a]	Specimen					
	1	2	3	4	5	6
	Week					
	36	31	30	29	28	27
	Corrosion Loss (µm)					
Conv.	13.3	10.8	8.61	7.50	10.4	6.09
ECR	0.13	0.21	0.27	0.17	0.30	0.24
ECR-ND	-0.02	-0.01	0.00	-	-	-
2304	0.18	0.06	-0.05	-0.03	-0.01	0.00
SSClad	0.11	0.03	0.01	0.17	-0.01	-0.01

[a] Conv. = conventional reinforcement, ECR = epoxy-coated reinforcement with ten 1/8-in. (3.2-mm) diameter holes through the epoxy, ECR-ND= undamaged ECR, 2304 = 2304 stainless steel, SSClad = undamaged stainless steel clad reinforcement.

- = No specimen cast in this batch.

Figures 53 and 54 show the average corrosion losses for Southern Exposure and cracked beam specimens, respectively, through week 31. Figure 53a shows the average corrosion losses for the control specimens, Conv., ECR, and ECR-ND, in the Southern Exposure test. Conventional reinforcement exhibits an average loss of 2.97 µm. The ECR specimens exhibit an average loss of 0.06 µm, while the ECR-ND specimens exhibit no significant losses. Individual corrosion loss data for all bench-scale specimens is located in Appendix C.

Figure 53b shows the average losses for the Southern Exposure specimens containing 2304 stainless steel and a mix of 2304 and conventional reinforcement. The mixed specimens with conventional steel in the top mat and 2304 stainless steel in the bottom mat (Conv./2304) exhibit average losses of 5.3 µm, which is greater than that observed for conventional reinforcement (Conv.) alone (2.97 µm) at week 31. The Conv./2304 specimens from the rapid macrocell test exhibited an average loss similar to that of the Conv. specimens at the conclusion of testing. The 2304 specimens and those with 2304 in the top mat and conventional

reinforcement in the bottom mat (2304/Conv.) show no significant losses. The latter trends are similar to those observed for losses in the rapid macrocell test.

Figure 53c compares the average losses for the Southern Exposure specimens containing stainless steel clad reinforcement (SSClad) and a mix of SSClad and conventional reinforcement with those for the Conv. specimens. None of the specimens with stainless steel clad reinforcement in the top mat, SSClad, SSClad-b, or SSClad/Conv., exhibit significant losses. One Conv./SSClad had a loss of 5.83 µm as of week 36. The other Conv./SSClad specimens have begun to corrode, but do not yet show losses above 1 µm as of 17 weeks (Table 8). The Conv./SSClad specimens in the rapid macrocell test also exhibited significant losses.

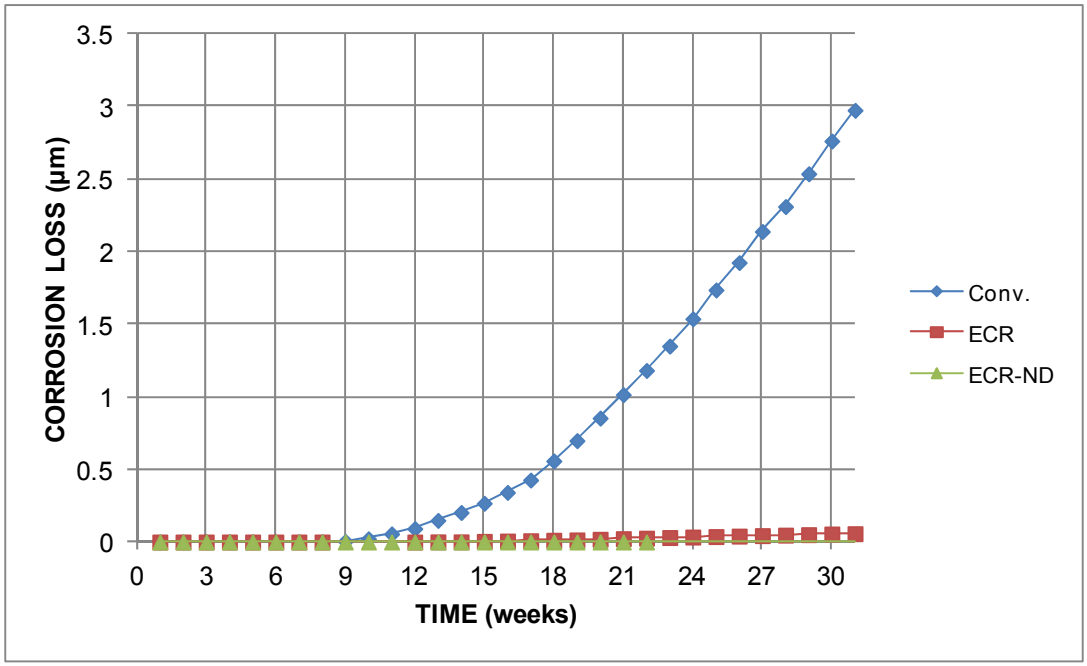

Figure 53a: Average corrosion losses (µm) based on total area for Southern Exposure specimens with conventional and epoxy-coated reinforcement.

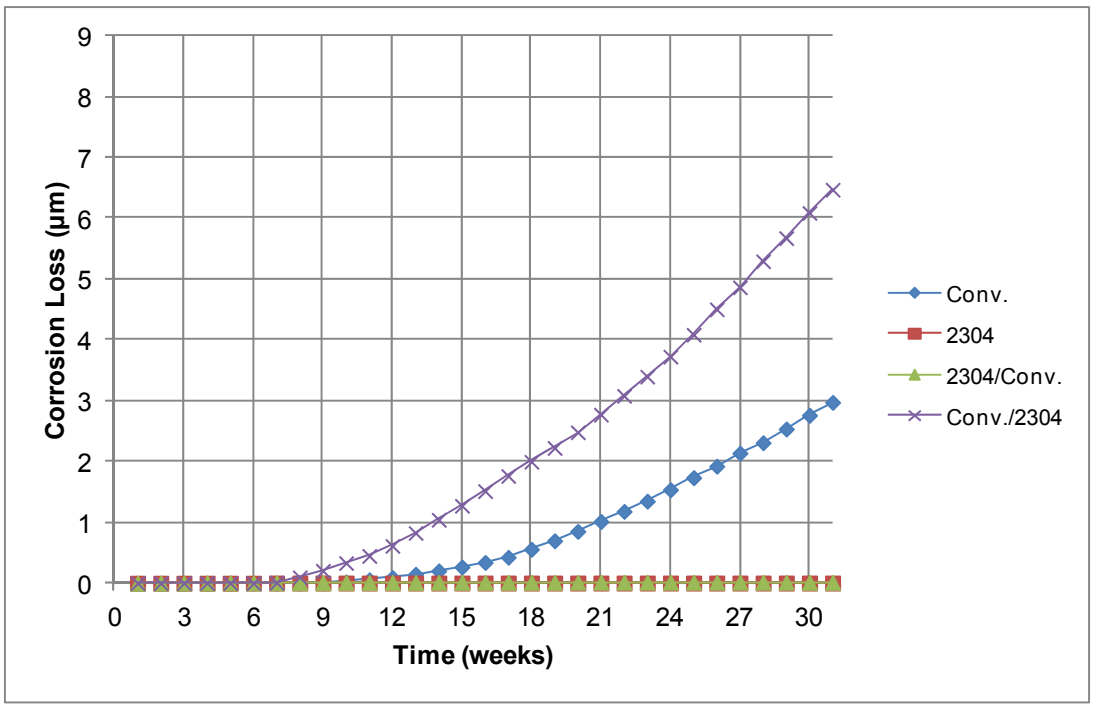

Figure 53b: Average corrosion losses based on total area for Southern Exposure specimens with conventional and 2304 stainless steel reinforcement (different scale).

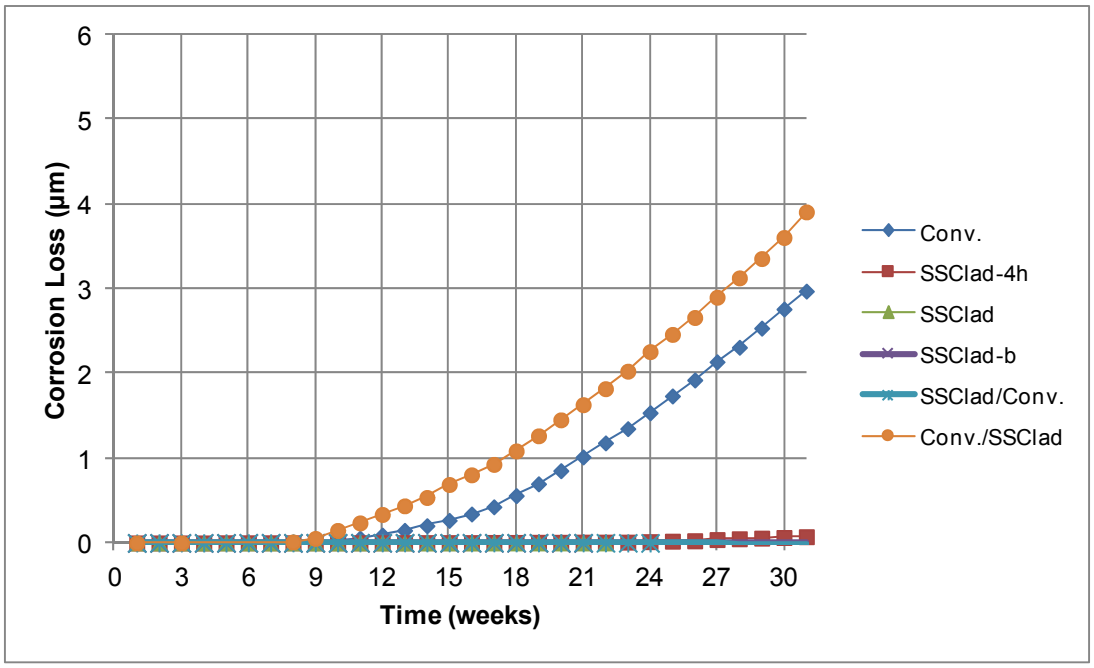

Figure 54c: Average corrosion losses based on total area for Southern Exposure specimens with conventional and stainless steel clad reinforcement (different scale).

Figures 55a and 55b show the average losses for the cracked beam specimens. Figure 55a shows that conventional reinforcement exhibits an average corrosion loss of 8.7 µm, which is far

greater than the other systems at week 31. Figure 55b examines the average losses of the more corrosion-resistant steels at a different scale. The ECR specimens exhibit the second greatest average loss at 0.20 µm, followed by undamaged stainless steel clad (SSClad) and 2304 stainless steel reinforcement, at 0.05 µm and 0.03 µm, respectively. Undamaged ECR exhibits no measurable corrosion loss as of week 31.

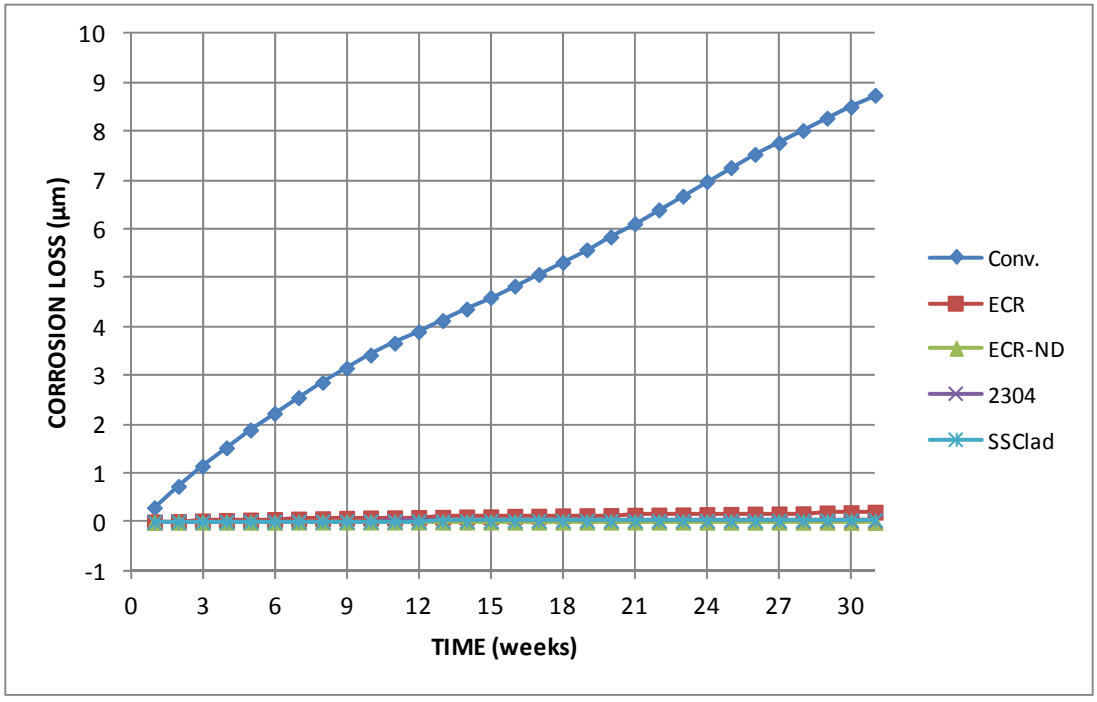

Figure 55a: Average corrosion losses based on total area for cracked beam specimens.

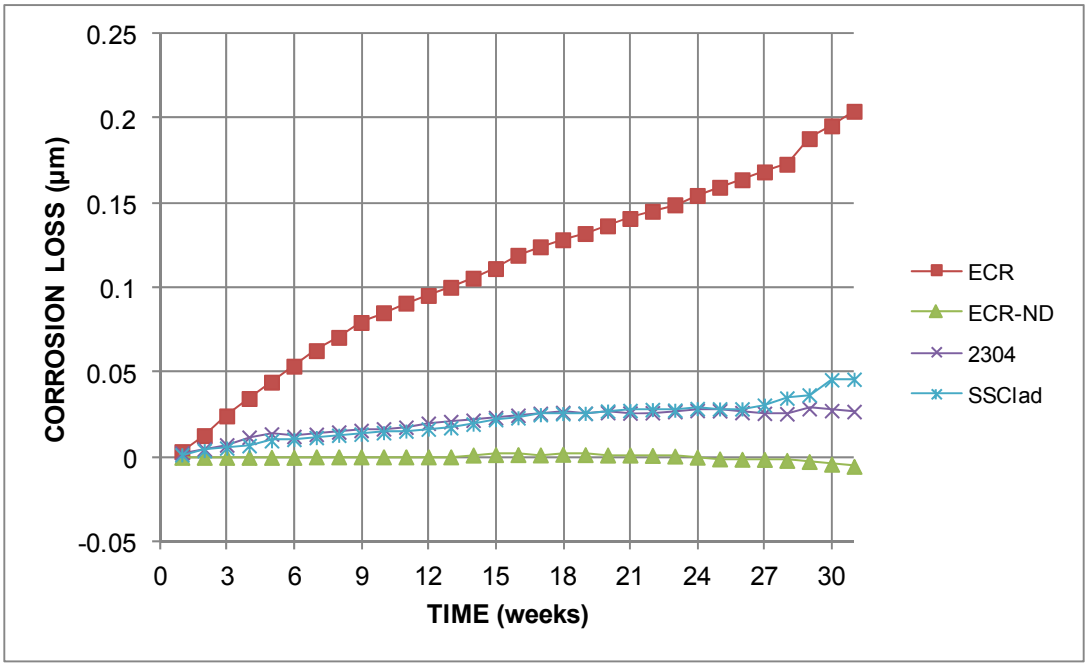

Figure 55b: Average corrosion losses based on total area for cracked beam specimens (different scale).

Figures 56a through 56c show the average mat-to-mat resistances for the Southern Exposure specimens. The resistances for epoxy-coated reinforcement are considerably higher than those for uncoated reinforcement. The ECR-ND specimens exhibit the highest average resistance during the first 26 weeks and are currently showing values similar to ECR specimens. The drop may indicate some penetration of ions through the undamaged coating. At 31 weeks, average resistances of 332, 4144, and 4579 ohms are observed for the Conv., ECR, and ECR-ND specimens, respectively.

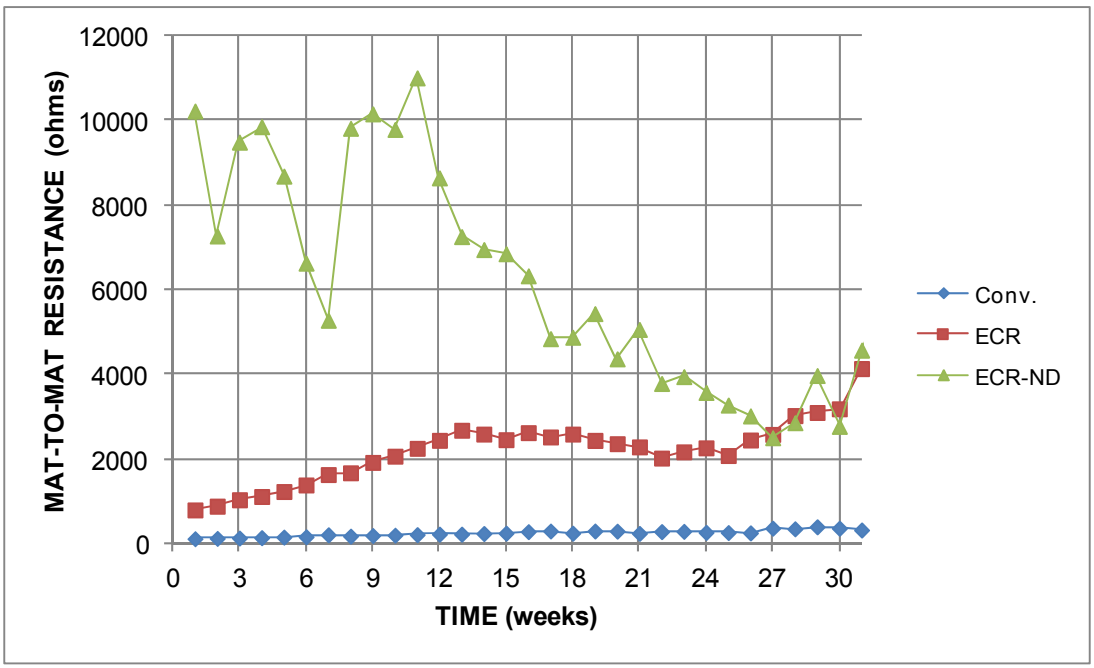

Figure 56a: Average mat-to-mat resistances based on total area for Southern Exposure specimens with conventional and epoxy-coated reinforcement.

4.2.2 Mat-to-mat resistance

Figure 56b shows that specimens with conventional and 2304 stainless steel reinforcement exhibit similar mat-to-mat resistances. Values have increased throughout the tests. Generally, the Conv. specimens exhibit somewhat higher resistances than do the other specimens. The same trends are observed in Figure 56c for with stainless steel clad specimens.

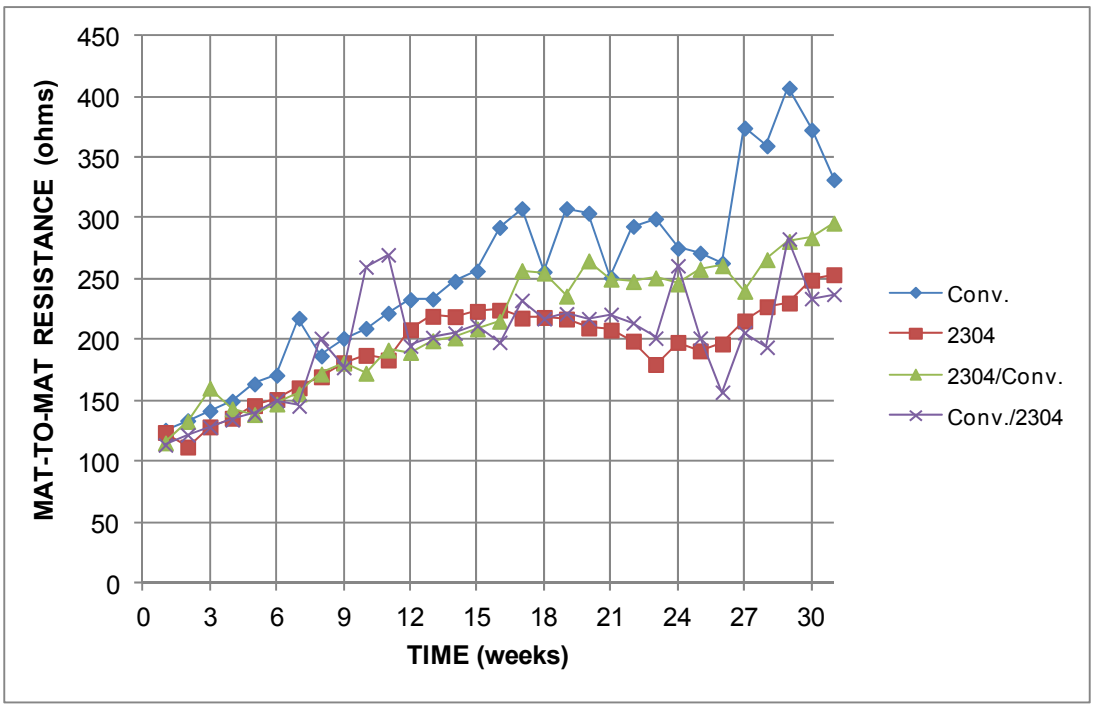

Figure 56b: Average mat-to-mat resistances based on total area for Southern Exposure specimens with conventional and 2304 stainless steel reinforcement (different scale).

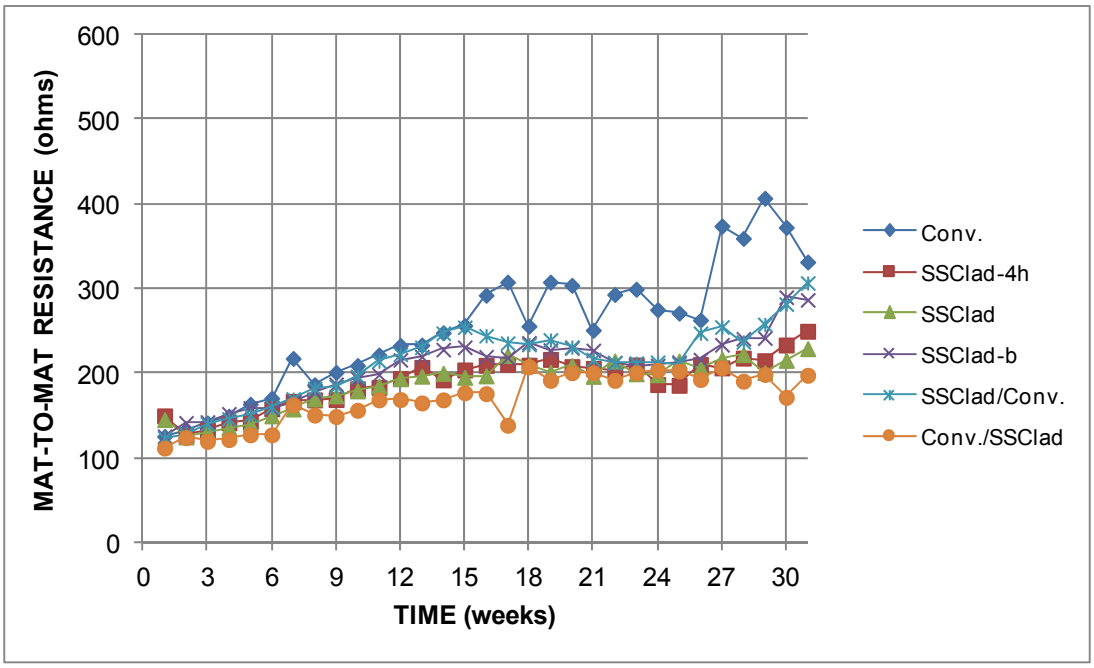

Figure 56c: Average mat-to-mat resistances based on total area for Southern Exposure specimens with conventional and stainless steel clad reinforcement (different scale).

The average mat-to-mat resistances for cracked beam specimens are shown in Figure 57.

As for the Southern Exposure specimens, the ECR-ND cracked beam specimens began with the

highest values but are currently exhibiting resistances near that of the ECR specimens. Uncoated bar specimens, Conv., 2304, and SSClad, exhibit similar values of resistance, with the Conv. and 2304 specimens averaging 588 ohms and the SSClad specimens averaging 510 ohms. Individual mat-to-mat resistance plots for all specimens are included in Appendix C.

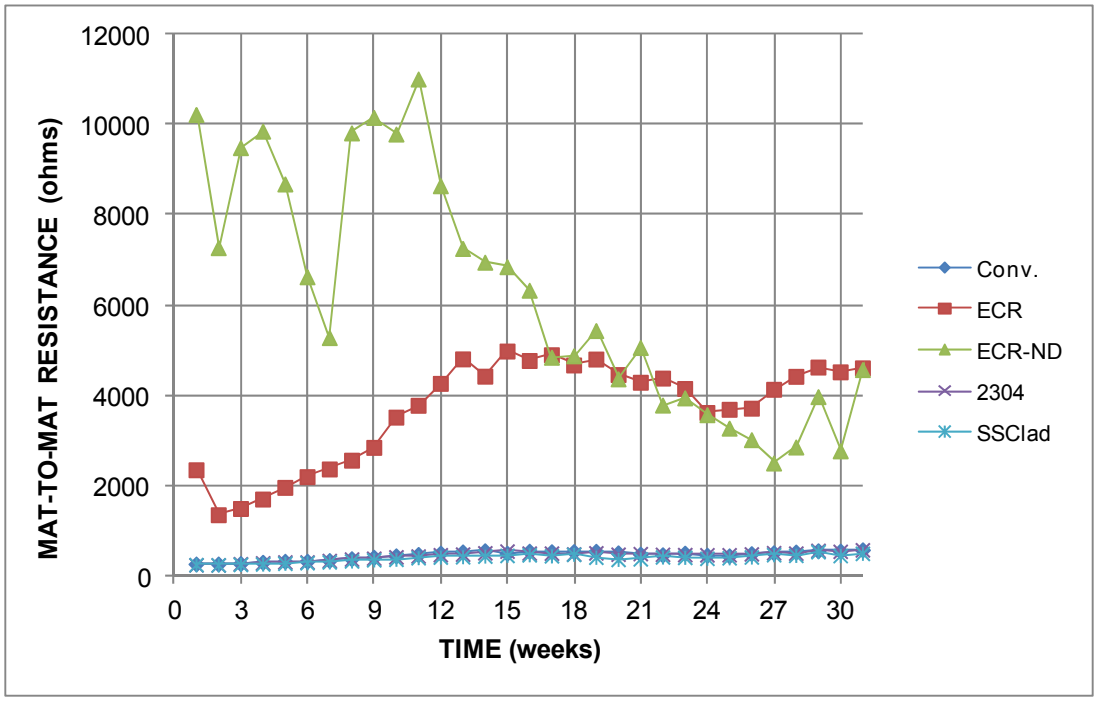

Figure 57: Average mat-to-mat resistances based on total area for cracked beam specimens.

4.2.3 Corrosion potential

Figure 58a compares the top-mat potentials for the Southern Exposure specimens with conventional and epoxy-coated reinforcement. Figures 58b and 58c compare the top-mat potentials for specimens containing, respectively, 2304 and SSClad bars with those containing only Conventional bars. As the potential of a bar or mat becomes more negative, the probability of corrosion increases. Throughout the tests, the top-mat resistances have dropped for specimens with exposed conventional steel in the top mat. Although the ECR-ND specimens are not exhibiting significant corrosion, the average top-mat potential is lower than that of the specimens with stainless steel in the top mat, as shown in Figures 58b and 58c. For the 2304 and mixed

Conv./2304 and 2304/Conv. specimens, those with higher corrosion rates (Conv. and Conv./2304) show the most negative corrosion potentials once the specimens initiate corrosion, with these potential ranging between –0.51 and –0.63 V. For the 2304 and 2304/Conv. specimens, top-mat potentials have remained more positive, with no value more negative than –-0.30 V for 2304/Conv. at 13 weeks. No 2304 or 2304/Conv. specimen has initiated corrosion to date. The same trends can be seen in Figure 58c for specimens with SSClad reinforcement. Again, the Conv. and Conv./SSClad specimens show the lowest potentials throughout the test. Four of the six damaged stainless steel clad specimens, SSClad-4h, have initiated corrosion and are currently exhibiting the next lowest potentials. SSClad, SSClad-b, and SSClad/Conv. specimens have not yet initiated corrosion and do not have potentials lower than –0.30 V.

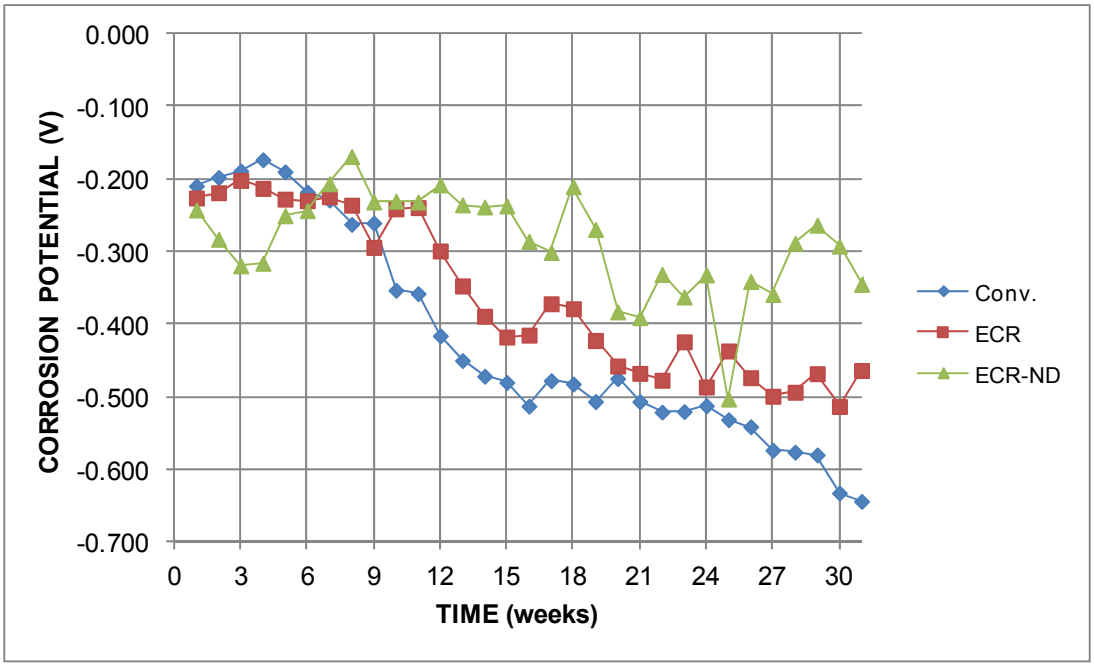

Figure 58a: Average top-mat potentials with respect to CSE for Southern Exposure specimens with conventional and epoxy-coated reinforcement.

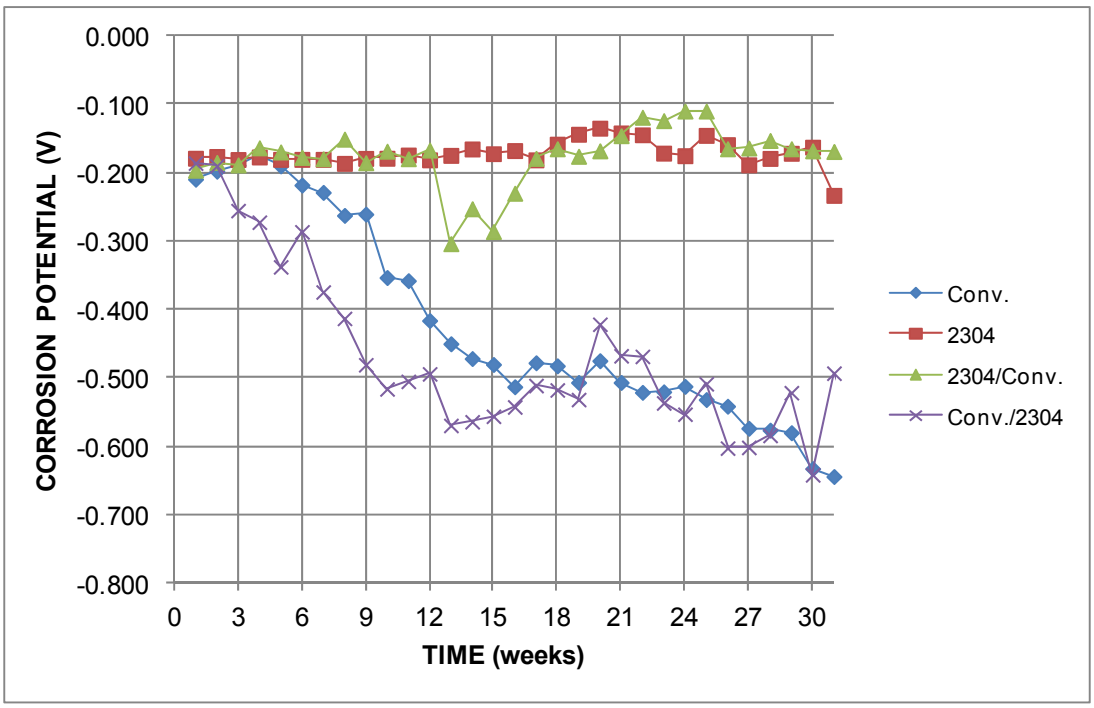

Figure 58b: Average top-mat potentials with respect to CSE for Southern Exposure specimens with conventional and 2304 stainless steel reinforcement.

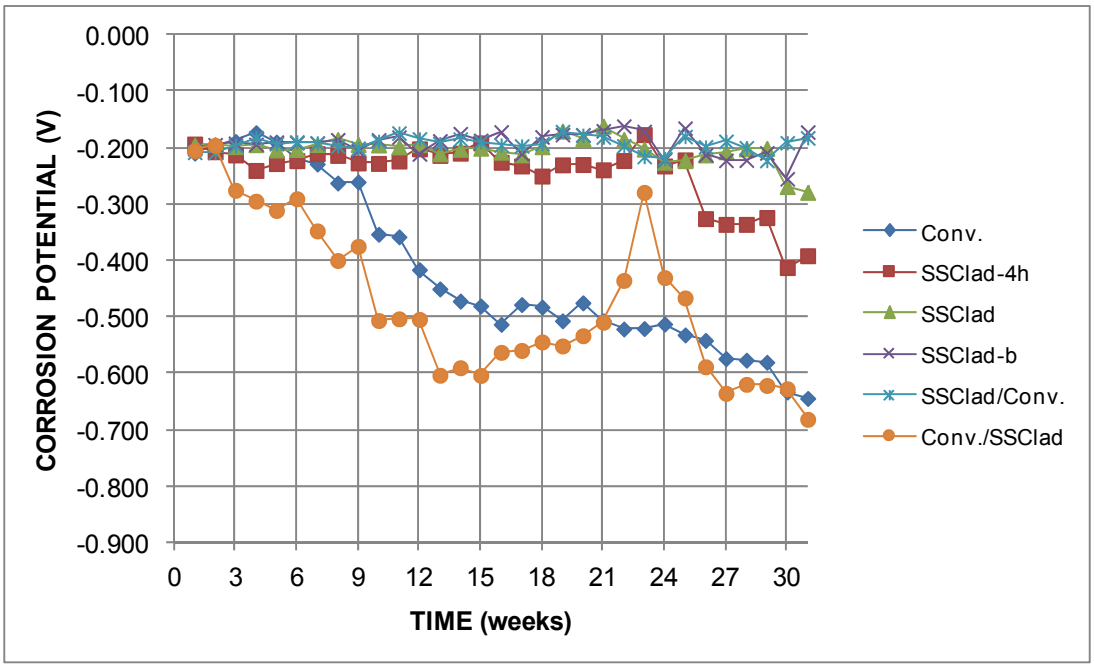

Figure 58c: Average top-mat potentials with respect to CSE for Southern Exposure specimens with conventional and stainless steel clad reinforcement.

The cracked beam top-mat potentials are shown in Figure 59. As for the Southern Exposure specimens, conventional reinforcement and damaged epoxy-coated reinforcement exhibit the most negative corrosion potentials throughout the test. The ECR specimens exhibit the lowest average potential, –0.63 V, at 31 weeks, followed by the Conv. specimens at -0.59 V The potentials for the ECR-ND specimens are higher than for the ECR and Conv. specimens but have been below –0.30 V since week 14. The potentials for the 2304 and SSClad specimens have been similar throughout the test, with values above –0.30 V. At 31 weeks, the SSClad and 2304 specimens exhibit corrosion potentials of –0.20 V and –0.17 V, respectively.

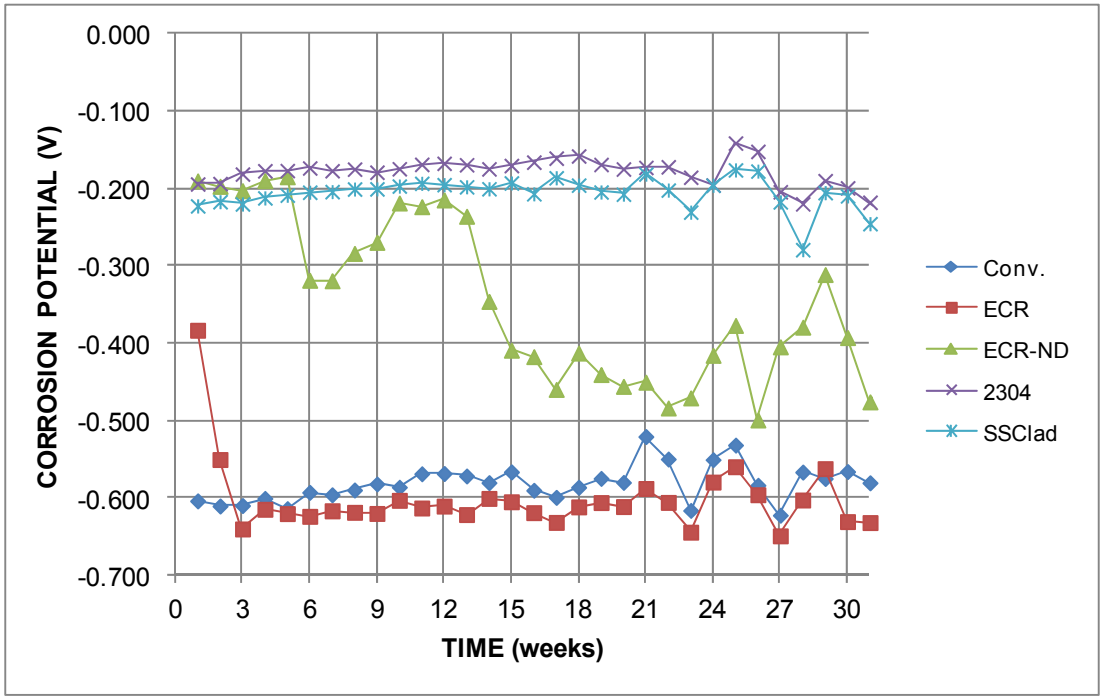

Figure 59: Average top-mat potentials with respect to CSE for cracked beam specimens.

The bottom-mat corrosion potentials are typically more positive than the top-mat potentials for all specimens, indicating a greater tendency to corrode in the top mat. For conventional and epoxy-coated reinforcement, shown in Figure 60a, the average bottom-mat potentials have exhibited similar values through week 31 with the exception of ECR-ND at week 26, where the average bottom-mat potential was –0.56 V.

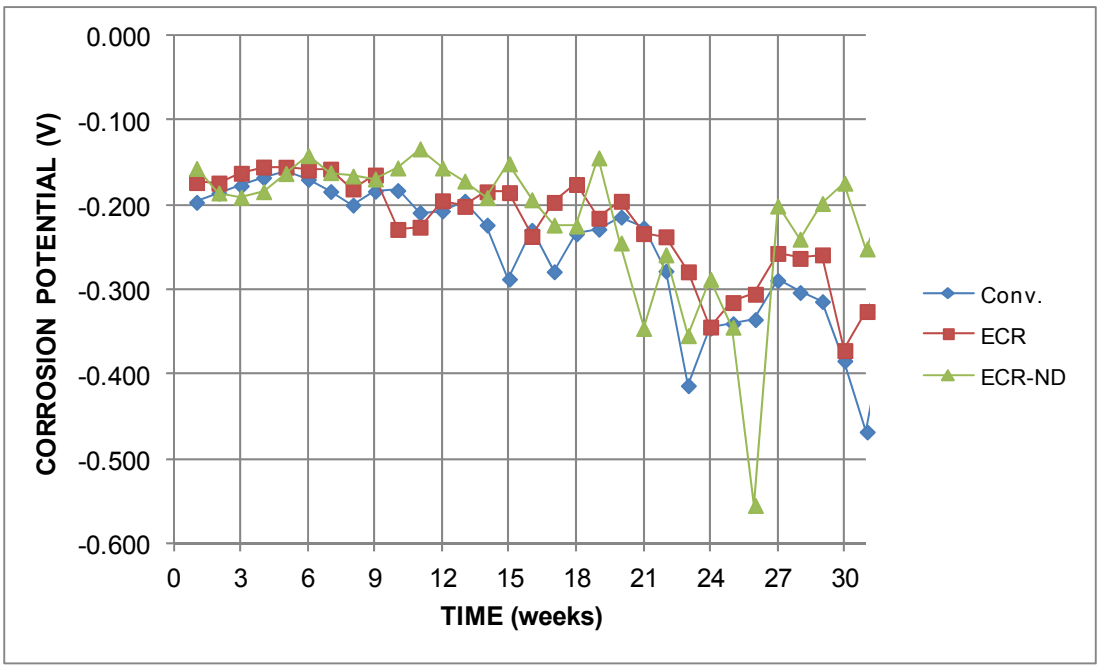

Figure 60a: Average bottom-mat potentials with respect to CSE Southern Exposure specimens with conventional and epoxy-coated reinforcement.

For the stainless steel specimens, the average bottom-mat potentials have remained in roughly the same range through week 31, as shown in Figures 60b and 60c. The bottom-mat potentials for the 2304 and SSClad specimens have remained higher than those of the Conv. specimens throughout tests.

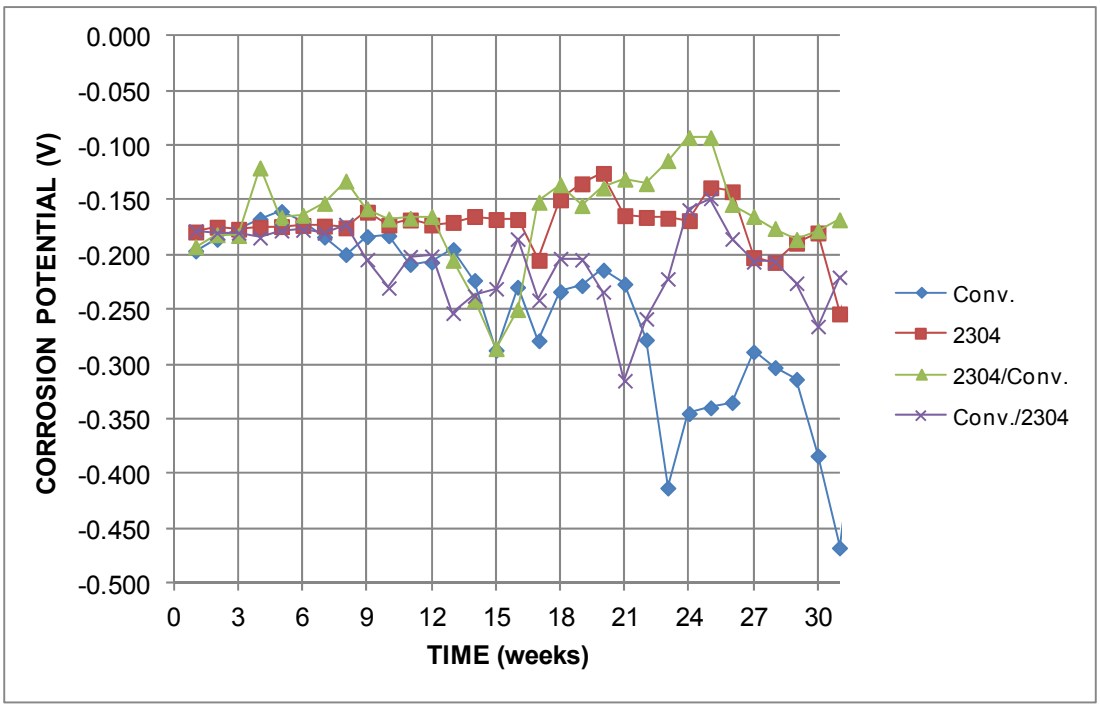

Figure 60b: Average bottom-mat potentials with respect to CSE Southern Exposure specimens with conventional and 2304 stainless steel reinforcement.

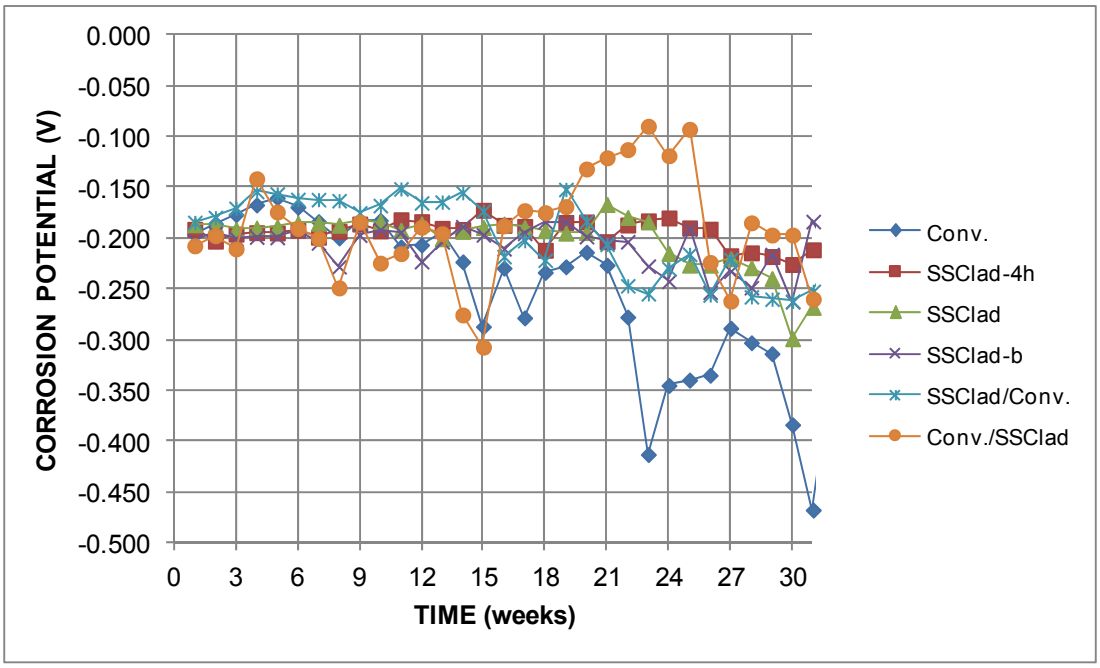

Figure 60c: Average bottom-mat potentials with respect to CSE Southern Exposure specimens with conventional and stainless steel clad reinforcement.

The average bottom-mat potentials for the cracked beam specimens are shown in Figure 61. As for the Southern Exposure specimens, the 2304 and SSClad specimens currently have the highest (most positive) average potentials. Also as observed for top mat, the potentials for the SSClad specimens are slightly lower than those for the 2304 specimens. These potentials are also close in value to top-mat potentials. For Conv., ECR, and ECR-ND specimens, average values are closely grouped and are generally on the order of – 0.10 to –0.20 V lower than those of the stainless steel specimens. Top and bottom mat potentials for each individual specimen is plotted in Appendix C.

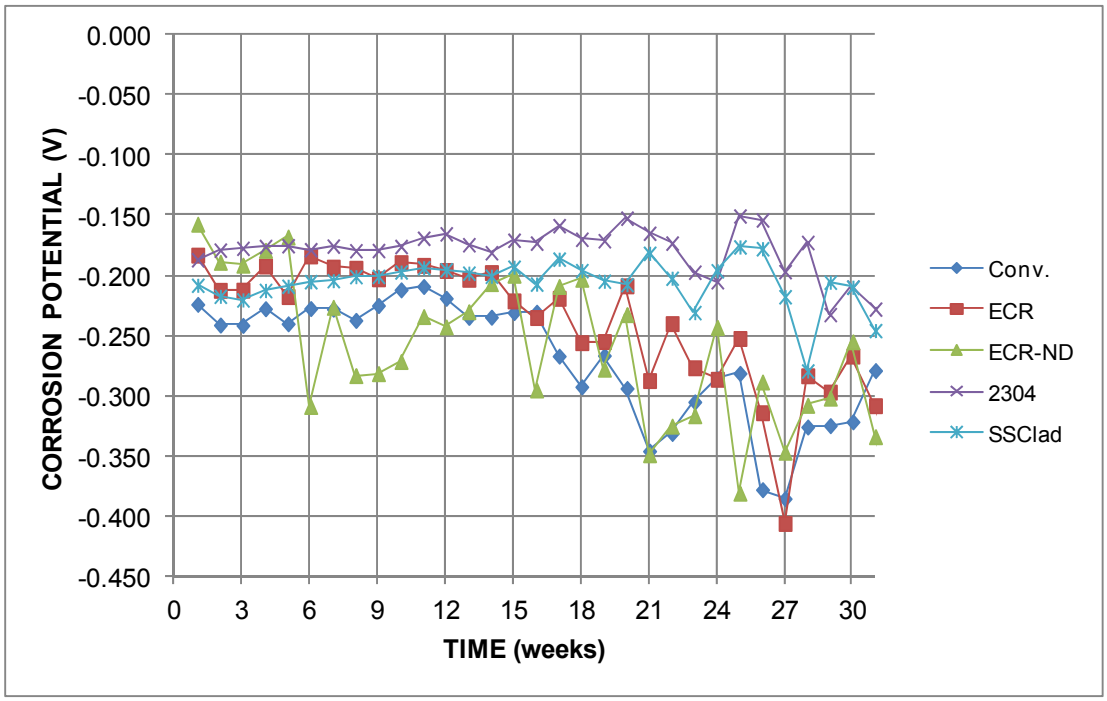

Figure 61: Average bottom-mat potentials with respect to CSE for cracked beam specimens.

4.2.4 Corrosion rates

ASTM A955 specifies that individual stainless steel cracked beam specimens must have corrosion rates no greater than 0.5 µm/yr and the average corrosion rate may not exceed 0.2 µm/yr. The individual corrosion rates for the cracked beam specimens with 2304 and undamaged stainless steel clad reinforcement are shown in Figures 62a and 62b, respectively.

As shown in Figure 62a, two of the six 2304 specimens have exceeded the maximum allowable corrosion rate of 0.5 μm/yr. Specimen CB-2304-1 exhibited corrosion rates exceeding 0.5 μm/yr at weeks 4, 5, 7, 8, 12, 15, and 17, while specimen CB-2304-2 exhibited rates exceeding 0.5 μm/yr at weeks 4, 5, and 29. For weeks 30-36, the corrosion rates for all 2304 specimens have been below 0.5 μm/yr. The average corrosion rates for the 2304 specimens exceeded 0.2 μm/yr at week 4 and have since remained below this limit.

The corrosion rates for the cracked beam specimens with stainless steel clad reinforcement are shown in Figure 62b. Specimen SSClad-1 exhibited a corrosion rate greater than 0.5 μm/yr at week 5 and equal to 0.5 μm/yr at week 15. This specimen has since shown a corrosion rate no higher than 0.27 μm/yr. Specimen SSClad-4 exhibited corrosion rates exceeding 0.5 μm/yr for weeks 27 through 30. However, upon investigation and replacement of the anode electrical connection at the terminal box at week 31, corrosion rates have since dropped to values near zero. Thus, the high rates exhibited by specimen SSClad-4 are considered invalid. With the exception of this specimen, the average corrosion rate has remained below 0.2 μm/yr throughout the test. Corrosion rate plots for all other individual specimens are included in Appendix C.

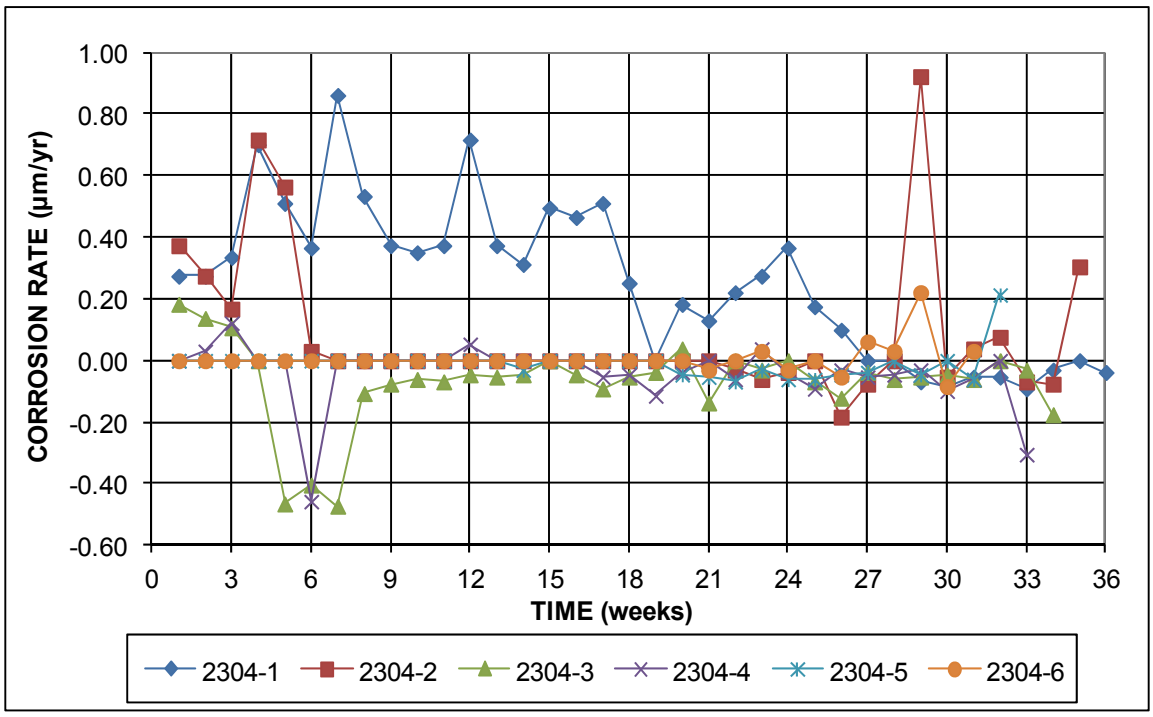

Figure 62a: Individual corrosion rates (µm/yr) based on total area for cracked beam specimens with 2304 reinforcement.

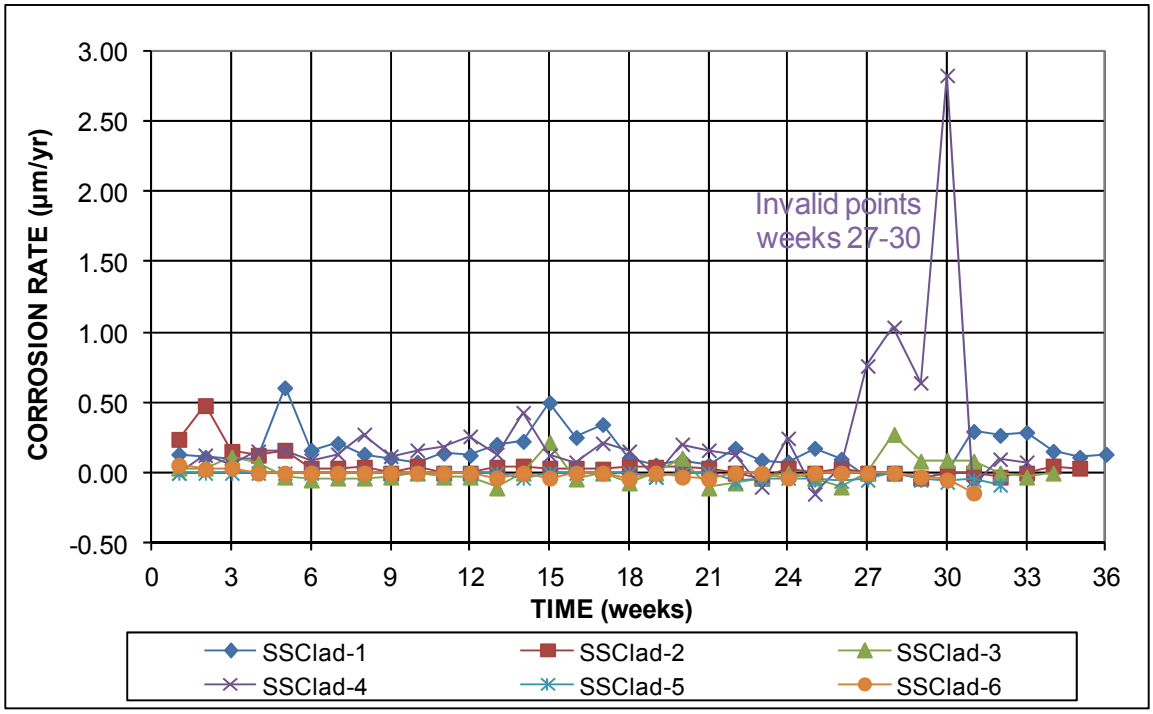

Figure 62b: Individual corrosion rates (µm/yr) based on total area for cracked beam specimens with stainless steel clad reinforcement

4.2.5 Critical Chloride Threshold for Southern Exposure Specimens

At the time of corrosion initiation, Southern Exposure specimens are sampled for chloride content. Tables 10a-10e give the individual and average chloride contents and ages at corrosion initiation. Table 10a shows the results for the specimens with conventional bars. The average time to initiation for the Conv. specimens is 12.5 weeks at an average chloride content of 1.78 lb/yd^3 with a standard deviation of 1.31 lb/yd^3. Initiation ages ranged from 9 to 18 weeks. Average chloride contents for individual specimens ranged from 1.14 to 2.78 lb/yd^3. Table 10b shows results for the mixed Conv./2304 specimens. The average time to initiation was 8.0 weeks with an average chloride content of 1.76 lb/yd^3 and a standard deviation of 1.13 lb/yd^3. Initiation ages ranged between 5 and 11 weeks, and the average chloride contents for individual specimens ranged from 0.88 to 2.42 lb/yd^3. Table 10c shows results for the mixed Conv./SSClad specimens. The average time to initiation was 9.3 weeks with an average of chloride content of 1.59 lb/yd^3 and standard deviation of 1.19 lb/yd^3. The ages of initiation for these specimens are 8 and 10 weeks. The average chloride contents for individual specimens ranged from 1.10 to 2.13 lb/yd^3.

Table 10a: Chloride contents for specimens with conventional reinforcement

Specimen	Initiation Age (weeks)	Chloride Content (lb/yd^3)						Average	Standard Deviation
		1	2	3	4	5	6		
Conv.-1	16	3.91	2.78	2.02	0.63	0.57	4.82	2.45	1.80
Conv.-2	18	1.69	0.50	2.59	1.64	0.44	1.14	1.33	1.41
Conv.-3	10	1.01	1.70	1.39	1.14	0.88	0.76	1.15	0.60
Conv.-4	10	3.03 2.59	0.44 0.63	2.33 2.02	0.38 0.32	1.58	2.02	1.53	1.02
Conv.-5	9	1.45	3.41	2.02	0.57	0.76	0.44	1.44	1.13
Conv.-6	12	6.43	0.32	1.27	5.43	2.78	0.44	2.78	2.04
Average	12.5							**1.78**	**1.31**

Table 10b: Chloride contents for specimens with conventional (top) and 2304 (bottom) reinforcement

Specimen	Initiation Age (weeks)	Chloride Content (lb/yd^3)						Average	Standard Deviation
		1	2	3	4	5	6		
Conv./2304-1	5	0.99	0.74	0.52	1.54	1.14	0.35	0.88	0.43
Conv./2304-2	11	5.11	2.08	1.45	1.15	1.01	1.14	1.99	1.58
Conv./2304-3	8	1.14	3.09	2.02	4.04	0.63	3.60	2.42	1.38
Average	8.0							**1.76**	**1.13**

Table 10c: Chloride contents for specimens with conventional (top) and stainless steel clad (bottom) reinforcement

Specimen	Initiation Age (weeks)	Chloride Content (lb/yd^3)						Average	Standard Deviation
		1	2	3	4	5	6		
Conv./SSClad-1	8	0.99	0.74	1.17	1.54	1.14	1.05	1.10	0.26
Conv./SSClad-2	10	3.03 3.91	0.44 0.63	2.33 0.69	0.38 0.50	1.58	2.02	1.53	1.02
Conv./SSClad-3	10	4.04 2.59	0.50 0.63	0.63 2.02	0.19 0.32	6.25	0.25	2.13	2.28
Average	9.3							**1.59**	**1.19**

Specimens containing coated reinforcement have shown longer times to initiation and higher chloride contents at initiation. Table 10d shows the results for epoxy-coated reinforcement. These specimens have initiation ages between 13 and 26 weeks with an average of 16.5 weeks. The average chloride content was 4.59 lb/yd^3 with a standard deviation of 2.33 lb/yd^3. The average chloride contents for individual specimens range from 2.14 to 7.98 lb/yd^3. The specimens with damaged stainless steel cladding show an average initiation time of 20.8 weeks. Specimens SSClad-4h-2 and SSClad-4h-1 have not yet initiated. The average chloride content is 7.37 lb/yd^3 with a standard deviation of 2.33 lb/yd^3. The average chloride contents for individual specimens range from 3.56 to 11.76 lb/yd^3. None of the undamaged and bent stainless steel clad or 2304 specimens have initiated corrosion.

Previous studies conducted at KU (O'Reilly et al. 2011, Darwin et al. 2009, Draper et al. 2009) have shown average chloride contents for specimens with conventional reinforcement of 1.68, 1.63, and 1.81 lb/yd^3 (1.00, 0.967, and 1.07 kg/m^3). These values are similar to those observed in this study. Damaged epoxy-coated reinforcement has shown average chloride thresholds between 7.30 and 10.30 lb/yd^3 (4.33 and 0.77 kg/m^3) in the earlier studies, about twice the average value observed in this study.

Table 10d: Chloride contents for specimens with epoxy-coated reinforcement

Specimen	Initiation Age (weeks)	Chloride Content (lb/yd^3)						Average	Standard Deviation
		1	2	3	4	5	6		
ECR-1	26	5.83	6.69	12.5	8.20	7.89	6.75	7.98	2.38
ECR-2	12	4.82	2.14	5.11	1.45	1.14	3.15	2.97	1.70
ECR-3	14	1.26	5.49	6.50	5.39	2.50	3.22	4.06	2.04
ECR-4	20	6.24	15.3	3.56	4.23	5.75	3.11	6.37	4.56
ECR-5	13	1.39	1.64	0.57	2.02	2.84	4.42	2.14	1.34
ECR-6	14	2.75	6.67	3.37	1.26	5.24	4.98	4.05	1.95
Average	16.5							**4.59**	**2.33**

Table 10e: Chloride contents for specimens with damaged stainless steel clad reinforcement

Specimen	Initiation Age (weeks)	Chloride Content (lb/yd^3)						Average	Standard Deviation
		1	2	3	4	5	6		
SSClad-4h-3	24	3.03	4.04	6.44	9.78	9.97	8.16	6.90	2.92
SSClad-4h-4	17	1.03	2.90	3.03	14.5	4.03	1.89	4.57	5.00
SSClad-4h-5	26	10.0 9.15	9.72 10.0	9.15 10.7	10.9 9.34	11.8	9.65	10.07	0.87
SSClad-4h-6	27	14.1 12.2	14.7 12.8	9.34 11.8	13.7 12.8	9.34	6.50	11.76	2.60
SSClad-4h-7	10	4.54 6.06	2.14 4.73	3.34 6.12	3.66 1.45	1.58	1.96	3.56	1.77
Average	20.8							**7.37**	**2.63**

5. SUMMARY AND CONCLUSIONS

The corrosion performance of 2304 duplex stainless steel reinforcement and NX-SCR™ stainless steel clad reinforcement was tested using the rapid macrocell, Southern Exposure, and cracked beam tests. The 2304 duplex stainless steel was evaluated in the as-received condition and after re-pickling in the macrocell tests. The NX-SCR™ stainless steel clad reinforcement was evaluated in the undamaged and damaged (0.83% damaged area) conditions and without a cap to protect the inner conventional steel core in the rapid macrocell test, in the undamaged condition in the Southern Exposure and cracked beam tests (known as bench-scale tests), and in the damaged condition (0.2% damaged area) in the Southern Exposure tests, and as a bent bar in the rapid macrocell and Southern Exposure tests. The performance of both steels was compared with that of epoxy-coated reinforcement in the damaged (0.83% damaged area for macrocells, 0.5% damaged area for bench-scale) and undamaged conditions and with conventional reinforcing steel. Tests of mixed specimens containing both stainless steel and conventional bars as either the anode or the cathode to evaluate possible galvanic effects were also performed. For specimens that initiated corrosion, the chloride content at the level of top reinforcement in the Southern Exposure specimens was also measured at the time of corrosion initiation. The results of the rapid macrocell and cracked beam tests are used to evaluate the stainless steel bars in accordance with the requirements of ASTM A955.

The following conclusions are based on the results and analyses presented in this report:

Rapid Macrocell Test

1. Epoxy-coated reinforcement exhibits a significant increase in corrosion resistance compared to conventional steel.

2. In the as-received condition, 2304 stainless steel did not satisfy the requirements of ASTM A955 – although it did exhibit an average corrosion rate below 0.25 μm/yr, the corrosion rate of individual specimens exceeded 0.50 μm/yr.
3. The re-pickled 2304 stainless steel satisfied the requirements of ASTM A955, with an average corrosion rate not exceeding 0.25 μm/yr and the corrosion rate of the individual specimens not exceeding 0.50 μm/yr.
4. The undamaged, capped NX-SCR^{TM} stainless steel clad bars satisfied the requirements of ASTM A955.
5. The ends of stainless steel clad bars must be protected by a protective cap to prevent corrosion of the conventional steel core.
6. Based on macrocell corrosion rates, the bent NX-SCR^{TM} stainless steel clad bars satisfied the requirements of ASTM A955.
7. The damaged NX-SCR^{TM} stainless steel clad bars exhibited measurable corrosion.
8. The macrocell corrosion rates of the mixed specimens containing NX-SCR^{TM} stainless steel clad bars and conventional reinforcement were driven by the corrosion resistance of the anode; the cathode material had little effect on the corrosion rate.
9. The macrocell corrosion rates of the mixed specimens containing 2304 stainless steel and conventional reinforcement were principally driven by the corrosion resistance of the anode; however, significant corrosion occurred in one of the specimens, thus increasing the average corrosion rate.
10. 2304 stainless steel in the as-received and re-pickled conditions and NX-SCR^{TM} stainless steel clad bars provide for a significant increase in corrosion performance when compared to conventional reinforcing steel.

Bench-Scale Tests

11. The corrosion loss exhibited by conventional reinforcement exceeds that of the other systems evaluated in the study.
12. Specimens with conventional reinforcement as top bars and stainless steel bars as bottom bars show greater average corrosion rates and losses than conventional reinforcement alone.
13. The specimens with conventional reinforcement as the top bars (Conv., Conv./2304 and Conv./SSClad) exhibit similar average chloride contents at corrosion initiation.
14. Epoxy-coated reinforcement with ten 1/8-in. (3.2-mm) holes through the epoxy on each bar exhibits a higher critical chloride corrosion threshold than does conventional reinforcement.
15. NX-SCR™ reinforcement with four 1/8-in. (3.2-mm) holes through the epoxy on each bar exhibits a higher critical chloride corrosion threshold than either the damaged epoxy-coated reinforcement or conventional reinforcement.
16. To date, the 2304, bent stainless steel clad, and undamaged NX-SCR™ stainless steel clad specimens exhibit no significant corrosion.
17. Some cracked-beam specimens containing 2304 duplex stainless steel in the as-received condition and NX-SCR™ stainless steel clad bars have exceeded the ASTM A955 requirements for maximum allowable corrosion rate.
18. Specimens containing damaged epoxy-coated bars exhibit higher corrosion rates than the stainless steel specimens.
19. Corrosion rates for 2304 and undamaged NX-SCR™ stainless steel clad specimens exhibit similar behavior in Southern Exposure and cracked beam tests.

20. Undamaged epoxy-coated specimens have exhibited the lowest corrosion rates to date.

6. REFERENCES

ASTM A775, 2007, "Epoxy-Coated Steel Reinforcing Bars (ASTM A955/A955M – 07b)," ASTM International, West Conshohocken, PA, 11 pp.

ASTM A955, 2010, "Standard Specification for Plain and Deformed Stainless-Steel Bars for Concrete Reinforcement (ASTM A955/A955M – 10)," ASTM International, West Conshohocken, PA, 11 pp.

Darwin, D., Browning, J.P., O'Reilly, M., Xing, L. and Ji, J., 2009, "Critical Chloride Corrosion Threshold of Galvanized Reinforcing Bars," *ACI Materials Journal*, Vol. 106, No. 2, March/April 2009, 8 pp.

Draper, J., Darwin, D., Browning, J., Locke, C. E., 2009, "Evaluation of Multiple Corrosion Protection Systems for Reinforced Concrete Bridge Decks," *SM Report* No. 96*,* University of Kansas Center for Research, Inc., Lawrence, Kansas, December 2009, 429 pp.

O'Reilly, M., Darwin, D., Browning, J.B., and Locke, C. E., "Evaluation of Multiple Corrosion Protected Systems for Reinforced Concrete Systems" *SM Report* No. 100, University of Kansas Center for Research, Inc., Lawrence, Kansas, January 2011, 535 pp.

Sturgeon, W. J., O'Reilly, M., Darwin, D., and Browning, J., "Rapid Macrocell Tests of ASTM A775, A615, and A1035 Reinforcing Bars" *SL Report* 10-4, University of Kansas Center for Research, Inc., Lawrence, Kansas, November 2010, 46 pp.

APPENDIX A: RAPID MACROCELL DATA
CORROSION RATES, CORROSION POTENTIALS FOR INDIVIDUAL SPECIMENS, AVERAGE CORROSION POTENTIALS, AND TOTAL CORROSION LOSSES

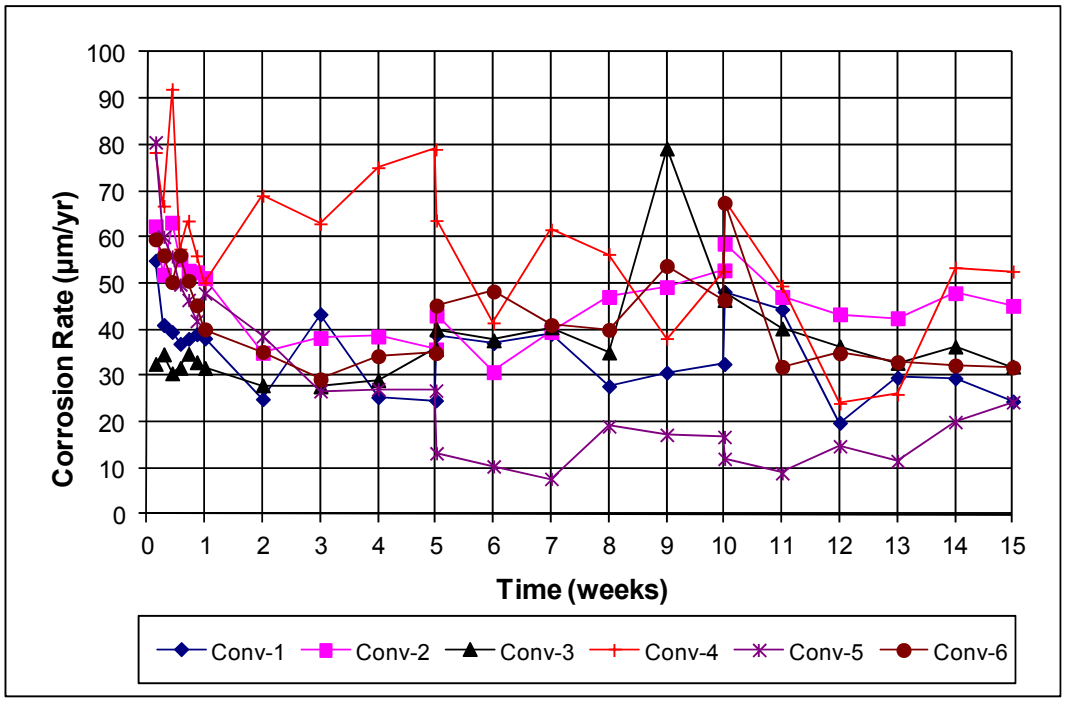

Figure A.1: Macrocell individual corrosion rate of conventional steel, specimens 1-6.

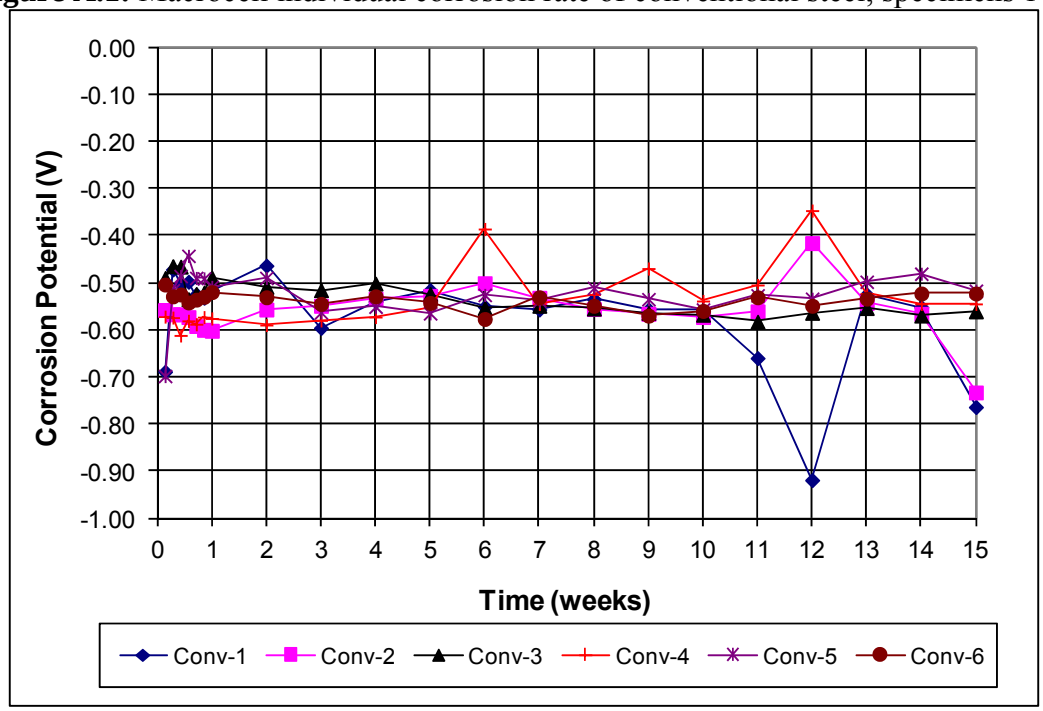

Figure A.2: Macrocell individual corrosion potentials with respect to SCE. Conventional steel bars in pore solution with salt (anode), specimens 1-6.

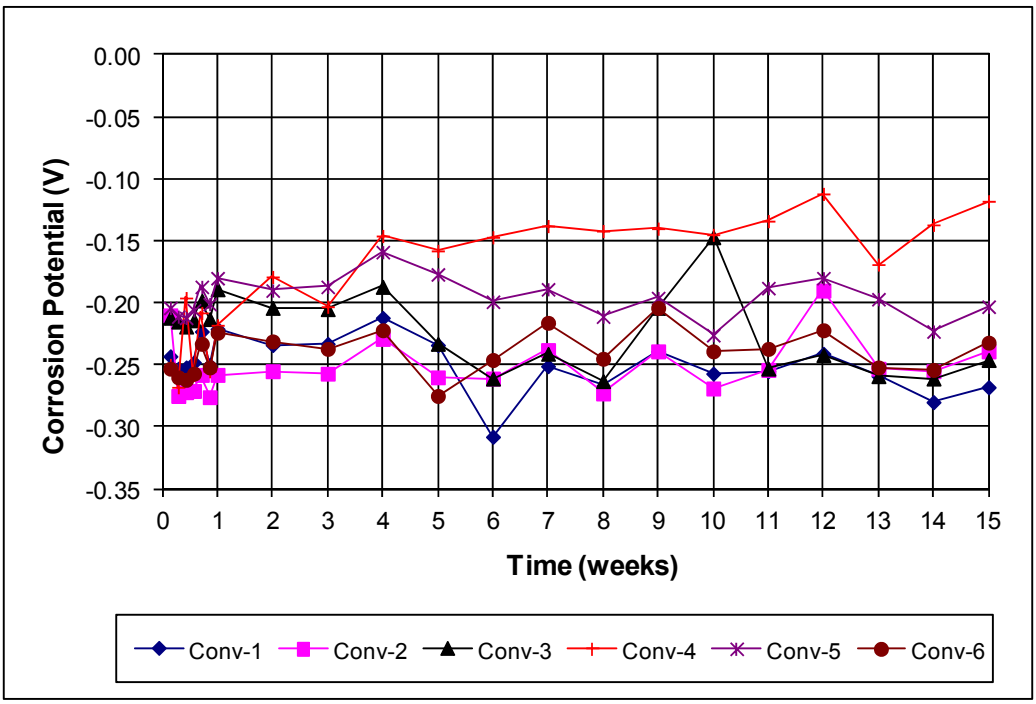

Figure A.3: Macrocell individual corrosion potentials with respect to SCE. Conventional steel bars in pore solution (cathode), specimens 1-6.

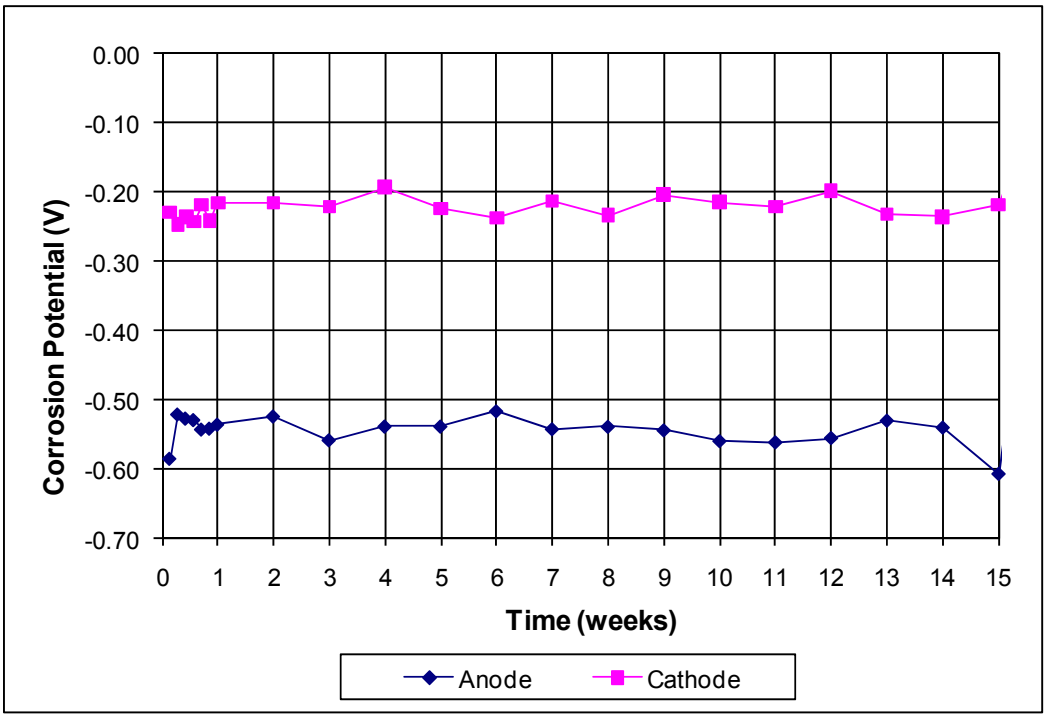

Figure A.4: Average corrosion potentials with respect to SCE. Conventional steel bars, specimens 1-6.

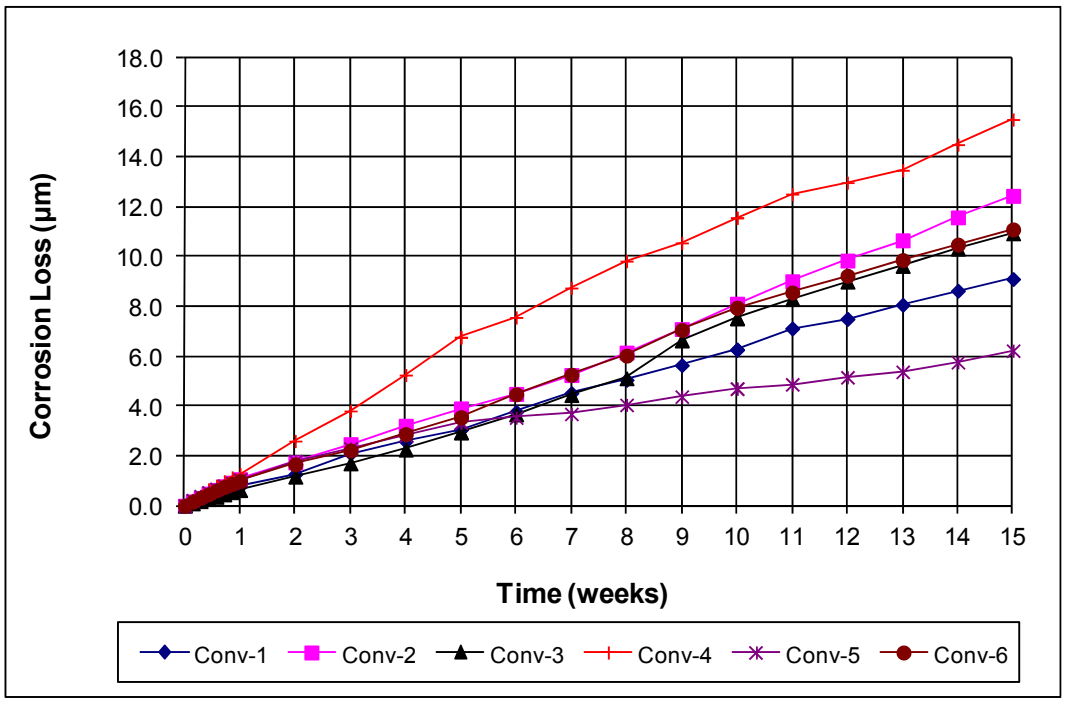

Figure A.5: Macrocell individual corrosion loss of conventional steel, specimens 1-6.

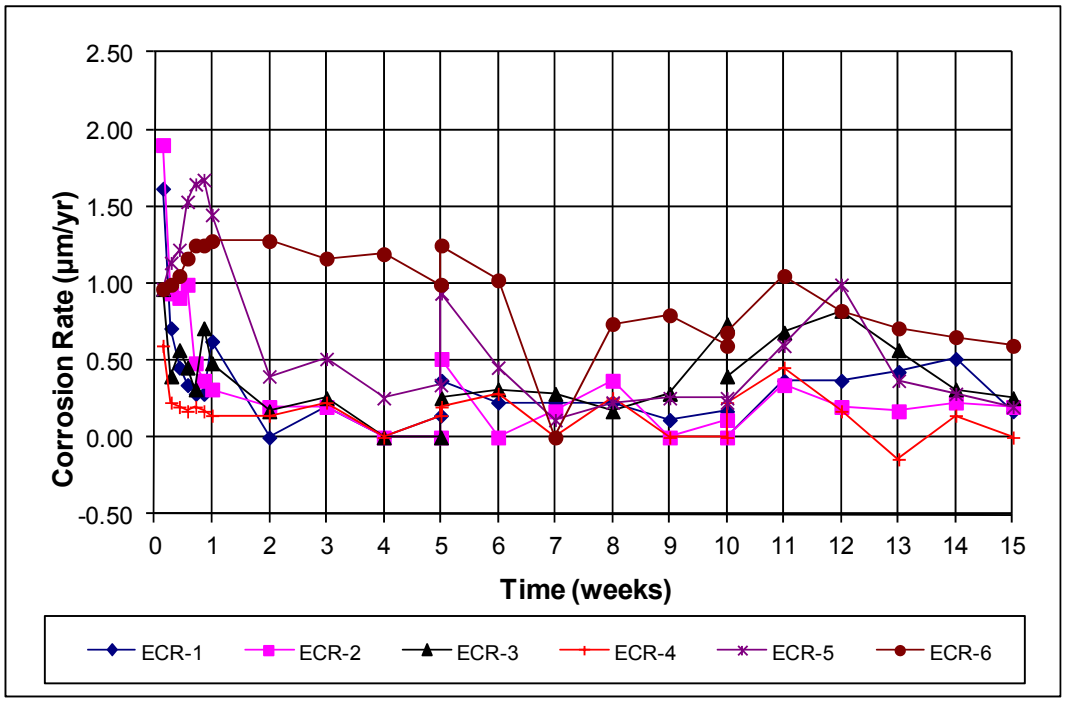

Figure A.6: Macrocell individual corrosion rates of 0.83% damaged area ECR, specimens 1-6.

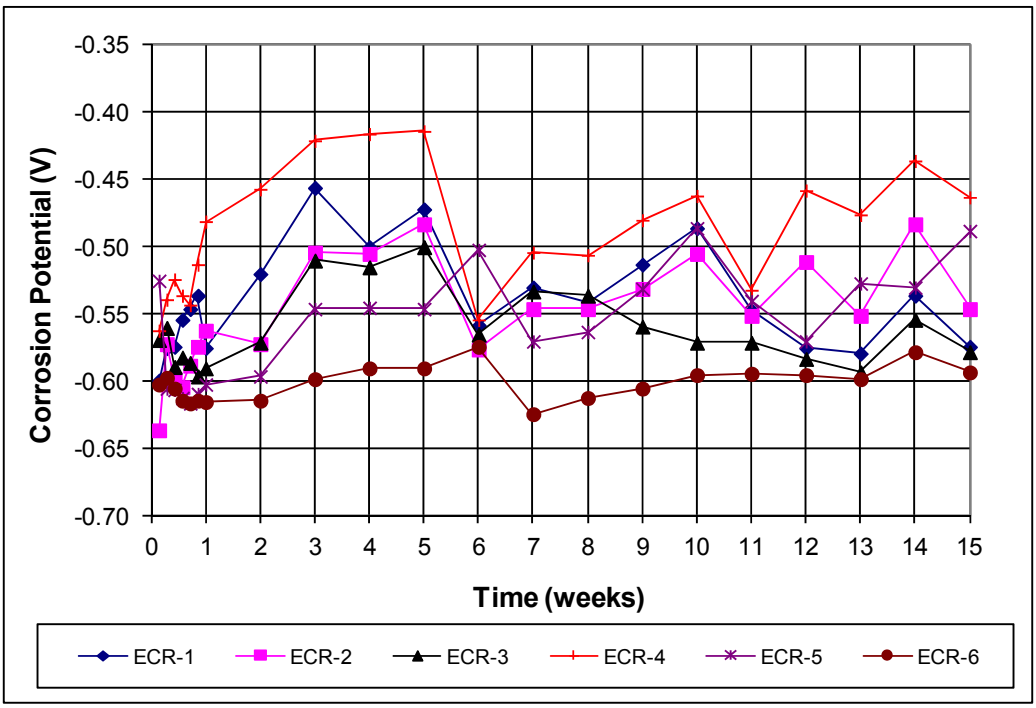

Figure A.7: Macrocell individual corrosion potentials with respect to SCE. 0.83% damaged area ECR in pore solution with salt (anode), specimens 1-6.

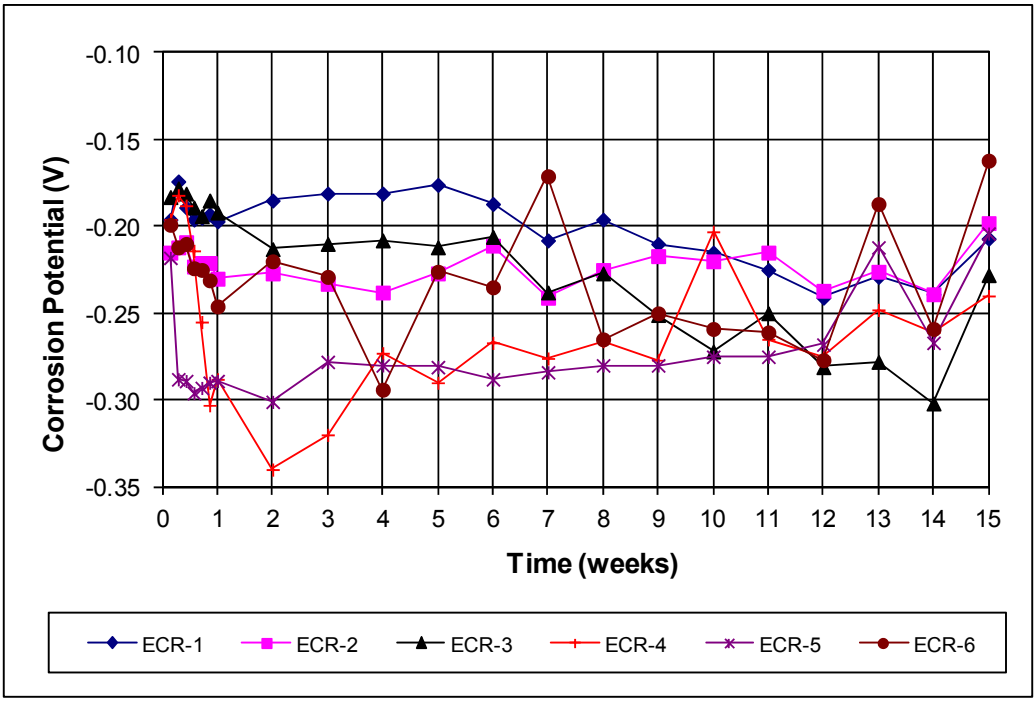

Figure A.8: Macrocell individual corrosion potentials with respect to SCE. 0.83% damaged area ECR in pore solution (cathode), specimens 1-6.

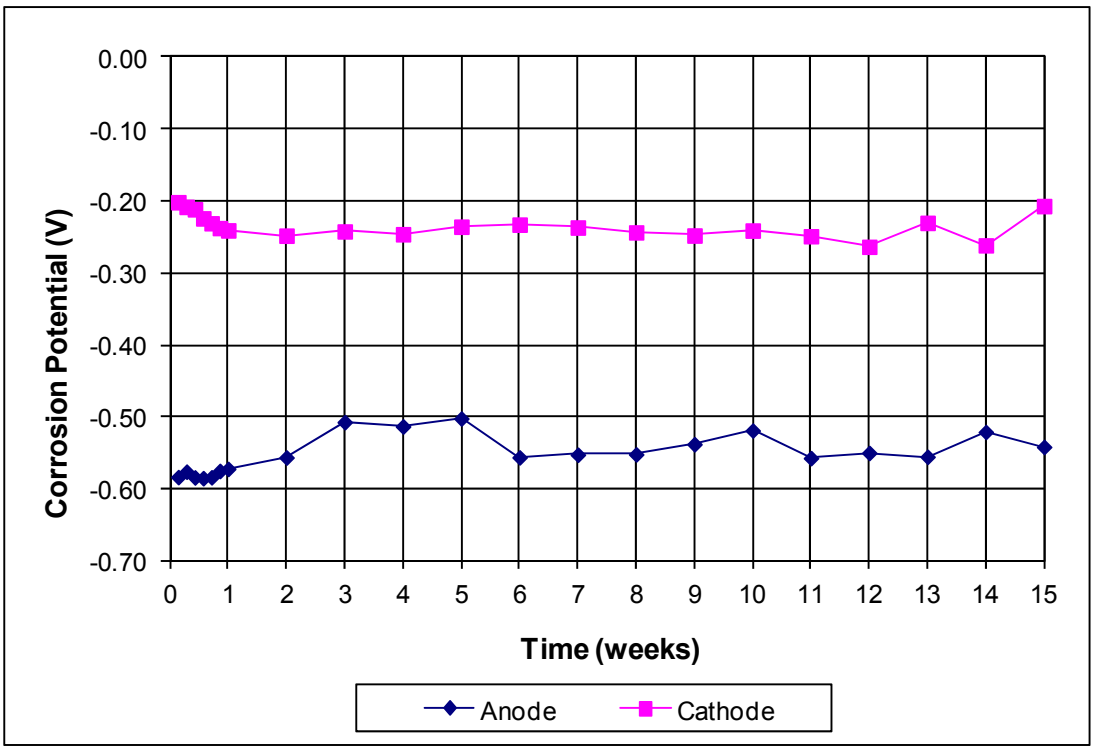

Figure A.9: Average corrosion potentials with respect to SCE. 0.83% damaged area ECR, specimens 1-6.

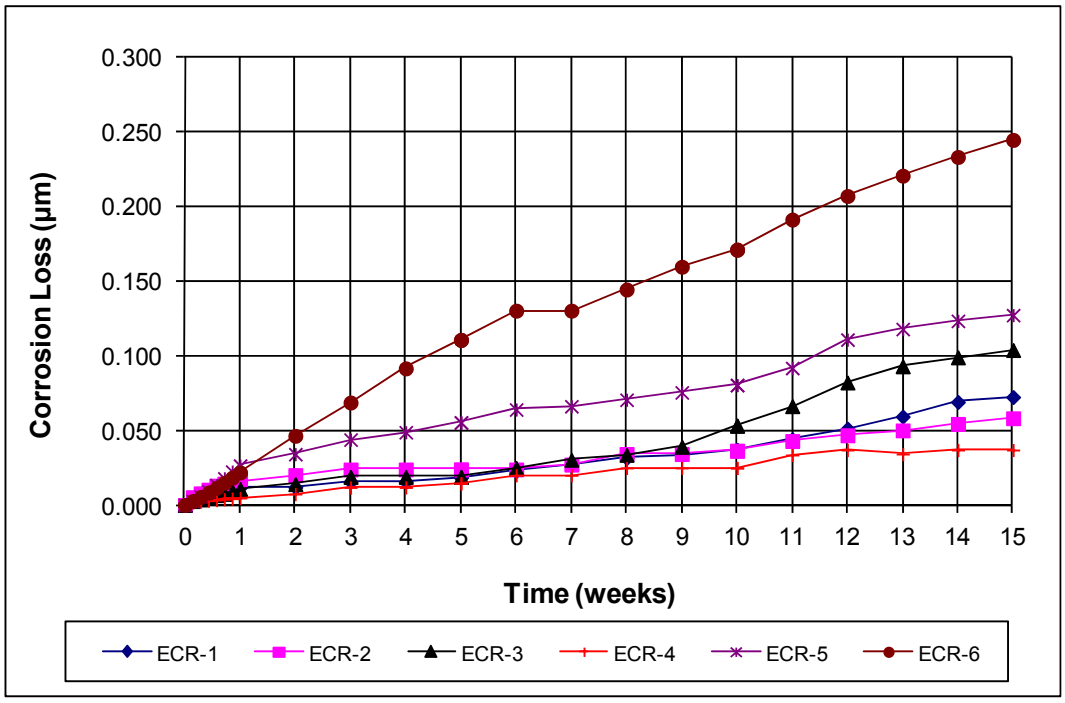

Figure A.10: Macrocell individual corrosion loss of 0.83% damaged area ECR, specimens 1-6.

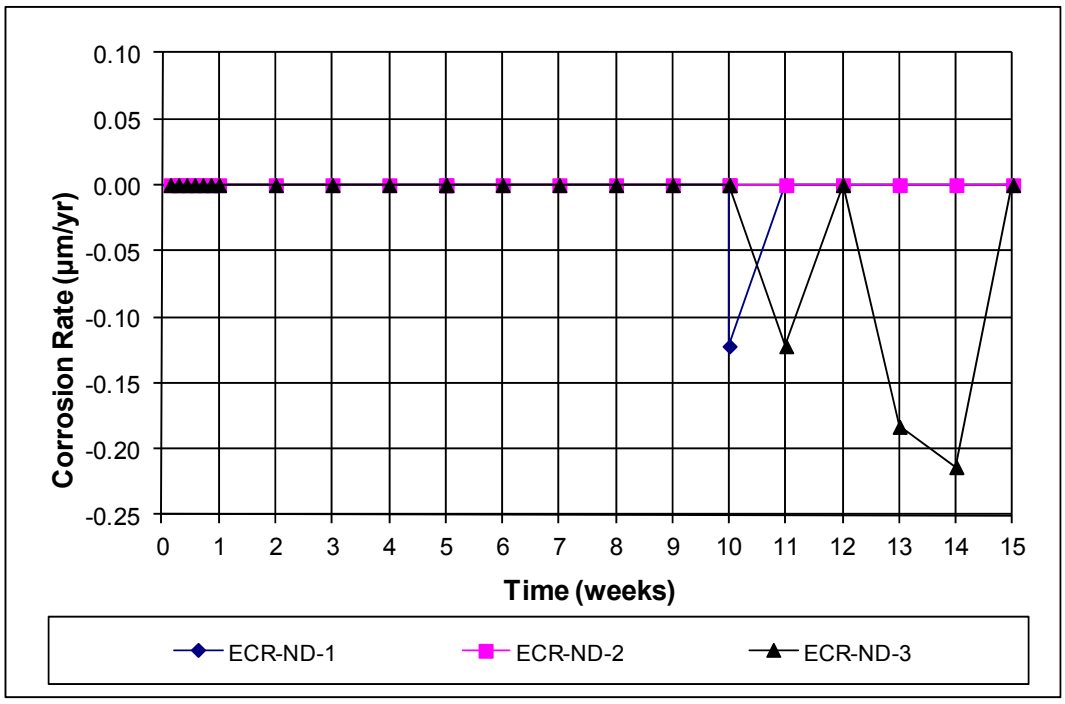

Figure A.11: Macrocell individual corrosion rates of undamaged ECR, specimens 1-6.

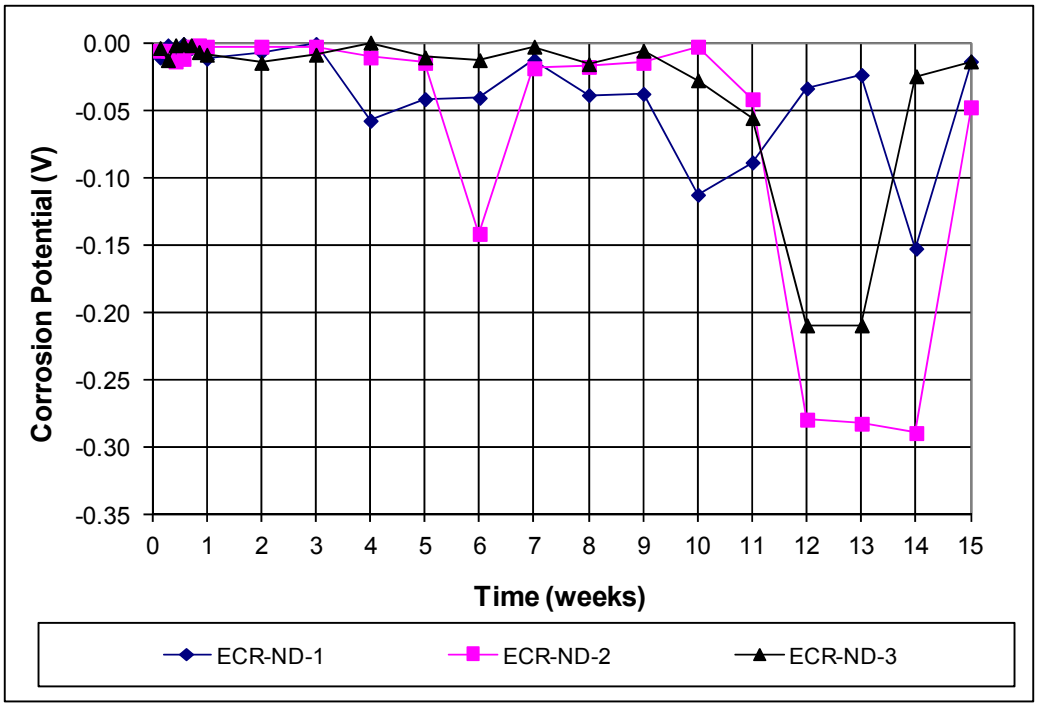

Figure A.12: Macrocell individual corrosion potentials with respect to SCE. Undamaged ECR in pore solution with salt (anode), specimens 1-6.

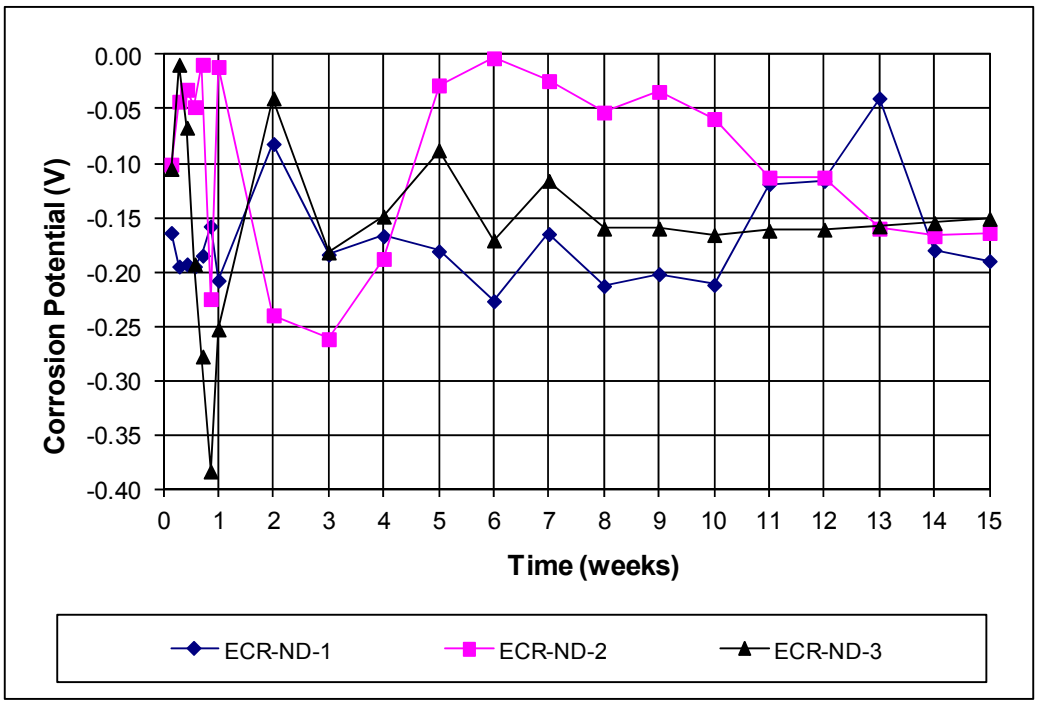

Figure A.13: Macrocell individual corrosion potentials with respect to SCE. Undamaged ECR in pore solution (cathode), specimens 1-6.

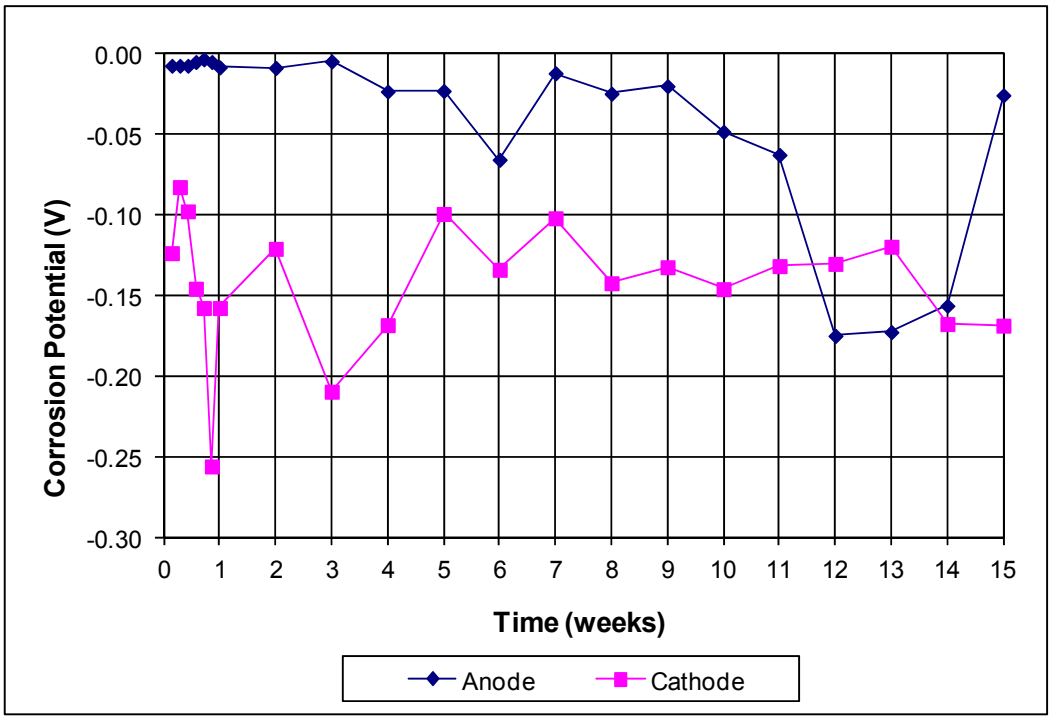

Figure A.14: Average corrosion potentials with respect to SCE. Undamaged ECR, specimens 1-6.

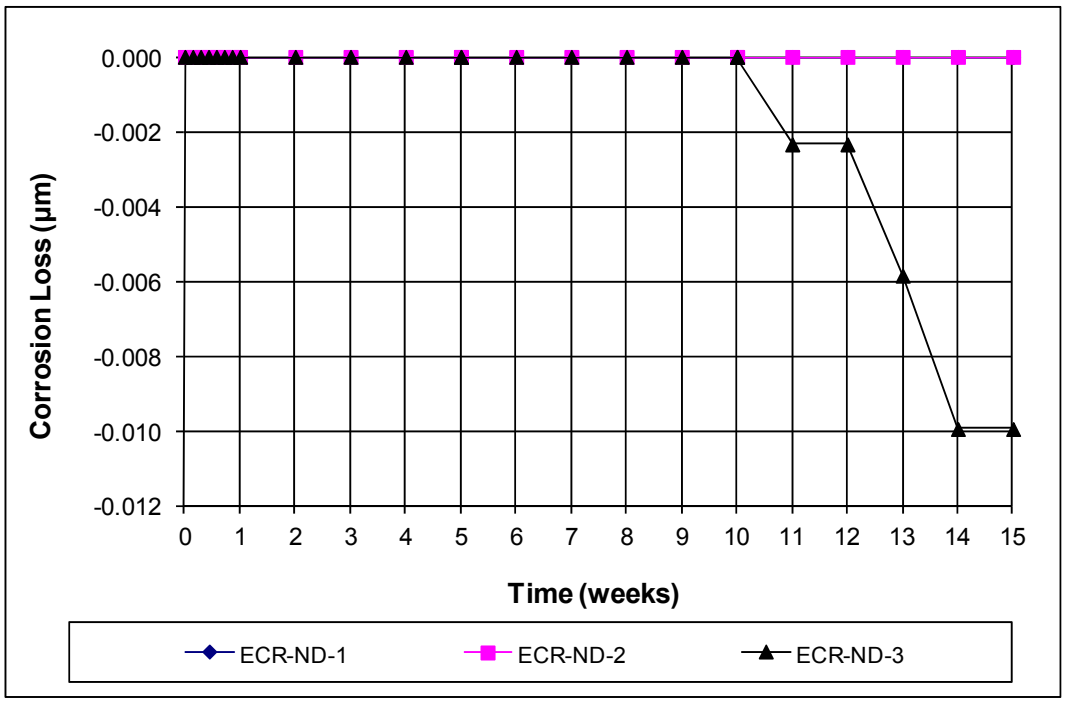

Figure A.15: Macrocell individual corrosion loss of undamaged ECR, specimens 1-3.

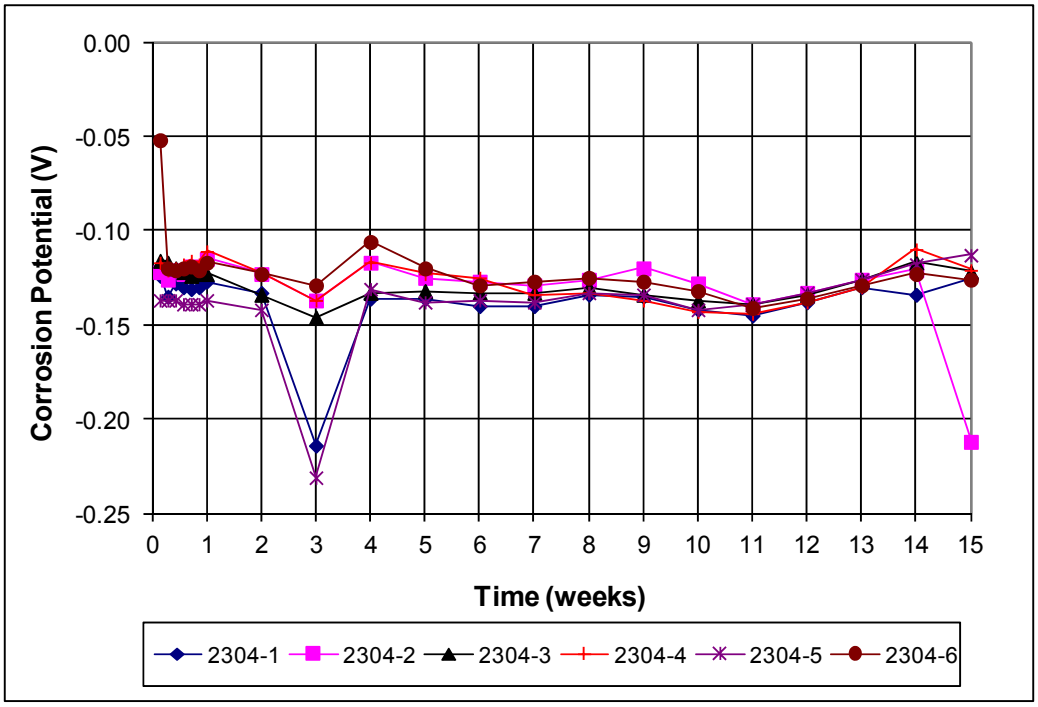

Figure A.16: Macrocell individual corrosion potentials with respect to SCE. 2304 stainless steel bars in pore solution with salt (anode), specimens 1-6.

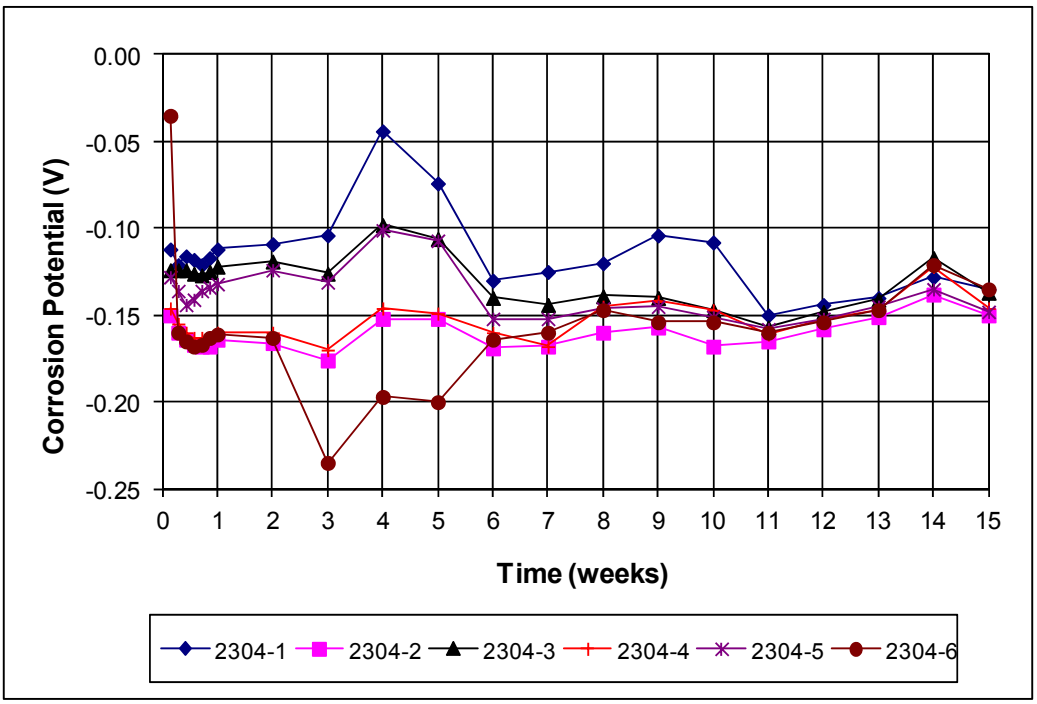

Figure A.17: Macrocell individual corrosion potentials with respect to SCE. 2304 stainless steel bars in pore solution (cathode), specimens 1-6.

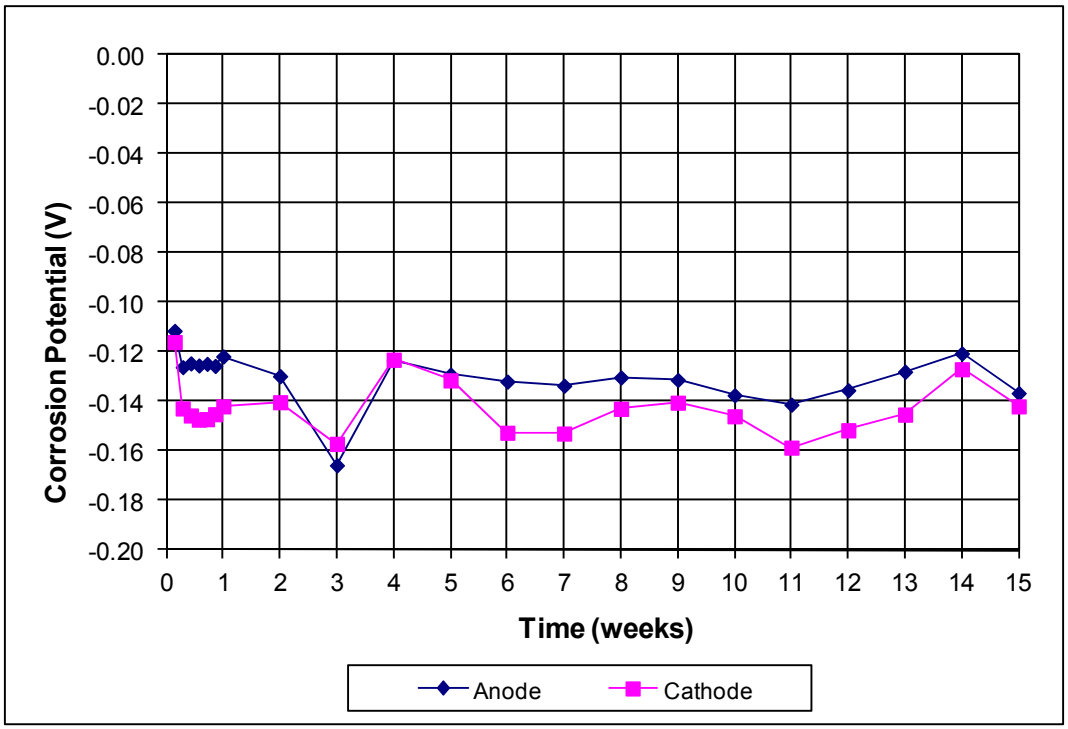

Figure A.18: Average corrosion potentials with respect to SCE. 2304 stainless steel bars, specimens 1-6.

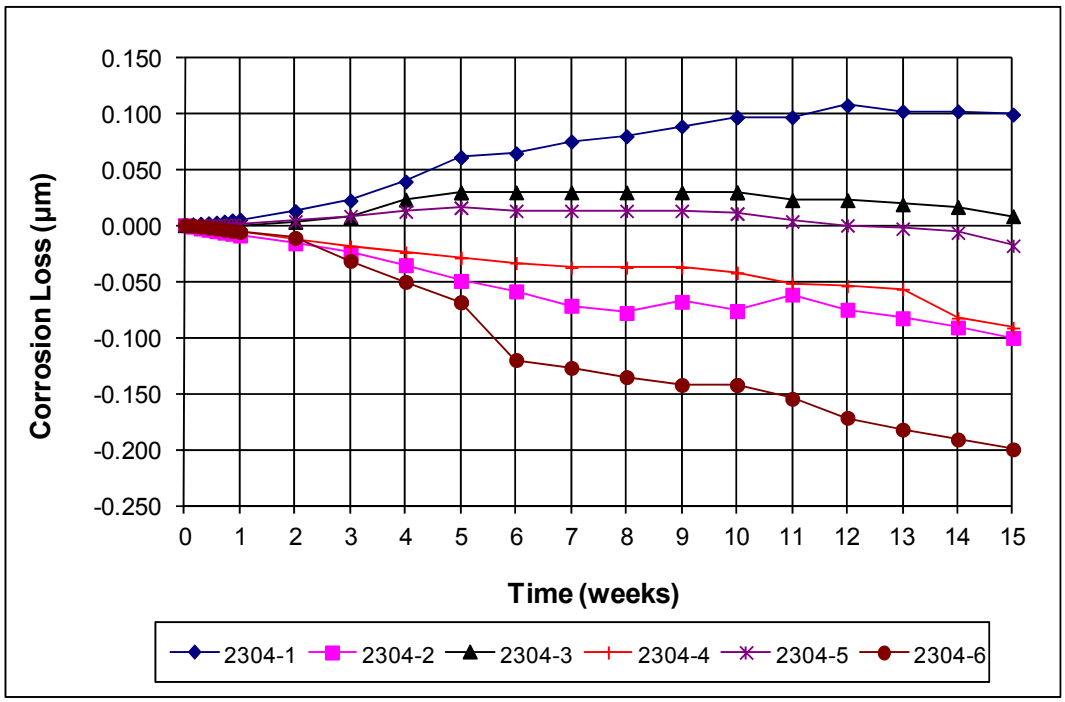

Figure A.19: Macrocell individual corrosion loss of 2304 stainless steel, specimens 1-6.

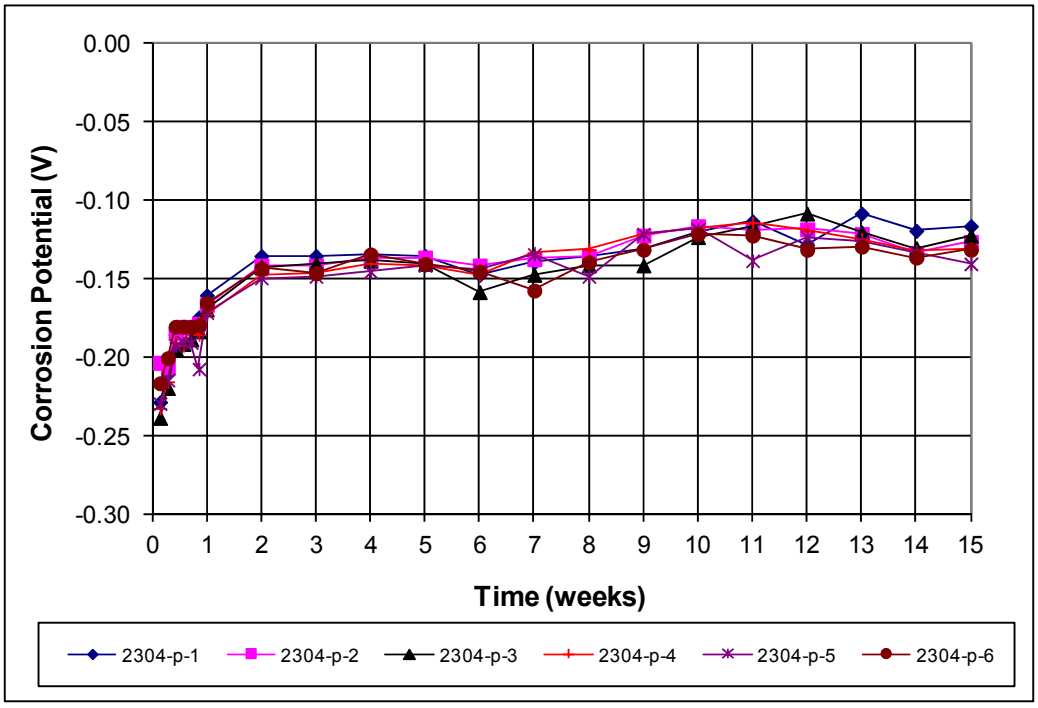

Figure A.20: Macrocell individual corrosion potentials with respect to SCE. Re-pickled 2304 stainless steel bars in pore solution with salt (anode), specimens 1-6.

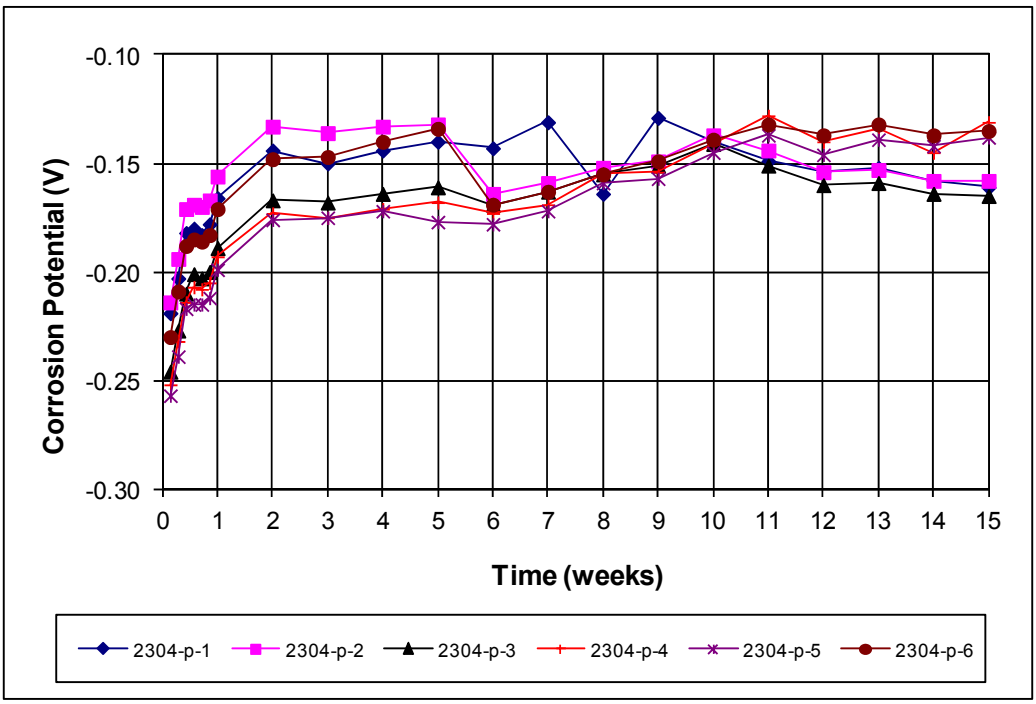

Figure A.21: Macrocell individual corrosion potentials with respect to SCE. Re-pickled 2304 stainless steel bars in pore solution with salt (cathode), specimens 1-6.

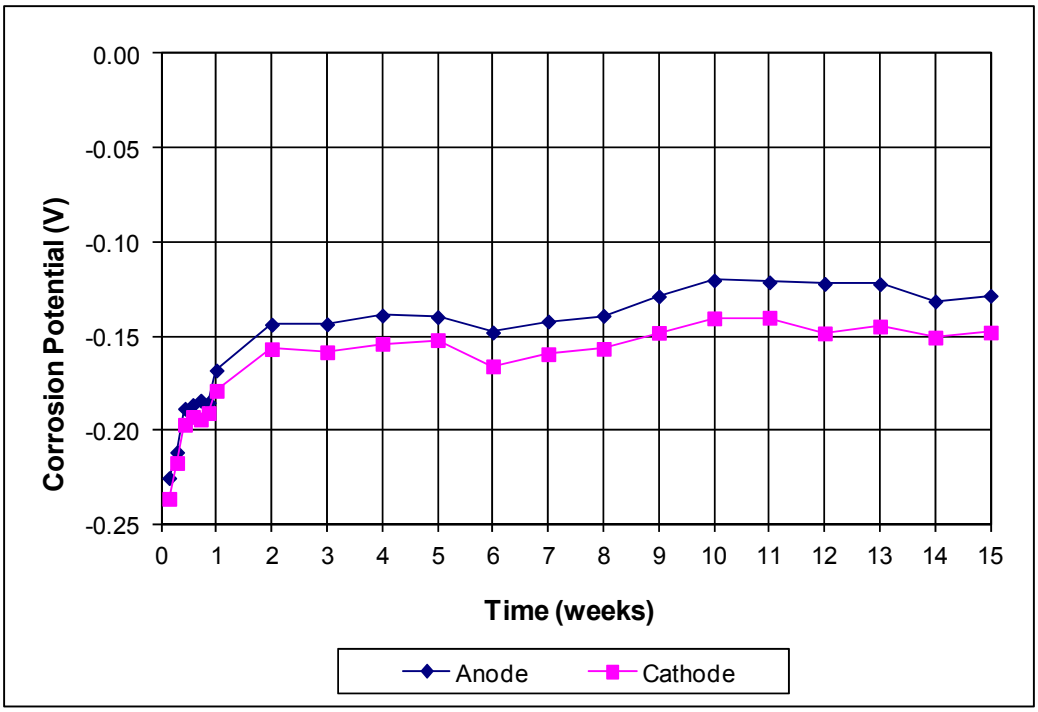

Figure A.22: Average corrosion potentials with respect to SCE. Re-pickled 2304 stainless steel bars, specimens 1-6.

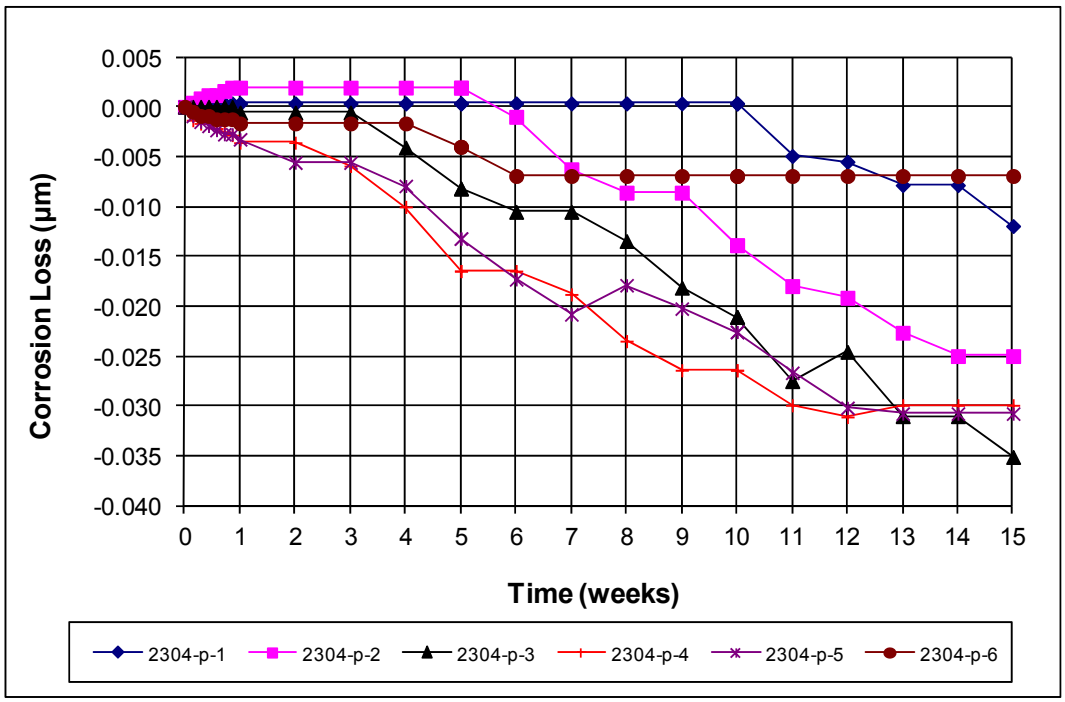

Figure A.23: Macrocell individual corrosion loss of 2304 re-pickled stainless steel, specimens 1-6.

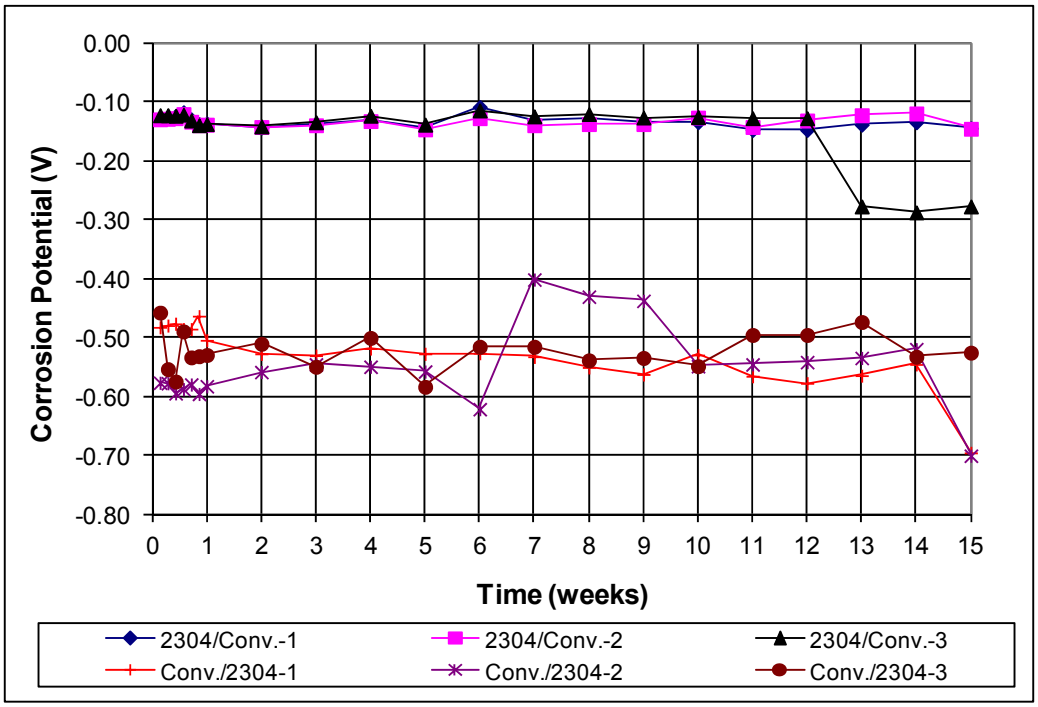

Figure A.24: Macrocell individual corrosion potentials with respect to SCE. Mixed 2304 stainless steel (anode/cathode) in pore solution with salt (anode), specimens 1-6.

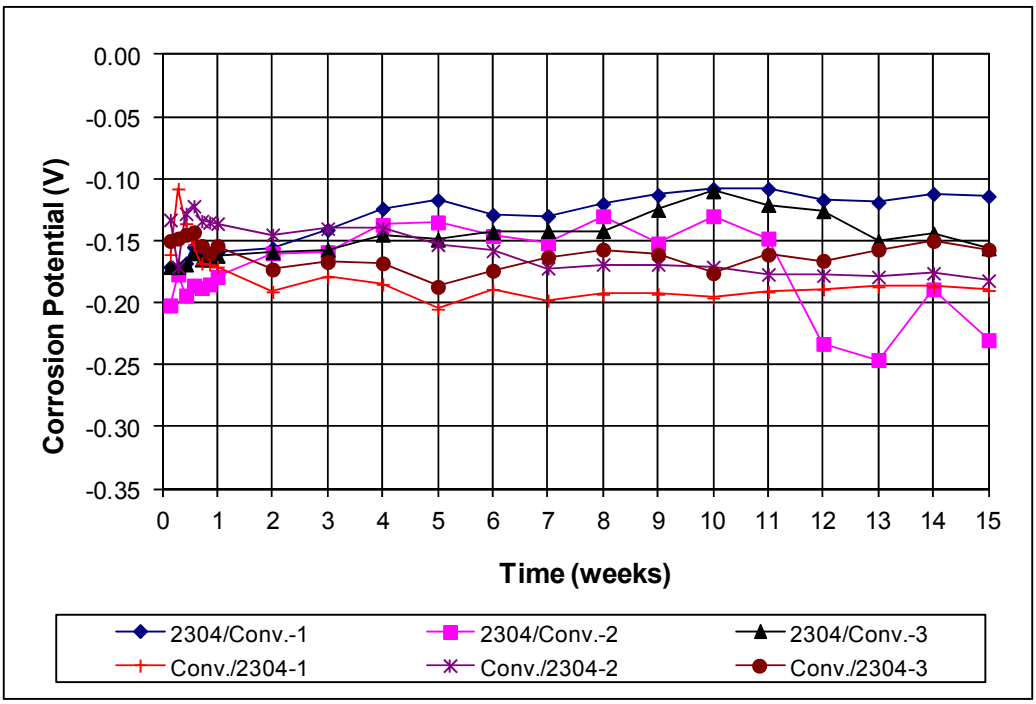

Figure A.25: Macrocell individual corrosion potentials with respect to SCE. Mixed 2304 stainless steel (anode/cathode) in pore solution (cathode), specimens 1-6.

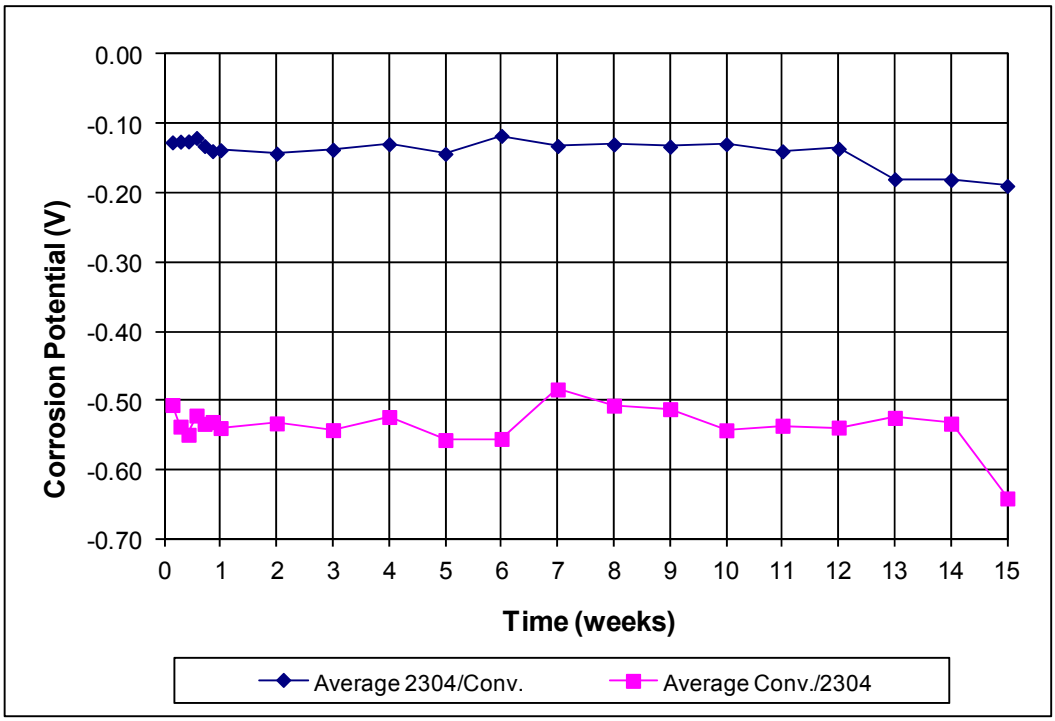

Figure A.26: Average anode corrosion potentials with respect to SCE. Mixed 2304 stainless steel (anode/cathode), specimens 1-6.

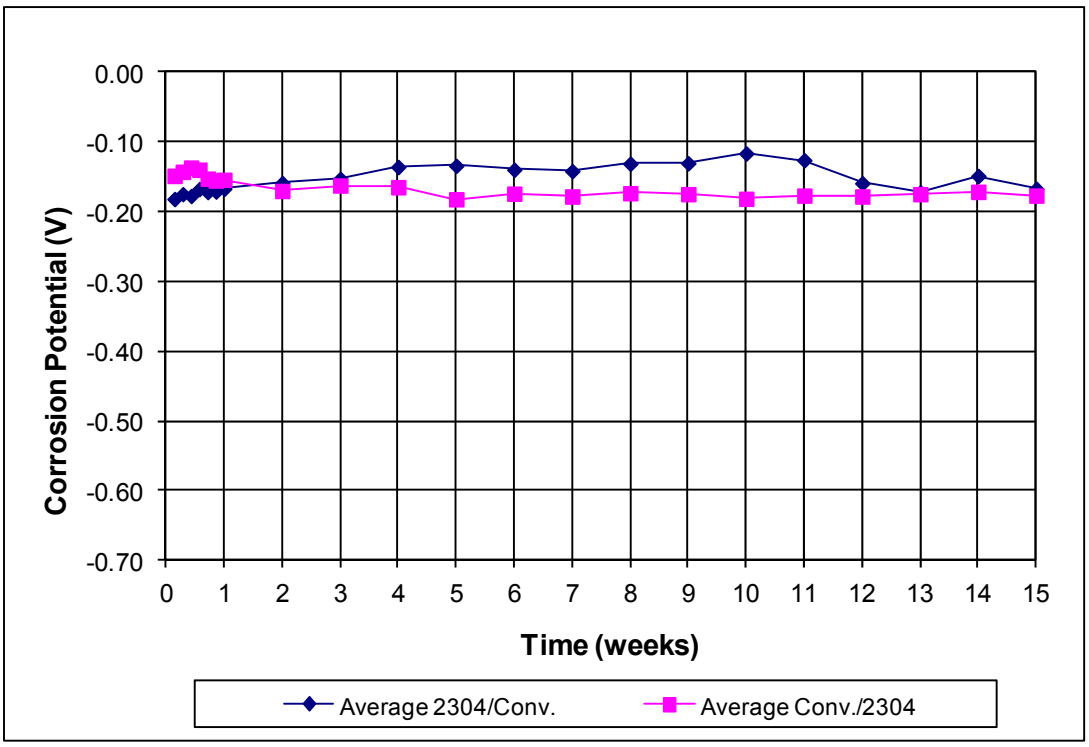

Figure A.27: Average cathode corrosion potentials with respect to SCE. Mixed 2304 stainless steel (anode/cathode), specimens 1-6.

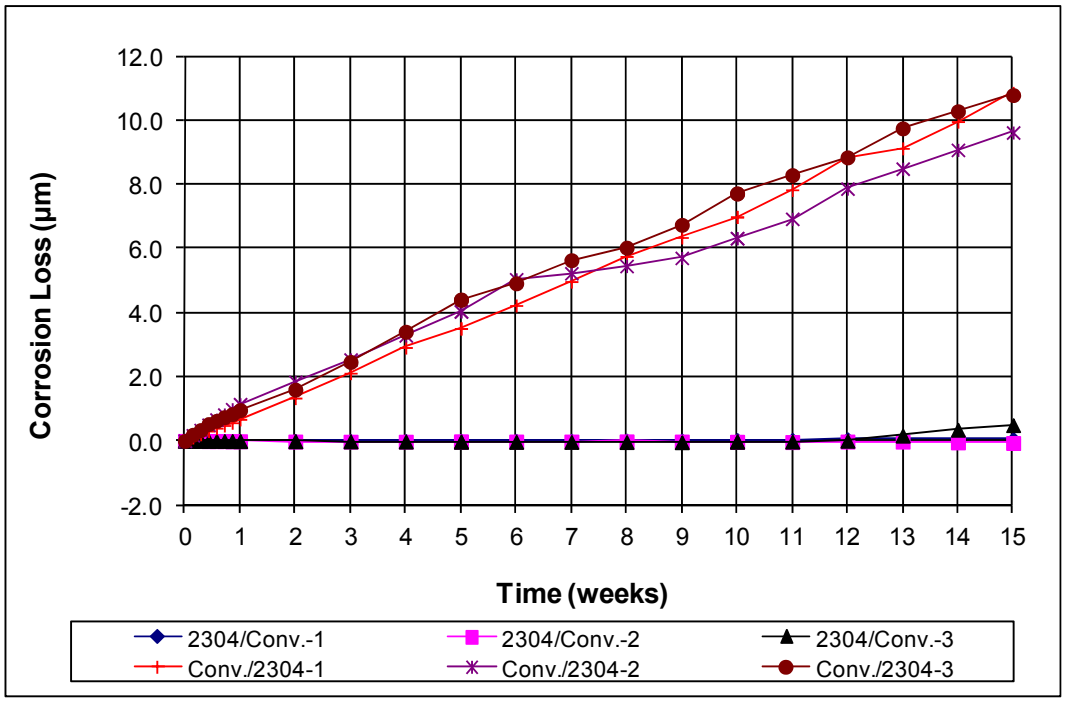

Figure A.28: Macrocell individual corrosion loss of mixed 2304 stainless steel, specimens 1-6.

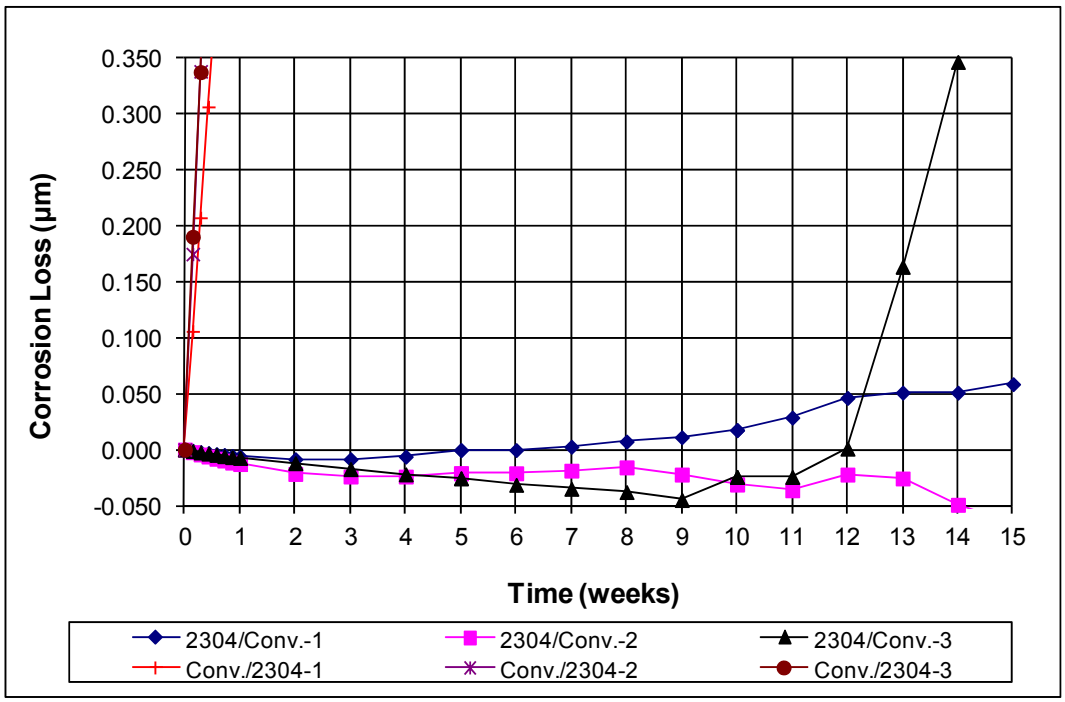

Figure A.29: Macrocell individual corrosion loss of mixed 2304 stainless steel, specimens 1-6 (different scale).

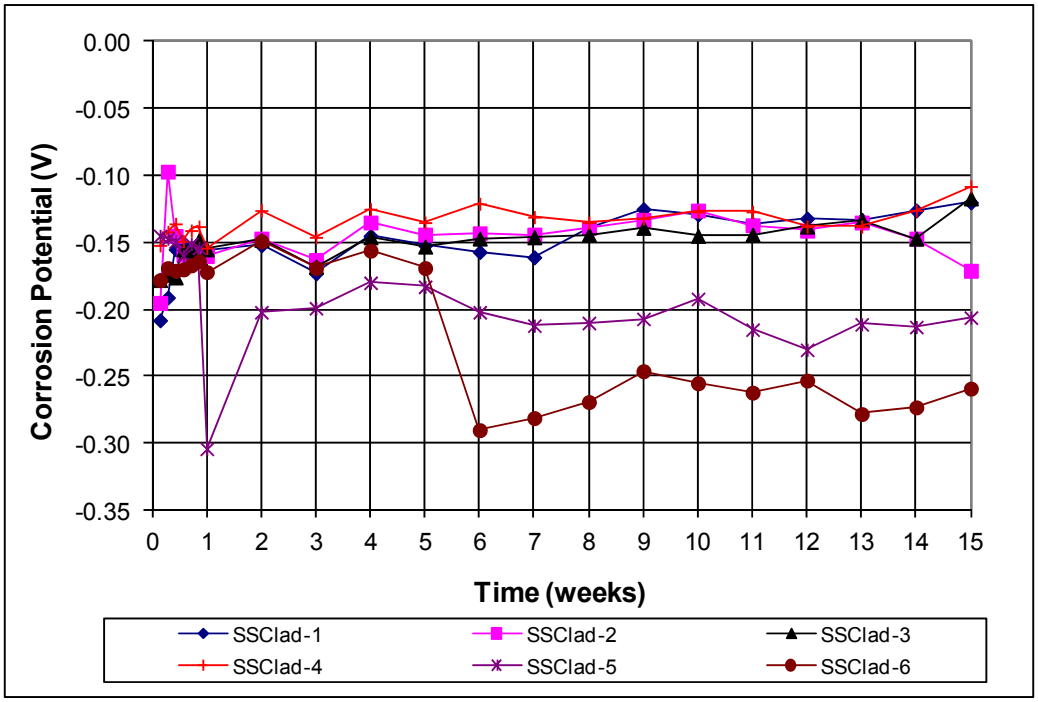

Figure A.30: Macrocell individual corrosion potentials with respect to SCE. Undamaged NX-SCR™ stainless steel clad bars in pore solution with salt (anode), specimens 1-6.

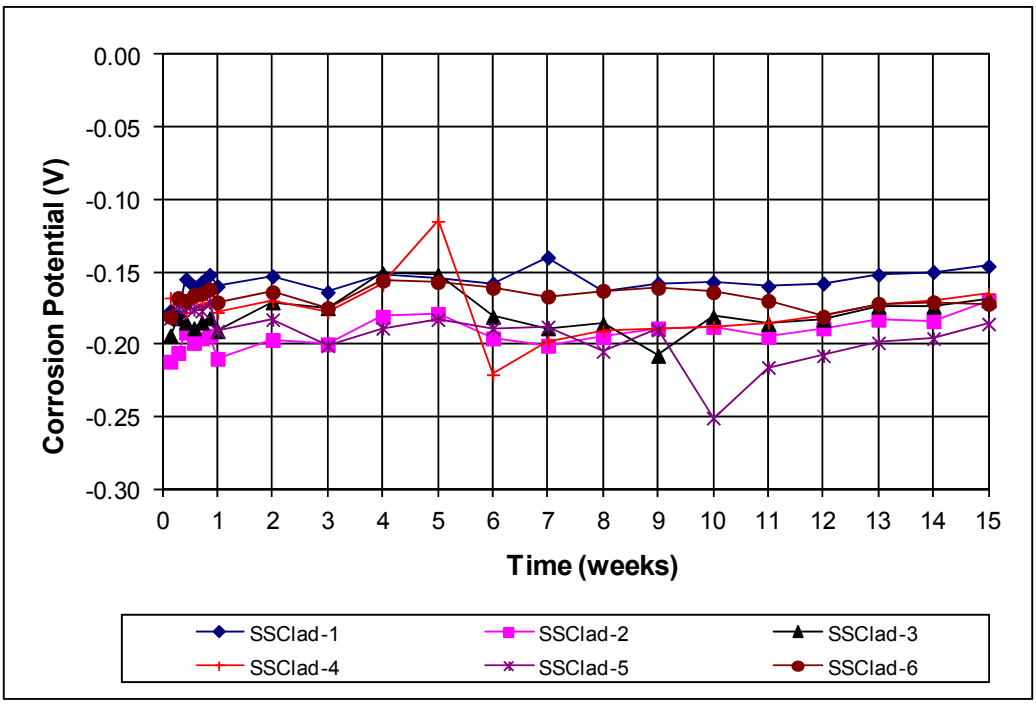

Figure A.31: Macrocell individual corrosion potentials with respect to SCE. Undamaged NX-SCR™ stainless steel clad bars in pore solution (cathode), specimens 1-6.

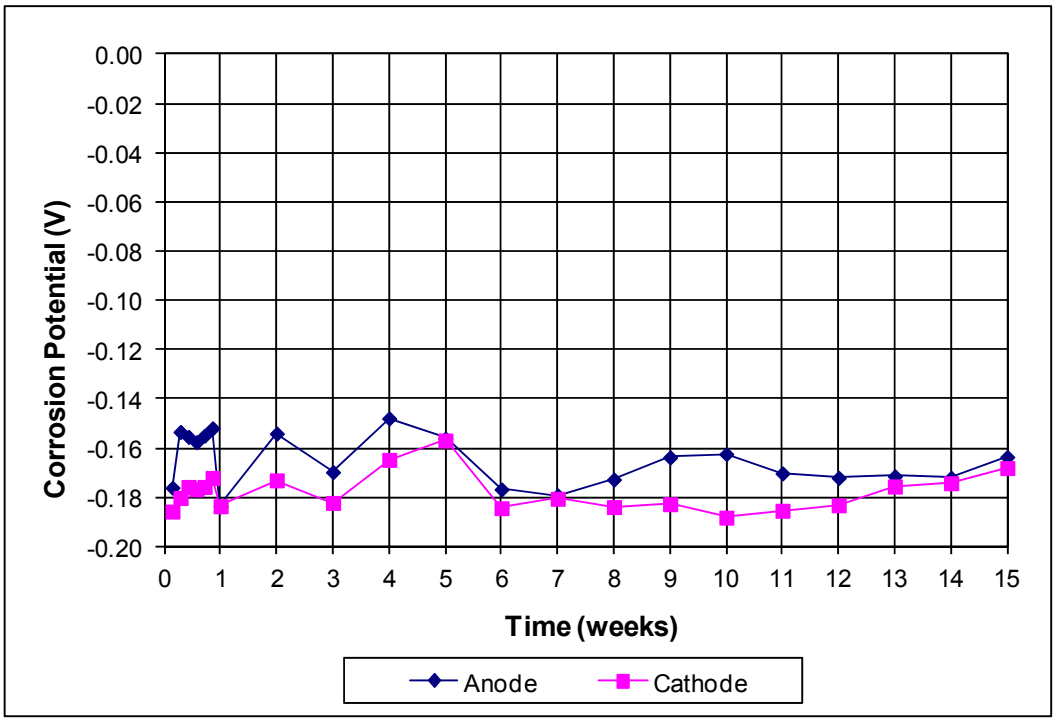

Figure A.32: Average corrosion potentials with respect to SCE. Undamaged NX-SCR™ stainless steel clad bars, specimens 1-6.

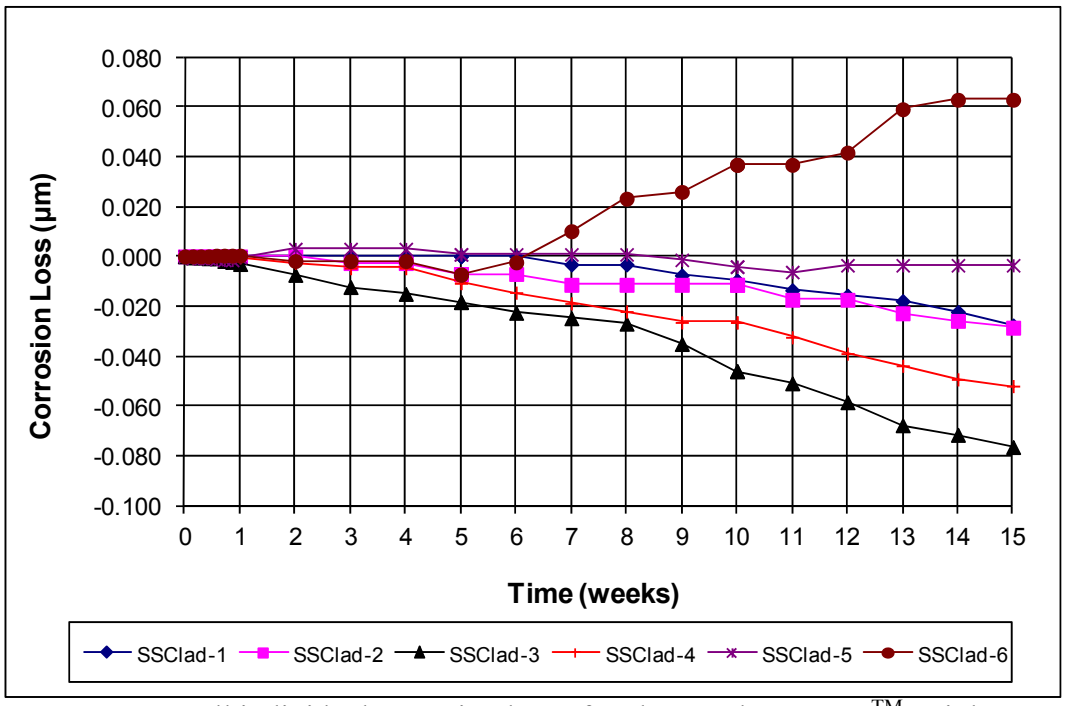

Figure A.33: Macrocell individual corrosion loss of undamaged NX-SCR™ stainless steel clad bars, specimens 1-6.

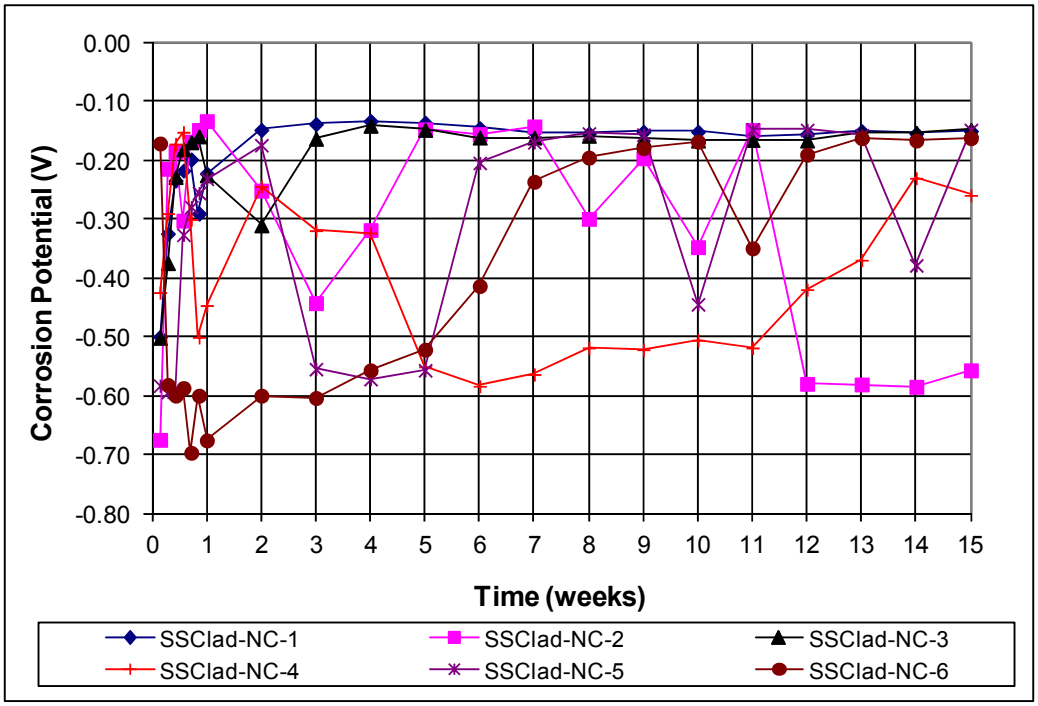

Figure A.34: Macrocell individual corrosion potentials with respect to SCE. Uncapped NX-SCR™ stainless steel clad bars in pore solution with salt (anode), specimens 1-6.

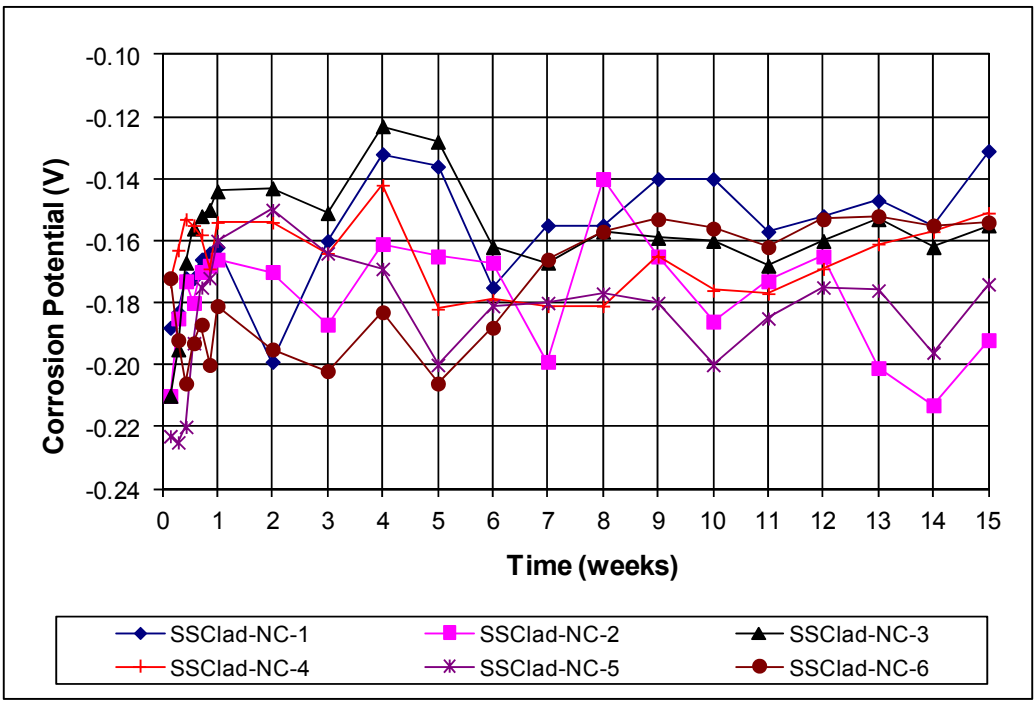

Figure A.35: Macrocell individual corrosion potentials with respect to SCE. Uncapped NX-SCR™ stainless steel clad bars in pore solution (cathode), specimens 1-6.

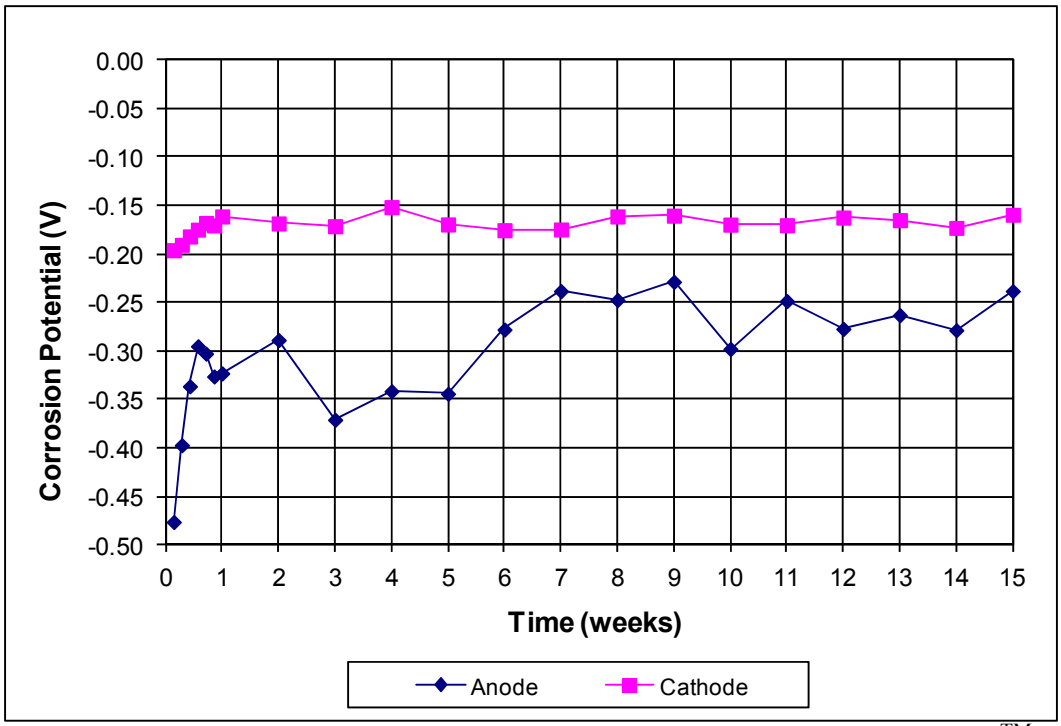

Figure A.36: Average corrosion potentials with respect to SCE. Uncapped NX-SCR™ stainless steel clad bars, specimens 1-6.

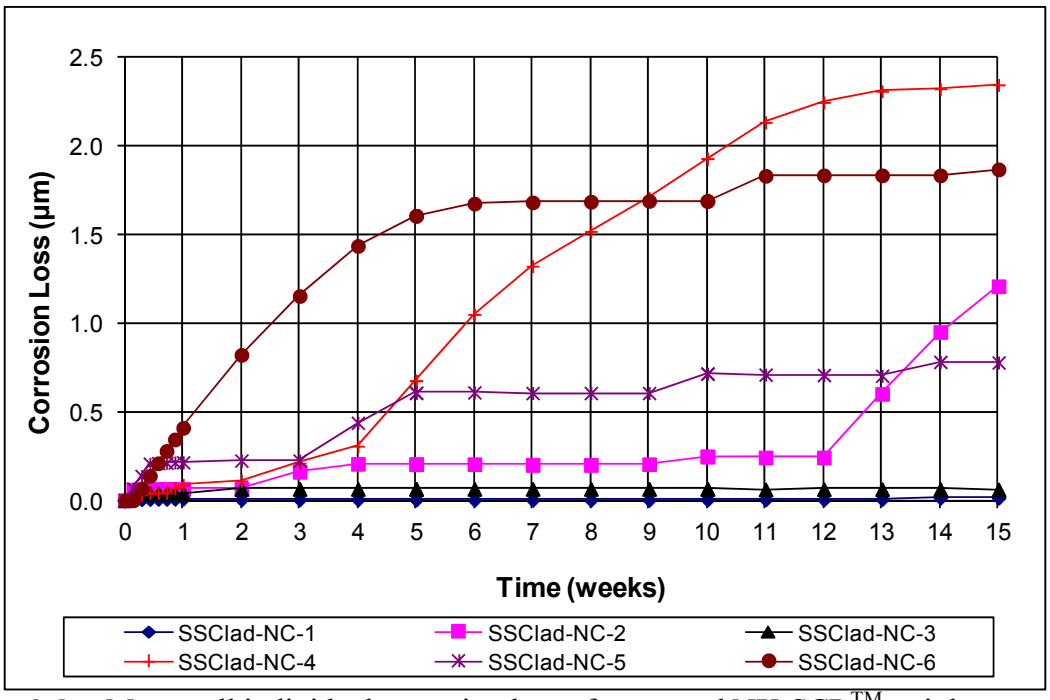

Figure A.37: Macrocell individual corrosion loss of uncapped NX-SCR™ stainless steel clad bars, specimens 1-6.

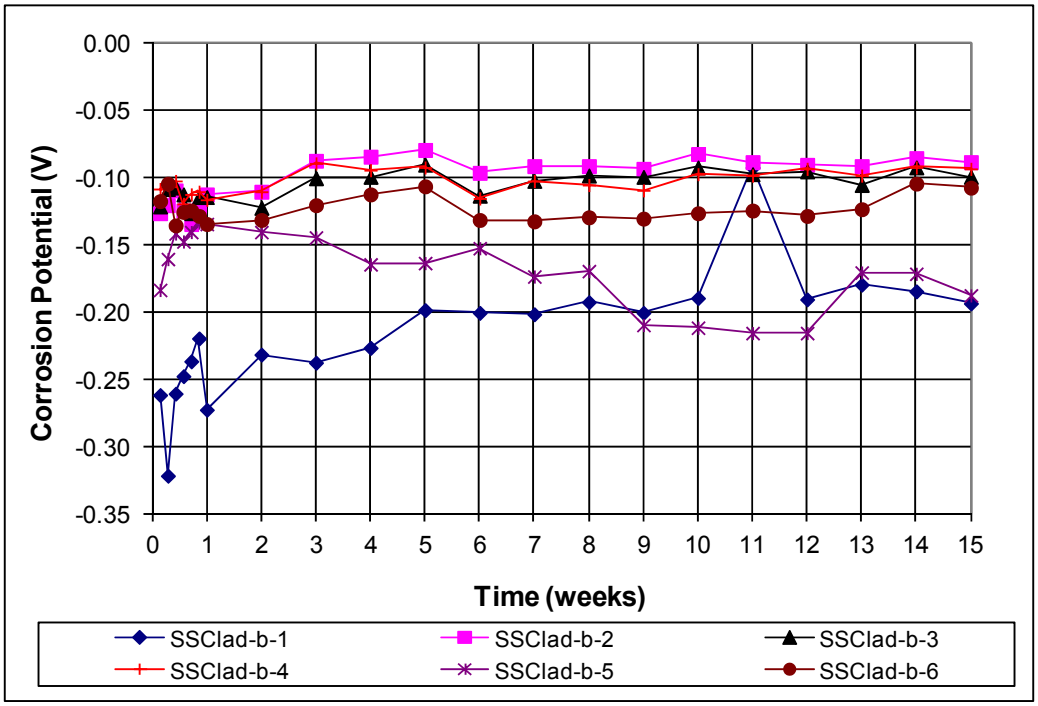

Figure A.38: Macrocell individual corrosion potentials with respect to SCE. Bent NX-SCR™ stainless steel clad bars in pore solution with salt (anode), specimens 1-6.

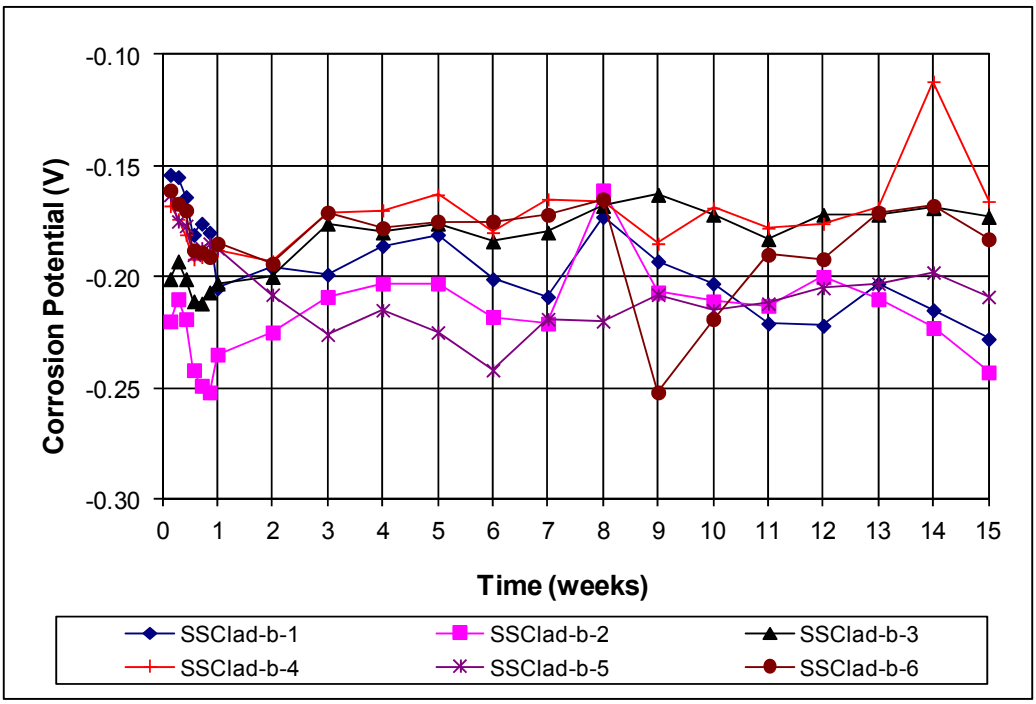

Figure A.39: Macrocell individual corrosion potentials with respect to SCE. Bent NX-SCR™ stainless steel clad bars in pore solution (cathode), specimens 1-6.

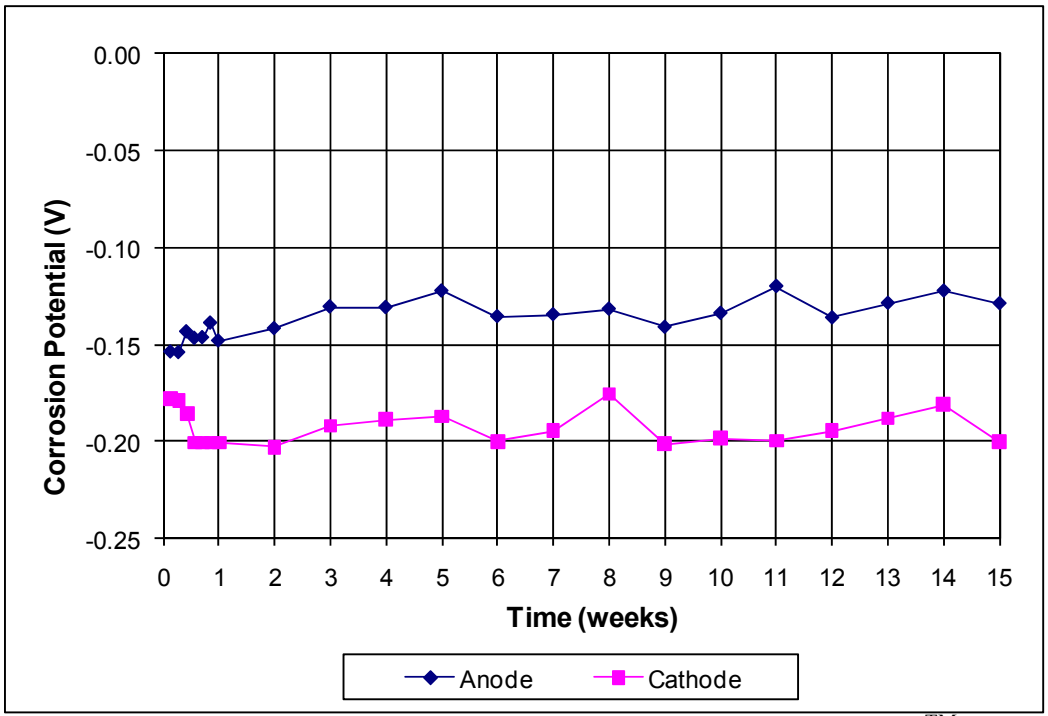

Figure A.40: Average corrosion potentials with respect to SCE. Bent NX-SCR™ stainless steel clad bars, specimens 1-6.

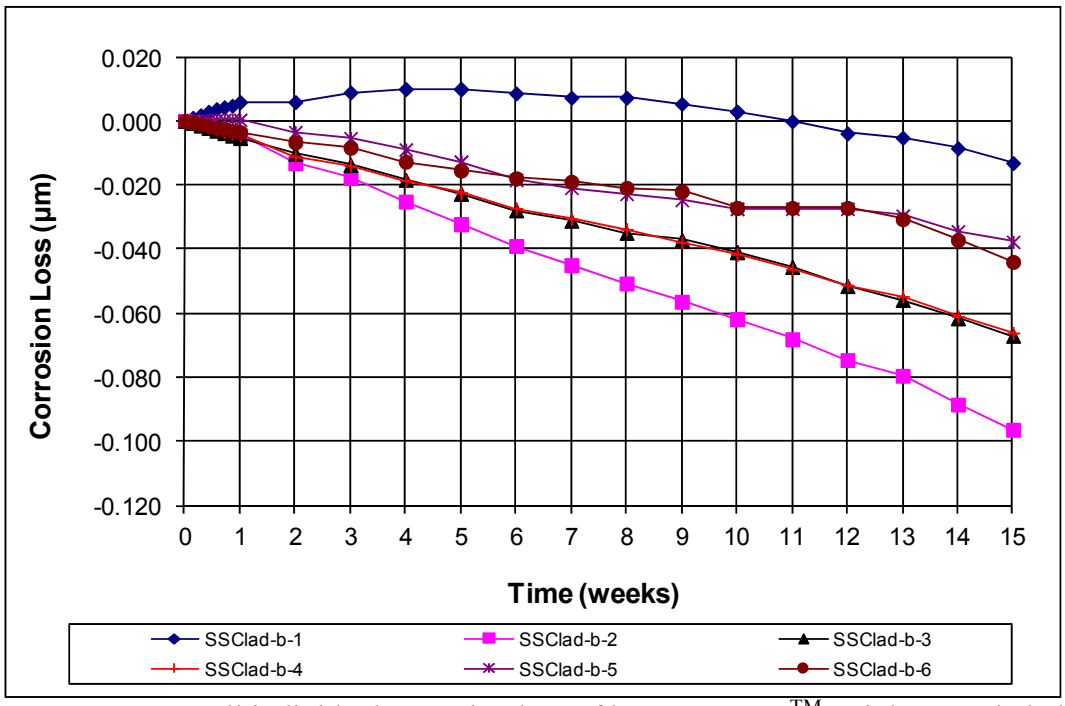

Figure A.41: Macrocell individual corrosion loss of bent NX-SCR™ stainless steel clad bars, specimens 1-6.

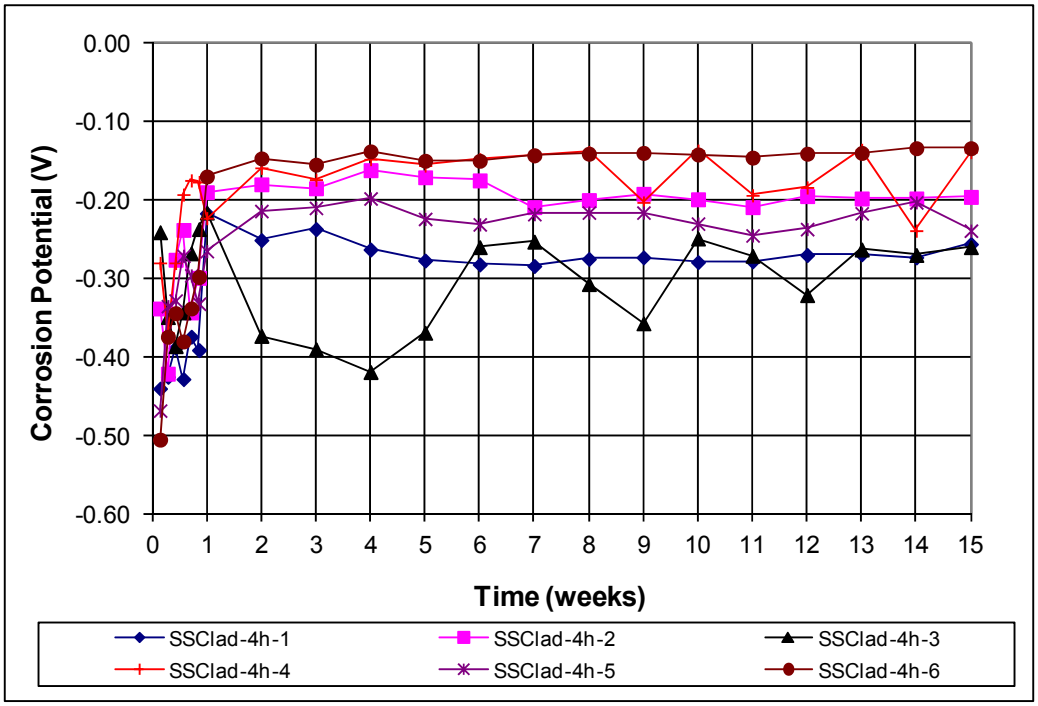

Figure A.42: Macrocell individual corrosion potentials with respect to SCE. 0.83% damaged area NX-SCR™ stainless steel clad bars in pore solution with salt (anode), specimens 1-6.

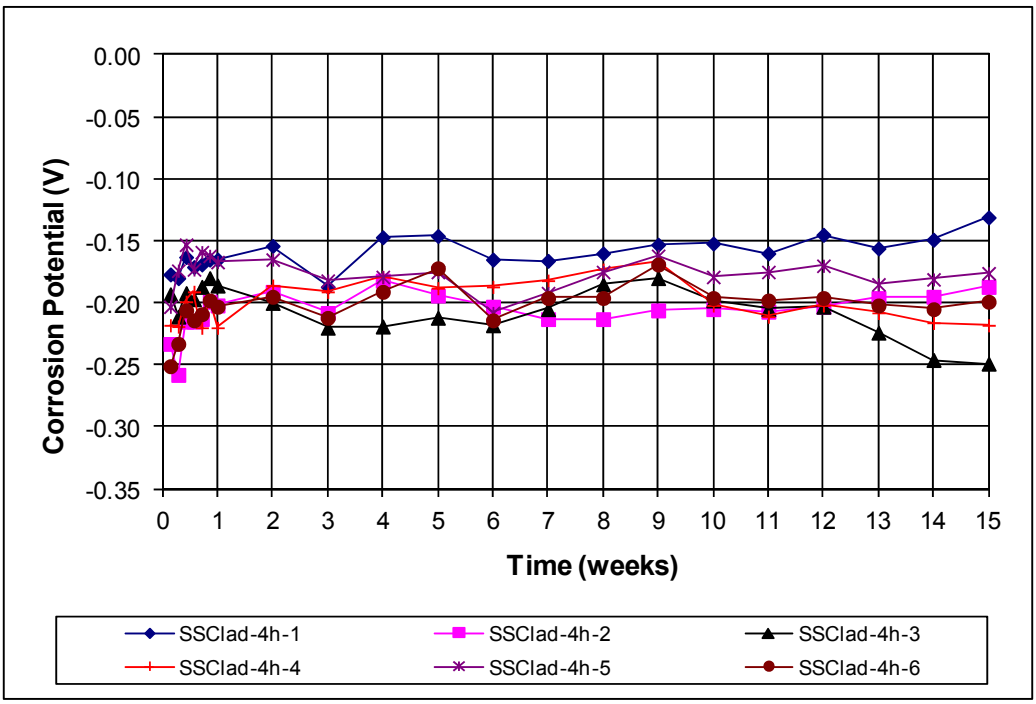

Figure A.43: Macrocell individual corrosion potentials with respect to SCE. 0.83% damaged area NX-SCR^{TM} stainless steel clad bars in pore solution (cathode), specimens 1-6.

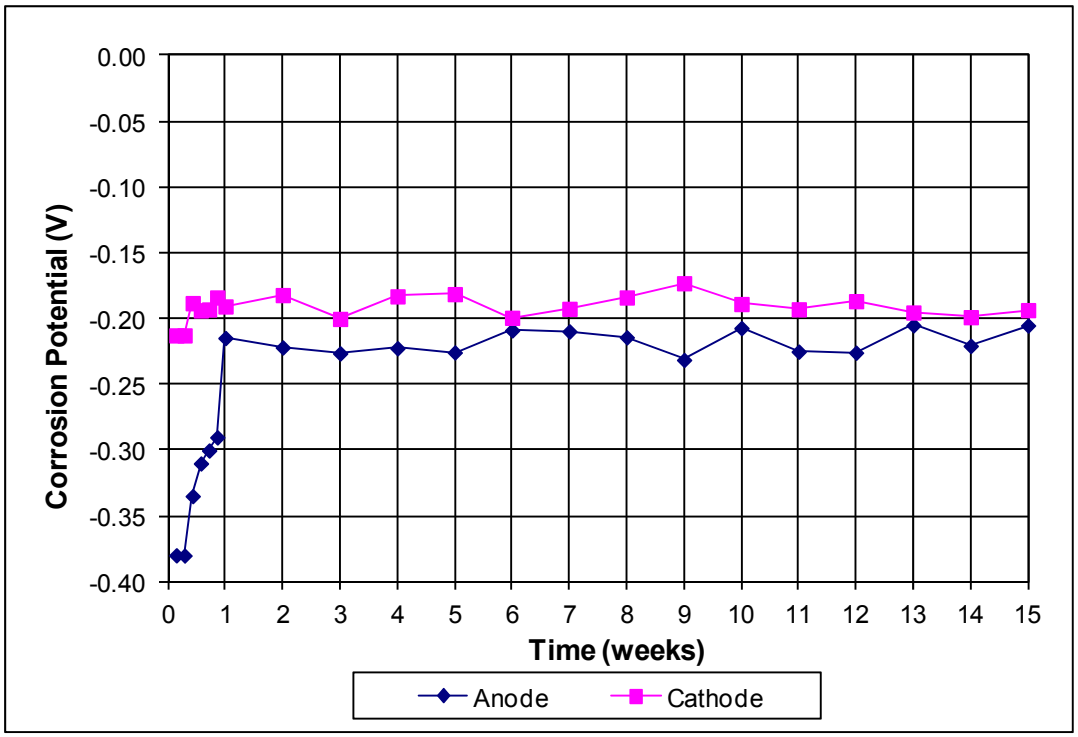

Figure A.44: Average corrosion potentials with respect to SCE. 0.83% damaged area NX-SCR^{TM} stainless steel clad bars, specimens 1-6.

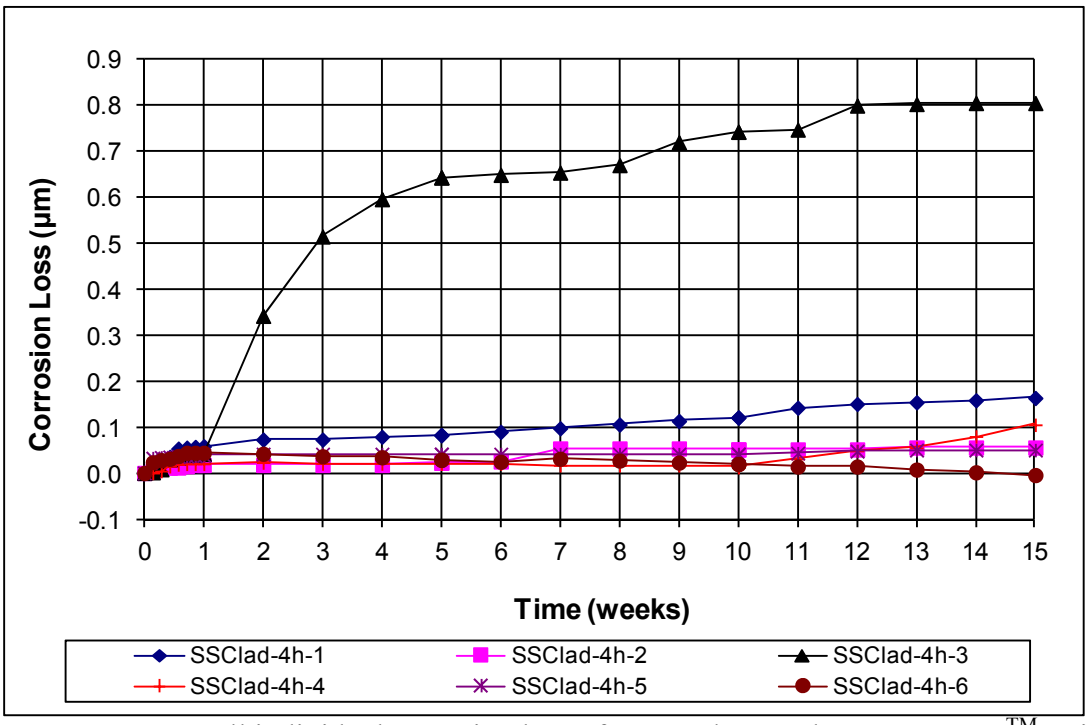

Figure A.45: Macrocell individual corrosion loss of 0.83% damaged area NX-SCR™ stainless steel clad bars, specimens 1-6.

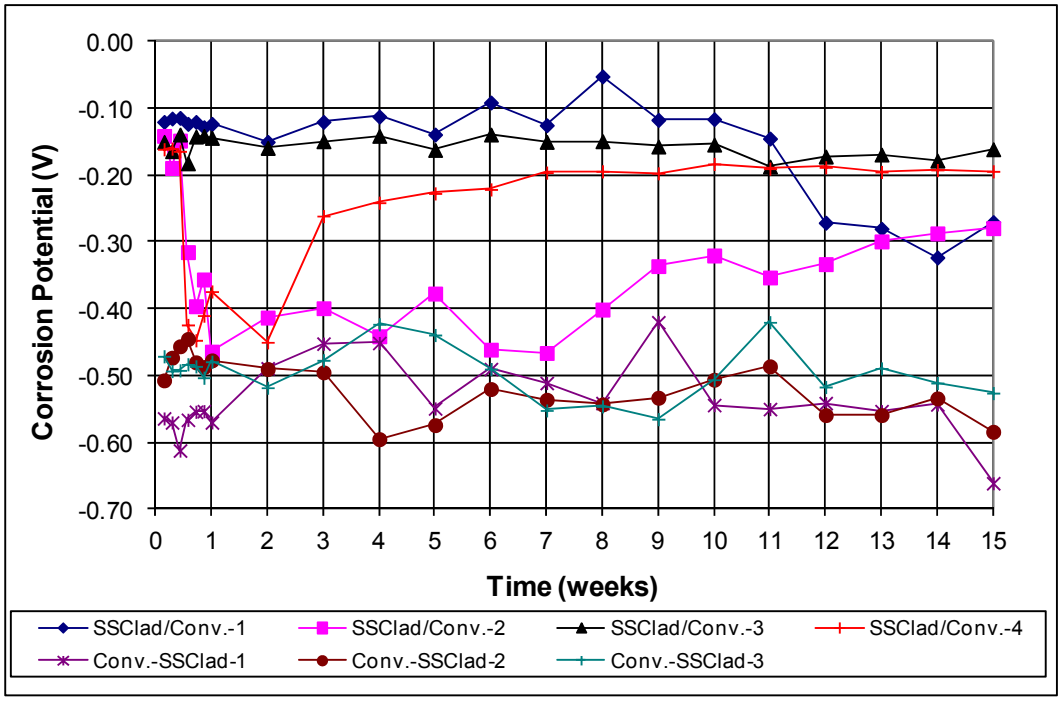

Figure A.46: Macrocell individual corrosion potentials with respect to SCE. Mixed NX-SCR™ stainless steel clad bars (anode/cathode) in pore solution with salt (anode), specimens 1-6.

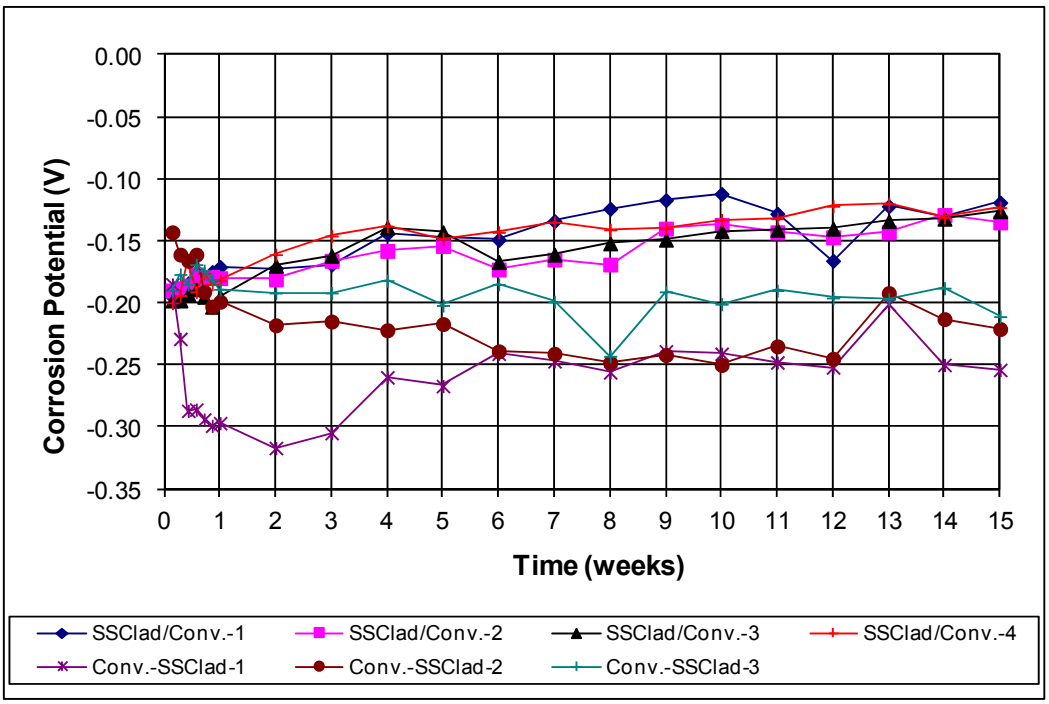

Figure A.47: Macrocell individual corrosion potentials with respect to SCE. Mixed NX-SCR™ stainless steel clad bars (anode/cathode) in pore solution (cathode), specimens 1-6.

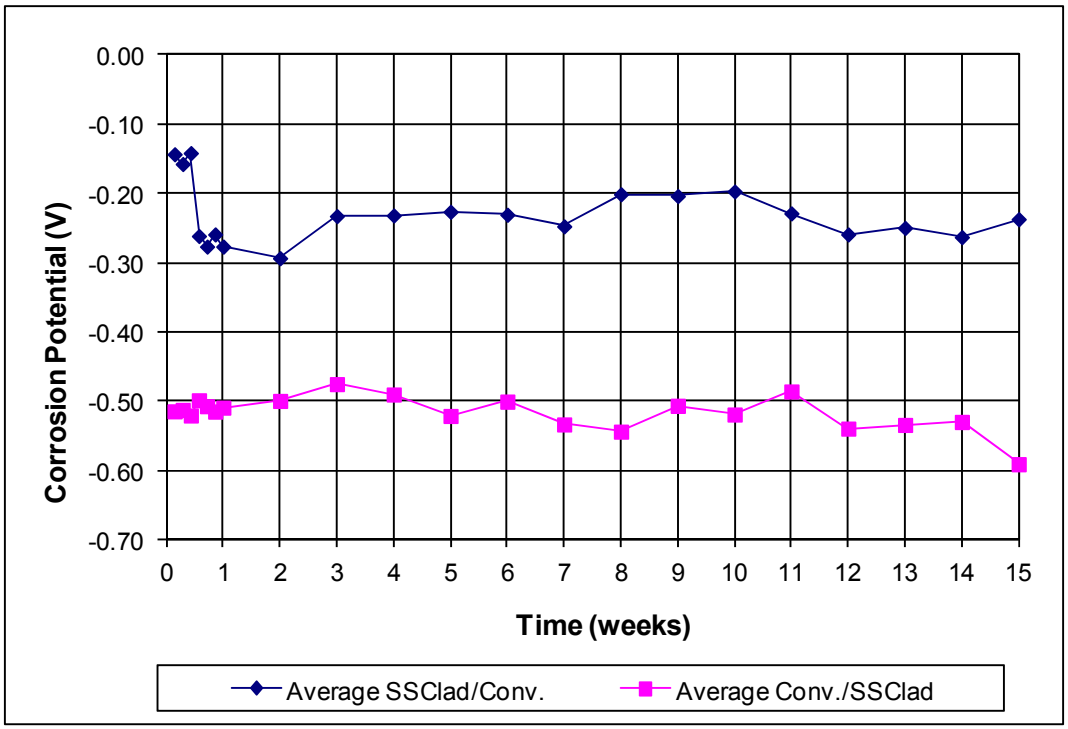

Figure A.48: Average anode corrosion potentials with respect to SCE. Mixed NX-SCR™ stainless steel clad bars (anode/cathode), specimens 1-6.

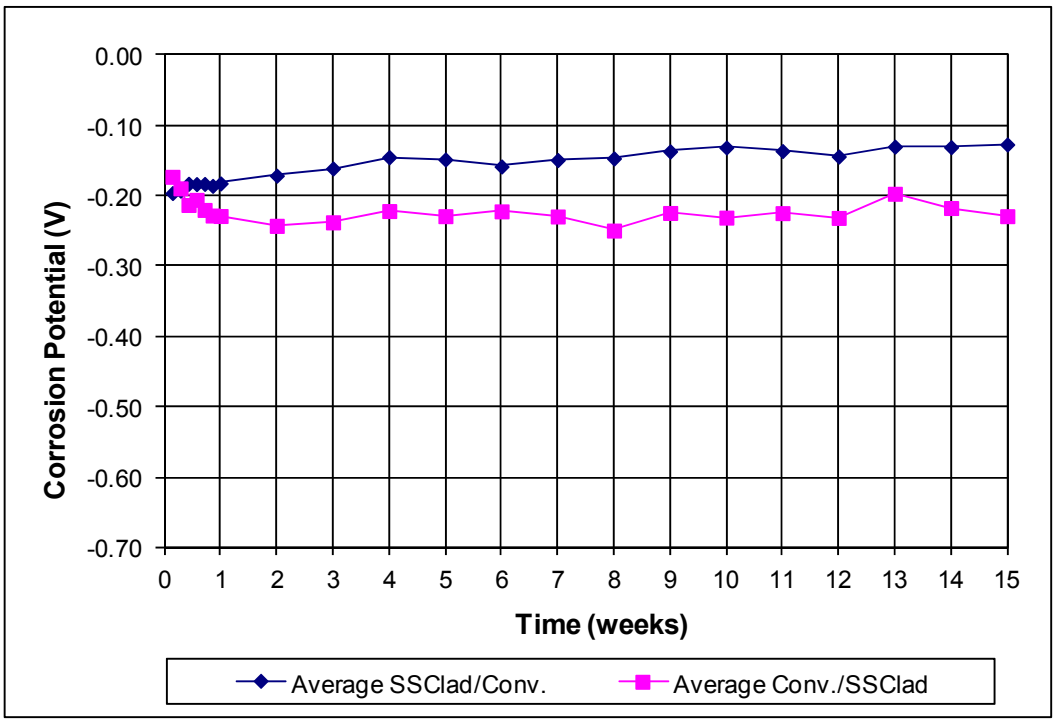

Figure A.49: Average cathode corrosion potentials with respect to SCE. Mixed NX-SCR^{TM} stainless steel clad bars (anode/cathode), specimens 1-6.

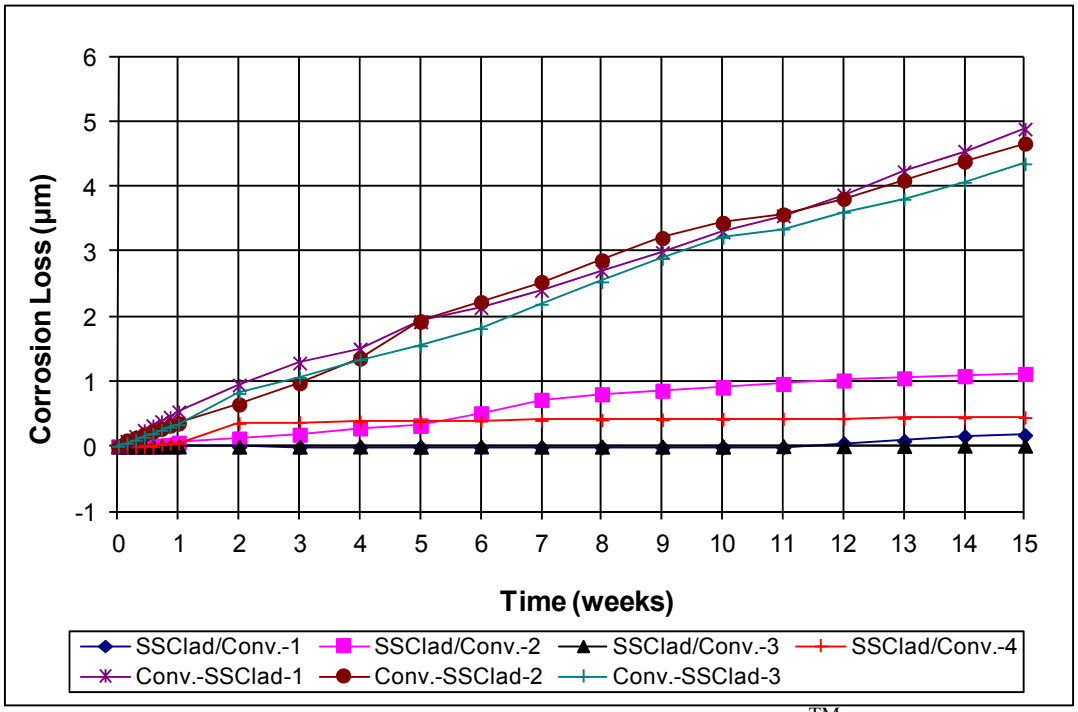

Figure A.50: Macrocell individual corrosion loss of mixed NX-SCR^{TM} stainless steel clad bars, specimens 1-6.

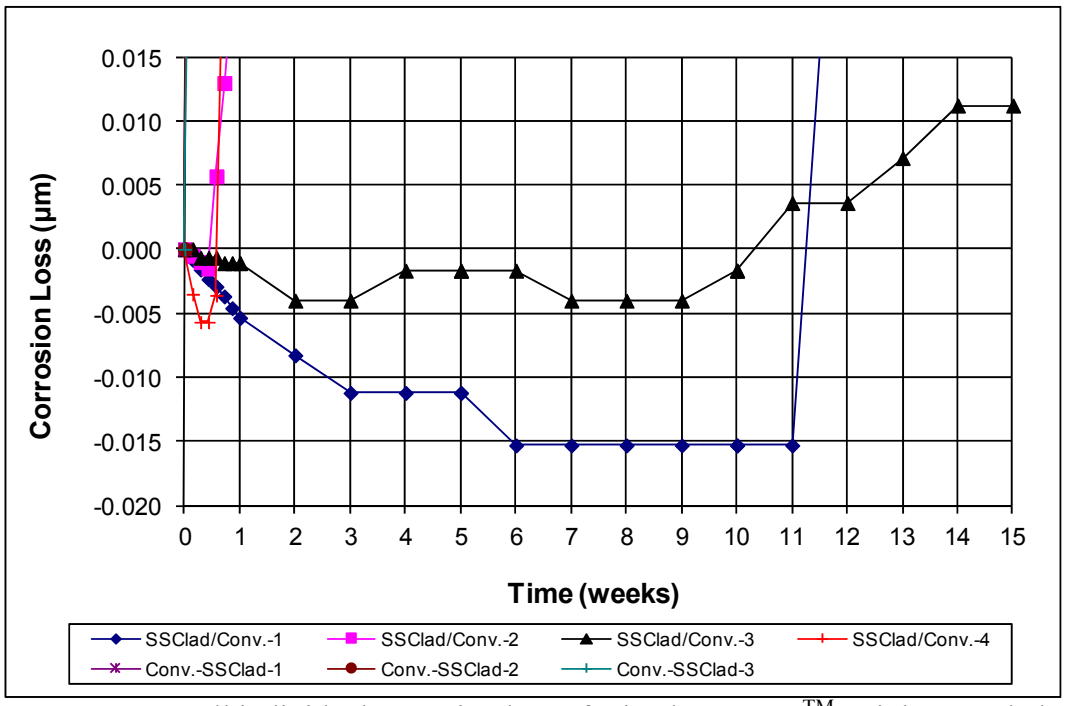

Figure A.51: Macrocell individual corrosion loss of mixed NX-SCR^{TM} stainless steel clad bars, specimens 1-6 (different scale).

APPENDIX B
LINEAR POLARIZATION DESCRIPTION, DATA

Linear polarization resistance tests were performed every three weeks throughout the rapid macrocell evaluation. It was performed in addition to the voltage drop and potential readings in order to verify data readings. The linear polarization resistance test provides a way in which the total corrosion rate of a metal, including microcell and macrocell corrosion rates, can be determined by measuring its response to an applied voltage, or polarization. Without an externally applied voltage, a metal will corrode with a current density i_{corr} and a potential E_{corr}. In the LPR test, the potential is forced to shift by an amount $\Delta\varepsilon$, which causes the current to shift by an amount Δi. The polarization resistance, which is the slope of the potential-current function, is also known as the polarization curve and is determined as follows:

$$R_p = \left[\frac{\Delta\varepsilon}{\Delta i}\right]_{\varepsilon\to 0}$$

where

R_p = polarization resistance

$\Delta\varepsilon$ = forced potential change

Δi = change in current density caused by $\Delta\varepsilon$

The polarization resistance, R_p, is determined by taking a series of current density measurements while changing the potential, $\Delta\varepsilon$, and measuring the resultant current, Δi. Another way in which the polarization resistance may be determined is by applying a range of currents to the metal and then measuring the resultant shifts in voltage. The polarization curve is linear when changes in potential are small. In this linear region, the polarization resistance is inversely proportional to the corrosion current density.

$$i_{corr} = \frac{\beta_a \beta_c}{2.3 R_p (\beta_a + \beta_c)}$$

where

β_a, β_c = anodic and cathodic Tafel constants, V/decade

R_p = polarization resistance

R_p is obtained by plotting the data and then finding the slope of the linear region. Using this value, the corrosion current density, i_{corr}, may be calculated. Using anodic and cathodic Tafel constant values, β_a and β_c, of 0.12 V/decade, a linear region for the polarization curve over a region of approximately ±10 mV with respect to E_{corr}. Using these Tafel constant values, the equation to determine current density is

$$i_{\text{corr}} = \frac{0.026}{R_p}$$

By multiplying this corrosion current density, i_{corr}, by surface area, the current is obtained. Using the current and plugging into Faraday's equation (Equation 1), corrosion loss is obtained. Corrosion losses are shown in Table B.1.

Table B.1: Total losses of rapid macrocell test specimens

Specimen[a]	Specimen						Average	Standard Deviation
	1	2	3	4	5	6		
Conv.	16.1	12.2	21.1	6.27	11.1	14.9	13.6	5.04
ECR	0.419	0.313	0.446	0.127	0.249	0.379	0.322	0.120
ECR-ND	0.001	0.000	0.000				0.000	0.000
2304	1.01	0.623	0.528	0.712	0.737	0.733	0.723	0.160
2304-p	0.501	0.377	0.811	0.502	0.532	0.754	0.580	0.167
2304/Conv.	1.46	1.29	1.96				1.57	0.348
Conv./2304	23.7	46.8	11.4				27.3	17.9
SSClad-4h	0.099	0.344	0.492	0.122	0.071	0.201	0.221	0.165
SSClad	0.284	0.184	1.023	0.118	0.277	0.094	0.330	0.348
SSClad-NC	2.87	2.218	0.183	1.79	0.223	1.78	1.51	1.09
SSClad-b	0.342	0.876	0.541	0.526	0.220	1.098	0.601	0.330
SSClad/Conv.	0.089	1.40	0.131	0.398			0.505	0.613
Conv./SSClad	10.5	20.4	11.8				14.2	5.36

[a] Conv. = conventional reinforcement, ECR = epoxy-coated reinforcement with ten 0.125-in. diameter holes through the epoxy, ECR-ND= undamaged ECR, 2304 = 2304 stainless steel, SSClad-4h = stainless steel clad reinforcement with four 0.125-in. diameter holes through the cladding, SSClad = undamaged stainless steel clad reinforcement, SSClad-b = bent stainless steel clad reinforcement, SSClad-NC=clad reinforcement with no cap over the cut end.

For mixed specimens, the reinforcement on the top mat is listed first.

APPENDIX C
BENCH-SCALE DATA
CORROSION RATES, TOTAL CORROSION LOSSES, MAT-TO-MAT RESISTANCES AND CORROSION POTENTIALS FOR INDIVIDUAL SPECIMENS

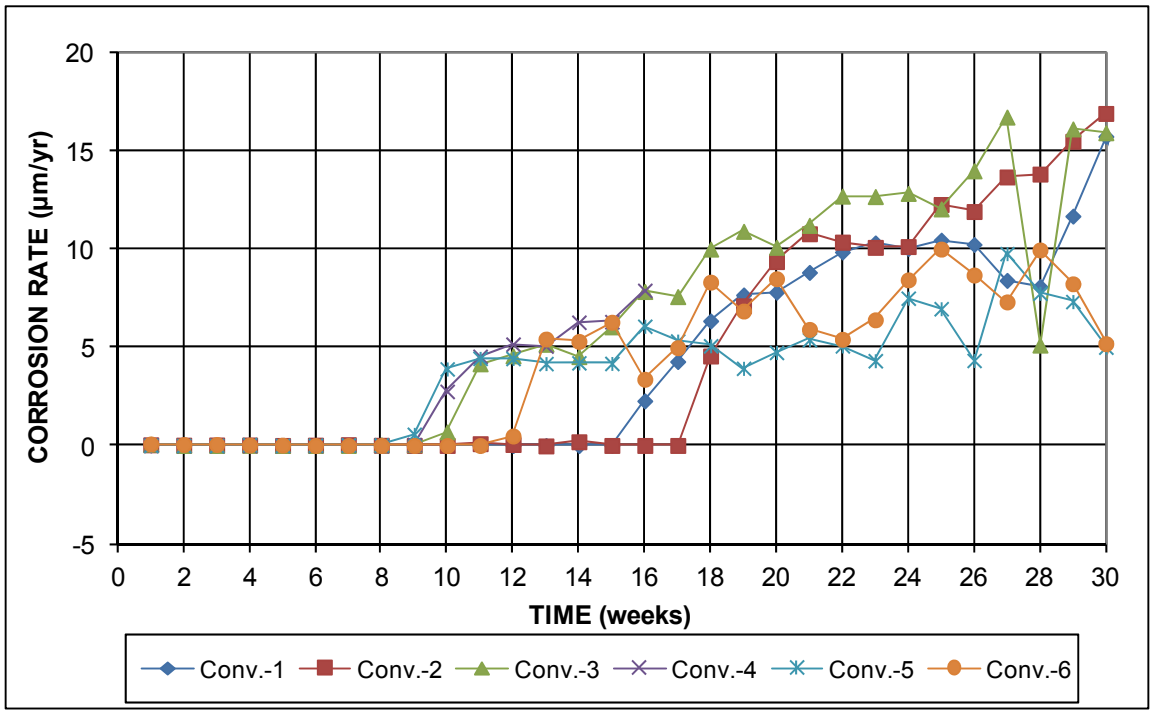

Figure C.1: Southern Exposure corrosion rates – conventional steel, w/c = 0.45

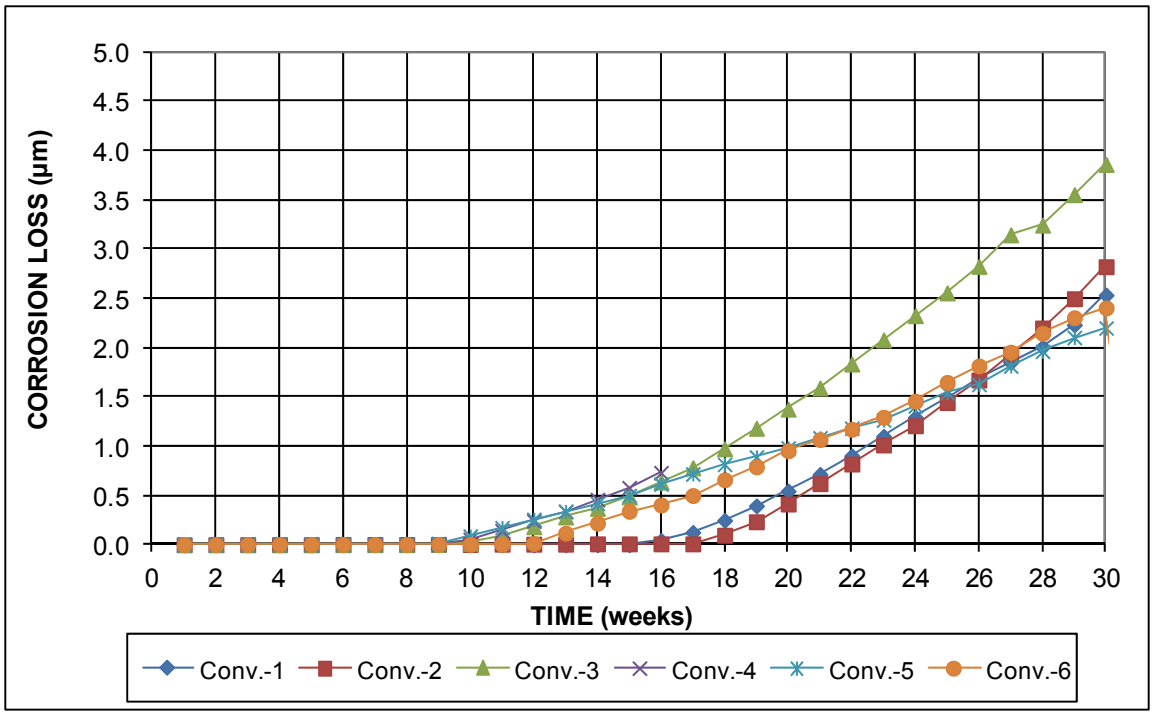

Figure C.2: Southern Exposure corrosion losses – conventional steel, w/c = 0.45

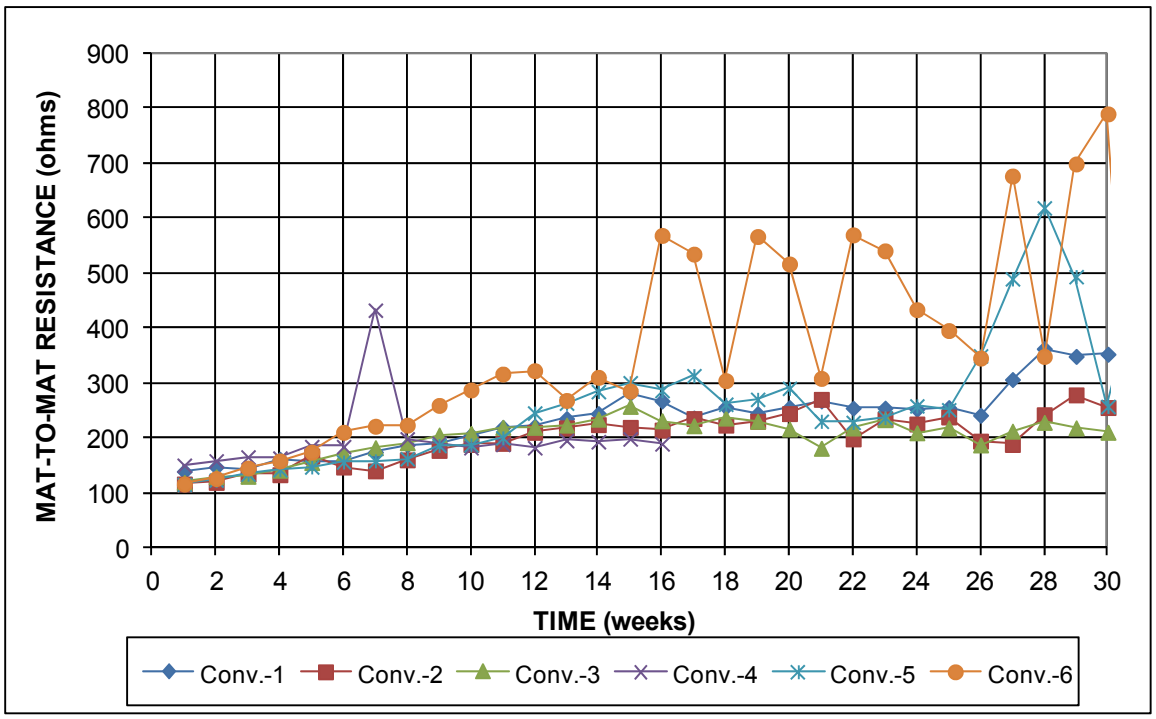

Figure C.3: Southern Exposure mat-to-mat resistances – conventional steel, w/c = 0.45

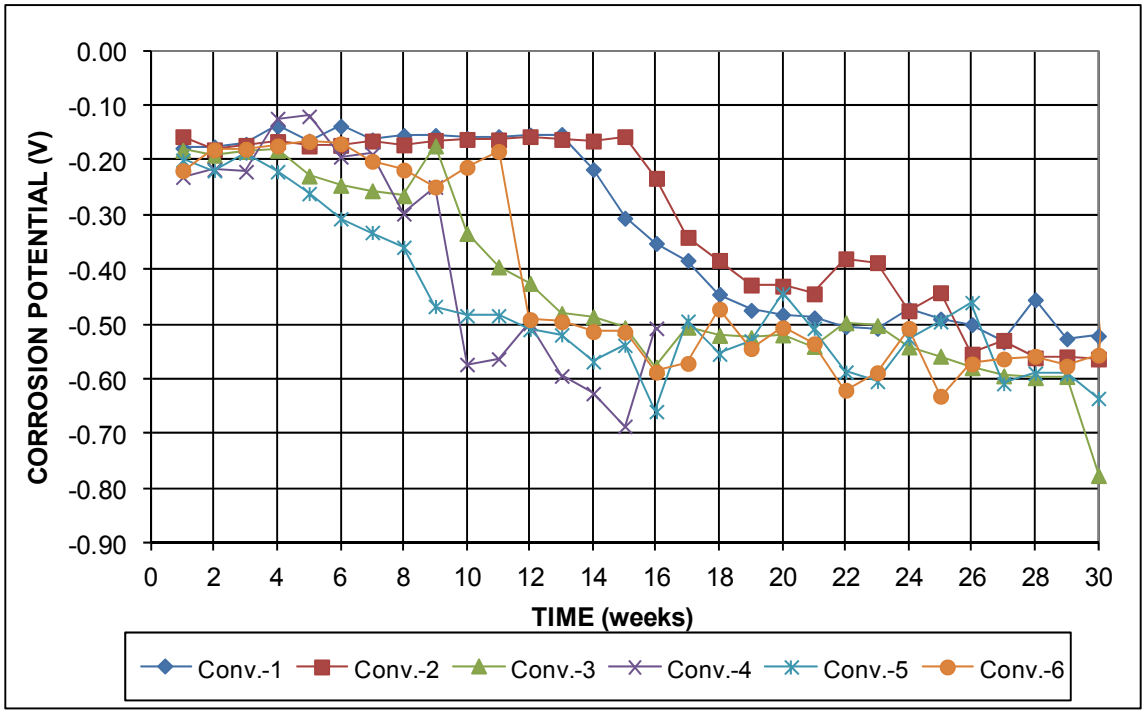

Figure C4: Southern Exposure corrosion potentials with respect to CSE – conventional steel, top mat, w/c = 0.45

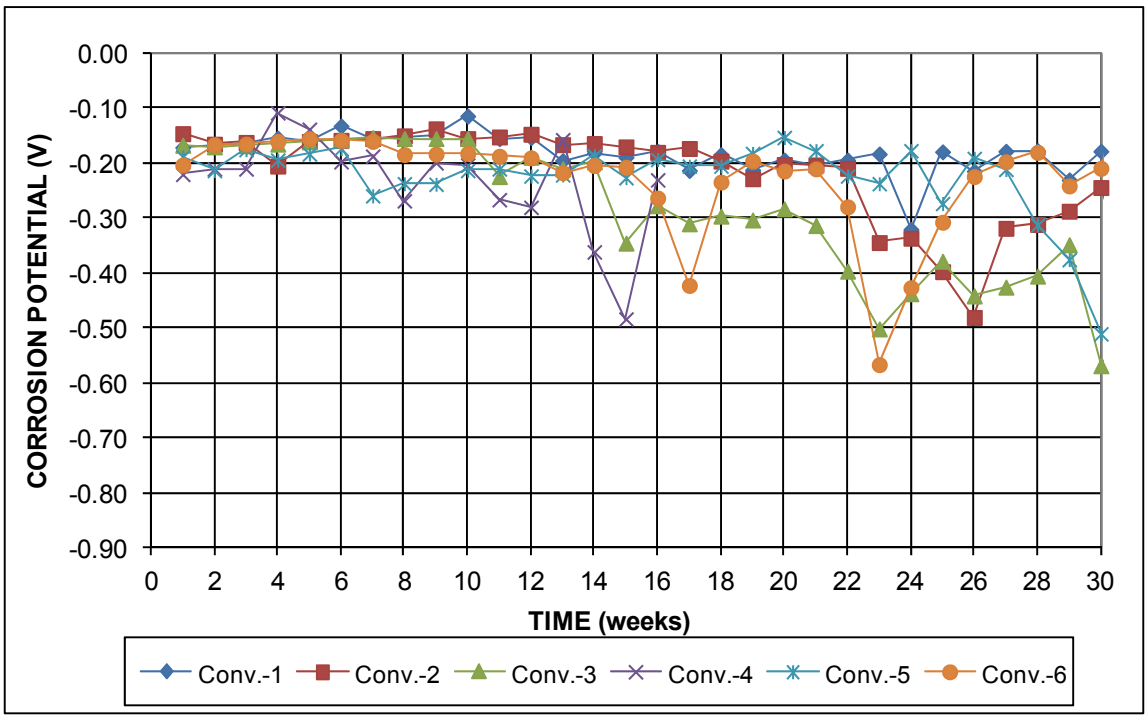

Figure C5: Southern Exposure corrosion potentials with respect to CSE – conventional steel, bottom mat, w/c = 0.45

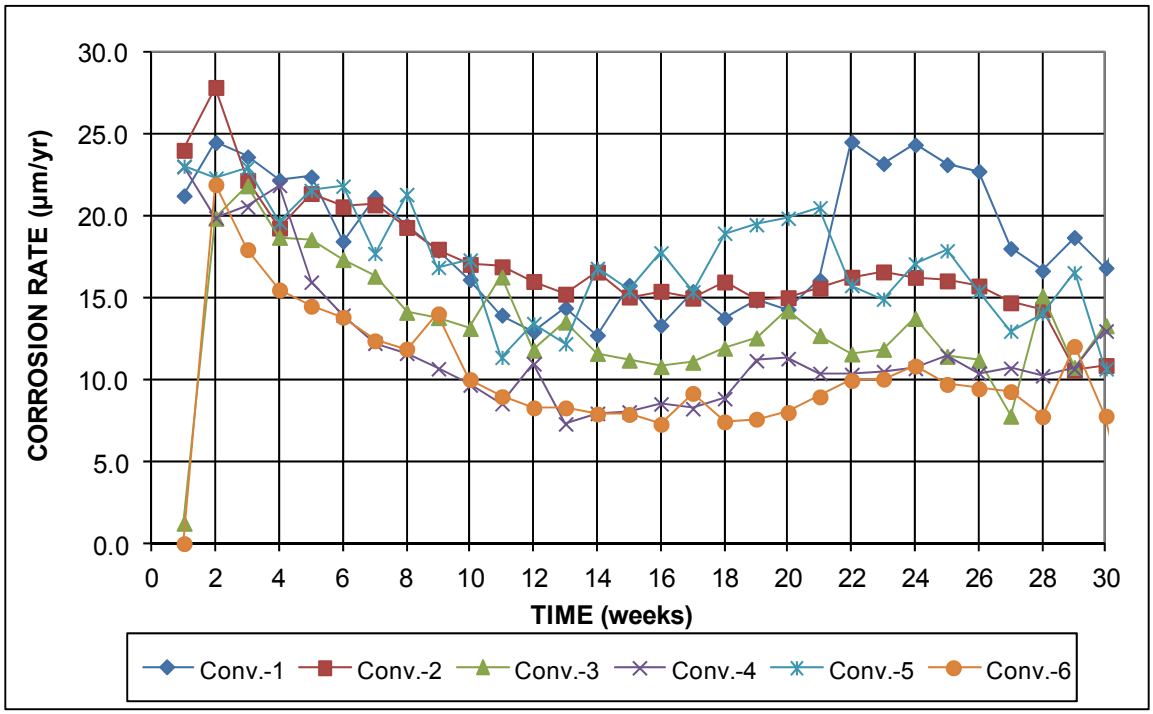

Figure C.6: Cracked beam corrosion rates – conventional steel, w/c = 0.45

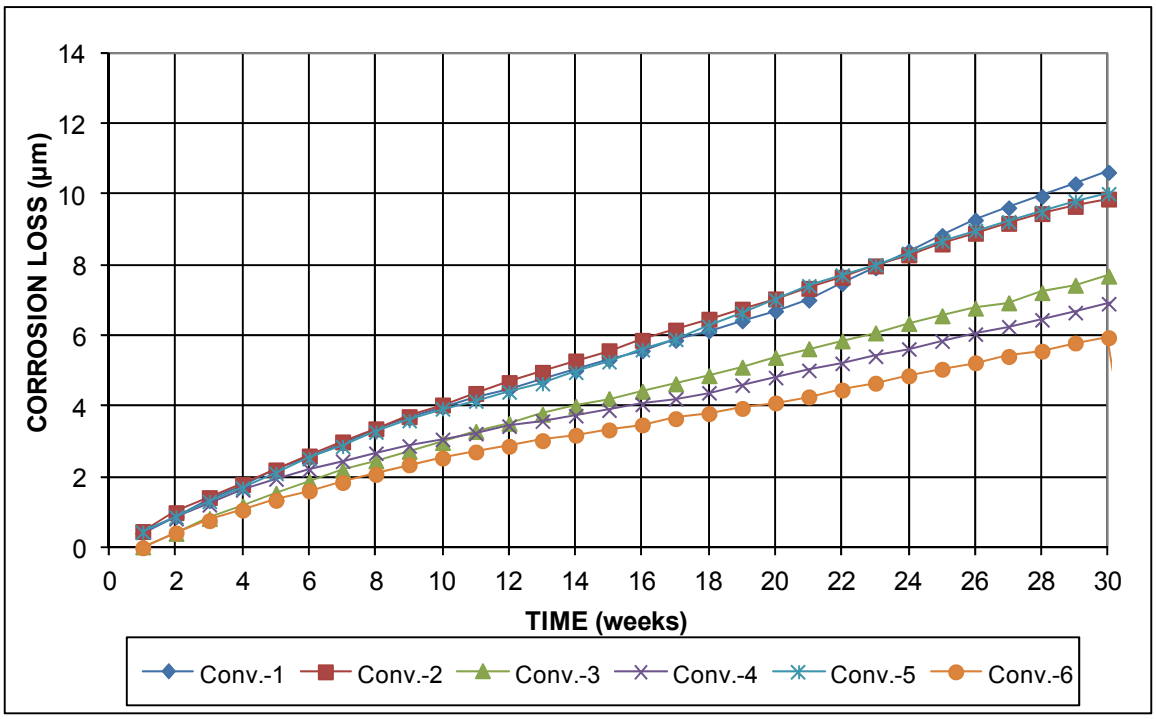

Figure C.7: Cracked beam corrosion losses – conventional steel, w/c = 0.45

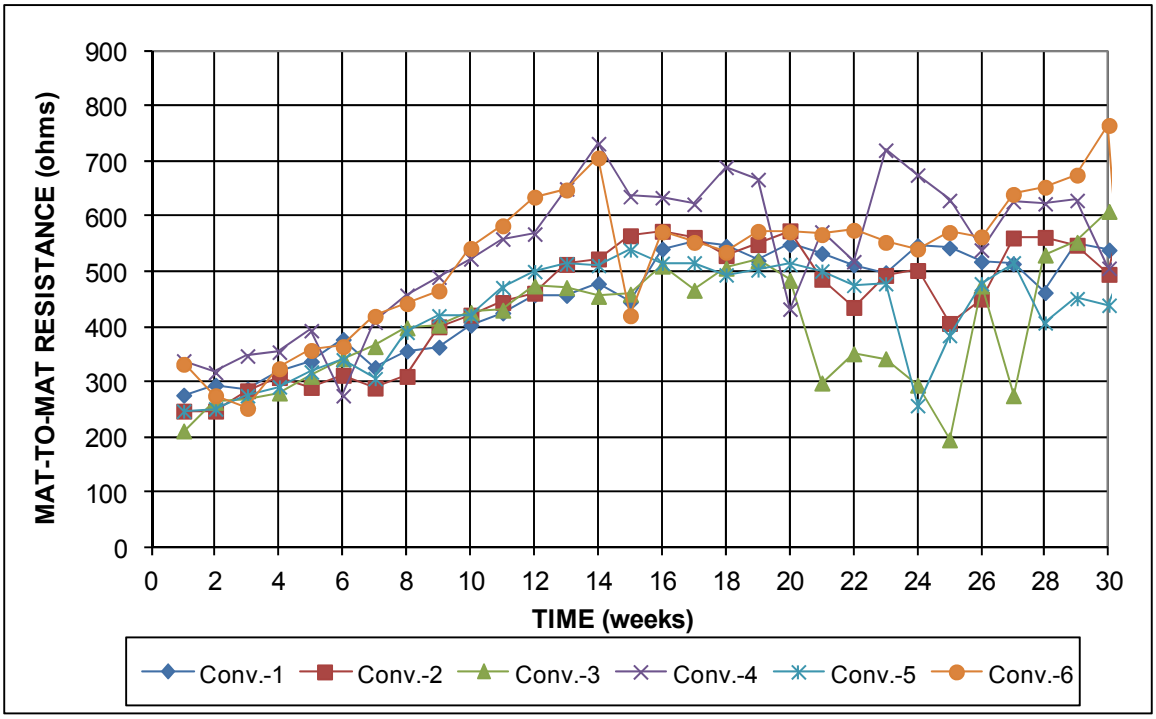

Figure C.8: Cracked beam mat-to-mat resistances – conventional steel, w/c = 0.45

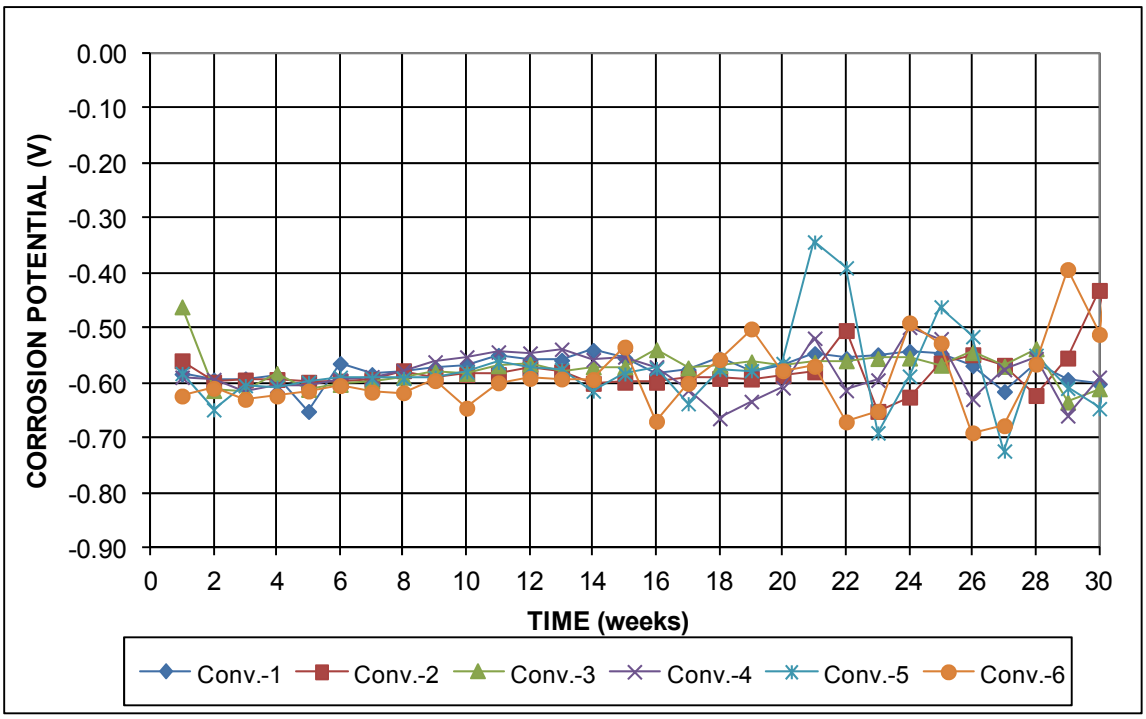

Figure C.9: Cracked beam corrosion potentials with respect to CSE – conventional steel, top mat, w/c = 0.45

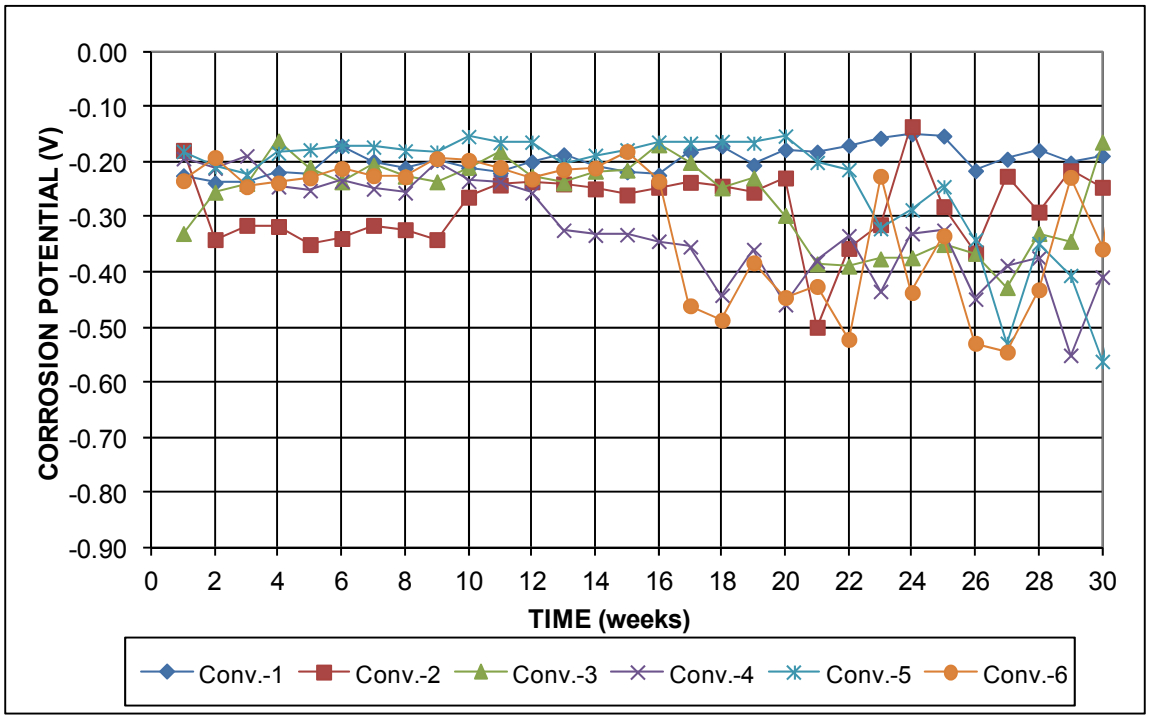

Figure C.10: Cracked beam corrosion potentials with respect to CSE – conventional steel, bottom mat, w/c = 0.45

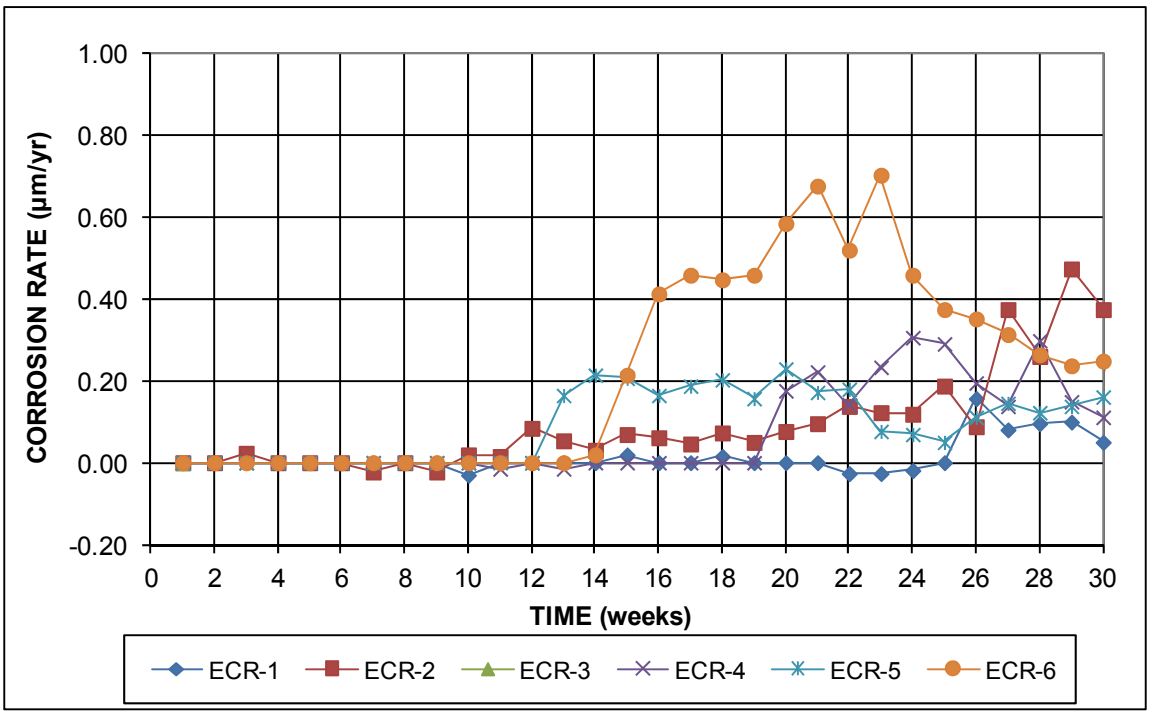

Figure C.11: Southern Exposure corrosion rates (based on total area) – epoxy coated steel, w/c = 0.45

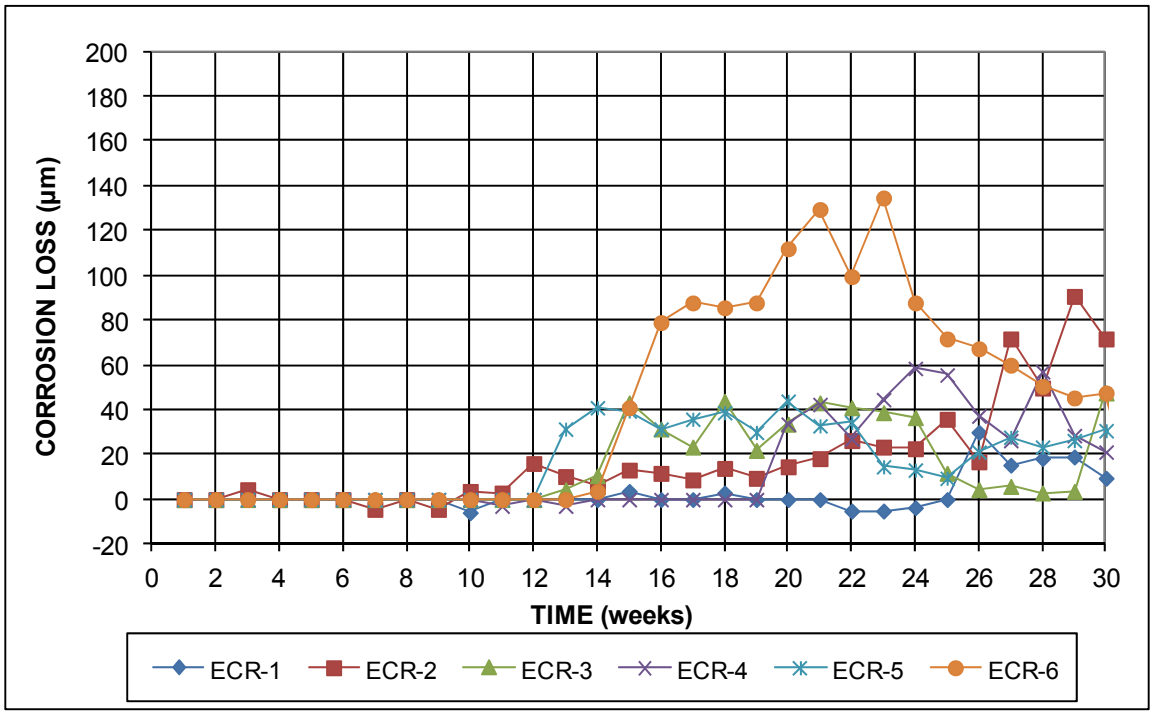

Figure C.12: Southern Exposure corrosion rates (based on exposed area) – epoxy coated steel, w/c = 0.45

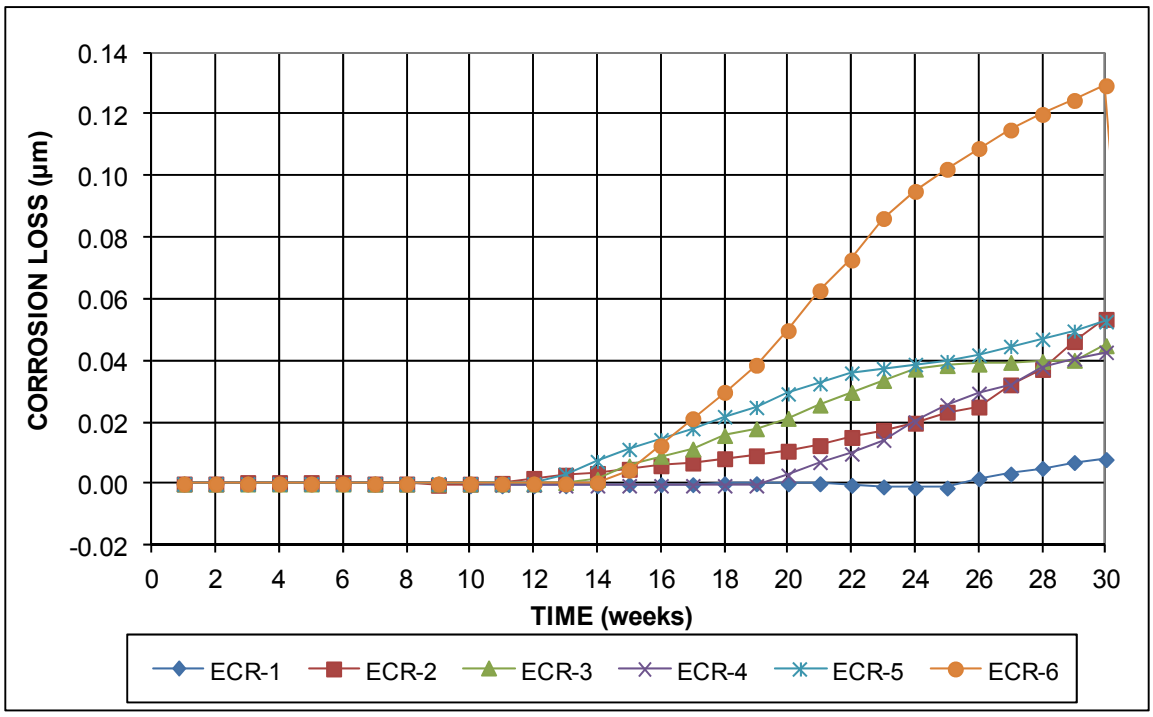

Figure C.13: Southern Exposure corrosion losses (based on total area) – epoxy coated steel, w/c = 0.45

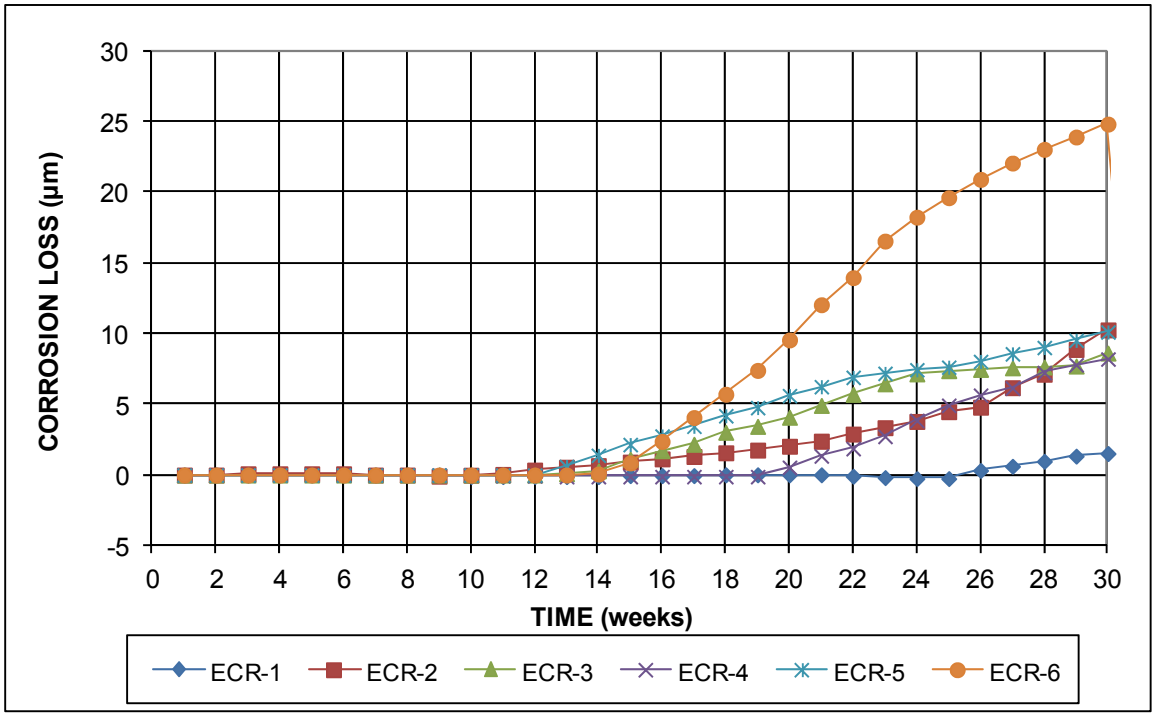

Figure C.14: Southern Exposure corrosion losses (based on exposed area) – epoxy coated steel

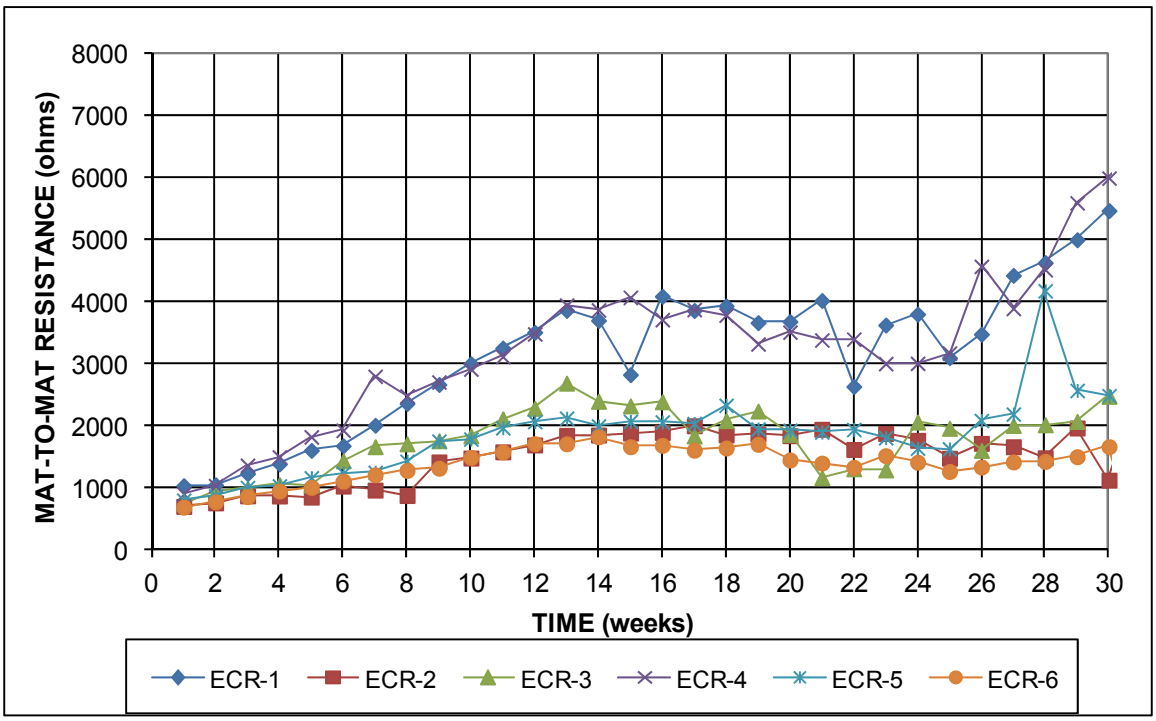

Figure C.15: Southern Exposure mat-to-mat resistances – epoxy coated steel, w/c = 0.45

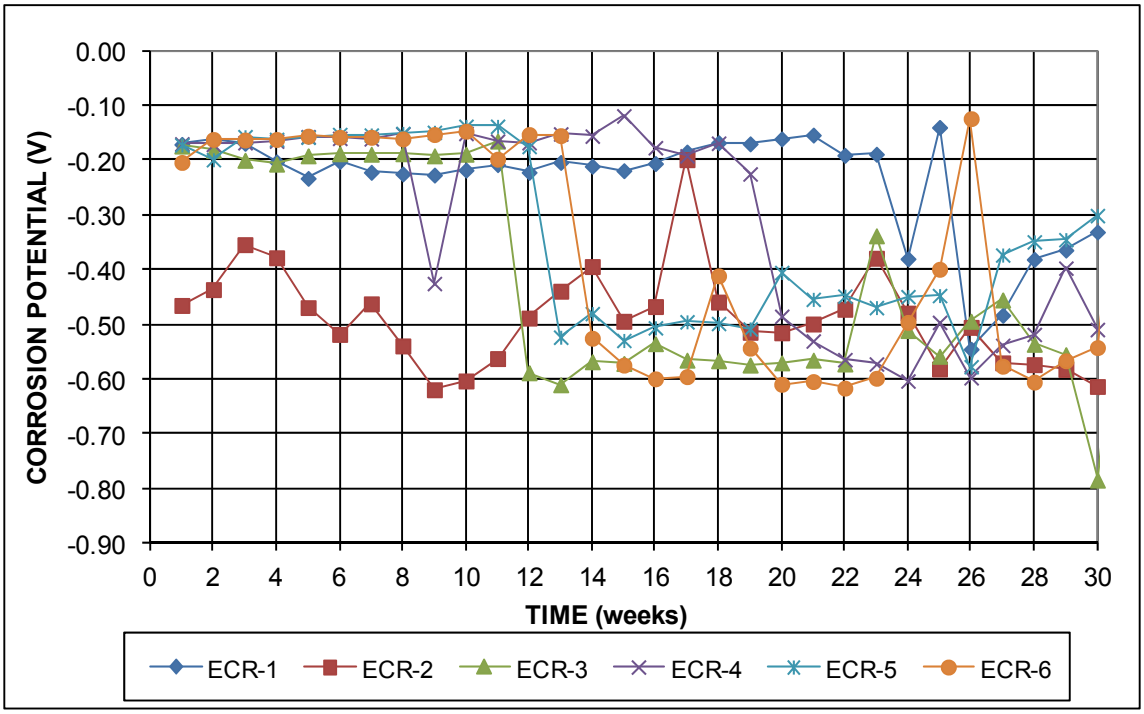

Figure C.16: Southern Exposure corrosion potentials with respect to CSE – epoxy coated steel, top mat, w/c = 0.45

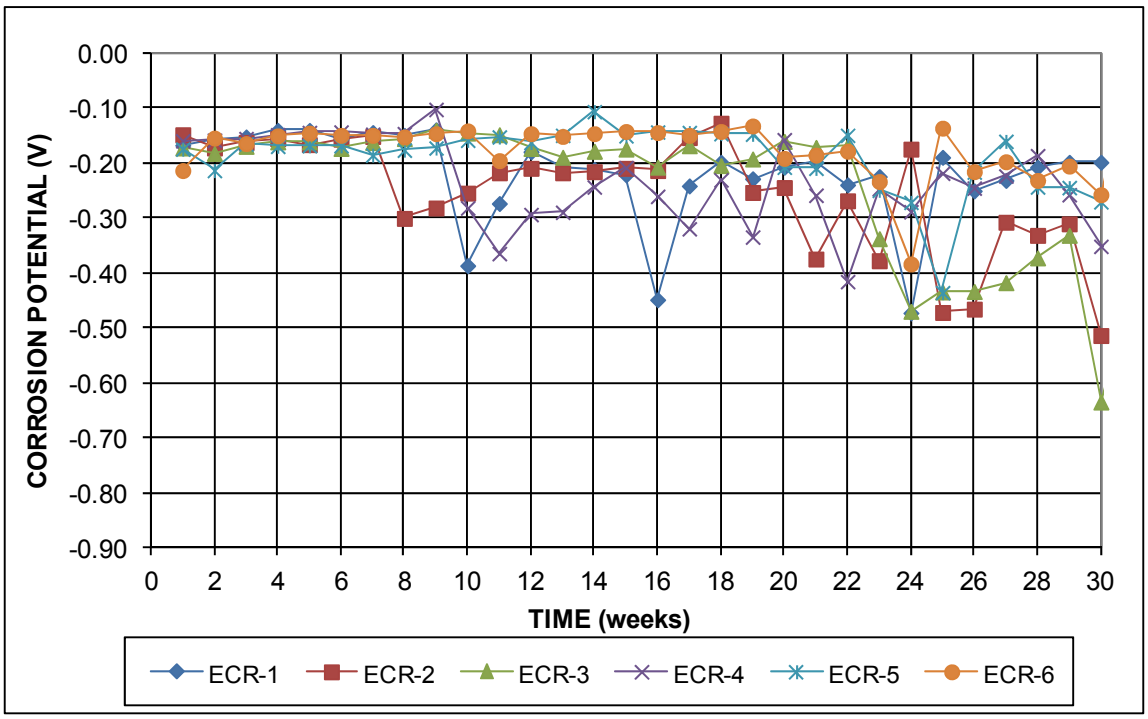

Figure C.17: Southern Exposure corrosion potentials with respect to CSE – epoxy coated steel, bottom mat, w/c = 0.45

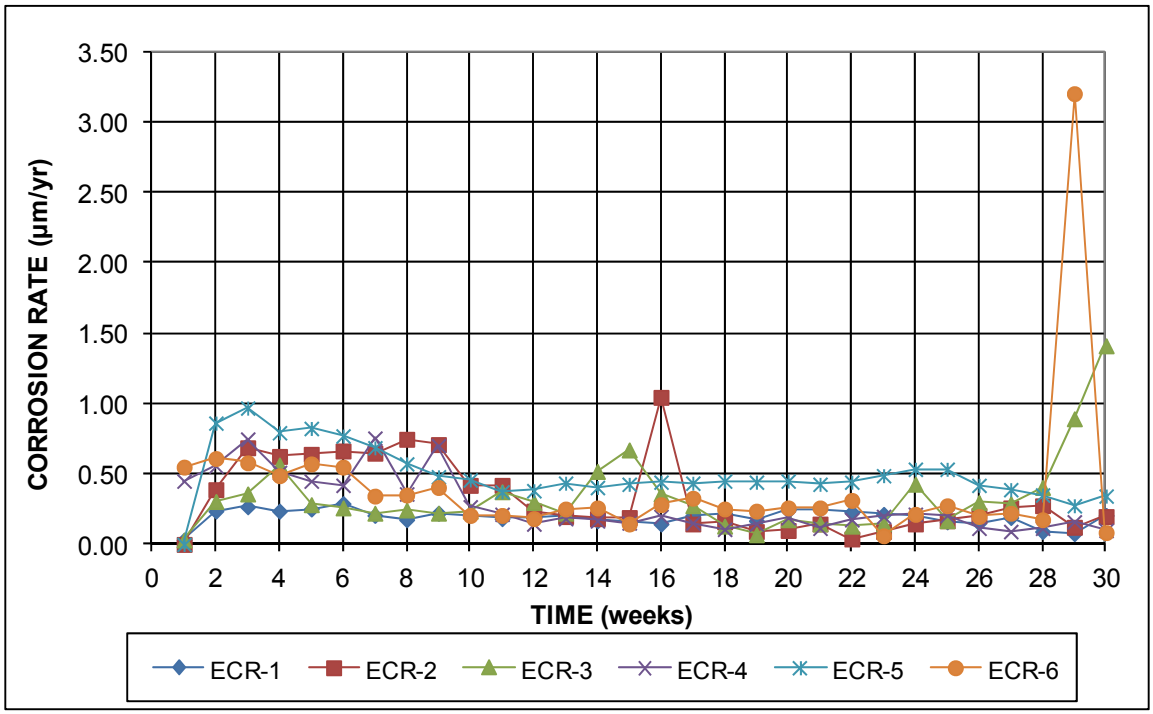

Figure C.18: Cracked beam corrosion rates (based on total area) – epoxy coated steel, w/c = 0.45

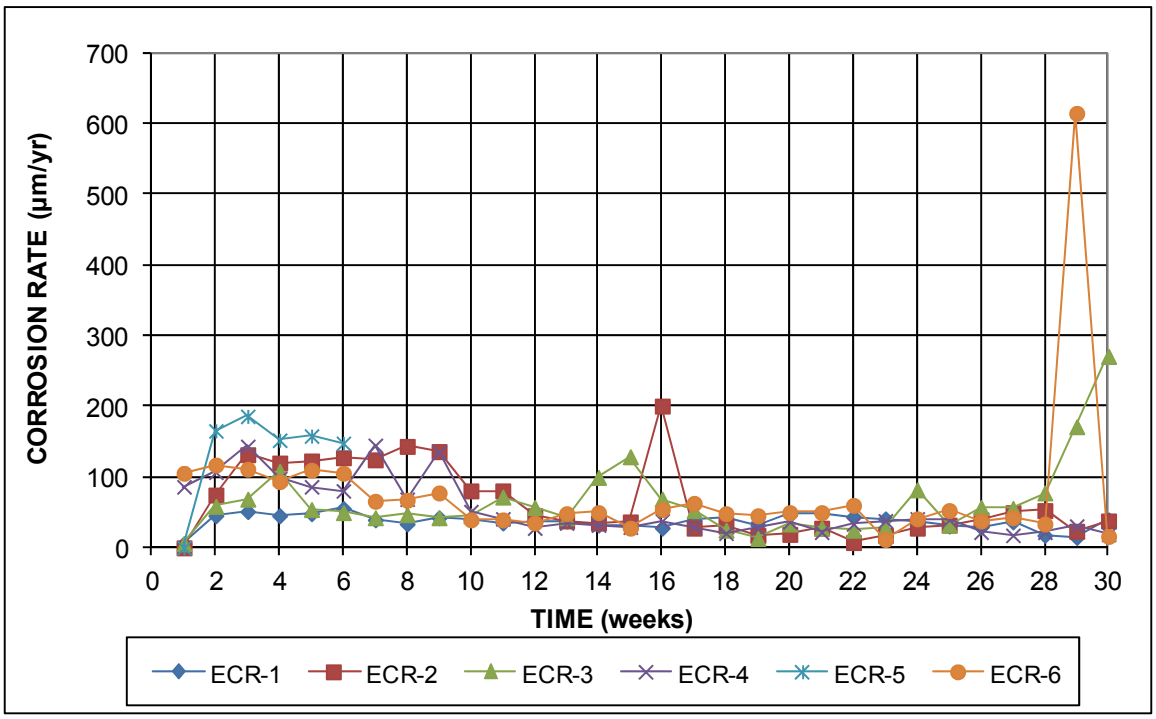

Figure C.19: Cracked beam corrosion rates (based on exposed area) – epoxy coated steel, w/c = 0.45

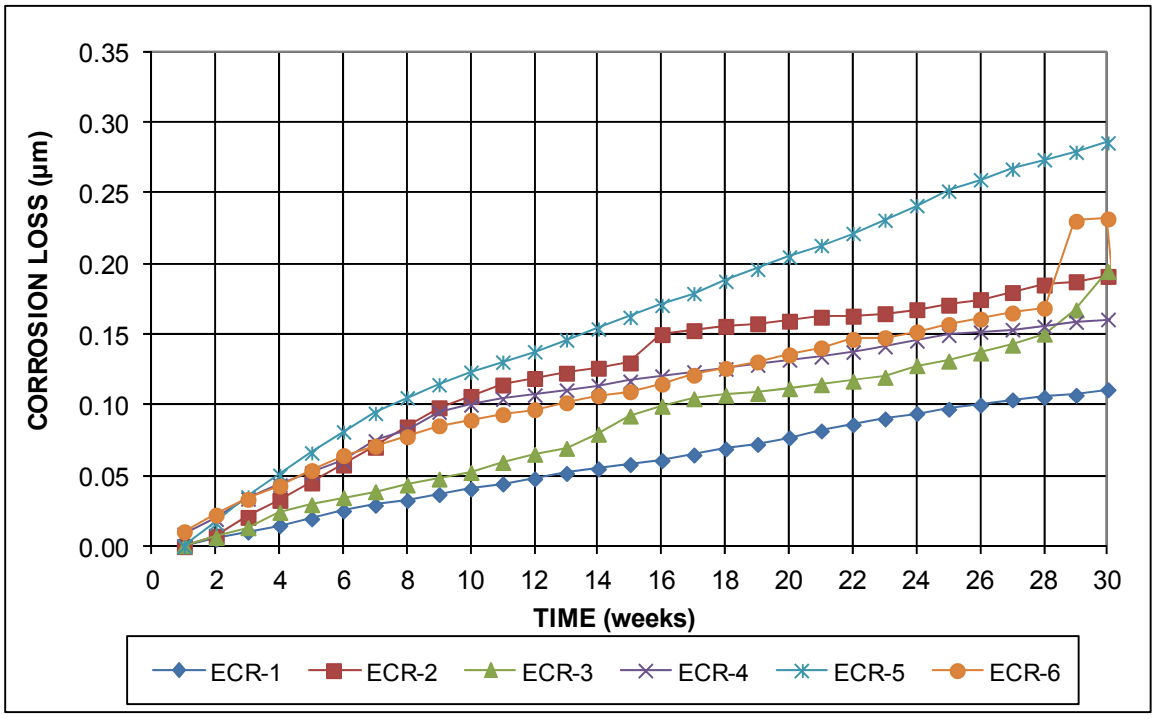

Figure C.20: Cracked beam corrosion losses (based on total area) – epoxy coated steel, w/c = 0.45

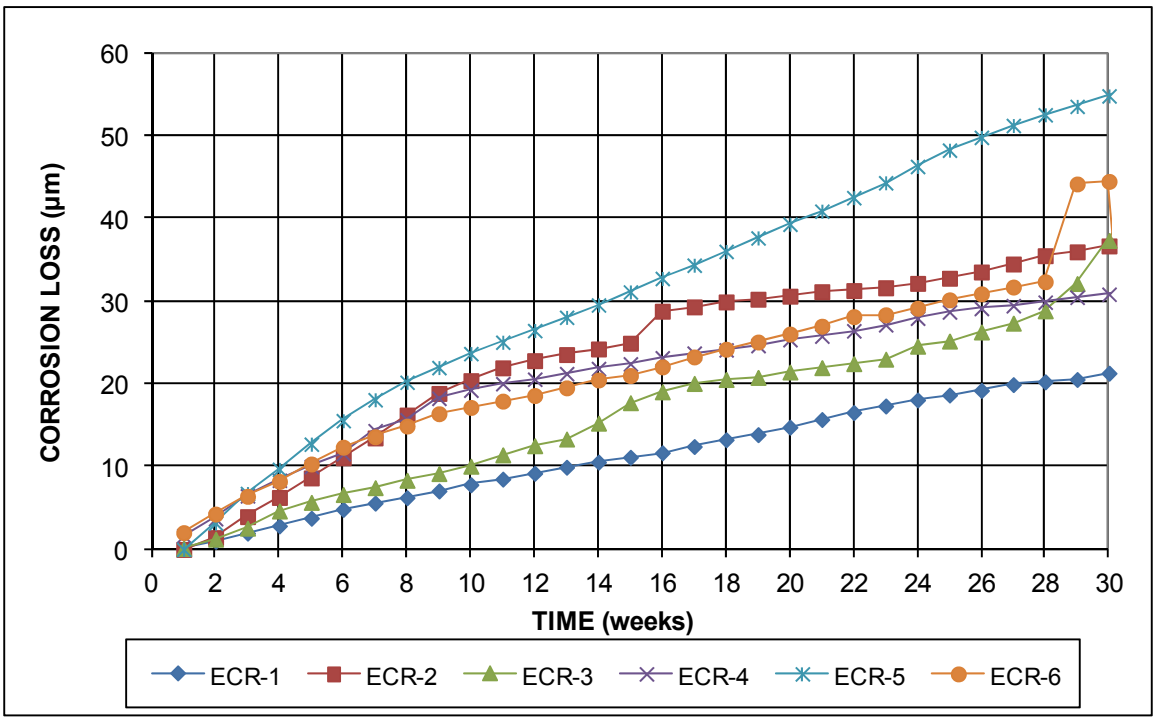

Figure C.21: Cracked beam corrosion losses (based on exposed area) – epoxy coated steel, w/c = 0.45

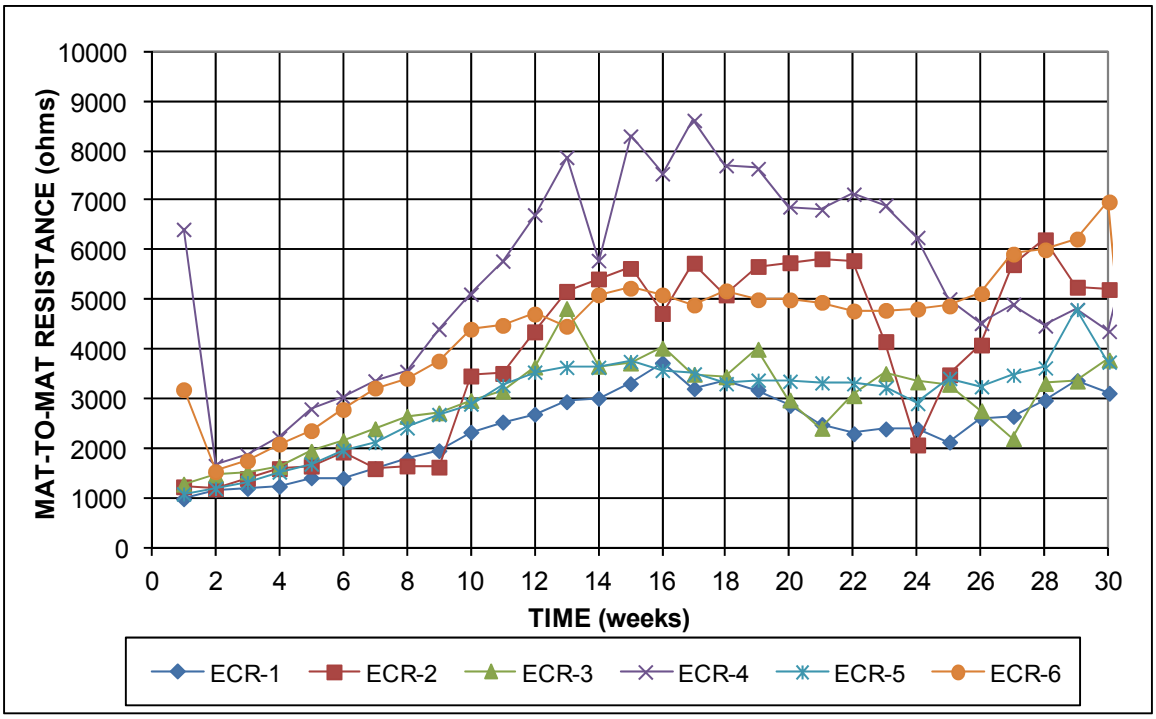

Figure C.22: Cracked beam mat-to-mat resistances – epoxy coated steel, w/c = 0.45

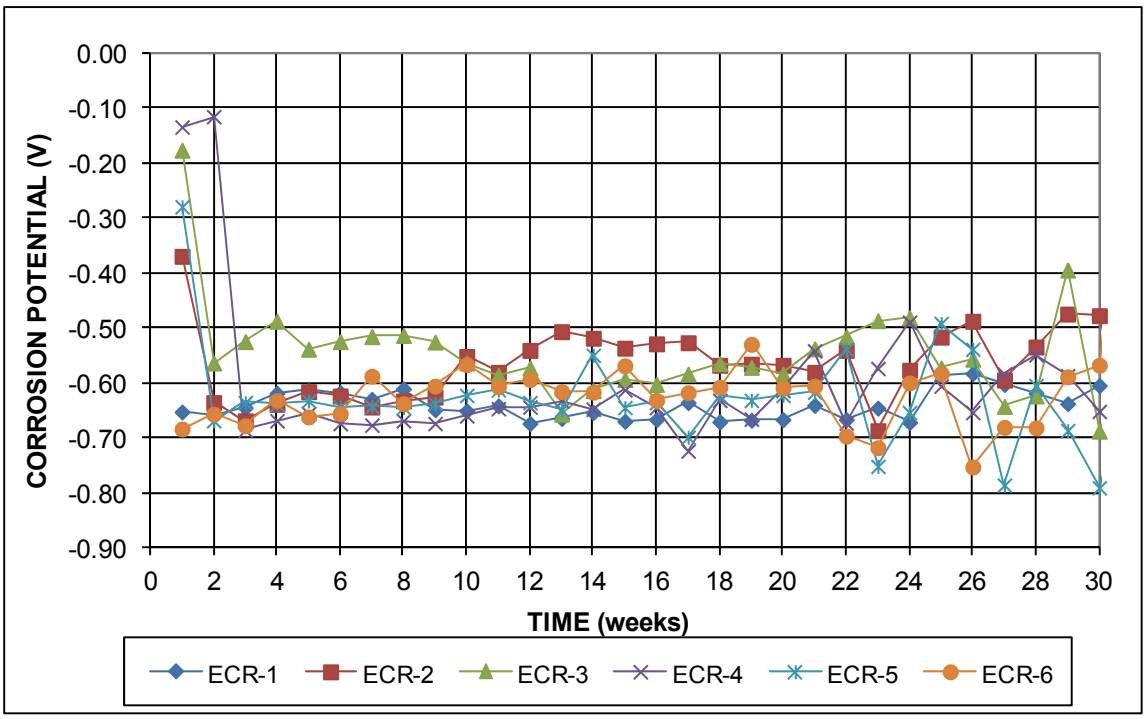

Figure C.23: Cracked beam corrosion potentials with respect to CSE – epoxy coated steel, top mat, w/c = 0.45

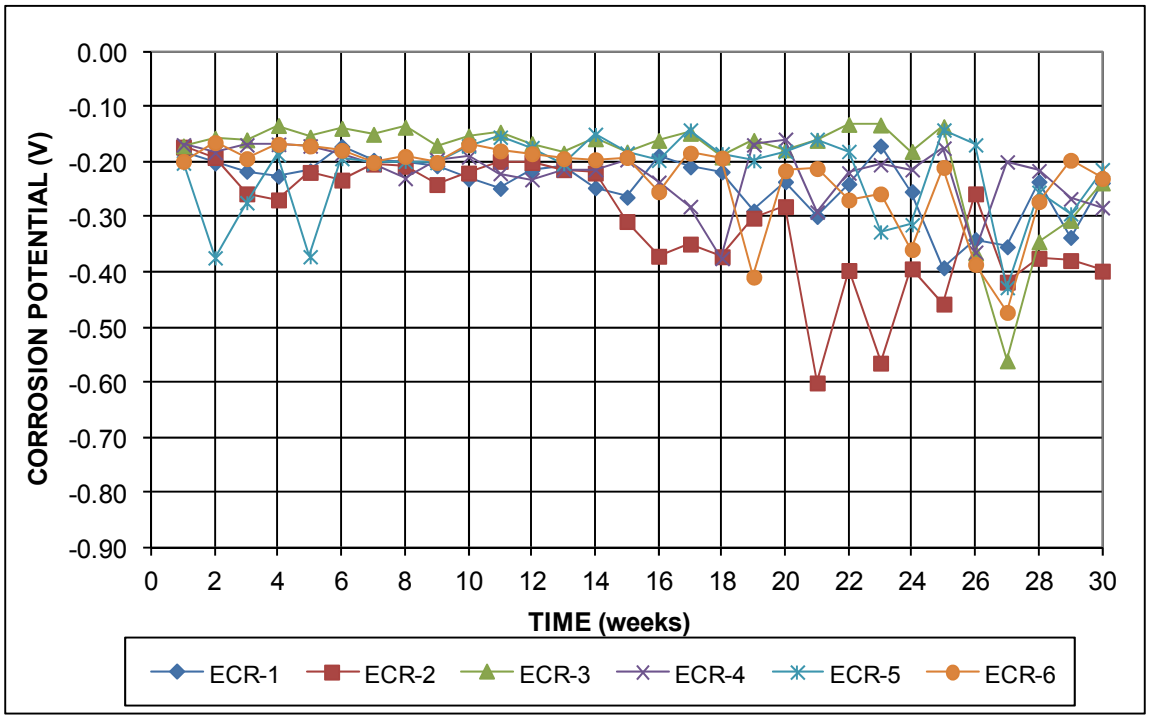

Figure C.24: Cracked beam corrosion potentials with respect to CSE – epoxy coated steel, bottom mat, w/c = 0.45

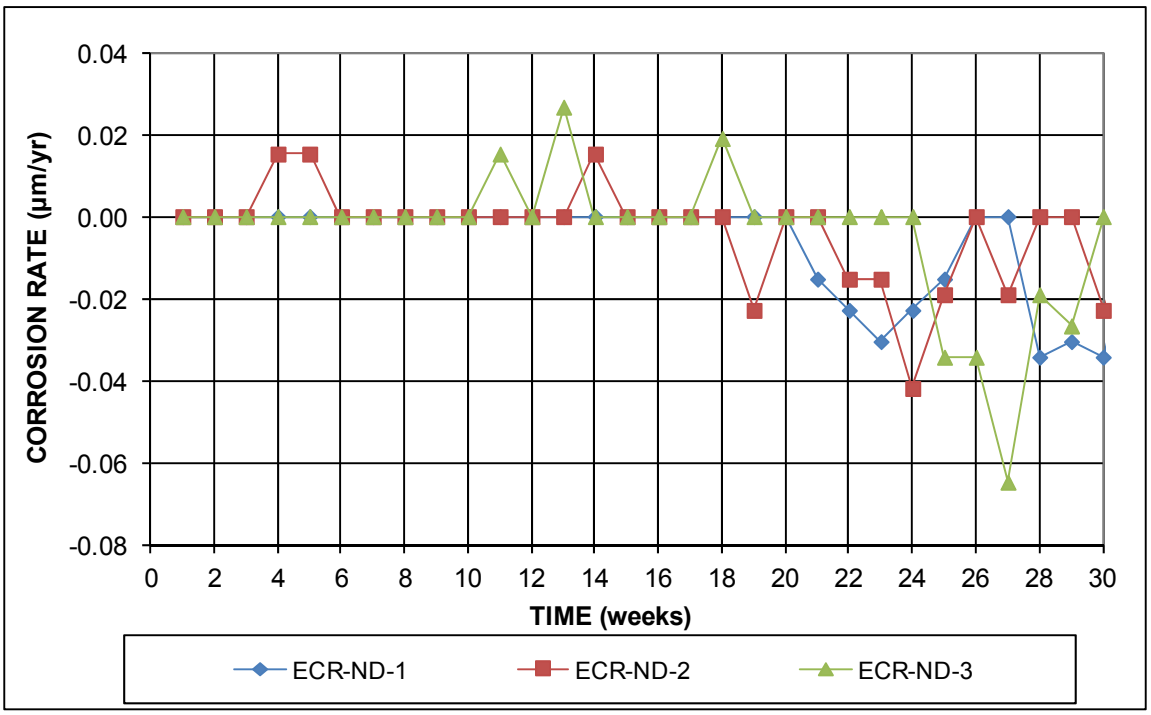

Figure C.25: Southern Exposure corrosion rates– epoxy coated (no damage) steel , w/c = 0.45

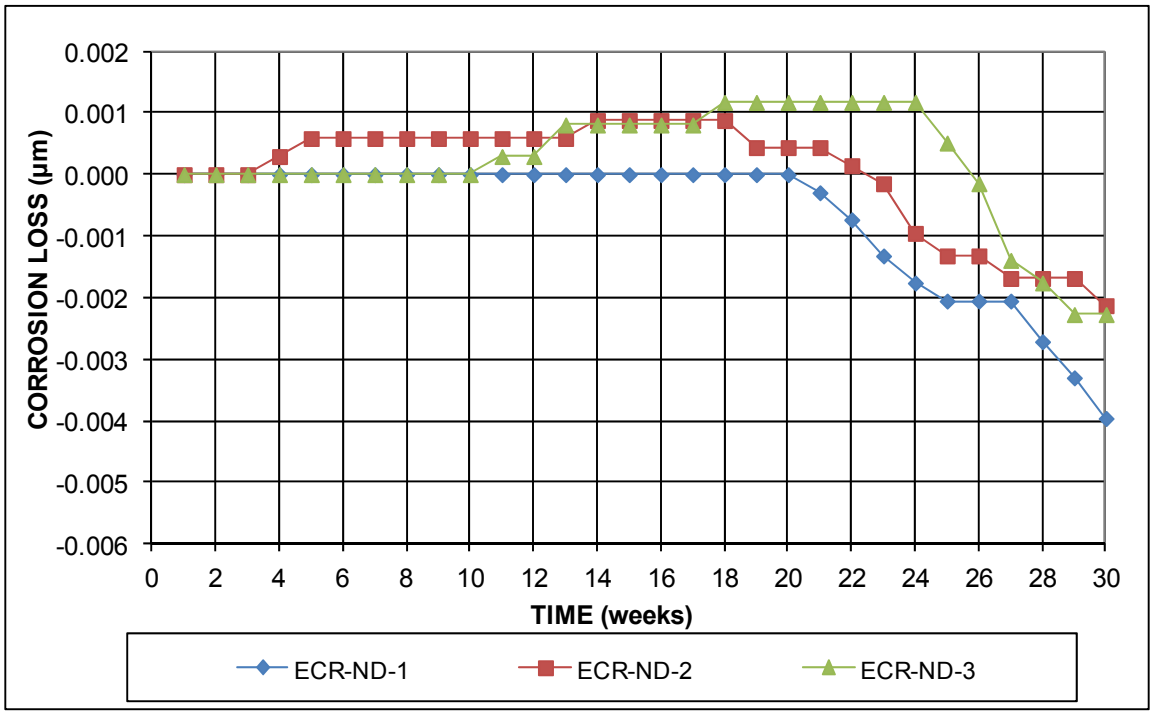

Figure C.26: Southern Exposure corrosion losses – epoxy coated (no damage) steel, w/c = 0.45

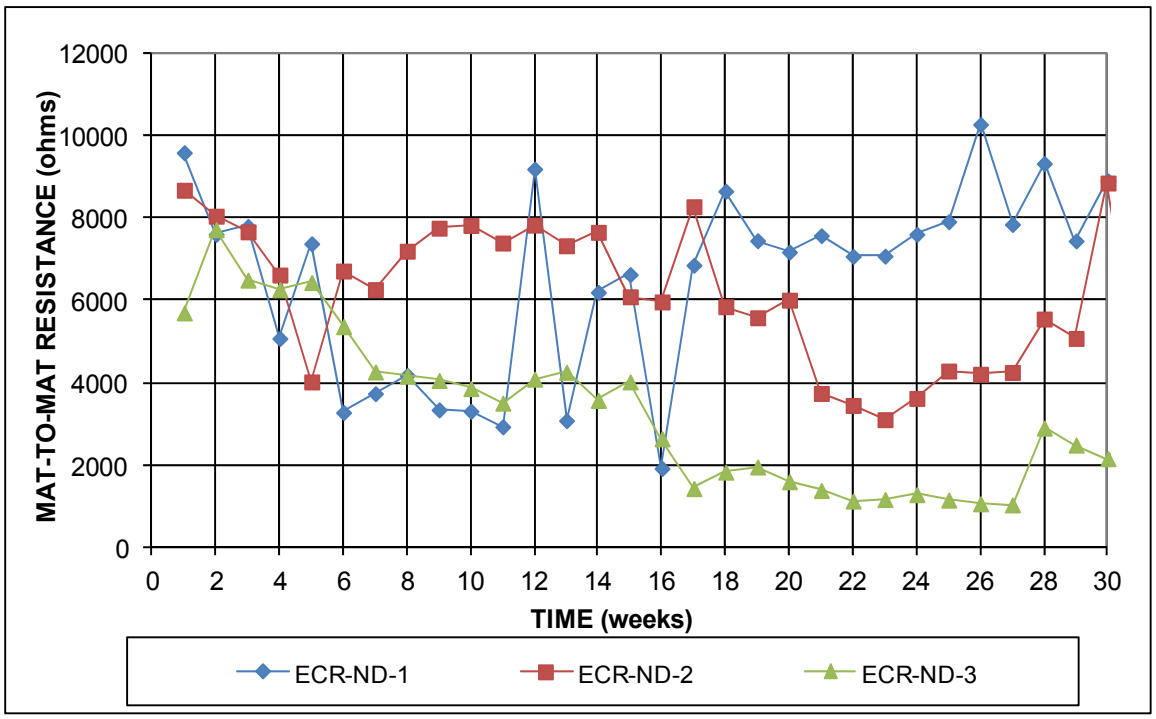

Figure C.27: Southern Exposure mat-to-mat resistances – epoxy coated (no damage) steel, w/c = 0.45

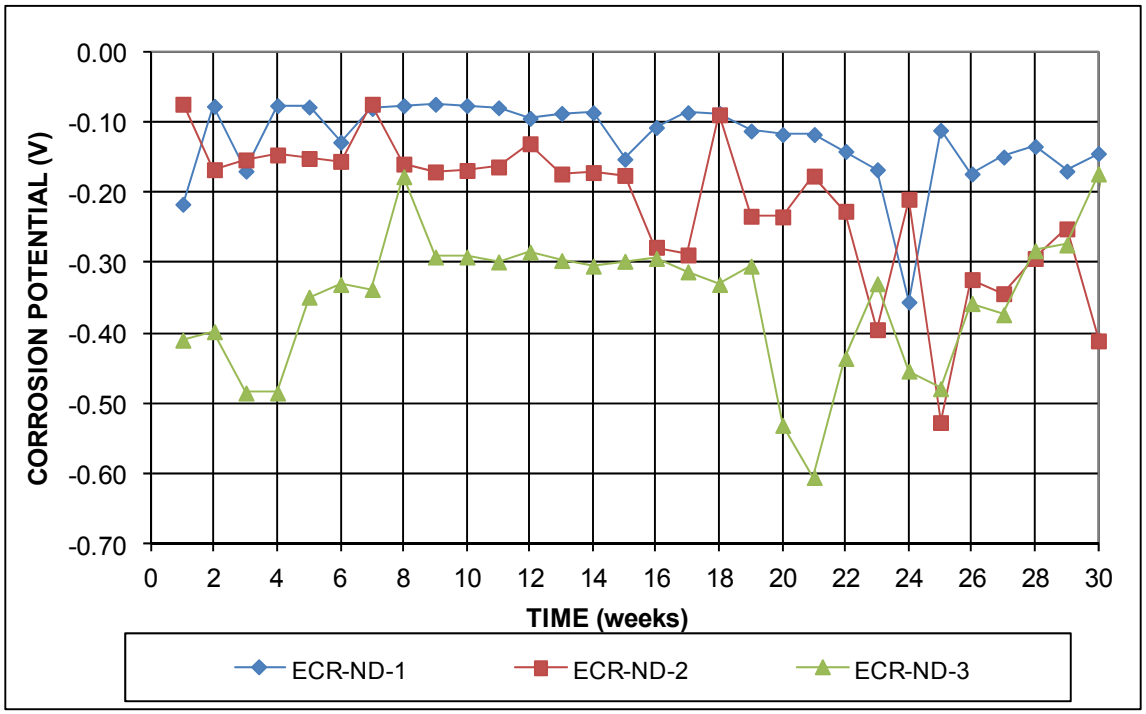

Figure C.28: Southern Exposure corrosion potentials with respect to CSE – epoxy coated (no damage) steel, top mat, w/c = 0.45

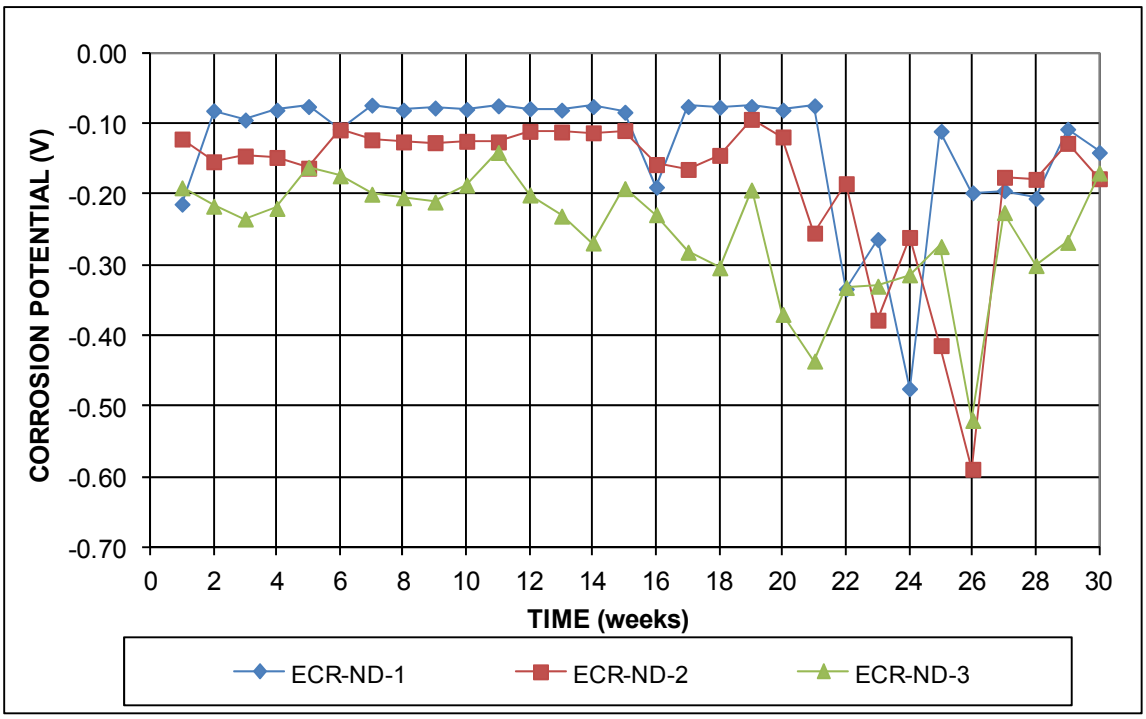

Figure C.29: Southern Exposure corrosion potentials with respect to CSE – epoxy coated (no damage) steel, bottom mat, w/c = 0.45

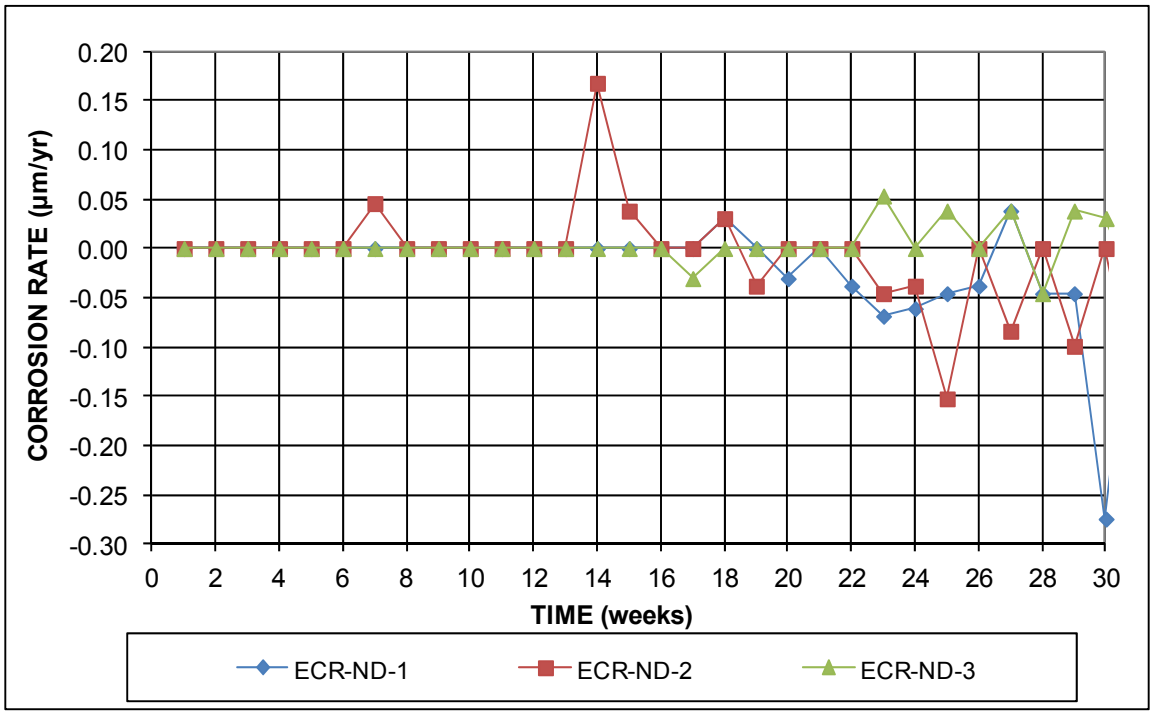

Figure C.30: Cracked beam corrosion rates – epoxy coated steel, w/c = 0.45

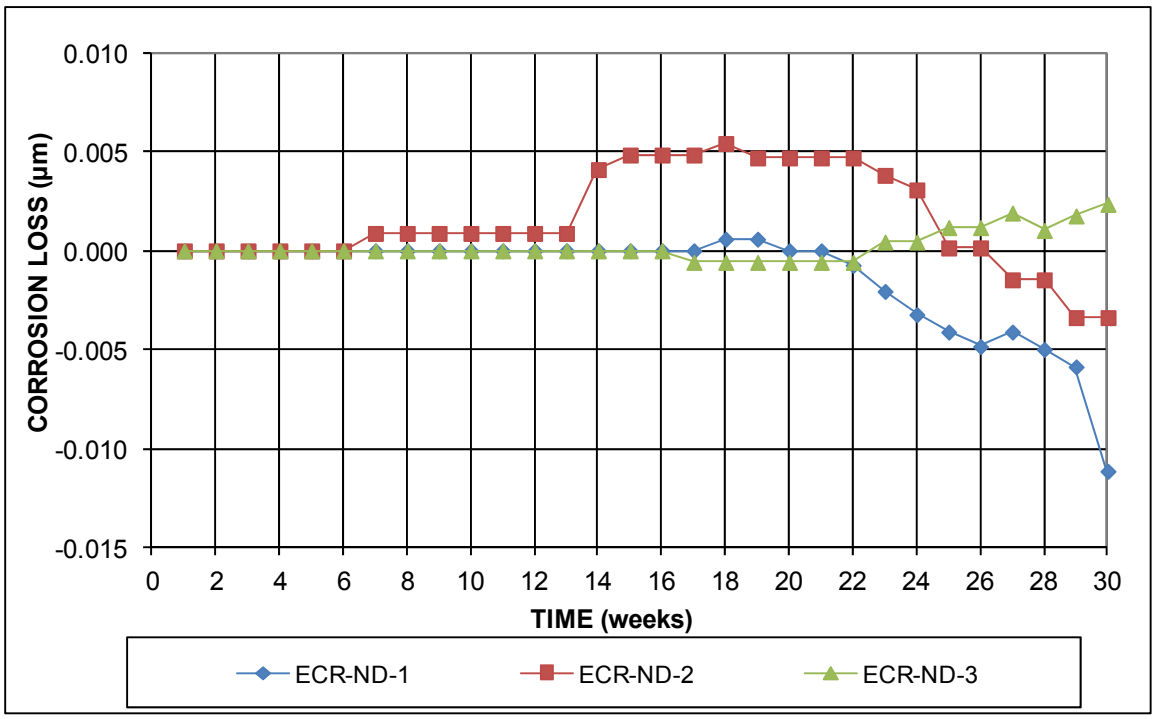

Figure C.31: Cracked beam corrosion losses – epoxy coated steel, w/c = 0.45

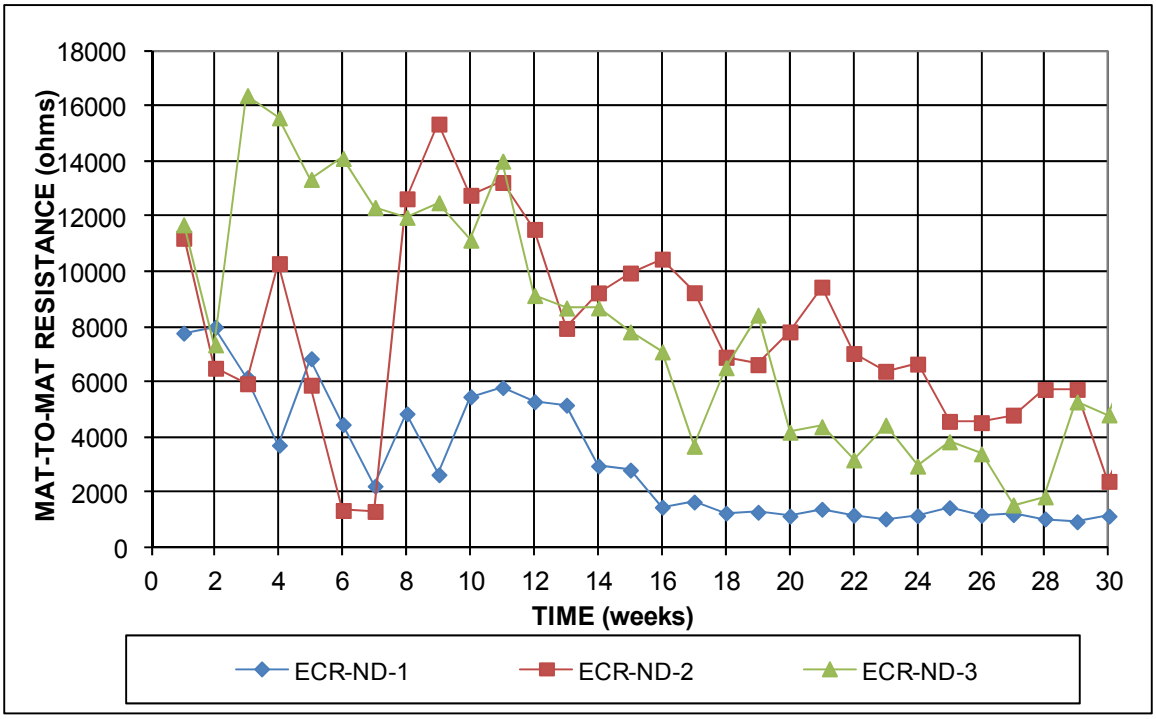

Figure C.32: Cracked beam mat-to-mat resistances – epoxy coated steel, w/c = 0.45

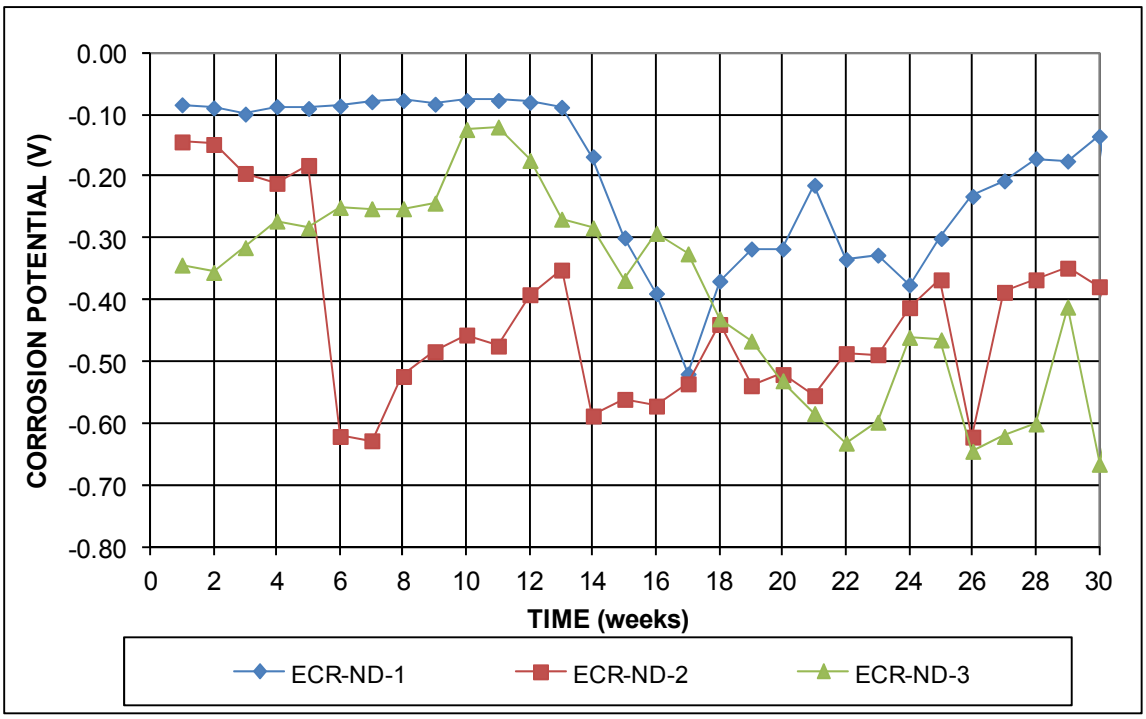

Figure C.33: Cracked beam corrosion potentials with respect to CSE – epoxy coated steel, top mat, w/c = 0.45

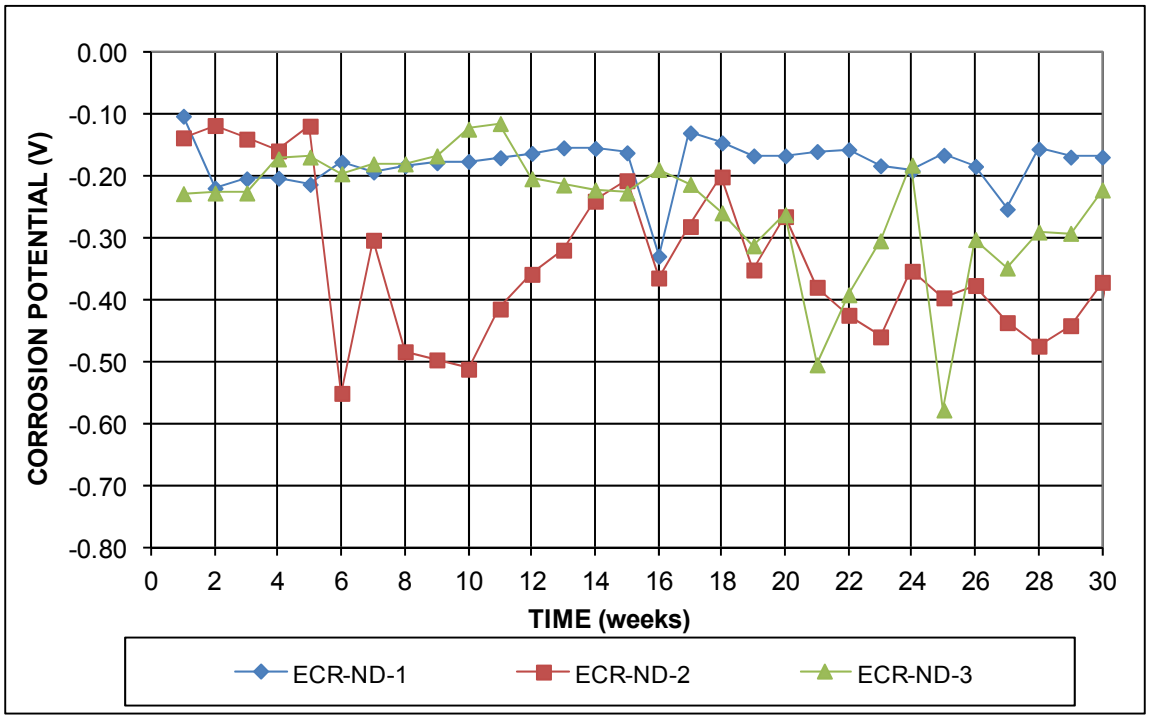

Figure C.34: Cracked beam corrosion potentials with respect to CSE – epoxy coated steel, bottom mat, w/c = 0.45

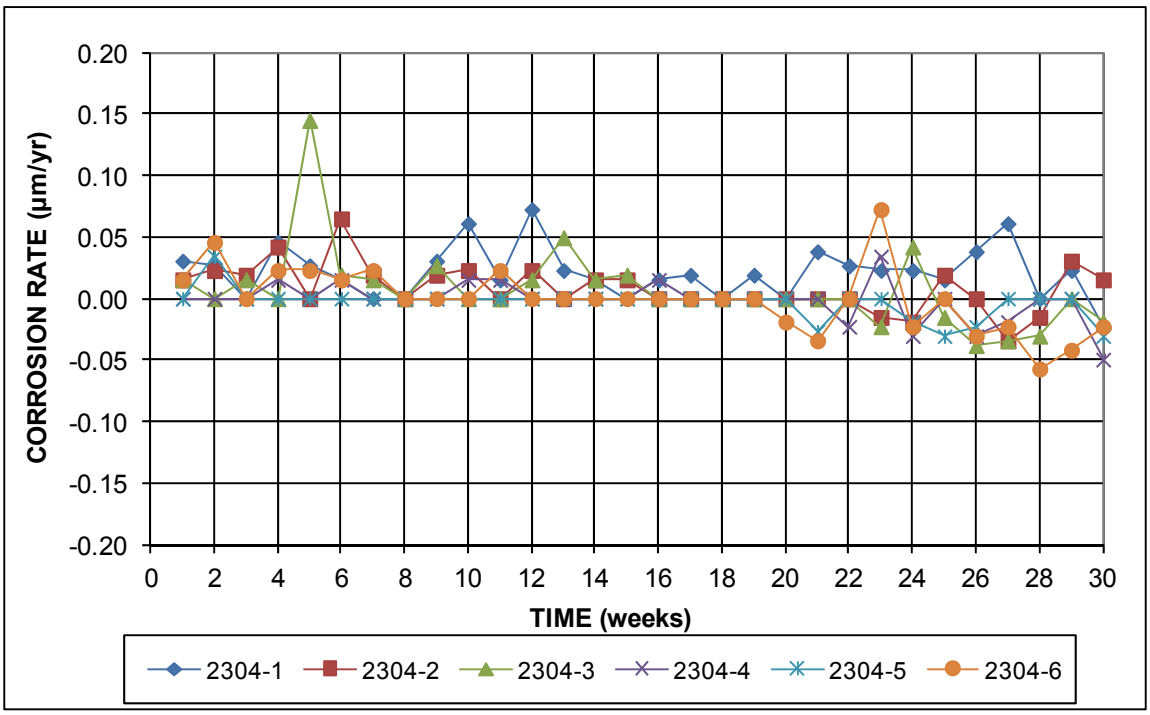

Figure C.35: Southern Exposure corrosion rates – 2304 steel, w/c = 0.45

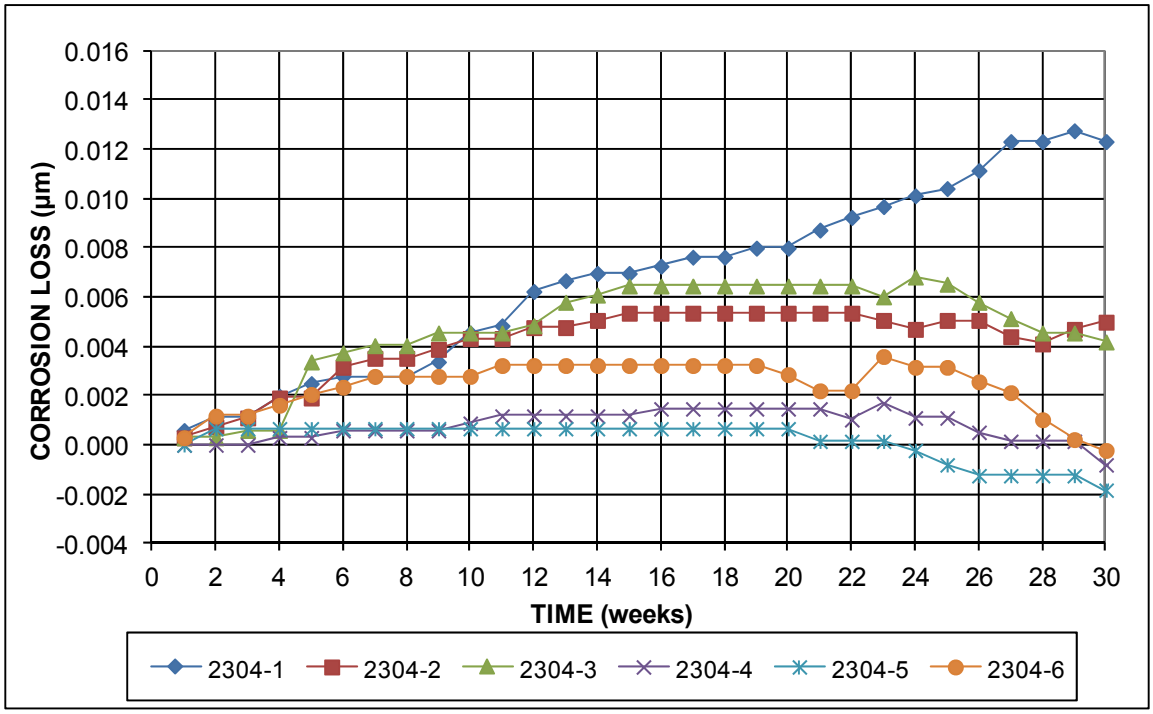

Figure C.36: Southern Exposure corrosion losses – 2304 steel, w/c = 0.45

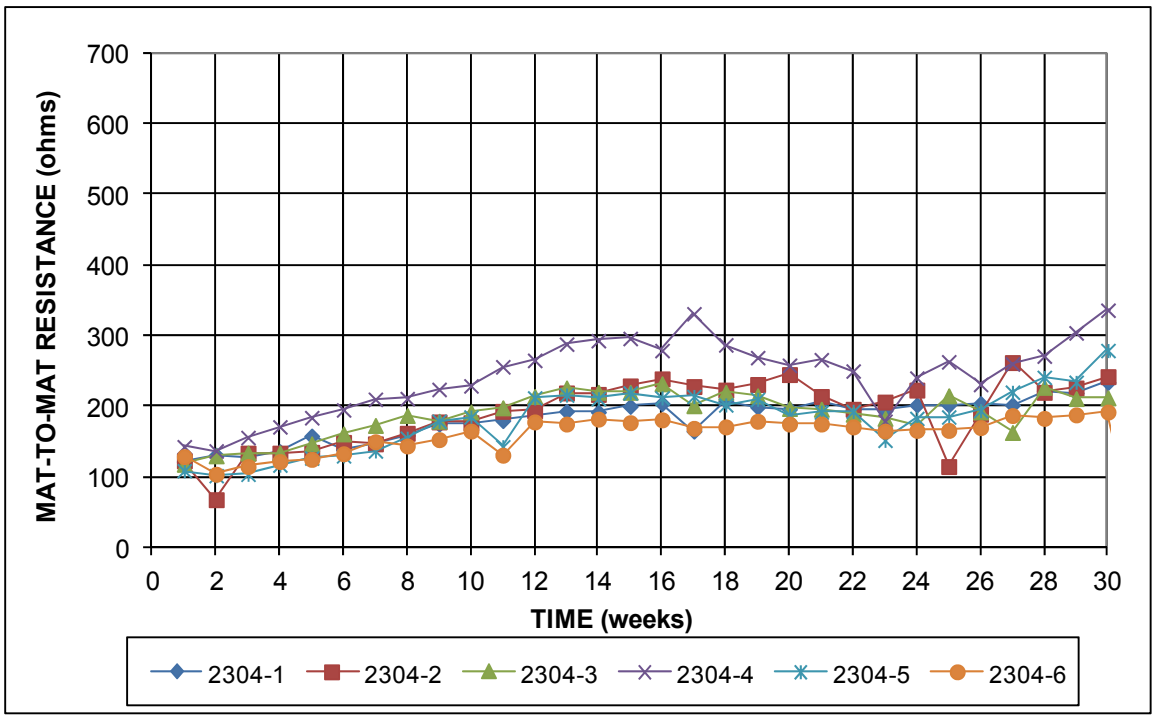

Figure C.37: Southern Exposure mat-to-mat resistances – 2304 steel, w/c = 0.45

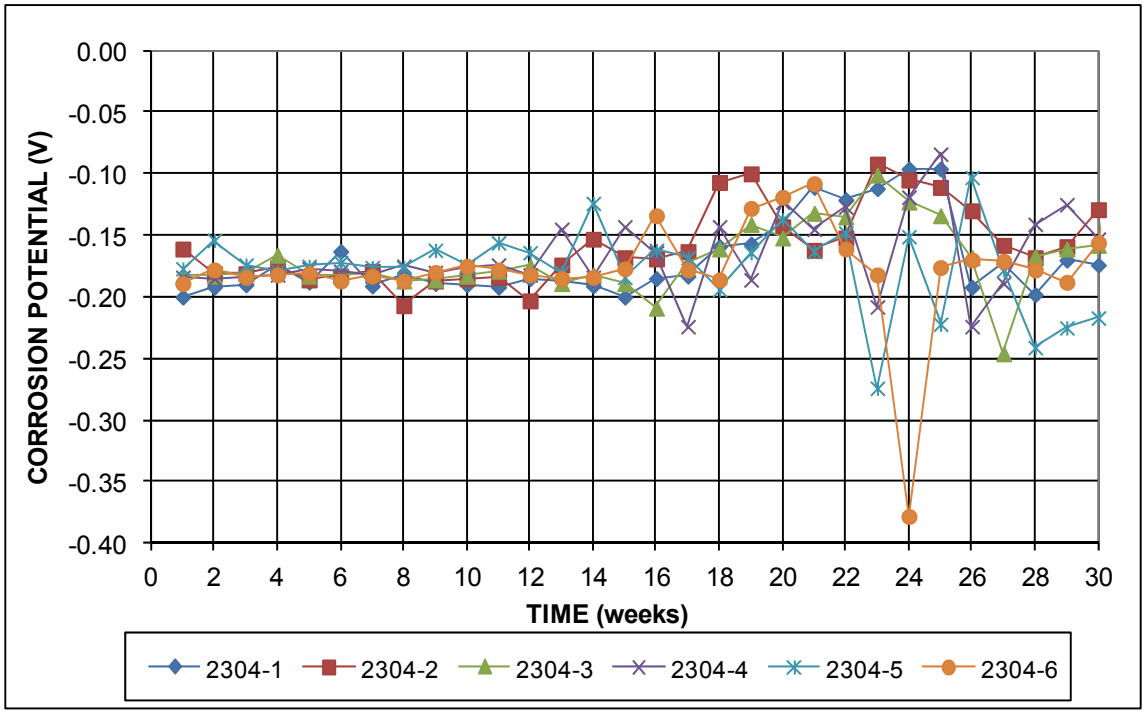

Figure C.38: Southern Exposure corrosion potentials with respect to CSE – 2304, top mat, w/c = 0.45

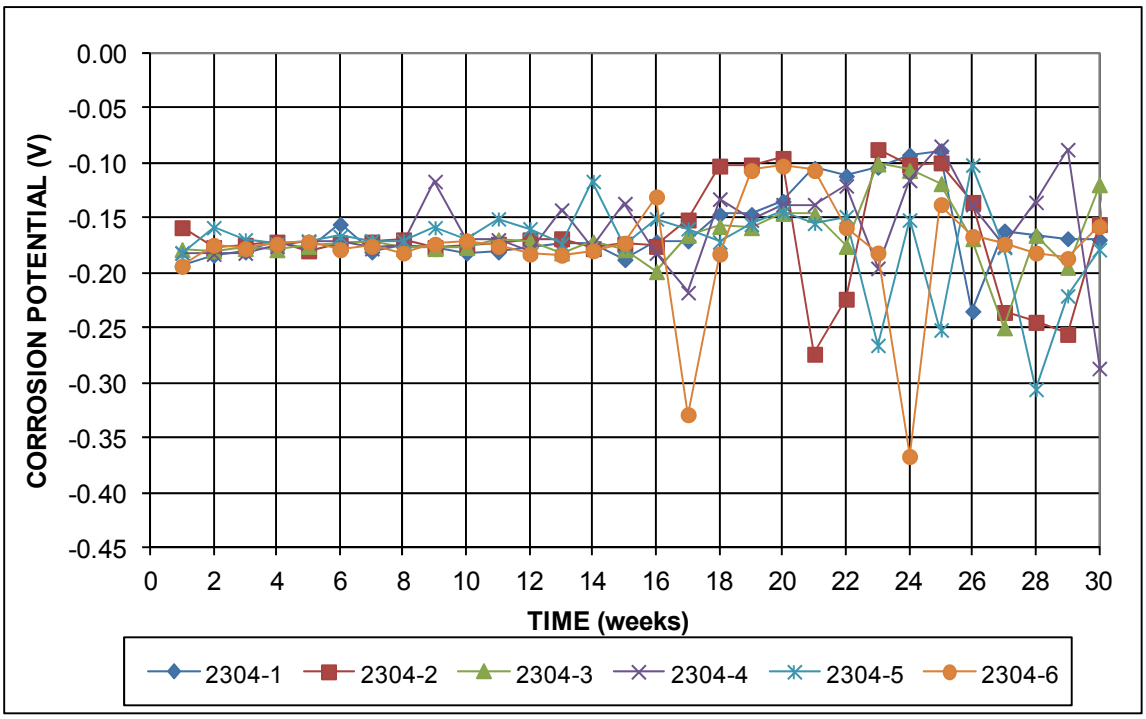

Figure C.39: Southern Exposure corrosion potentials with respect to CSE –2304, bottom mat, w/c = 0.45

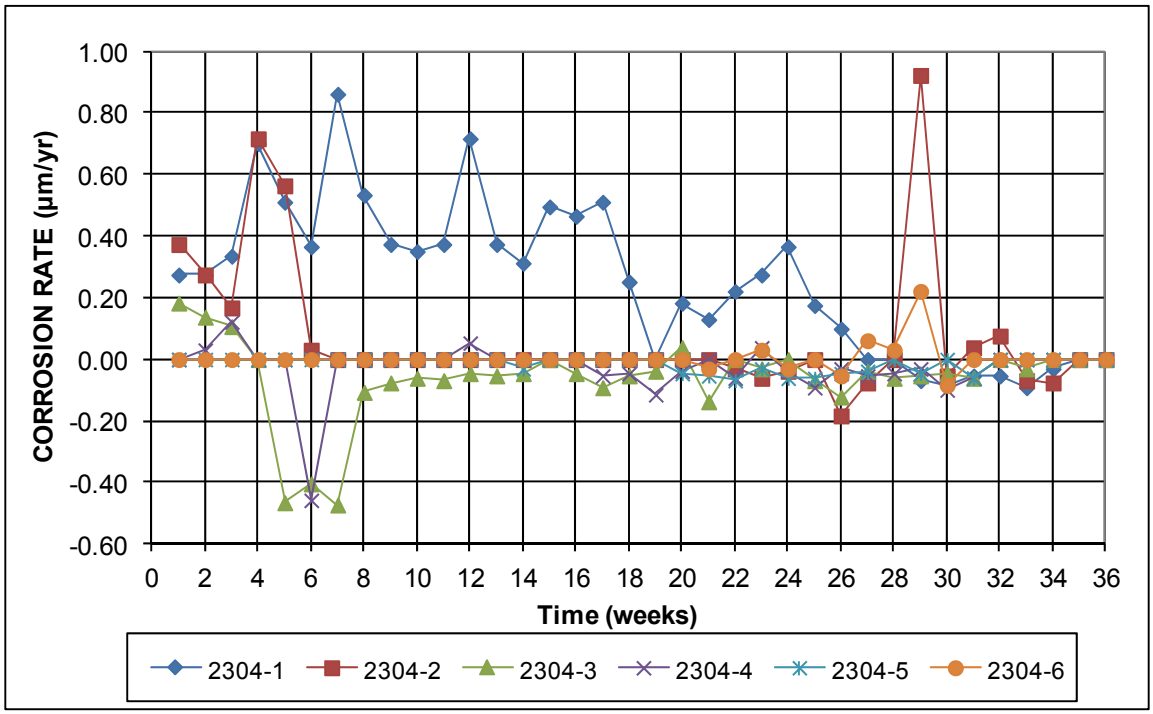

Figure C.40: Cracked beam corrosion rates – 2304 steel, w/c = 0.45

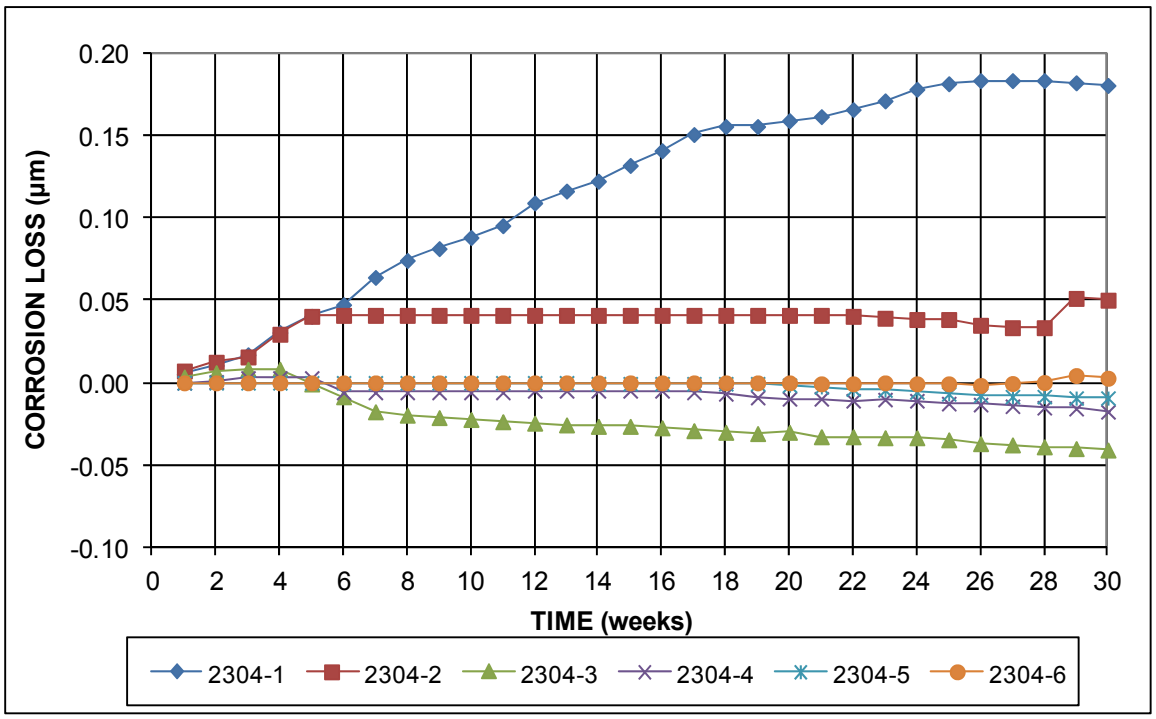

Figure C.41: Cracked beam corrosion losses – 2304 steel, w/c = 0.45

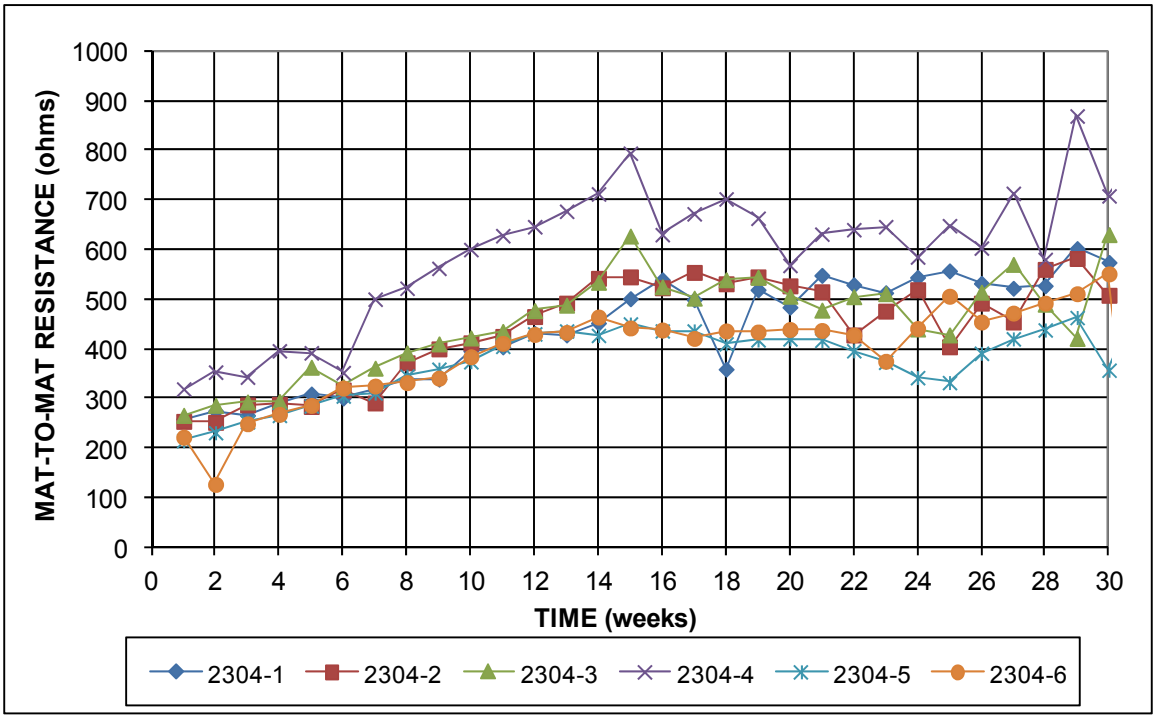

Figure C.42: Cracked beam mat-to-mat resistances – 2304 steel, w/c = 0.45

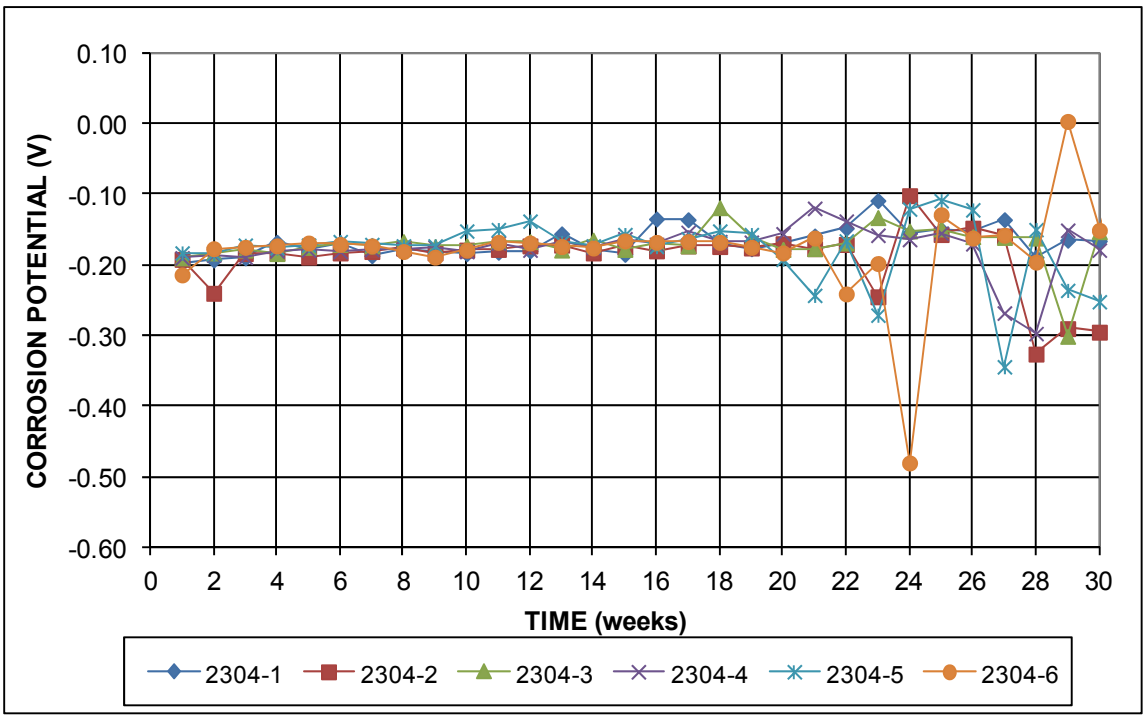

Figure C.43: Cracked beam corrosion potentials with respect to CSE – 2304, top mat, w/c = 0.45

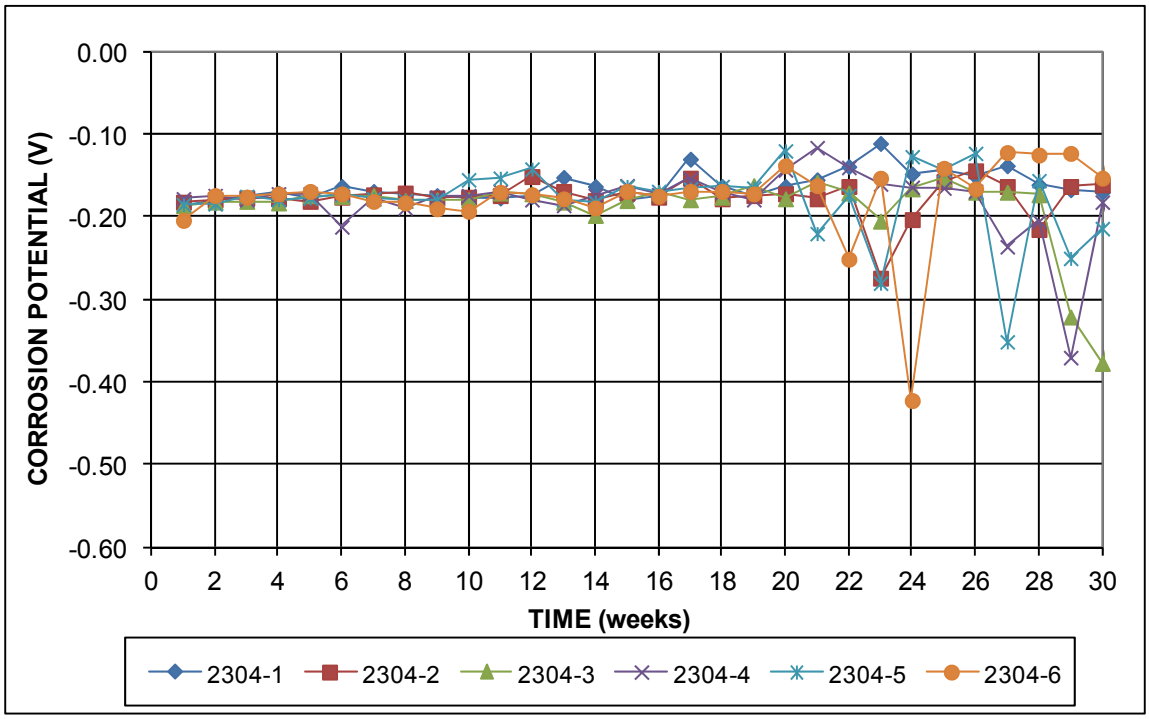

Figure C.44: Cracked beam corrosion potentials with respect to CSE – 2304, bottom mat, w/c = 0.45

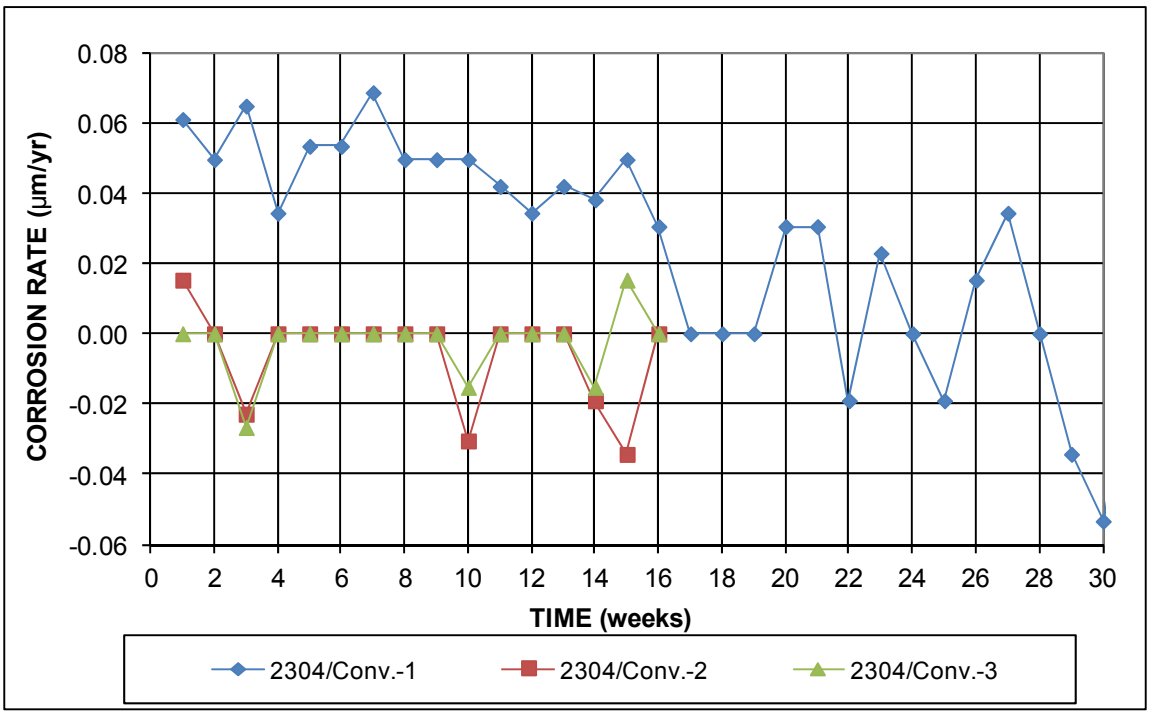

Figure C.45: Southern Exposure corrosion rates – 2304 (top mat) / conventional steel (bottom mat) , w/c = 0.45

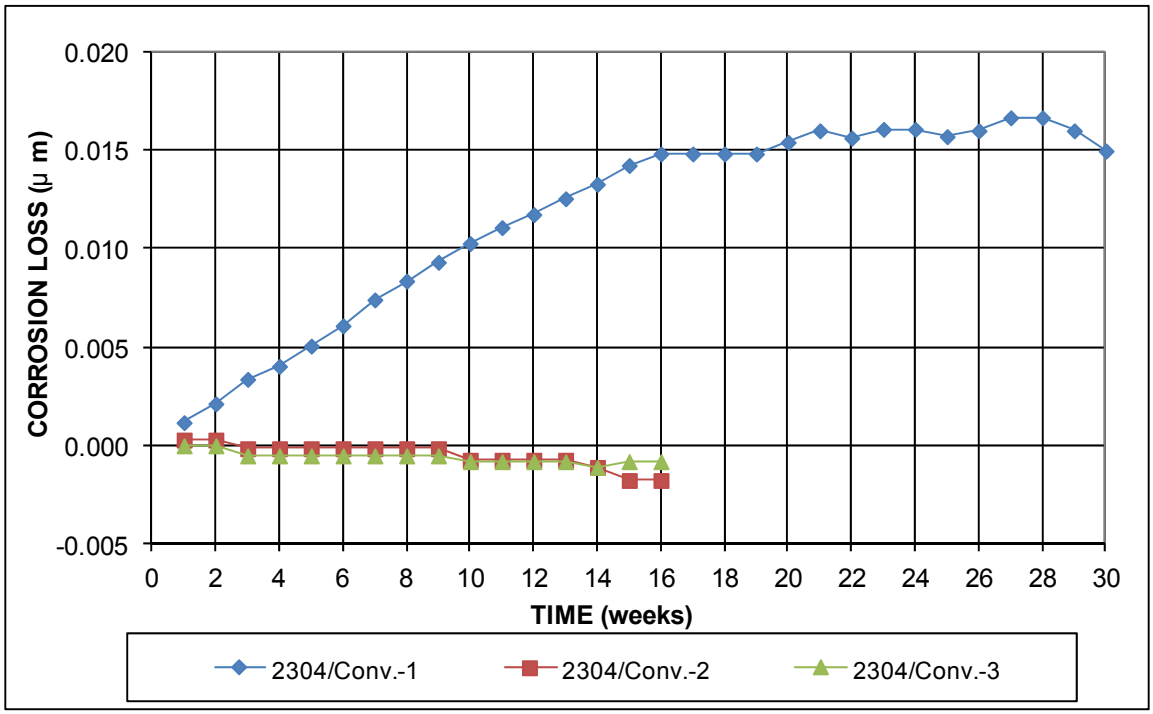

Figure C.46: Southern Exposure corrosion losses – 2304 (top mat) / conventional steel (bottom mat) , w/c = 0.45

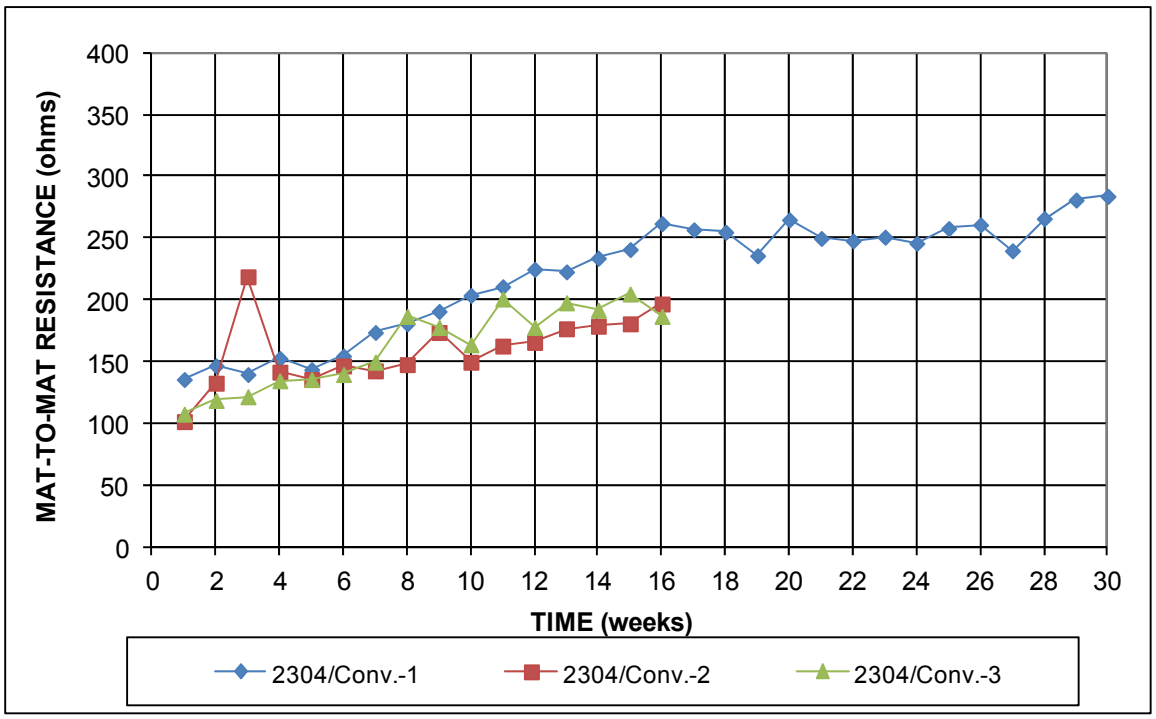

Figure C.47: Southern Exposure mat-to-mat resistances – 2304 (top mat) / conventional steel (bottom mat) , w/c = 0.45

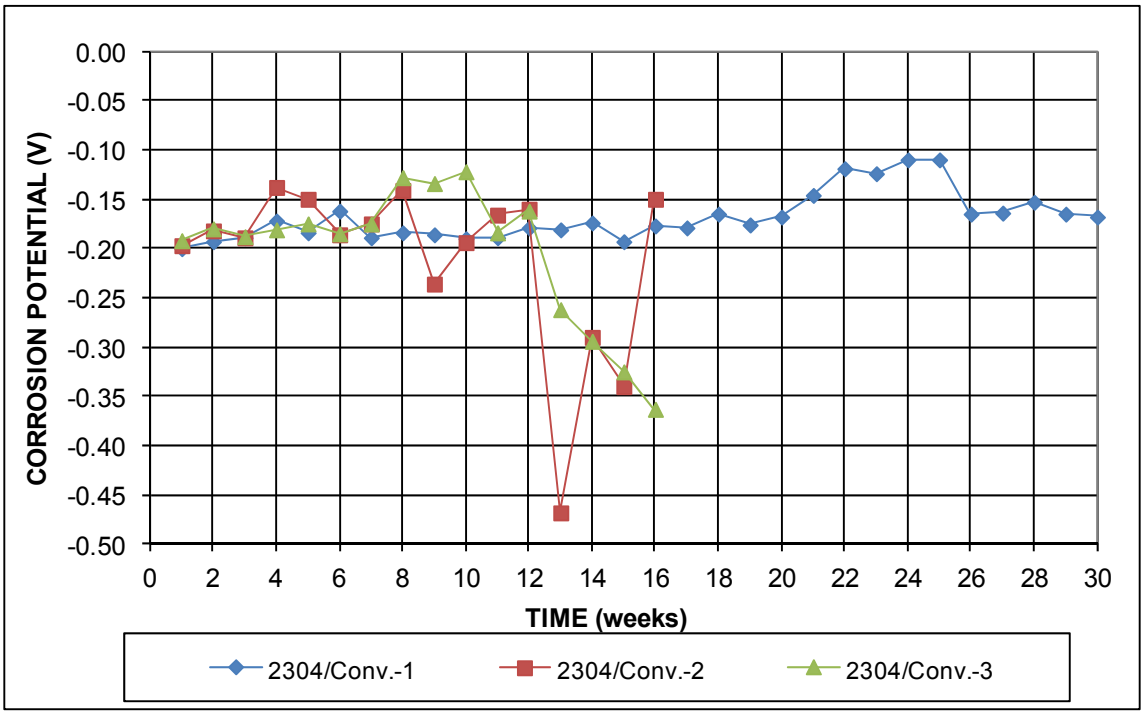

Figure C.48: Southern Exposure corrosion potentials with respect to CSE – specimens with 2304 (top mat) / conventional steel (bottom mat), top mat potentials, w/c = 0.45

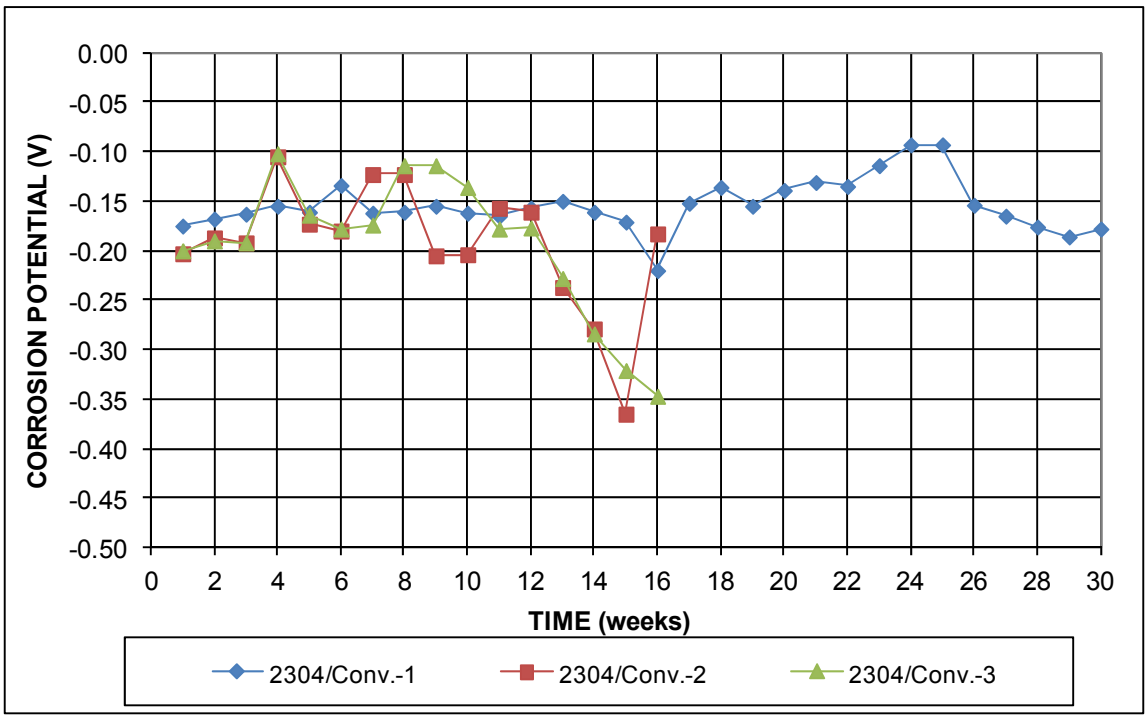

Figure C.49: Southern Exposure corrosion potentials with respect to CSE – specimens with 2304 (top mat) / conventional steel (bottom mat), bottom mat potentials, w/c = 0.45

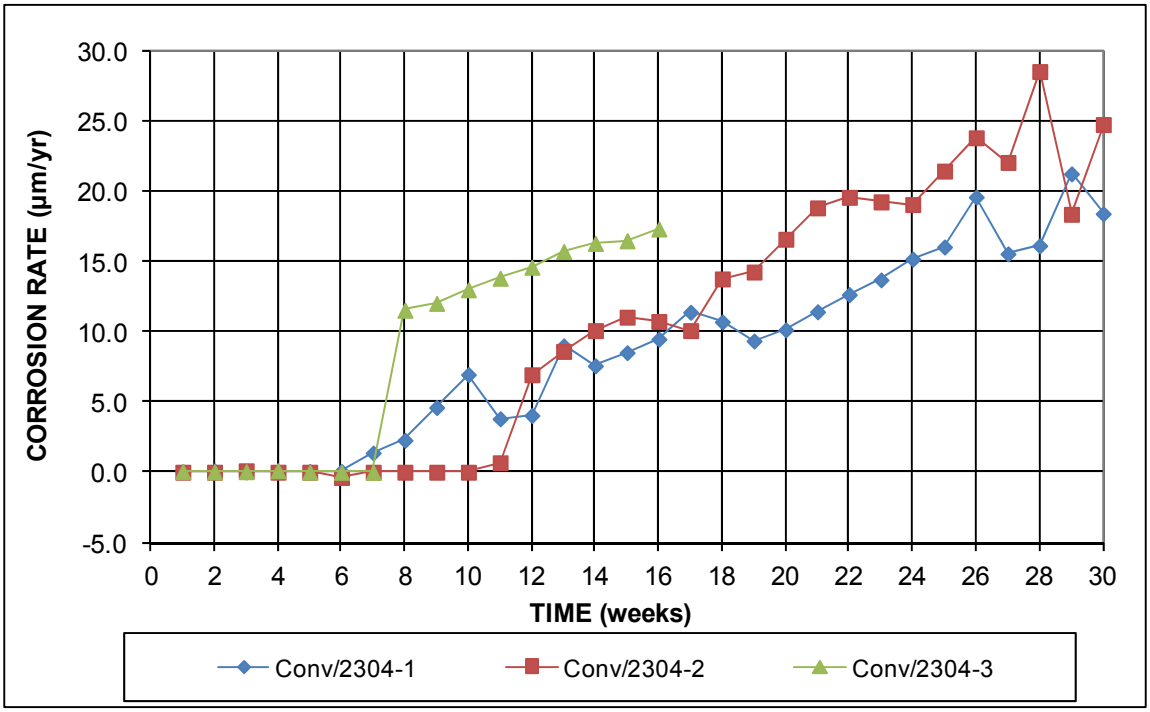

Figure C.50: Southern Exposure corrosion rates – conventional steel (top mat) / 2304 (bottom mat) , w/c = 0.45

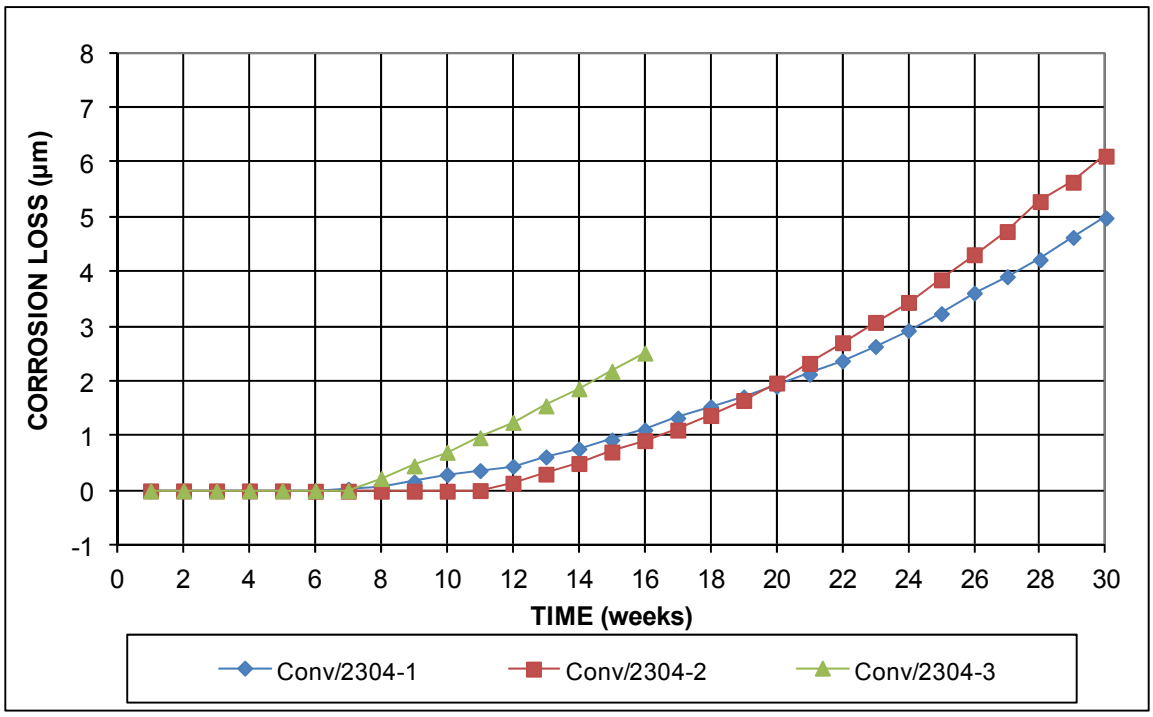

Figure C.51: Southern Exposure corrosion losses – conventional steel (top mat) / 2304 (bottom mat) , w/c = 0.45

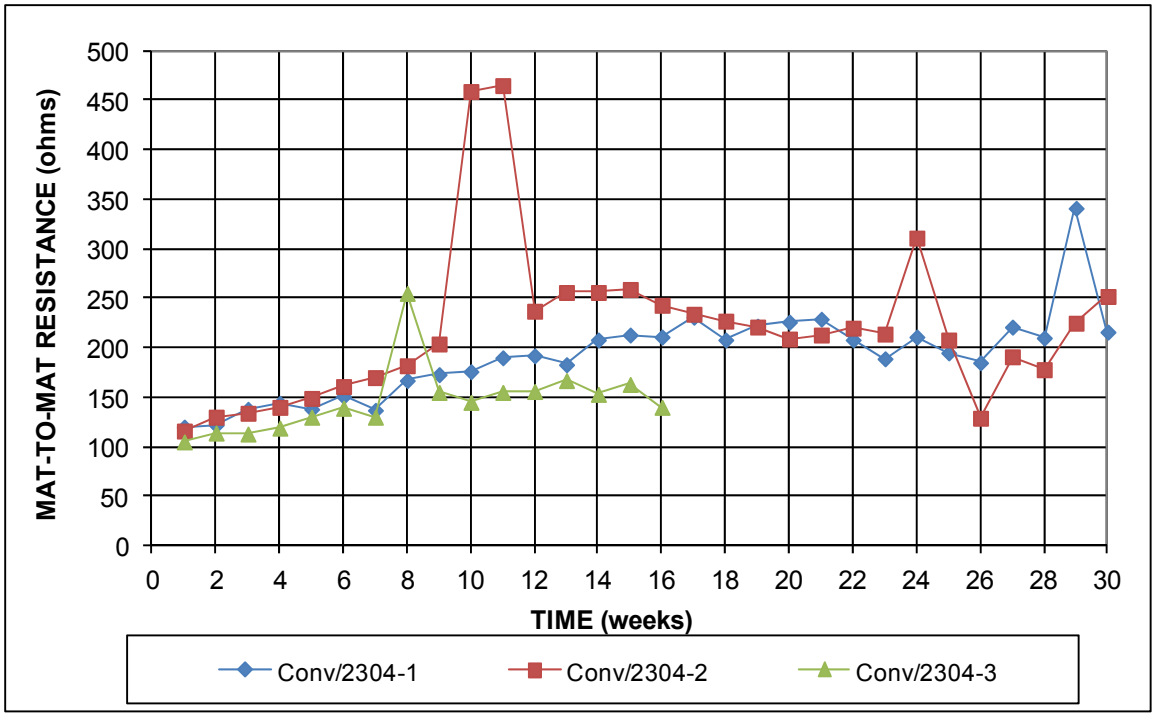

Figure C.52: Southern Exposure mat-to-mat resistances – conventional steel (top mat) / 2304 (bottom mat) , w/c = 0.45

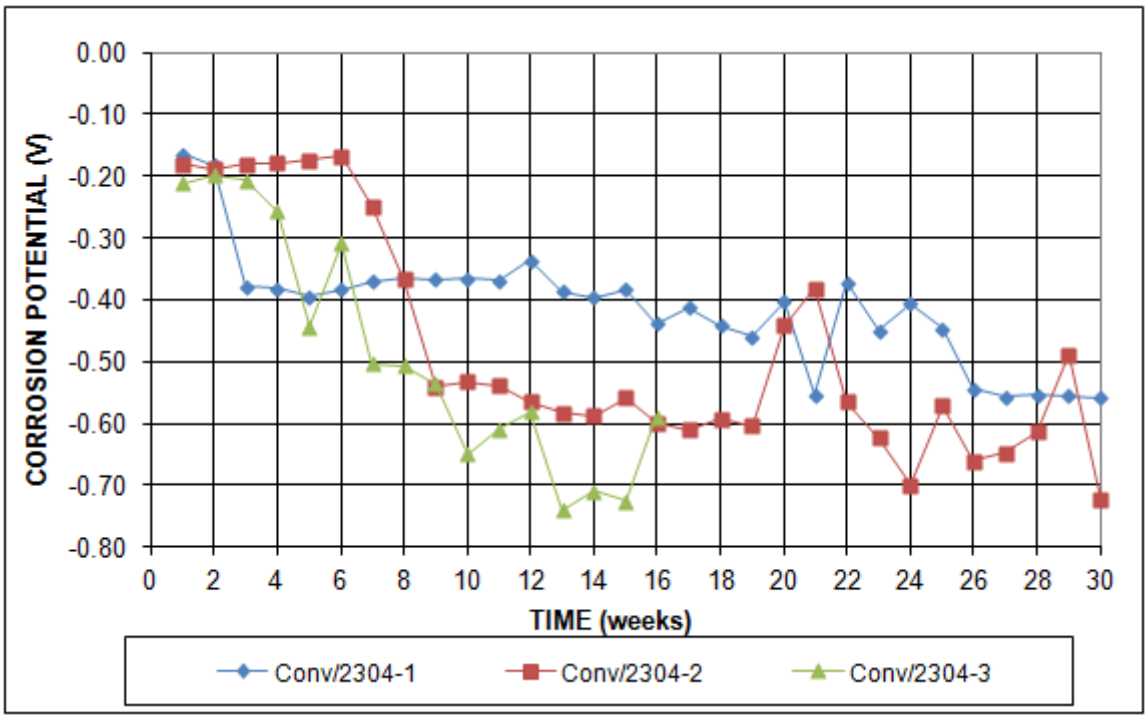

Figure C.53: Southern Exposure corrosion potentials with respect to CSE – specimens with conventional steel (top mat) / 2304 (bottom mat), top mat potentials, w/c = 0.45

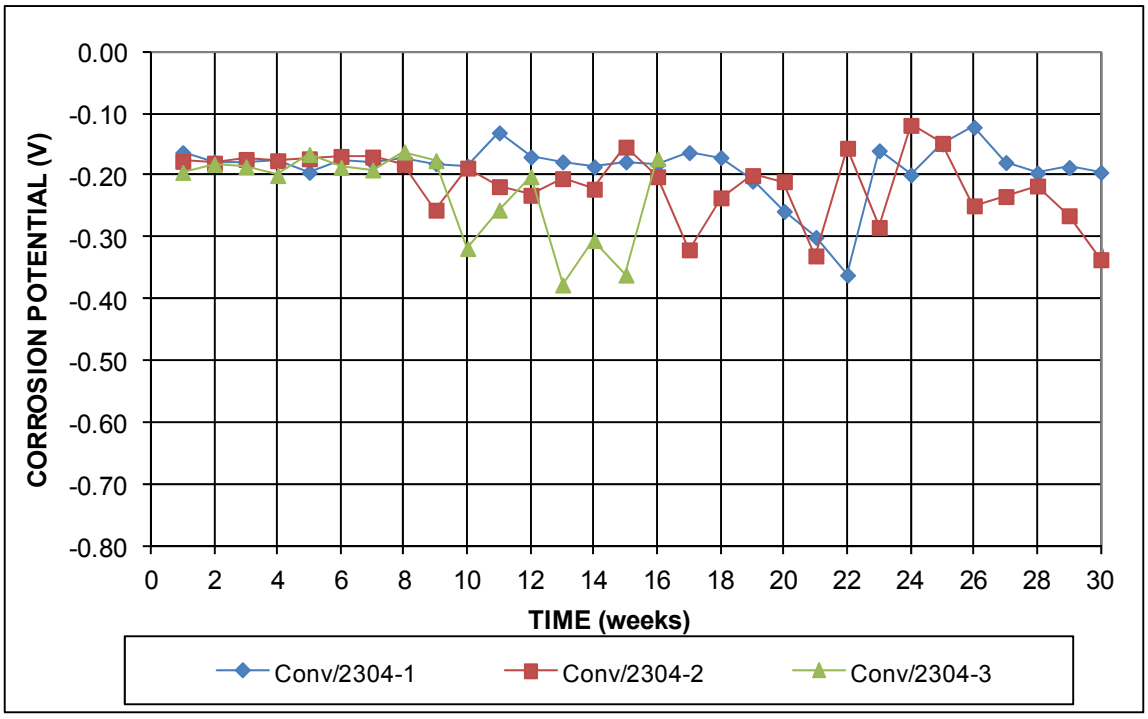

Figure C.54: Southern Exposure corrosion potentials with respect to CSE – specimens with conventional steel (top mat) / 2304 (bottom mat), bottom mat potentials, w/c = 0.45

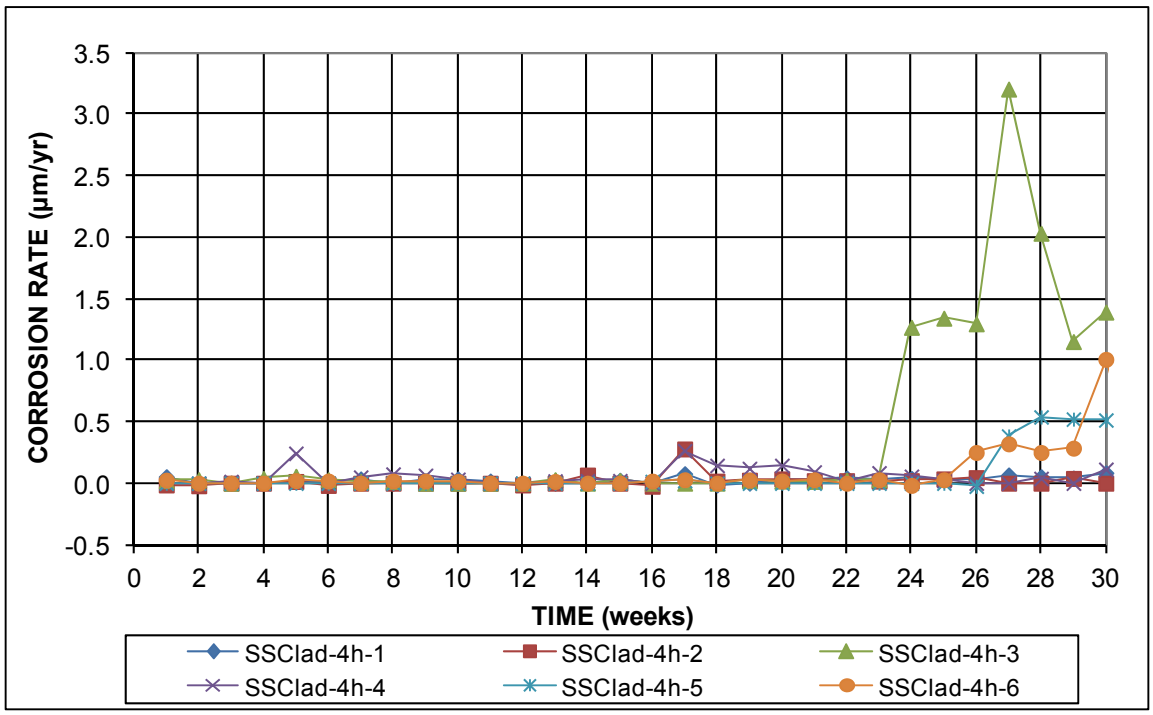

Figure C.55: Southern Exposure corrosion rates (based on total area) – stainless steel clad (damaged) , w/c = 0.45

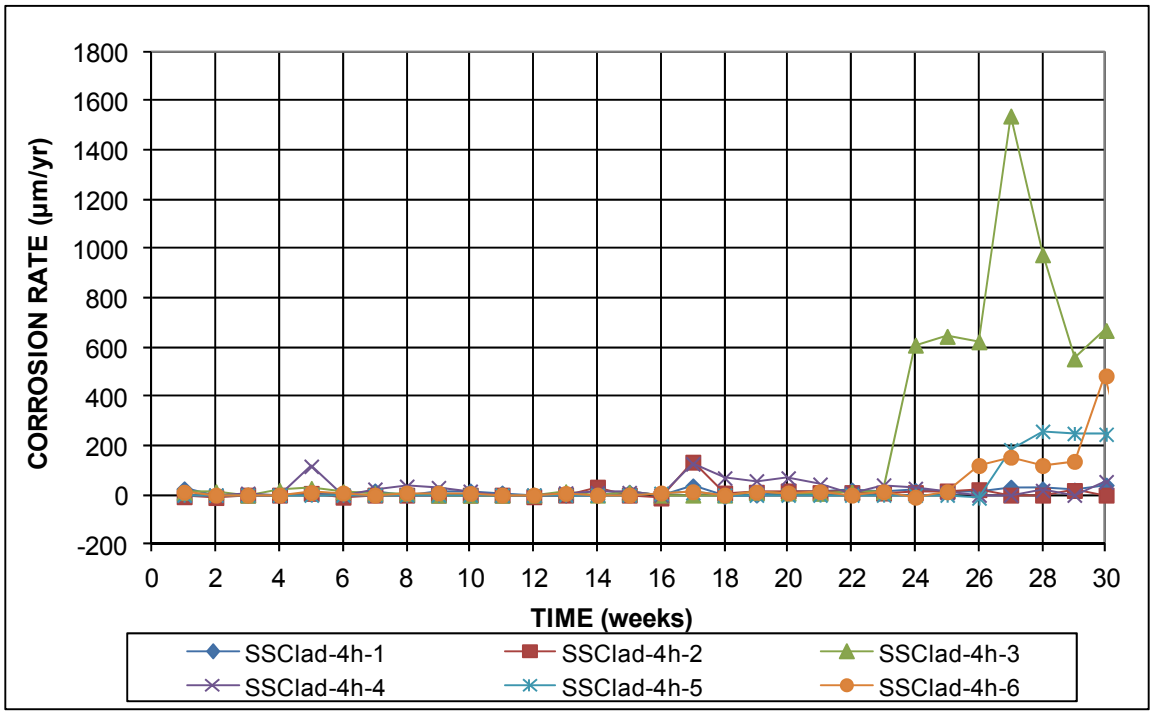

Figure C.56: Southern Exposure corrosion rates (based on exposed area) – stainless steel clad (damaged) , w/c = 0.45

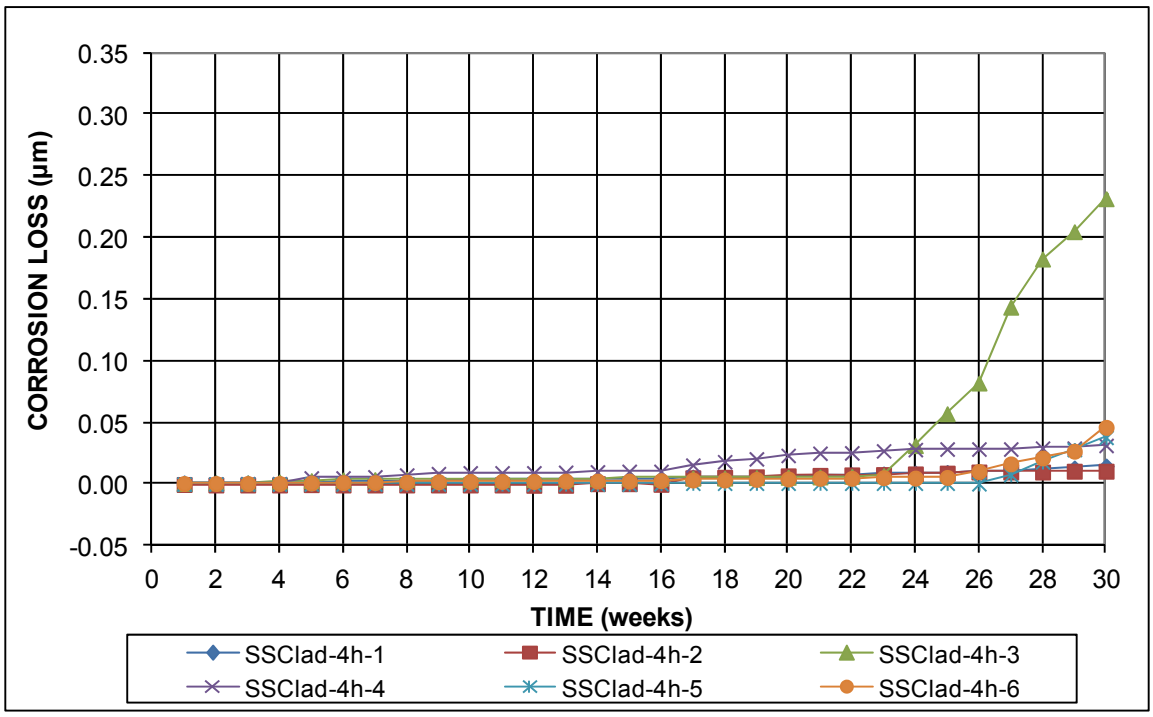

Figure C.57: Southern Exposure corrosion losses (based on total area) – stainless steel clad (damaged) , w/c = 0.45

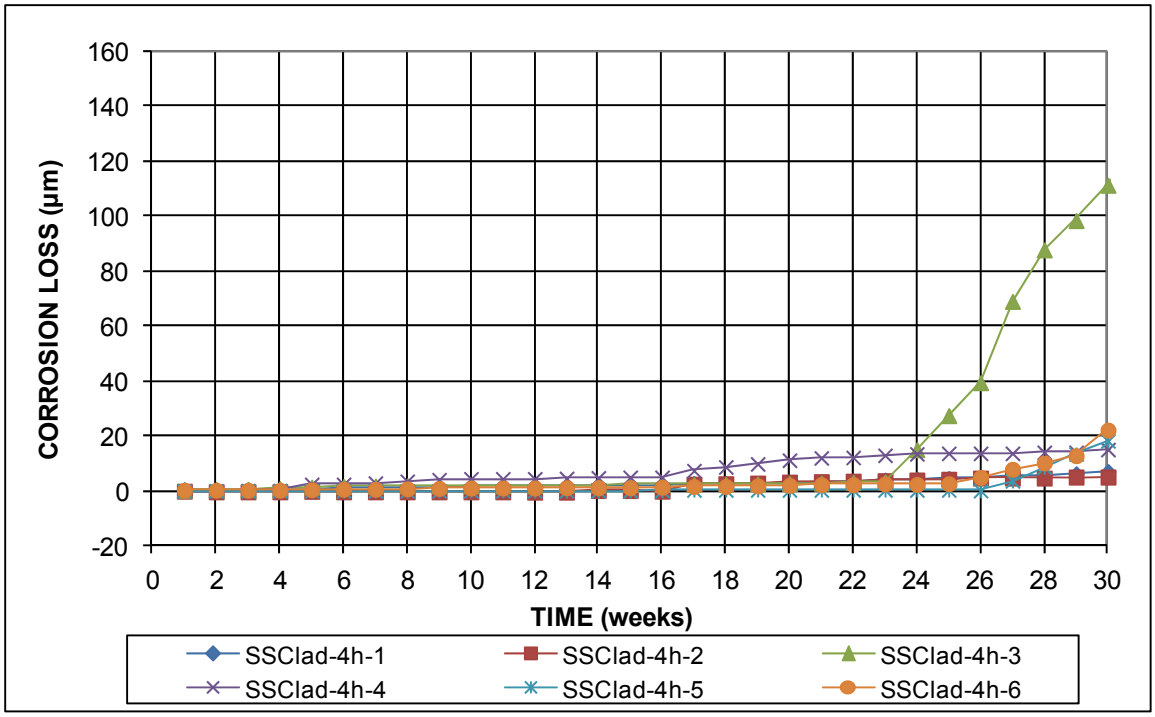

Figure C.58: Southern Exposure corrosion losses (based on exposed area) – stainless steel clad (damaged) , w/c = 0.45

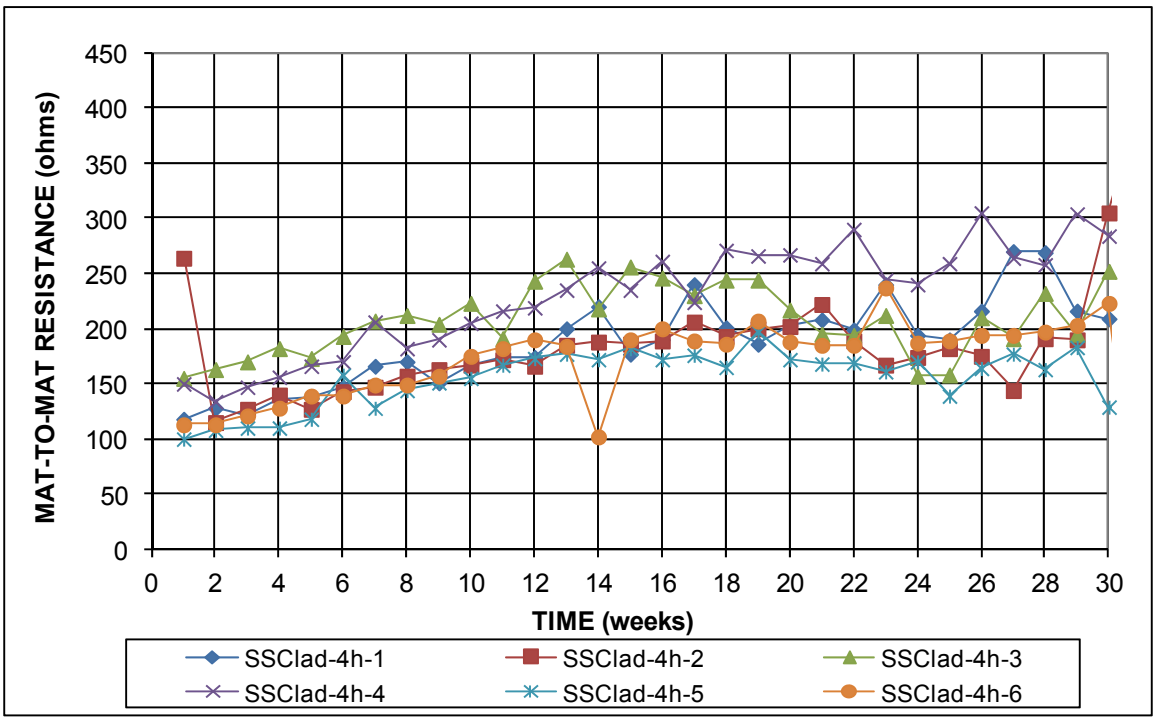

Figure C.59: Southern Exposure mat-to-mat resistances – stainless steel clad (damaged) , w/c = 0.45

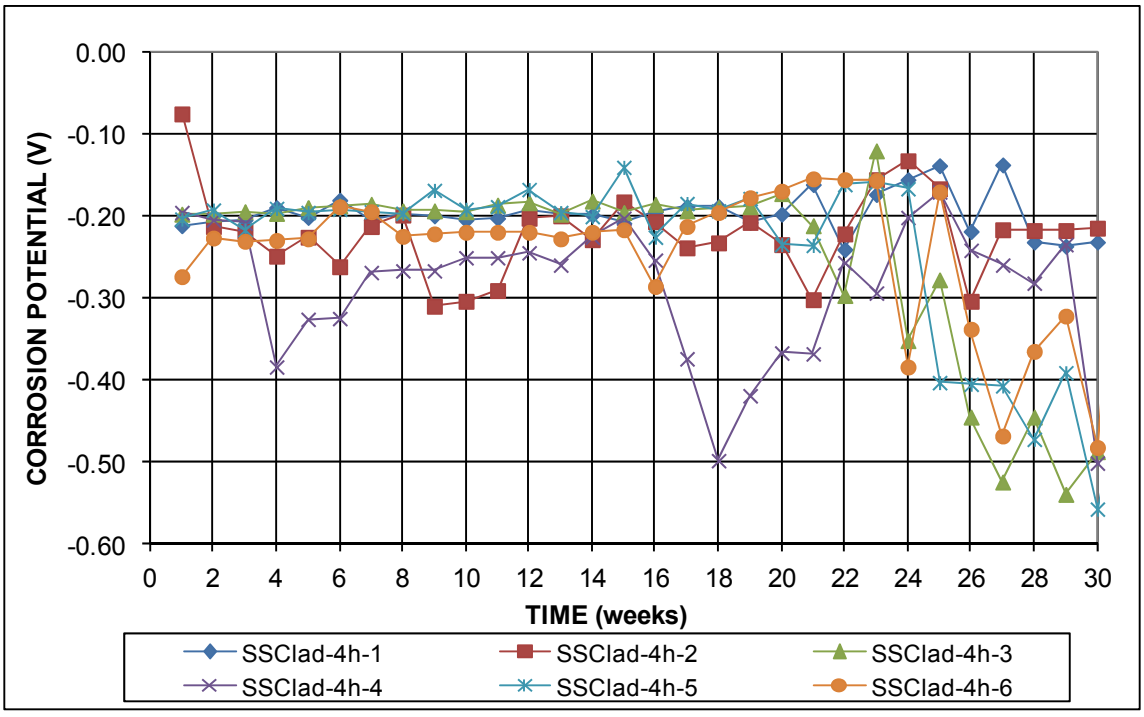

Figure C.60: Southern Exposure corrosion potentials with respect to CSE – stainless steel clad (damaged), top mat, w/c = 0.45

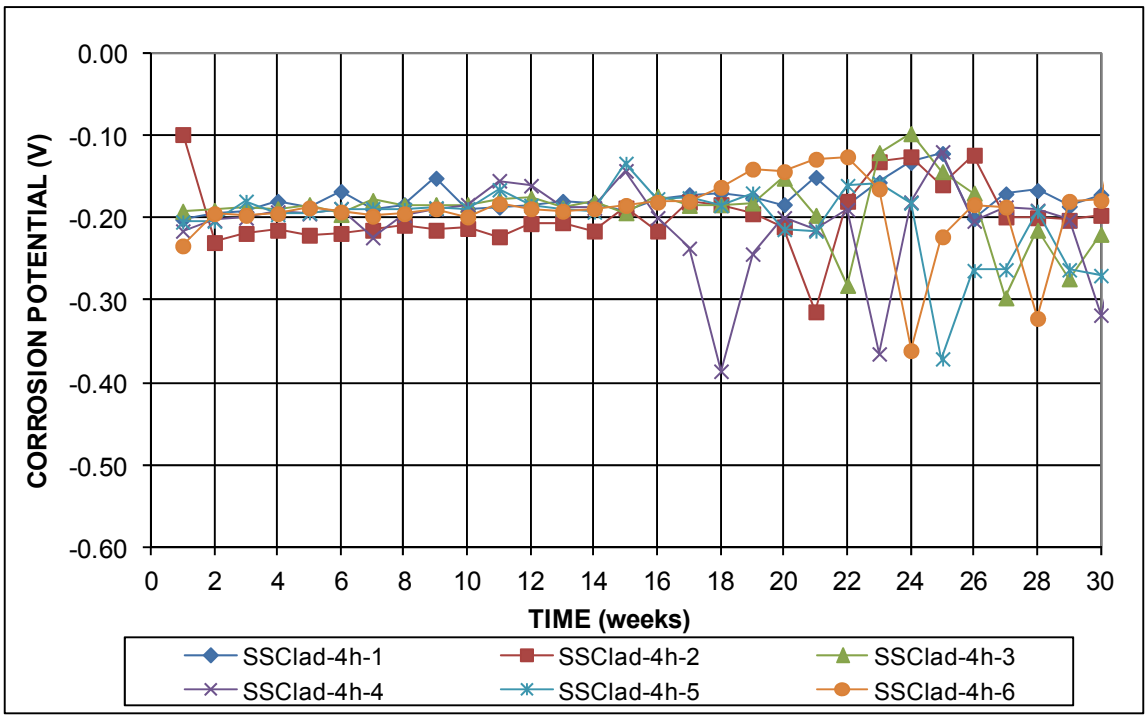

Figure C.61: Southern Exposure corrosion potentials with respect to CSE – stainless steel clad (damaged), bottom mat, w/c = 0.45

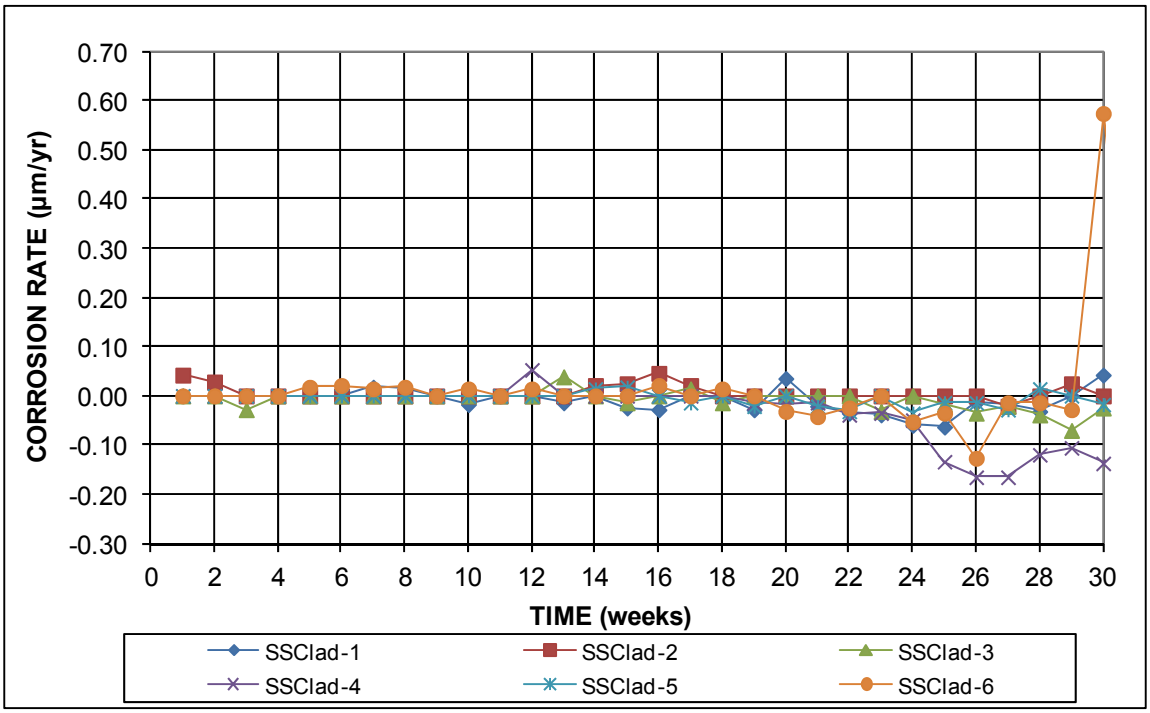

Figure C.62: Southern Exposure corrosion rates – stainless steel clad, w/c = 0.45

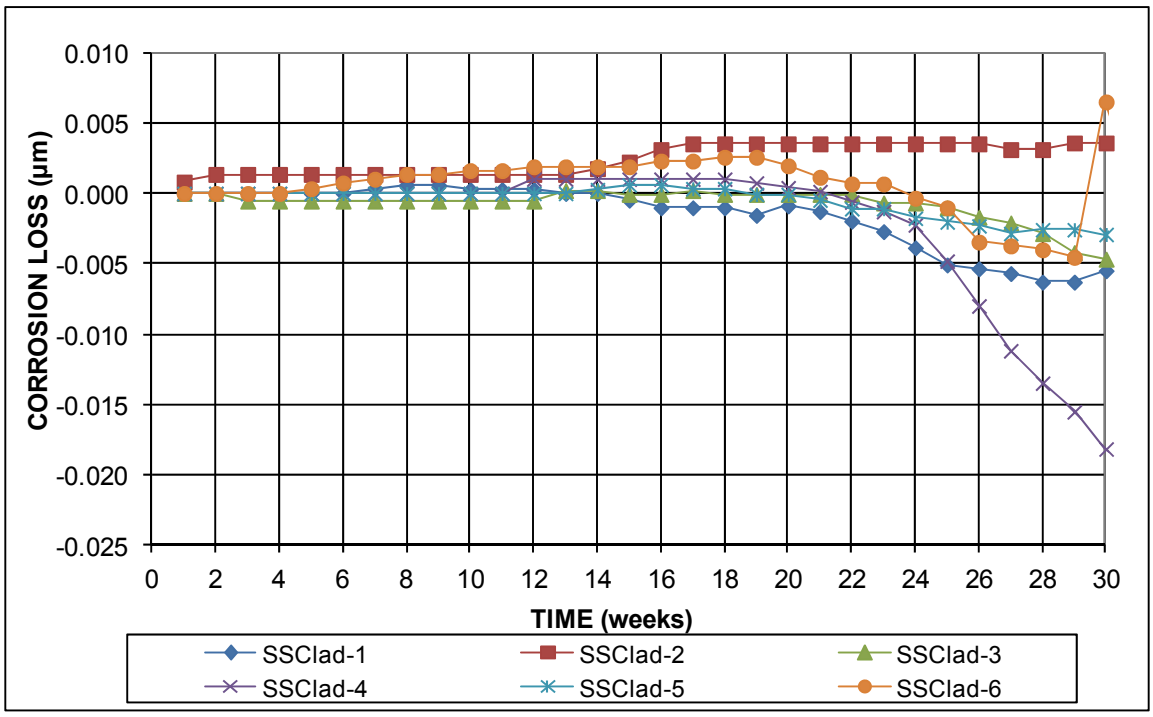

Figure C.63: Southern Exposure corrosion losses – stainless steel clad, w/c = 0.45

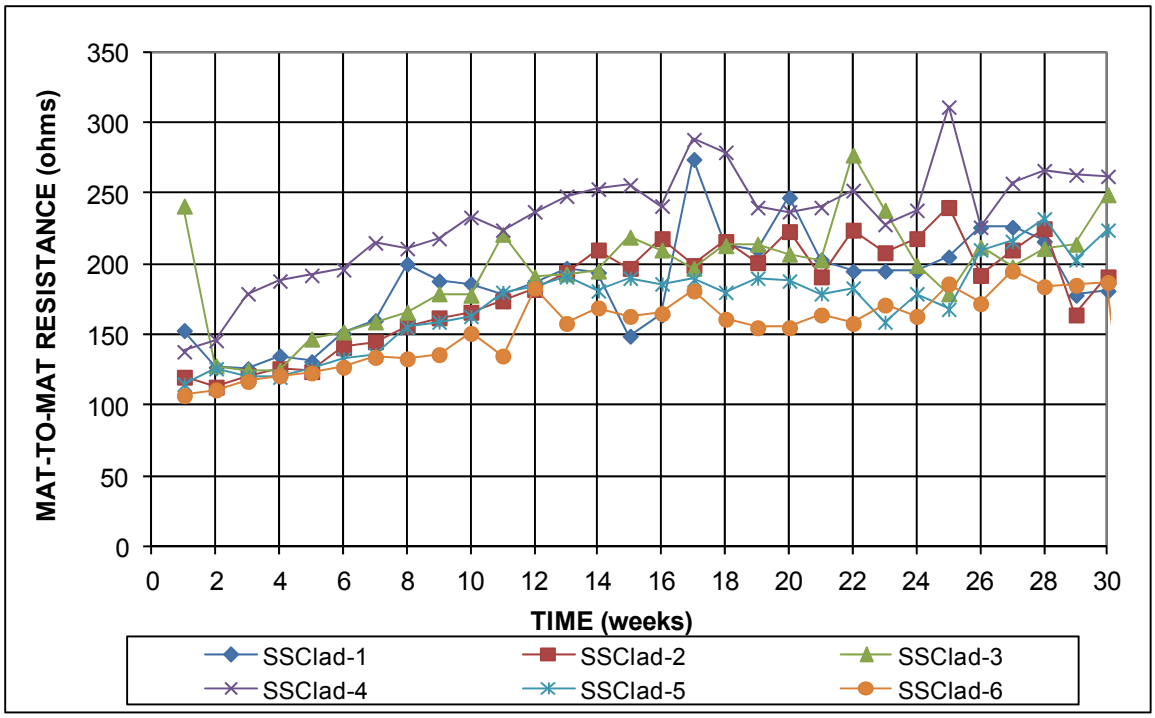

Figure C.64: Southern Exposure mat-to-mat resistances – stainless steel clad, w/c = 0.45

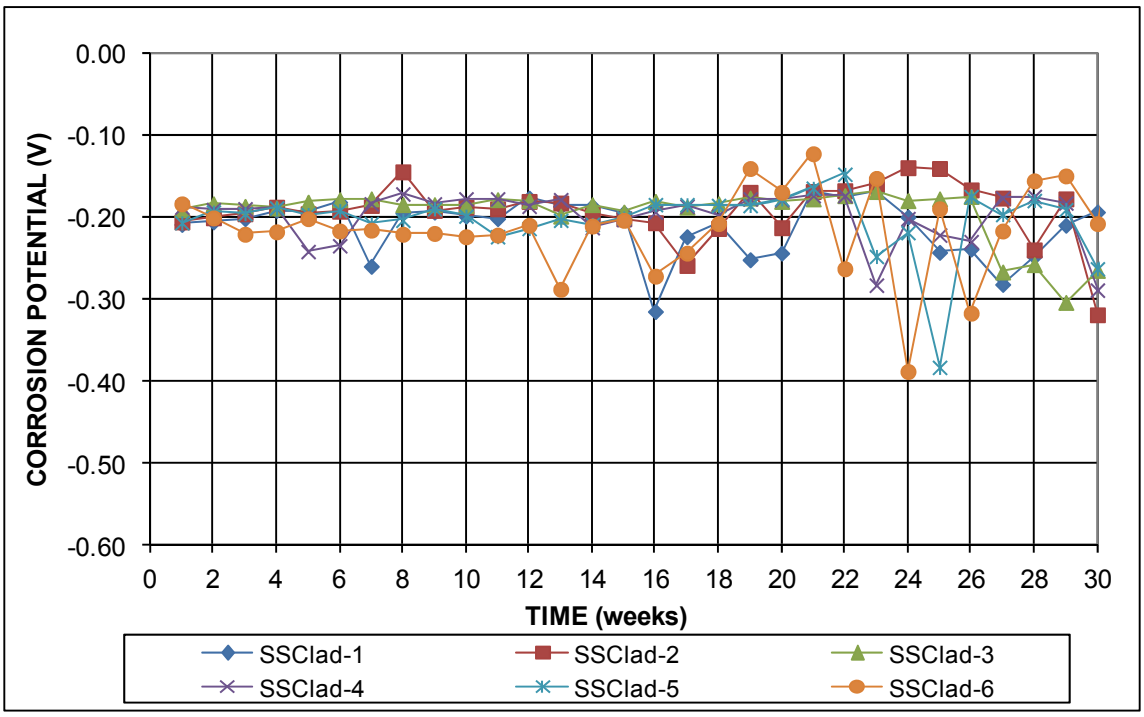

Figure C.65: Southern Exposure corrosion potentials with respect to CSE – stainless steel clad, top mat, w/c = 0.45

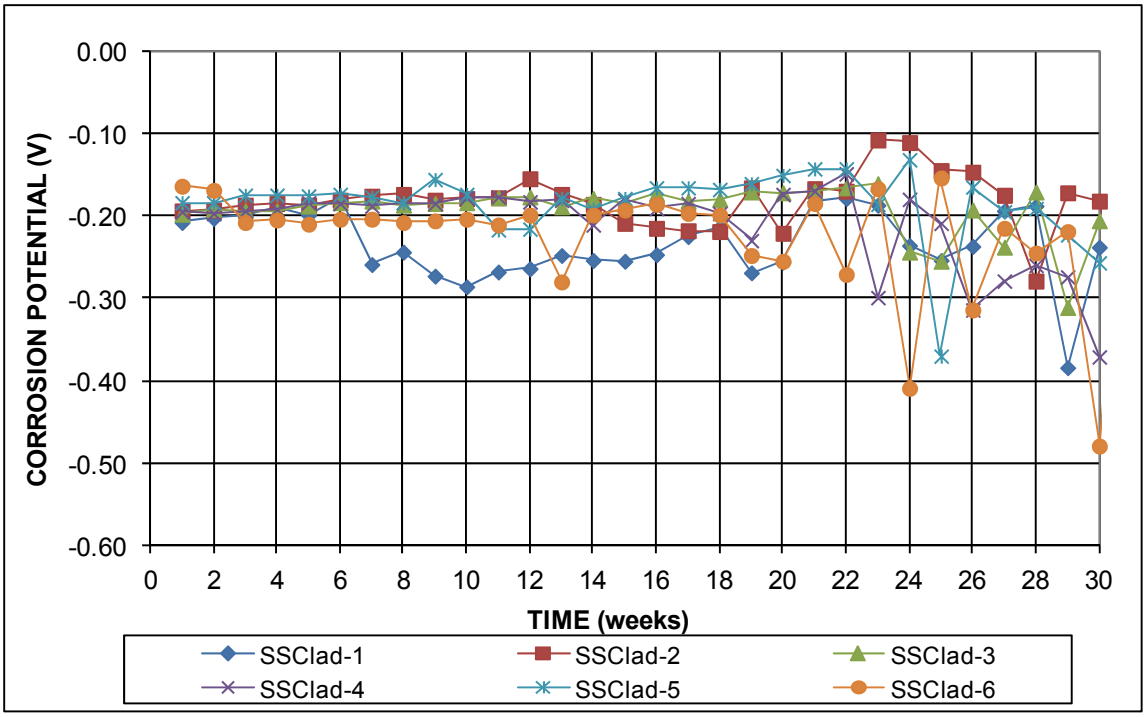

Figure C.66: Southern Exposure corrosion potentials with respect to CSE – stainless steel clad, bottom mat, w/c = 0.45

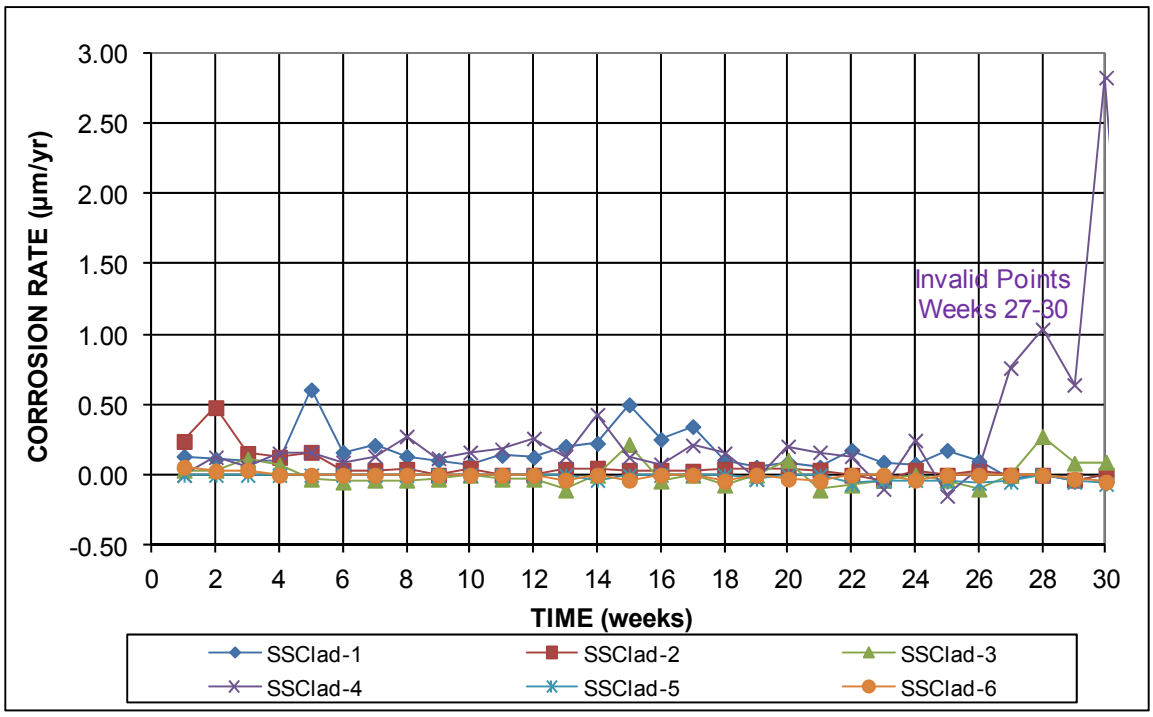

Figure C.67: Cracked beam corrosion rates – stainless steel clad, w/c = 0.45

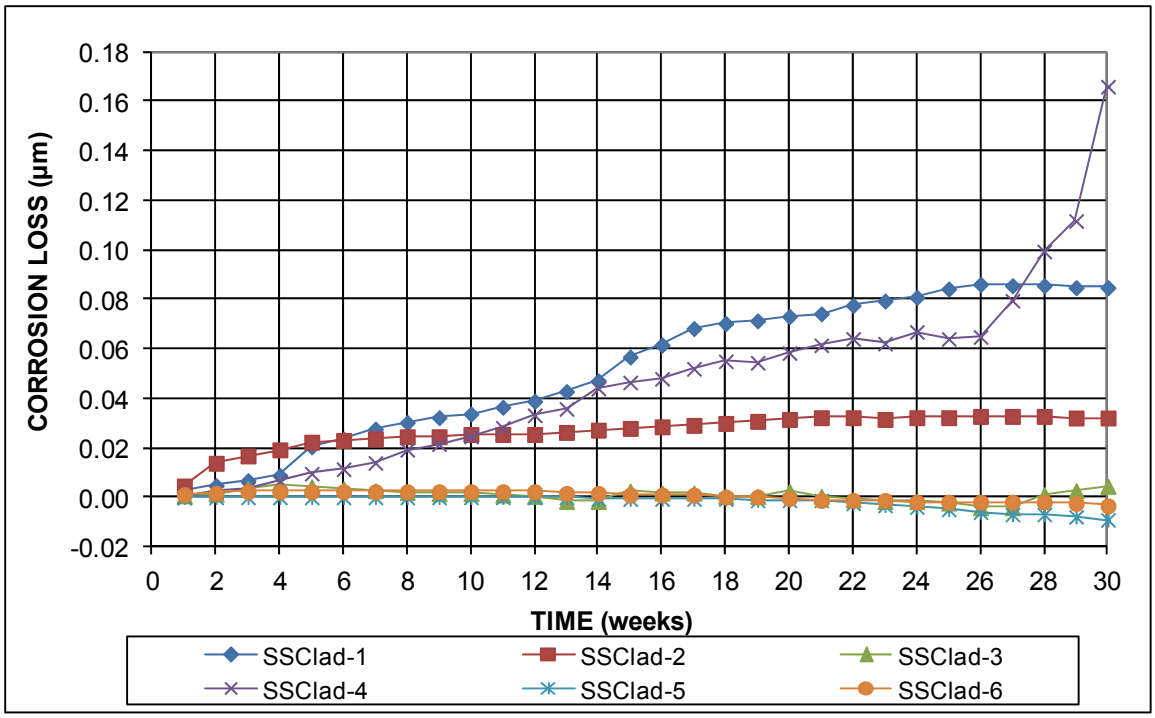

Figure C.68: Cracked beam corrosion losses – stainless steel clad, w/c = 0.45

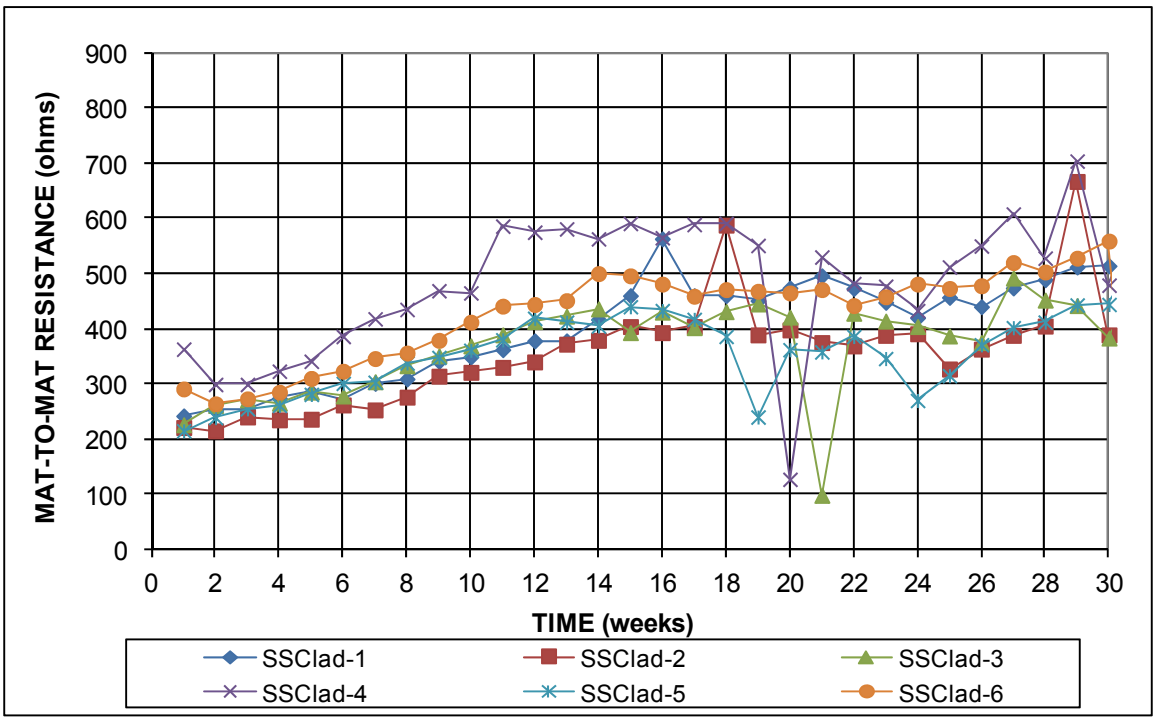

Figure C.69: Cracked beam mat-to-mat resistances – stainless steel clad, w/c = 0.45

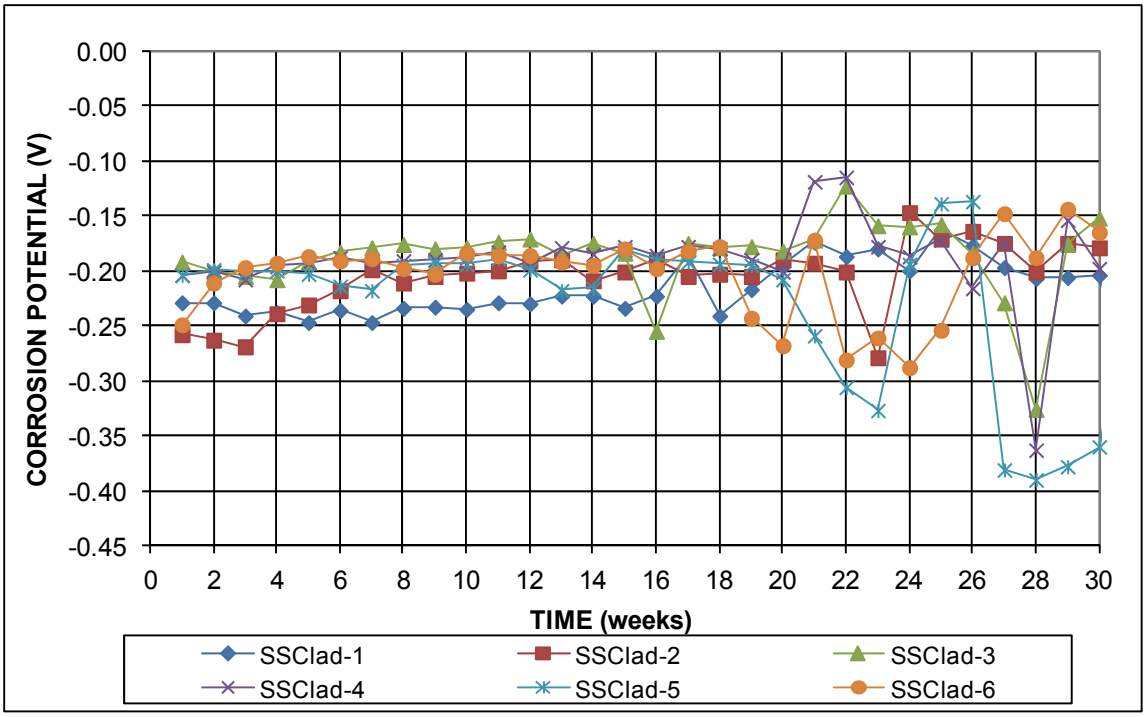

Figure C.70: Cracked beam corrosion potentials with respect to CSE – stainless steel clad, top mat, w/c = 0.45

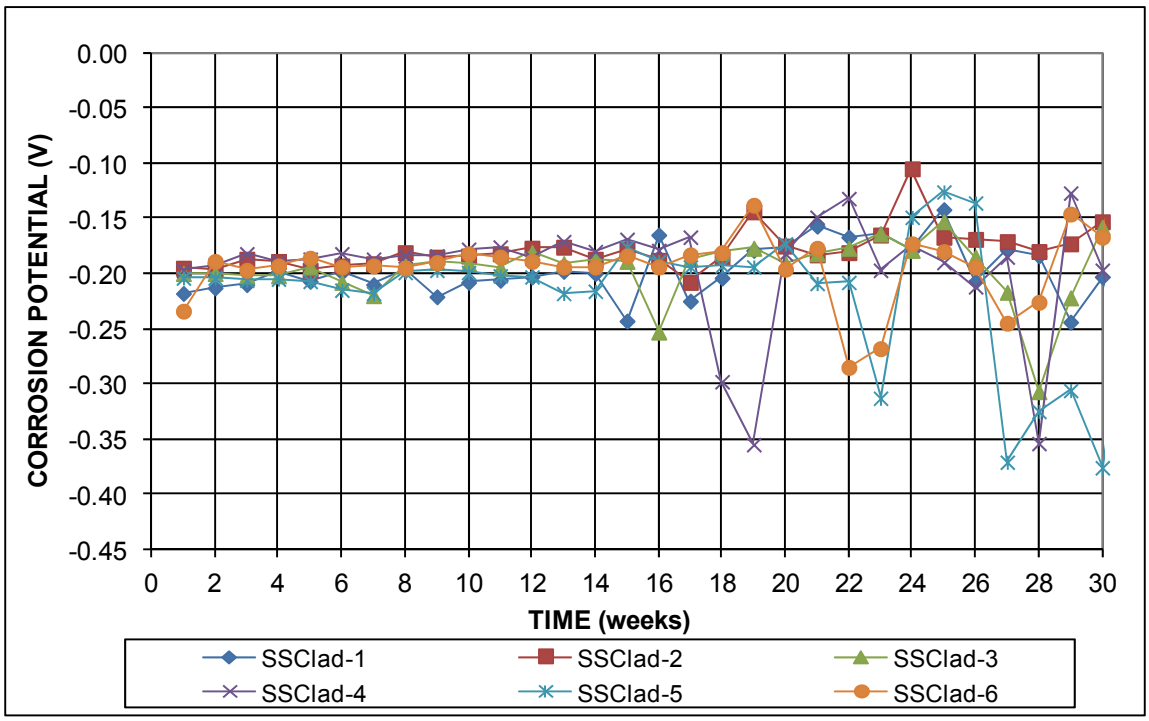

Figure C.71: Cracked beam corrosion potentials with respect to CSE – stainless steel clad, bottom mat, w/c = 0.45

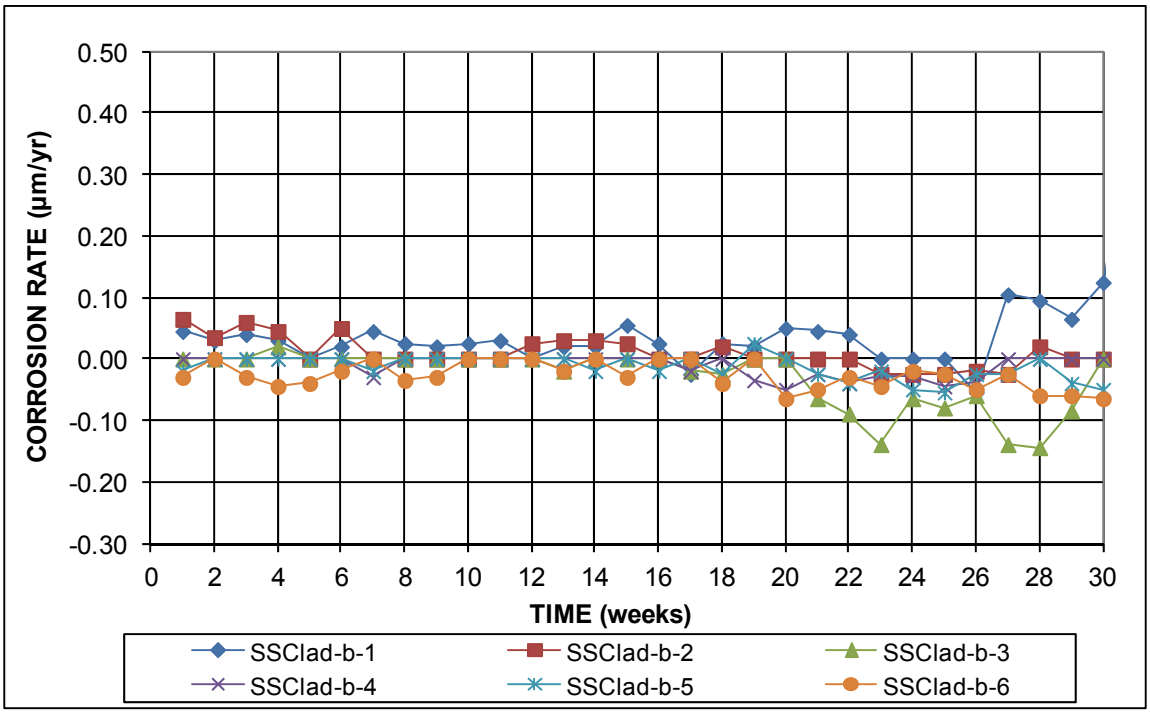

Figure C.72: Southern Exposure corrosion rates – stainless steel clad (180° bend) , w/c = 0.45

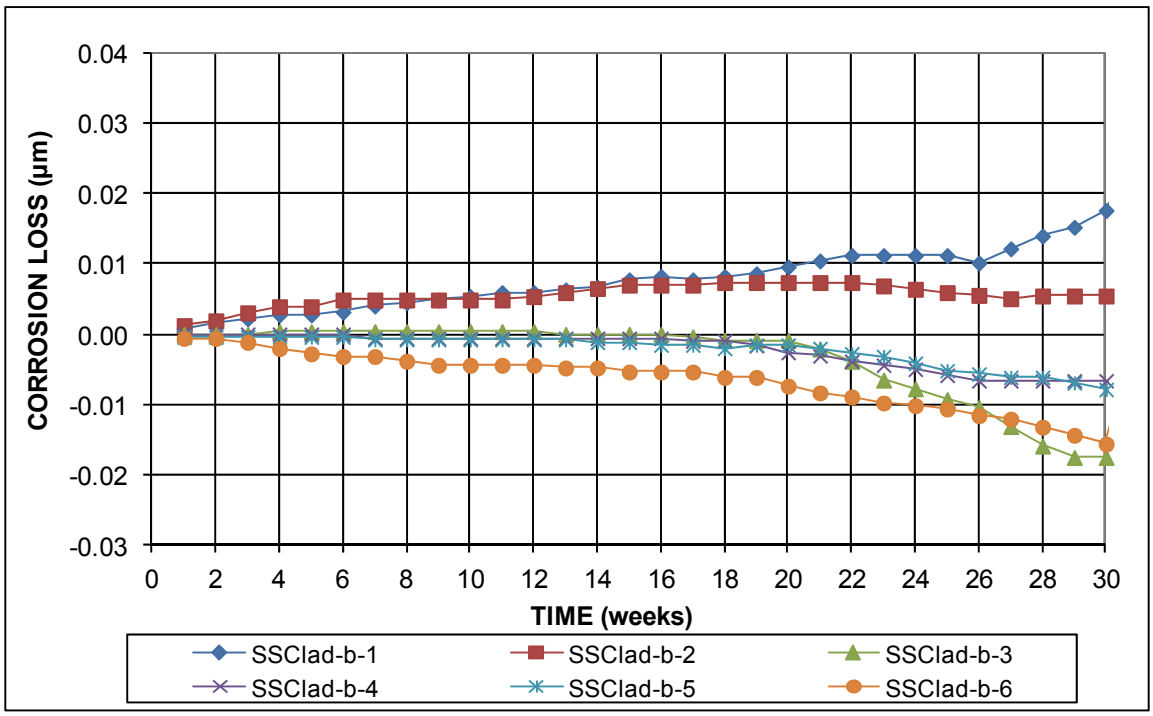

Figure C.73: Southern Exposure corrosion losses – stainless steel clad (180° bend) , w/c = 0.45

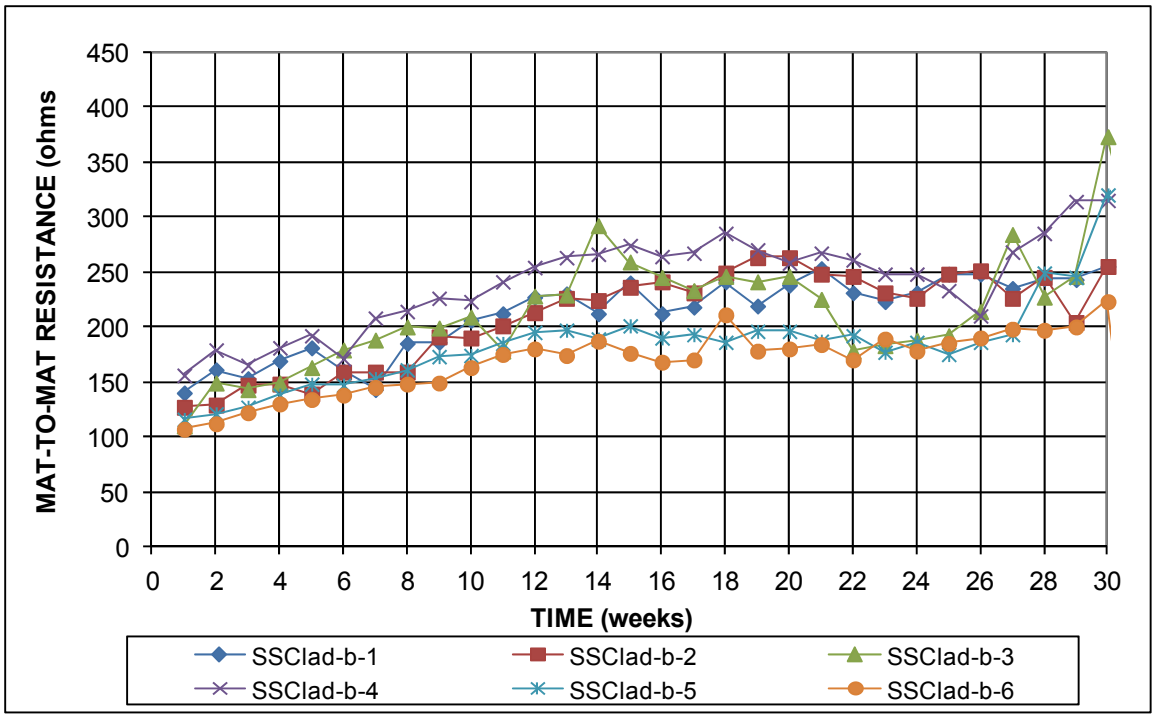

Figure C.74: Southern Exposure mat-to-mat resistances – stainless steel clad (180° bend) , w/c = 0.45

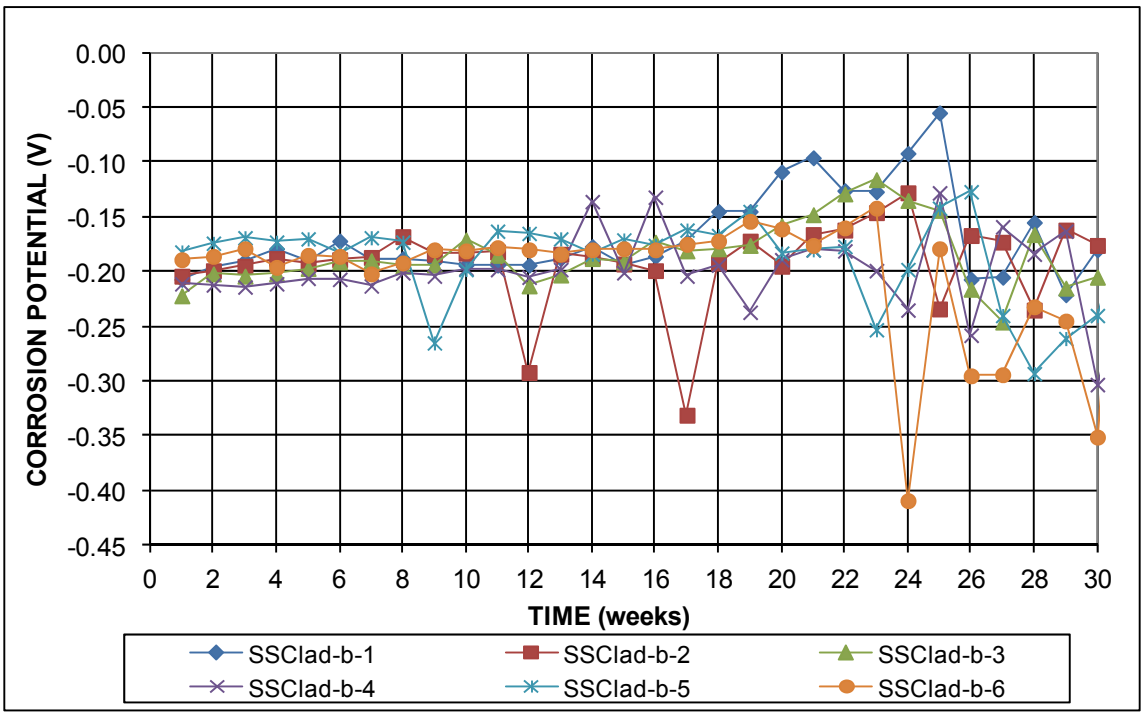

Figure C.75: Southern Exposure corrosion potentials with respect to CSE – stainless steel clad (180° bend), top mat, w/c = 0.45

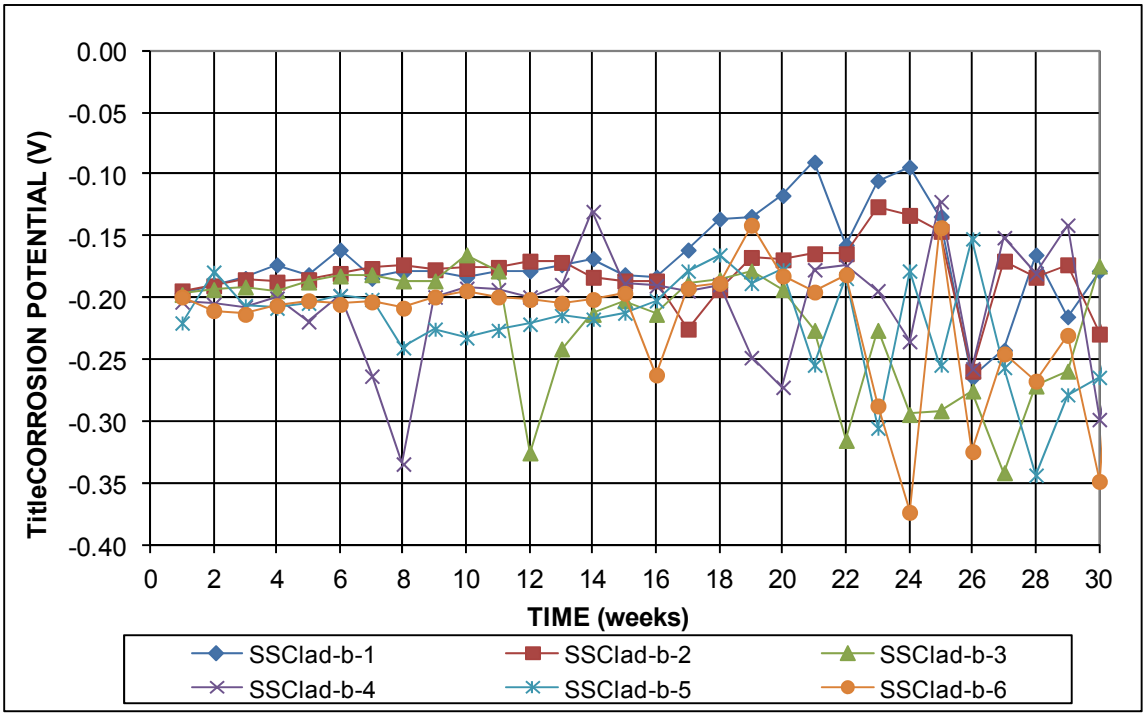

Figure C.76: Southern Exposure corrosion potentials with respect to CSE – stainless steel clad (180° bend), bottom mat, w/c = 0.45

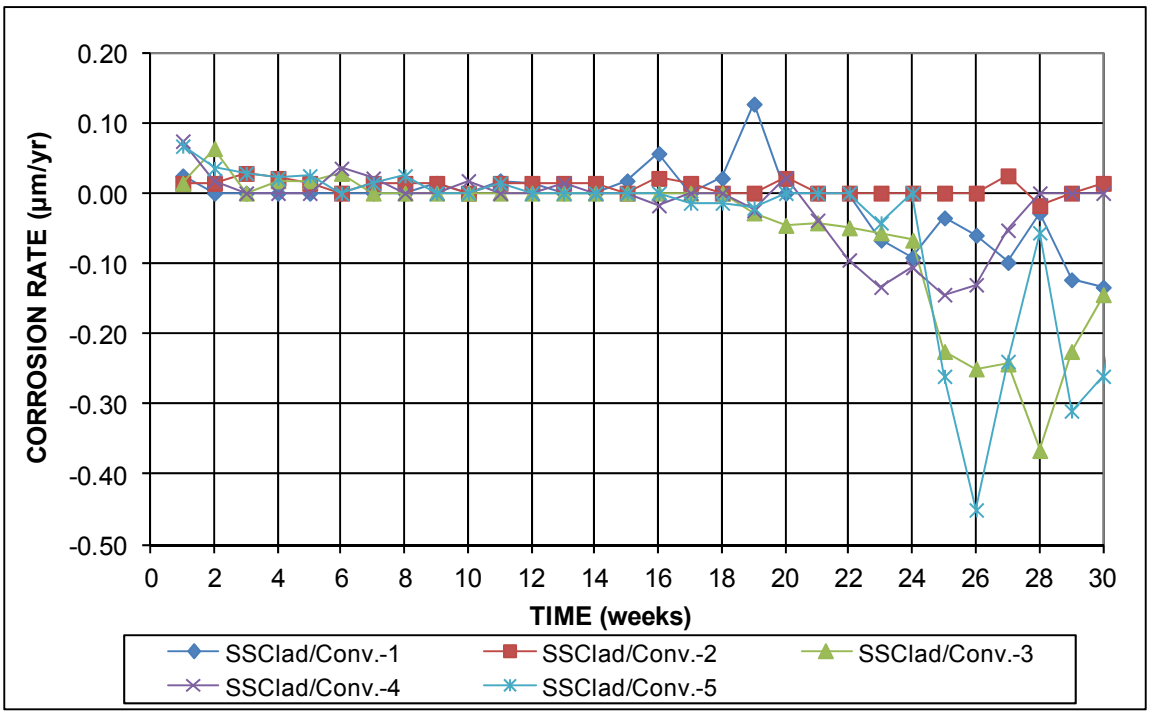

Figure C.77: Southern Exposure corrosion rates – stainless steel clad (top mat) / conventional steel (bottom mat) , w/c = 0.45

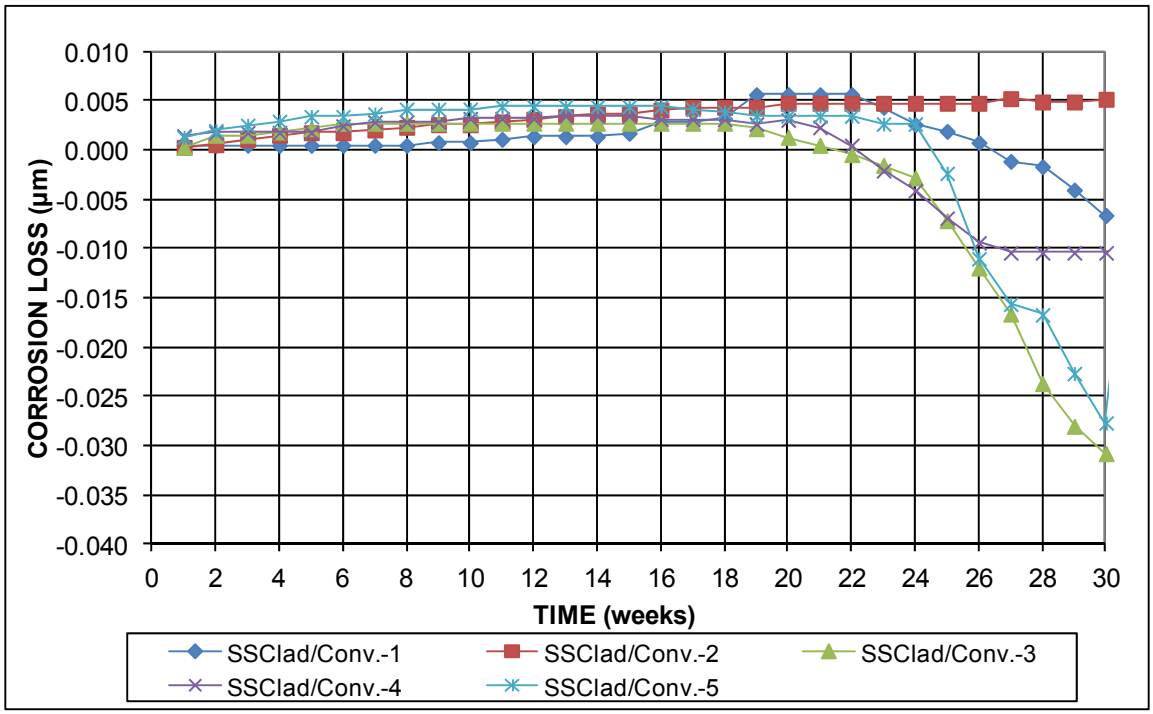

Figure C.78: Southern Exposure corrosion losses – stainless steel clad (top mat) / conventional steel (bottom mat) , w/c = 0.45

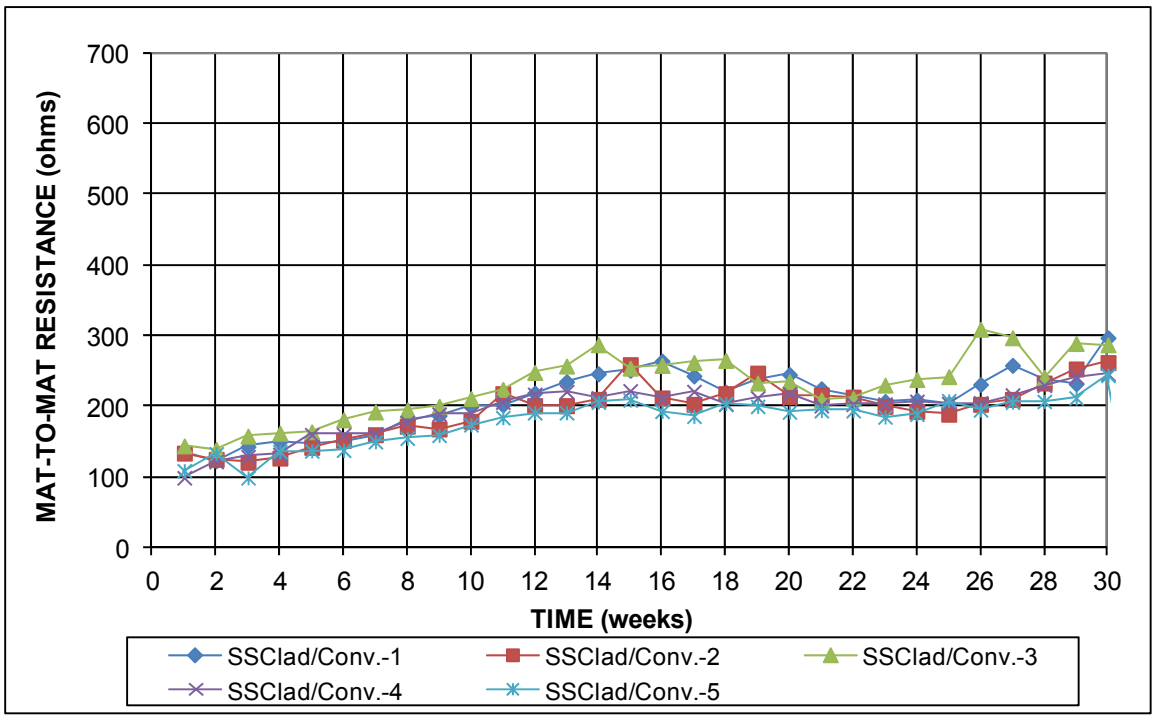

Figure C.79: Southern Exposure mat-to-mat resistances – stainless steel clad (top mat) / conventional steel (bottom mat) , w/c = 0.45

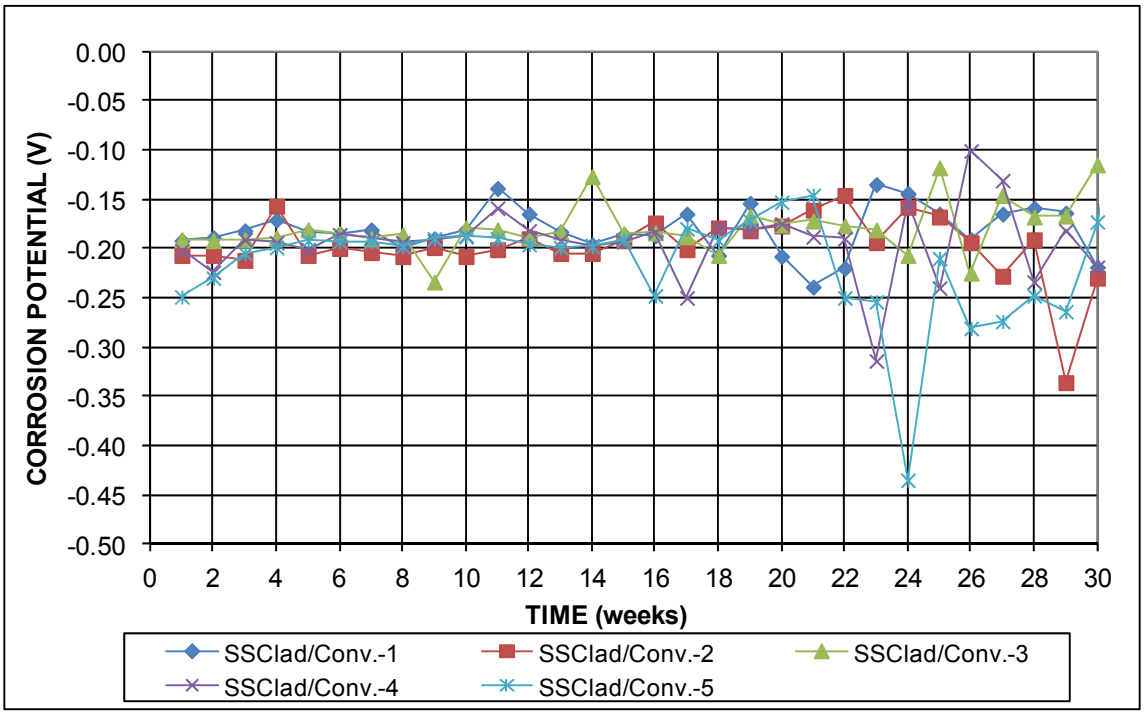

Figure C.80: Southern Exposure corrosion potentials with respect to CSE – stainless steel clad (top mat) / conventional steel (bottom mat), top mat, w/c = 0.45

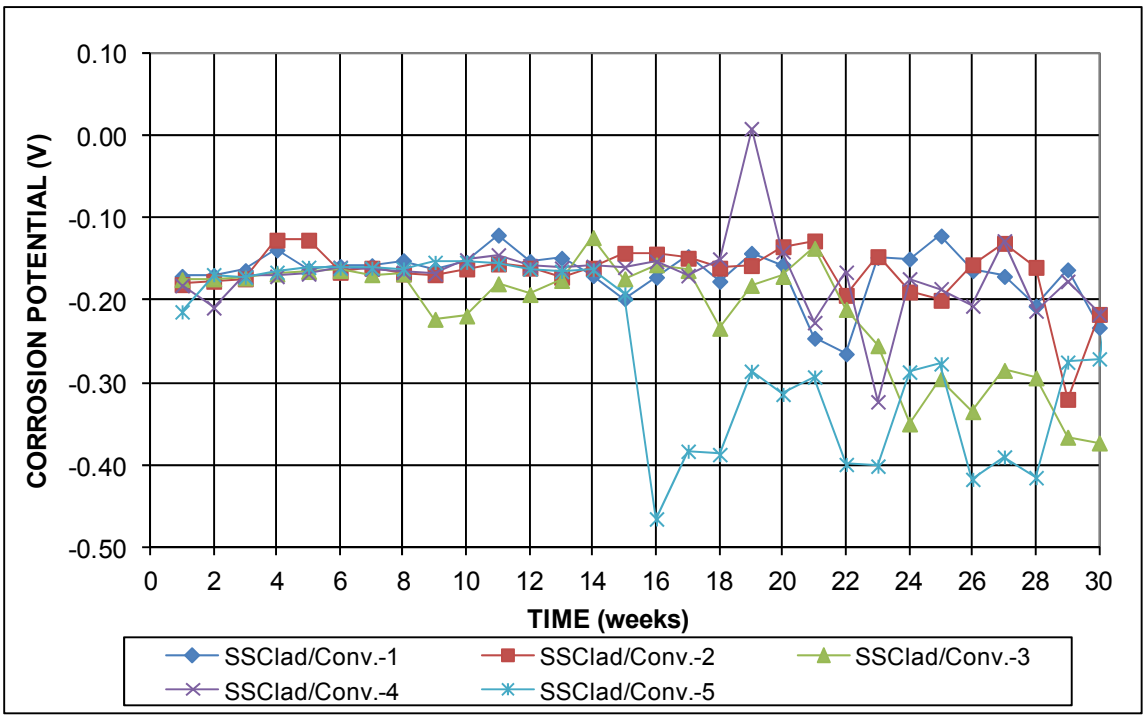

Figure C.81: Southern Exposure corrosion potentials with respect to CSE – stainless steel clad (top mat) / conventional steel (bottom mat), bottom mat, w/c = 0.45

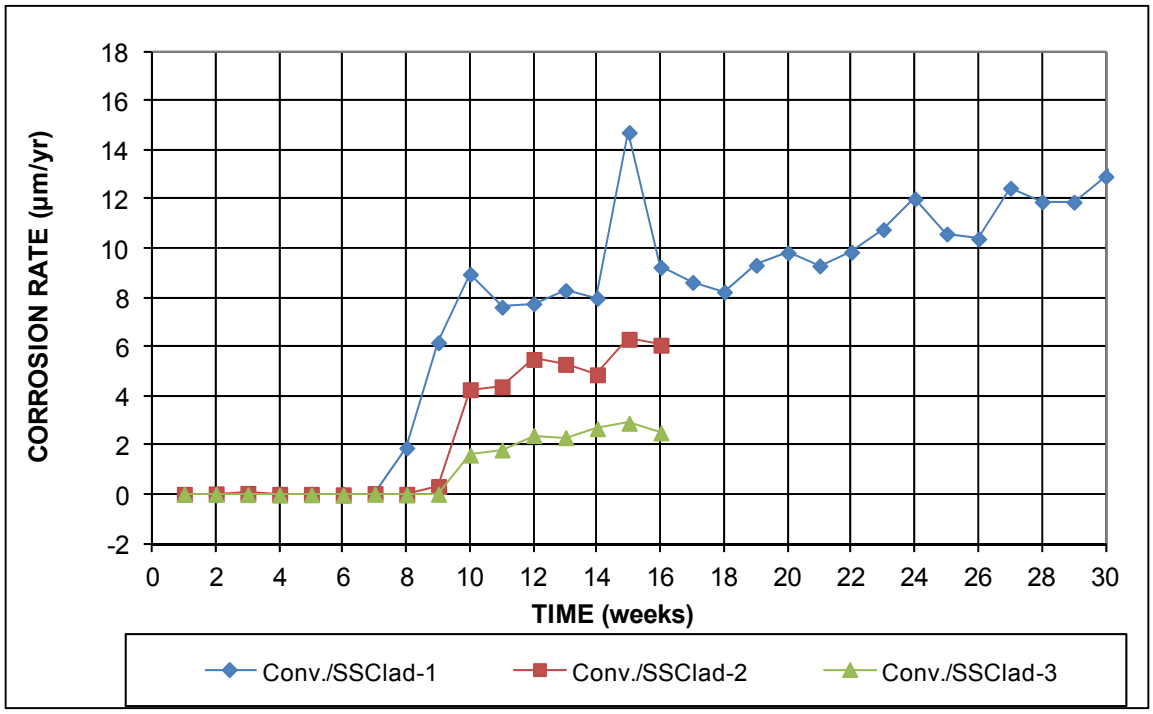

Figure C.82: Southern Exposure corrosion rates – conventional steel (top mat) / stainless steel clad (bottom mat) , w/c = 0.45

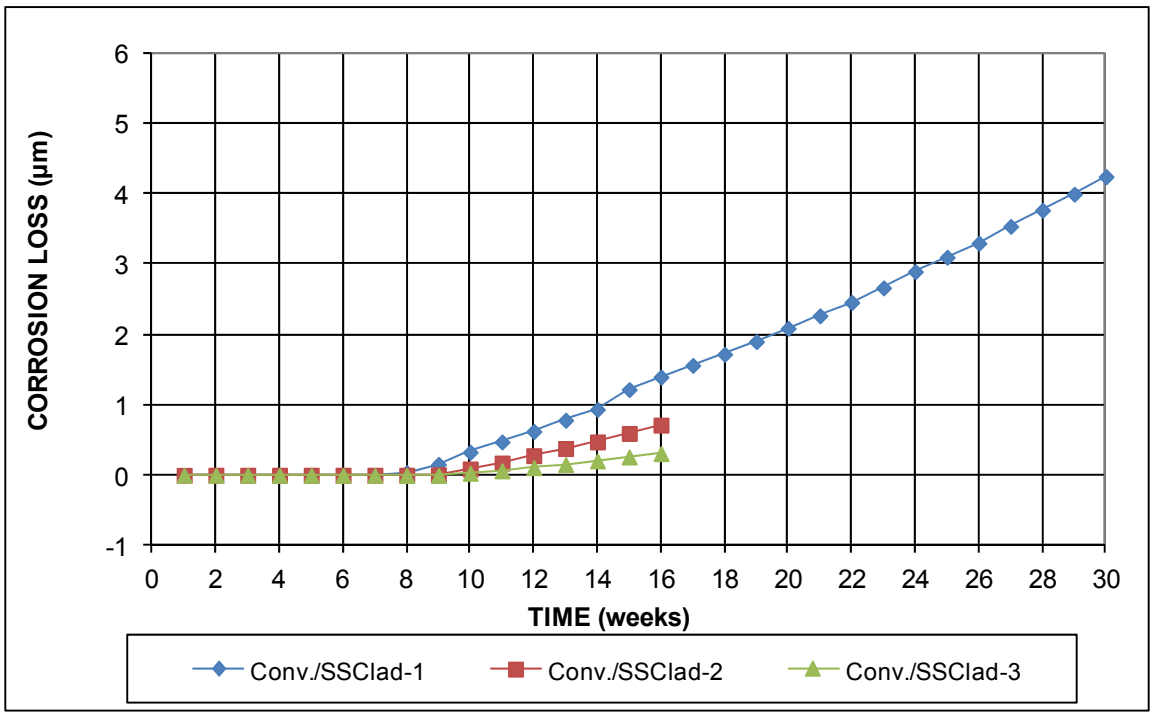

Figure C.83: Southern Exposure corrosion losses – conventional steel (top mat) / stainless steel clad (bottom mat) , w/c = 0.45

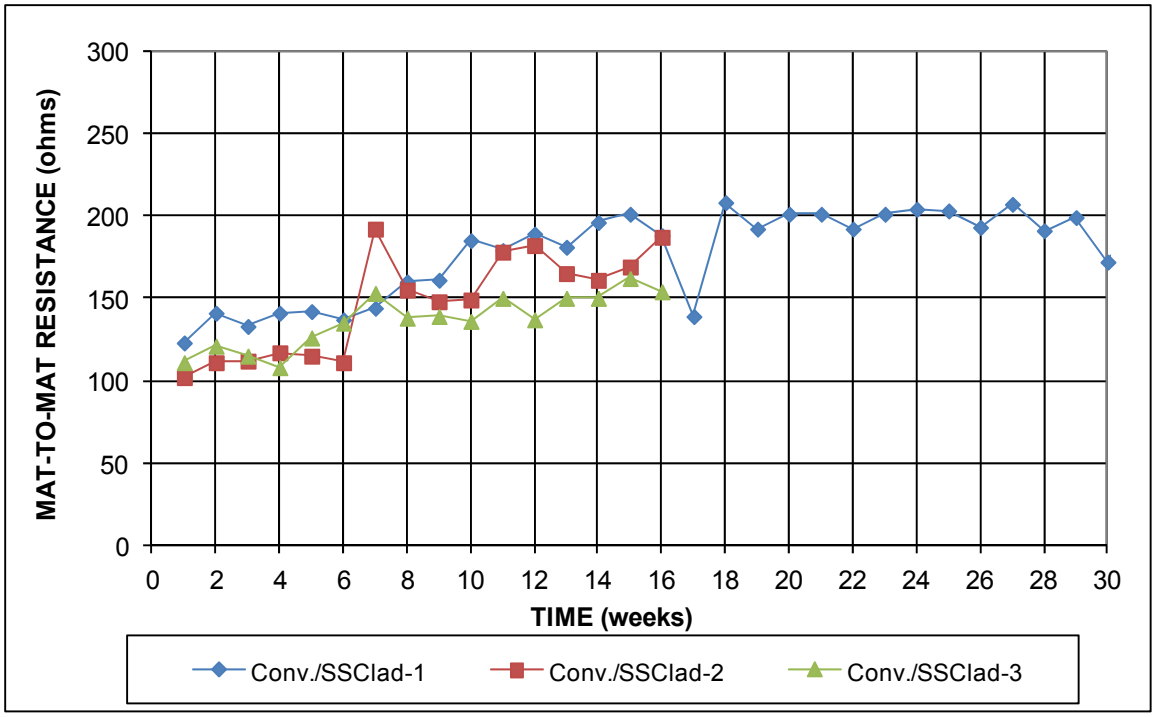

Figure C.84: Southern Exposure mat-to-mat resistances – conventional steel (top mat) / stainless steel clad (bottom mat) , w/c = 0.45

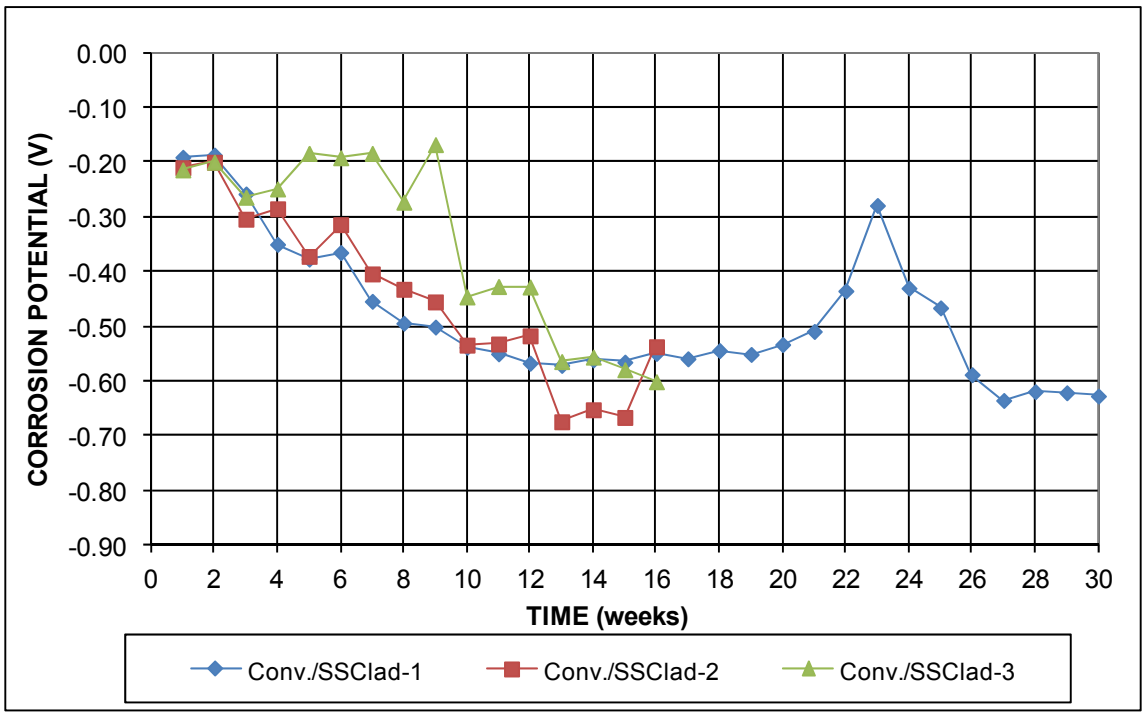

Figure C.85: Southern Exposure corrosion potentials with respect to CSE – conventional steel (top mat) / stainless steel clad (bottom mat), top mat, w/c = 0.45

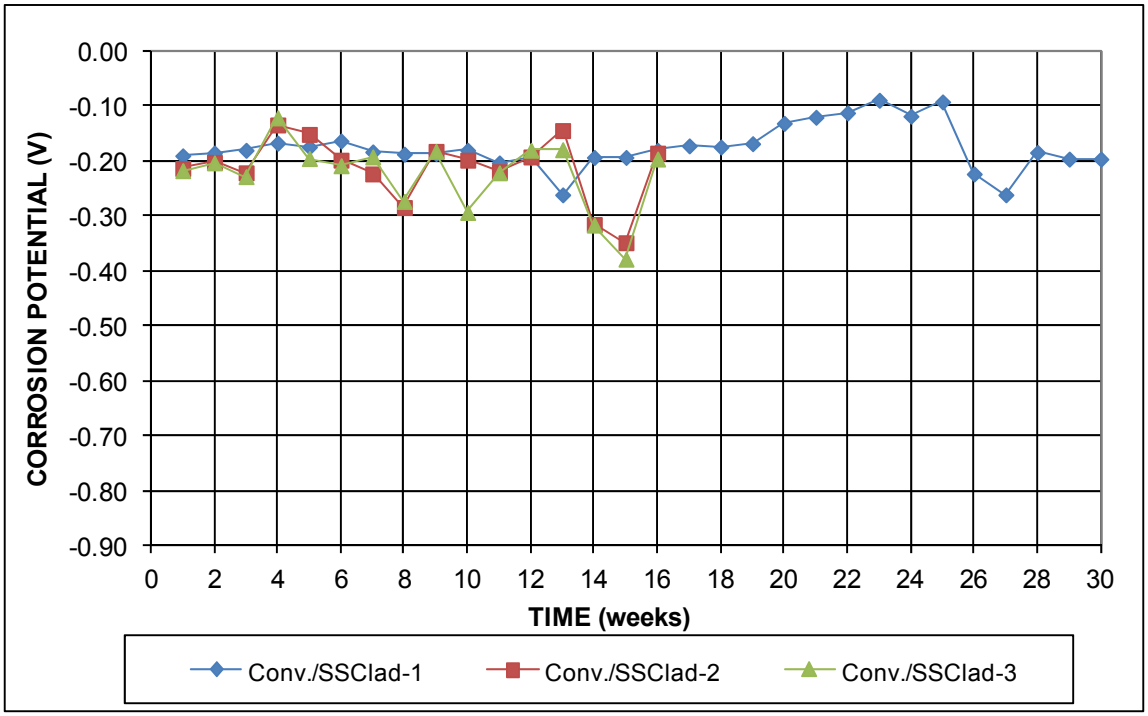

Figure C.86: Southern Exposure corrosion potentials with respect to CSE – conventional steel (top mat) / stainless steel clad (bottom mat), bottom mat, w/c = 0.45